Investigation of Telomere maintenance in BRCA2 defective mammalian cell lines

A thesis submitted for the degree of doctorate of philosophy

By

Yaghoub Gozaly Chianea

Division of Biosciences

School of Health Sciences and Social Care

January 2014

Declaration

I hereby declare that the research presented in this thesis is my own work, except where otherwise specified, and has not been submitted for any other degree.

Yaghoub Gozaly Chianea

Abstract

BRCA2 is a highly penetrant breast cancer predisposing gene. The protein product of the *BRCA2* gene mediates repair of breaks in DNA, through Homologous Recombination (HR). Understanding the mechanism(s) behind *BRCA2* involvement in HR will help clarify its clinical importance and may pave the way for possible therapy.

In this work we show that *BRCA2* affects telomere maintenance in mammalian cells. Telomeres are physical ends of chromosomes implicated in cell senescence and carcinogenesis. In particular, the enzyme telomerase that synthesizes telomeric DNA is highly active in ~90% cancers and it is considered one of the cancer markers. The remaining 10% of cancers do not show telomerase activity and they maintain their telomeres by an alternative pathway known as Alternative Lengthening of Telomeres (ALT). We observed telomere shortening, loss of telomere function in the form of end chromosome fusions and increased incidence of Telomere Sister Chromatid Exchanges (T-SCE), one of the recognized markers of ALT, in 3 sets of Chinese hamster and human *BRCA2* defective cell lines, all of which maintained telomeres by conventional mechanisms.

We have also inhibited *BRCA2* expression in ALT positive cells by transfecting them with si (short interfering) RNA oligonucleotides specific for *BRCA2* and monitored its expression by Real Time-PCR and Western blot. Results indicate that BRCA2 knock-down in ALT positive human cells that causes reduction in T-SCE frequencies, thus suggesting that ALT cells and those that maintain telomeres by conventional mechanisms differ in this respect. One interesting scenario that emerges from these results is that BRCA2 deficiency could potentially suppress the ALT pathway. We wanted to explore this possibility further by creating a permanent BRCA2 knock-down. Our preliminary results suggest that our method for the permanent BRCA2 knock-down based on the SMARTvector 2.0 system and sh (short hairpin)

RNA approach is still not working effectively. We identified hyper-methylation of the promoter within the vector as a possible cause.

Finally, we examined repair kinetics of interstitial telomeric sites (ITSs) in BRCA2 deficient Chinese hamster cells in order to test the hypothesis that defective DNA double strand break repair may be responsible for their increased sensitivity to DNA damaging agents. Our results indicate that DNA damage within ITSs is repaired effectively thus disproving the above hypothesis. In conclusion, this work demonstrates the involvement of *BRCA2* in telomere maintenance.

Acknowledgments

My continuous thanks are for Allah, the creator of the universe. I also would like to express my deepest gratitude to my supervisor, Dr. Predrag Slijepcevic for his encouragement and continues help and support throughout this study.

I must personally thank Dr. Hemad Yasaei, for his support and helpful guidance. Many thanks also go to my colleagues in our group, Dr. Maryam, Savi, Chetana, Parisa, and Sheila for their help and support. I also must thank, Dr. Parris, Dr. Terry, Dr. Al-Mahdavi, Dr. Sandi and Dr. Matthew for their help and for encouragement and for being there for me whenever I needed chat or discussion.

My acknowledgement also goes for my office colleagues, Hannah, Jessica, Dr. Asif, Dr. Najmunisa, Gabriele, Dr. Olesya and Valentina. Moreover, I wanted to say many thanks to my friends Mohammad, Hassan, Dr. Punam and special thanks for Dr. Azadeh, for her help in molecular biology studies.

Last but not least, I would like to send my special appreciations to my parents and my sisters for their love, support and long-suffering listening to my difficulty throughout my PhD studies.

Dedicated from my bottom of my heart to love of my life

I.H

Publications

- **Yaghoub Gozaly Chianea**, Savneet Bains, Hemad Yasaei and Predrag Slijepcevic: BRCA2 may be involved in interstitial telomeric maintenance. In preparation

- AS Qaseem, AA. Pathan, JA Layhadi, **Y. Gozaly-Chianea**, SR Durham, U. Kishore, and MH Shamji: Recombinant human pulmonary surfactant protein-D (rhSP-D) suppresses IgE-facilitated allergen binding to B cells. Manuscript in preparation.

- Hemad Yasaei, **Yaghoub Gozaly-Chianea** and Predrag Slijepcevic: Analysis of telomere length and function in radiosensitive mouse and human cells in response to DNA-PKcs inhibition. 2013 Mar 22, Genome Integrity, 4, 2. doi: 10.1186/2041-9414-4-2.

- Ester Sapir, **Yaghoub Gozaly-Chianea**, Suliman Al-Wahiby, Sainu Ravindran, Hemad Yasaei and Predrag Slijepcevic: Effects of BRCA2 deficiency on telomere recombination in non-ALT and ALT cells. 2011 Dec 09, *Genome Integrity*, **2**, 9. doi: 10.1186/2041-9414-2-9.

- Gayani Nadika Pitiyage, Predrag Slijepcevic, Aliya Gabrani,**Yaghoub Gozaly Chianea**, Kue Peng Lim , Stephen Stewart Prime, Wanninayake Mudiyanselage Tilakaratne, Farida Fortune, and Eric Kenneth Parkinson: Senescent Mesenchymal Cells Accumulate in Human Fibrosis by a Telomere-Independent Mechanism and Ameliorate Fibrosis through Matrix Metalloproteinases. 2011 Feb 21, *Journal of Pathology*, **223**, 604-617

Abbreviations

ALT	Alternative lengthening of telomeres
APB	ALT Promyelocytic leukemia Bodies
APS	Ammonium persulphate
ATM	Ataxia telangastia mutated protein
ATR	ATM-and Rad3-related proteins
BCA	Bicinchoninic acid
BER	Base excision repair
Bp	Base pair
BRCA1	Breast Cancer susceptibility gene 1
BRCA2	Breast Cancer 2 susceptibility protein
BRCT	BRCA1 C-terminal
BSA	Bovine Serum Albumin
CCFL	Corrected Calibrated Fluorescence
cDNA	Complementary DNA
CF	Correction Factor
COD-FISH	Chromosome Orientation and Direction FISH
CO-FISH	Chromosome Orientation Fluorescence in situ Hybridization
DDR	DNA damage response
DMEM	Dulbecco's modified eagle medium
DMSO	Dimethylsulfoxide
DNA-PKcs	DNA-protein kinase catalytic-subunit
dNTP	Deoxynucleotide triphosphate
DSB	Double strand breaks
DTT	Dithiothreitol
DW	Distilled water
ECL	Enhanced chemiluminescence
ECF	Chromosome End fusions
EDTA	Ethylene diamine-tetra acetic acid
ES	Embryonic stem cells
FA	Fanconi's Anemia
FBS	Fetal bovine serum
FCS	Fetal calf serum
FISH	Fluorescence in-situ hybridization
FITC	Fluorescein isothiocynate
gDNA	Genomic DNA
Gy	Gray
hCMV	Human cytomegalovirus
HR	Homologous recombination
HRP	Horseradish peroxidise
IF	Immunofluorescence
IQ-FISH	Interphase Q-Fish
IR	Ionising Radiation
Kb	Kilobase
KCL	Potassium Chloride
kDa	Kilo Dalton

LY-R	Radioresistant mouse lymphoma cells
LY-S	Radio-sensitive mouse lymphoma cells
MgCl2	Magnesium chloride
MOI	Multiplicities of infection
miRNA	MicroRNA
MMEJ	Microhomology-mediated end joining
MRN	MRE11/RAD50/NSB1
NBS	Nuclear bodies
NER	Nucleotide Excision Repair
NHEJ	Non-homologous end joining
PAR	Poly ADP-ribose
PBS	Phosphate buffer saline
PCR	Polymerase chain reaction
PNA	Peptide nucleic acid
POT1	Protection of telomeres 1
PVDF	Polyvinylidene fluoride
Q-FISH	Quantitative in-situ hybridization
RNA	Ribonucleic acid
RNAi	Ribonucleic acid interference
RPA	Replication protein A
RPM	Rotations per minute
RPMI	Roswell Park Memorial Institute
RS-SCID	Radio sensitive severe combined immunodeficiency
RT	Room Temperature
RT-PCR	Reverse transcriptase-polymerase chain reaction
SDS	Sodium dodecyl sulphate
shRNA	short hairpin RNA
siRNA	Short interfering ribonucleic acid
ss	Single stranded
SSB	Single strand breaks
SSC	Sodium chloride sodium citric acid
ssDNA	Single stranded DNA
TBE	Tris-borate-EDTA
TBST	Tris-buffered saline tween-20
TEMED	Tetramethylethylenediamine
TERT	Telomerase Reverse Transcriptase
TFUs	Telomere fluorescence units
TIF	Telomere dysfunction induced foci
TIN2	TRF1-interacting factor
T-loop	Telomeric-loop
TRF1	Telomeric repeat binding factor 1
TRF2	Telomeric repeat binding factor 2
T-SCEs	Telomere Sister Chromatid Exchanges
TU	Transducing Unit
UV	Ultra violet
H2AX	Histone H2AX phosphorylated on serine-139

Contents

List of Tables

List of Figures

Chapter-1

General Introduction

1.1 Telomere biology

Telomeres are specialised nucleoprotein structures located at the ends of linear chromosomes responsible for maintenance of chromosome stability. The absence of these specialized structures causes fusion of chromosomes and subsequent breakage-fusion-breakage cycles leading to genomic instability (King et al., 1994). Here, we will review telomere biology, assess the importance of telomeres in DNA damage response and discuss the role of BRCA2 in telomere maintenance.

1.2 Structure and function of telomeres

In the early 1930s, Hermann J. Muller and Barbara McClintock showed that chromosomes carry a distinct component at their ends, which provides their long-term stability (Greider and Blackburn, 1996). Muller named this component the "telomere", using Greek words "telos" for end and "meros" for part. Today we know that telomeres consist of specific DNA sequences and a set of specialized proteins (Olovnikov, 1971). However, telomeres were initially defined functionally; the definition was based on the Muller/McClintock's observations that naturally occurring chromosome ends behave in a different way from broken chromosome ends. Today we know that the telomere protective function is due to the formation of a specialized nucleoprotein complex, which occupies the end of the chromosome and most likely prevents the activation of DNA damage response pathways that normally recognize DNA ends resulting from DNA breakage (Viscardi et al., 2007).

In mammalian cells telomeres are composed of the repeated DNA sequence (TTAGGG)n (Greider and Blackburn, 1985). When DNA replicates, one strand is replicated by the leading-strand DNA synthesis and the other strand is replicated by the lagging-strand synthesis (Figure 1.1). Most of the telomeric tract is double stranded DNA, but there is also a short (normally

between 50 and 200 base pairs) single 3' strand overhang at both chromosome ends (Makarov et al., 1997, Greider and Blackburn, 1996, Lingner and Cech, 1998) (Figure 1.1).

Due to replication properties of mammalian polymerases it has been thought that two strands of telomeric DNA would have different terminal structures at the end of DNA replication: the leading strand telomere would be blunt-ended and the lagging strand telomere will have 3` overhang (Figure 1.1). The size of this 3` overhang has to be equal to the size of an RNA primer i.e. 8-12 base pairs (bp) (see Figure 1.1A).

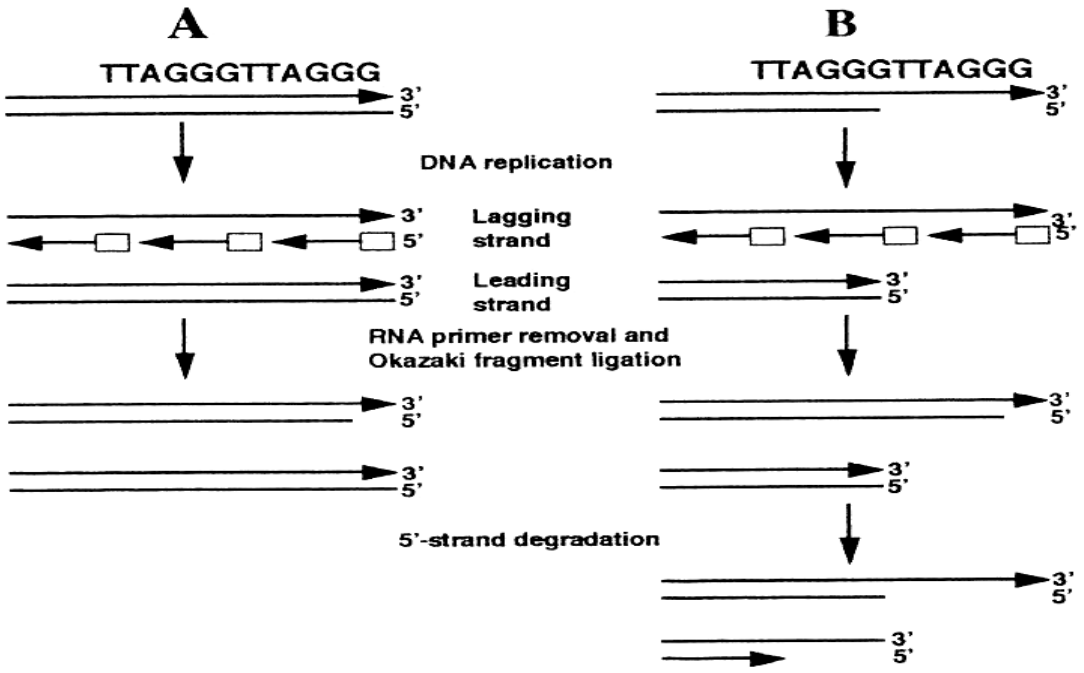

Figure 1.1 Schematic outline of telomere replication (adapted from Slijepcevic, 1998).

A) conventional model, B) revised model. Because an RNA primer (R) primes the synthesis process of the lagging strand, removal of the RNA primer leaves a gap of 8-12 bp (Conventional model) (Weinrich et al., 1997). However, degradation of the 5` ends by exonuclease activity works to shorten the strand a little further (Revised model) (Wellinger and Sen, 1997, Makarov et al., 1997).

However, it has been shown that all chromosome ends have 3' single strand overhangs most likely created by exonucleolytic degradation (Wellinger and Sen, 1997, Makarov et al., 1997) (Figure 1.1B). Therefore, the replication of telomeric DNA results in sequence loss due to end-replication problem and exonucleolytic degradation (Figure 1.1B).

Examination of chromosomal ends by electron microscopy revealed that telomeric DNA is not linear. Instead, it forms a loop called t (telomeric)-loop (Griffith et al. 1999). T-loops can be as large as several kb and it has been suggested, based on indirect evidence, that the G-rich 3` overhang invades the telomeric duplex DNA. The G-rich overhang is able to fold backwards, invade duplex telomere strands thus resulting in a t-loop formation (Figure 1.2).

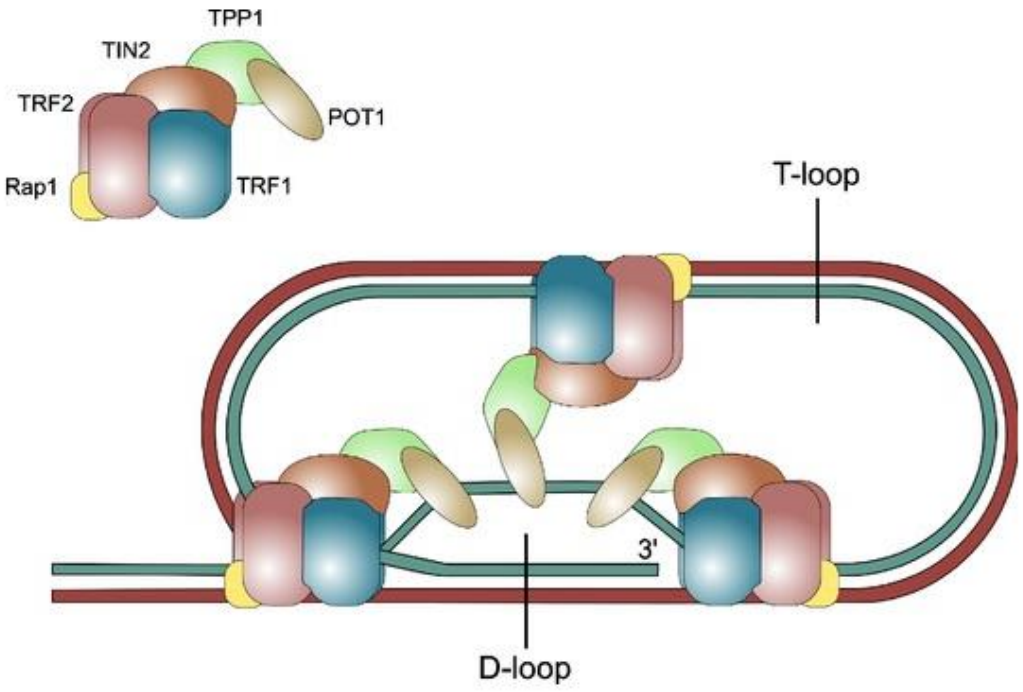

Figure 1.2 A schematic of how shelterin might be positioned on telomeric DNA.
The TTAGGG repeats of mammalian chromosome ends associate with the six-protein complex. Highlighting the duplex telomeric DNA interactions of TRF1 and TRF2 and the binding of POT1 to the single-stranded TTAGGG repeats. Although one of the shelterin complexes may have the depicted structure, telomeres contain numerous copies of the complex bound along the double strand TTAGGG repeat array (adapted from Titia de Lange, 2005).

The G-rich overhang inserts between the two strands, which forms a minor D-loop (Figure 1.2). Free 3`-end can possibly be recognised as DNA strand breaks which are able to activate the checkpoints of the DNA repair apparatus. These could probably initiate the process of cellular senescence and apoptosis. Therefore, the loop structures sequester the free 3`-ends, preventing DNA damage recognition. This structure is also considered to be dynamic. This is because numerous proteins must be able to access the extreme terminus of DNA in its linear form in order to regulate processes associated with telomere function (Bryan et al., 1997). The essential function of telomere is to protect ends of chromosomes from irregular chromosomal recombination, end-to-end fusions and DNA degradation (Blackburn, 1991) in order to avoid DNA damage response activation (de Lange 2005). In addition to this function, telomeres play other roles including organisation of cell nucleus, meiosis associated processes and regulation of stem proliferation (Hackett et al., 2001). In the next section telomeric proteins will be described.

1.2.1 Telomere-associated proteins

Various proteins have been recognised as telomere-associated proteins. They associate with telomeres in two different ways. Some associate by binding telomeric DNA directly. However, other proteins are not able to bind telomeric DNA directly. Instead, they interact with proteins which bind telomeric DNA. Together, these two groups of proteins mediate formation of a specialized tri-dimensional t-loop structure discussed earlier. The core group of telomeric proteins are known by a collective name shelterin. Shelterin components include: TRF1, TRF2, POT1, TIN2, RAP1 and TPP1 (Liu et al., 2004). Some of these proteins, namely TRF1, TRF2 and POT1 directly interact with the sequences of telomeric DNA (as illustrated in Figure 1.2) (Liu et al., 2004).

TRF2 is involved in the establishment of t-loop (Cesare and Griffith, 2004) whereas TRF1 is involved in the telomere length homeostasis control (van Steensel and de Lange, 1997).

Expression of truncated forms of TRF1 and the interacting factor present in it, TIN2, induce unsuitable elongation of telomeres in telomerase-positive cells (van Steensel and de Lange, 1997, Kim et al., 1994, Smogorzewska et al., 2000). Inhibition of TRF2 in cultured cells results in deprotection of chromosome ends and covalently fused telomeres (van Steensel et al., 1998). Additionally, loss of TRF2 function would possibly lead to growth arrest and ATM/p53 mediated apoptosis (van Steensel et al., 1998). Both TRF1 and TRF2 are also recognised as the negative telomere length regulators i.e. overexpression of either results in gradual length decline (Van Steensel and de Lange, 1997; Smogorzewska et al., 2000). POT1 is the only protein that can bind the 3' single strand telomeric overhang. TIN2 (TRF1-Interacting Nuclear protein-2) and RAP1 (Repressor Activator Protein-1) do not bind telomeric DNA directly but instead interact with TRF1 and TRF2. In addition, TPP1, thereby providing a bridge between the shelterin components that bind to ds and single strand telomeric DNA (Houghtaling et al., 2004). Thus, members of the shelterin complex are considered to be vital regulators of telomere structure and function.

In addition to shelterin components, several other proteins have been shown to associate with telomeres. For example, Tankyrase 1 and 2 are identified as proteins that associate with telomeres through interactions with TRF1 (Ye and de Lange, 2004). They are also known by their shorter names TANK1 (TRF1-interacting ankyrin-related ADP-ribose polymerase) and TANK2. They belong to a family of proteins known as poly (ADP-ribose) polymerases (PARPs) that play a role in DNA metabolism in particular DNA damage response. Two prominent members of this family, PARP 1 and 2 operate in base excision repair (BER) and single strand break (SSB) repair (Slijepcevic, 2006, Herceg and Wang, 2001, Ame et al., 2004).

Furthermore, some other DNA damage response proteins associate with telomeres. For example, the MRE11-RAD50-NBS1 (MRN) complex, the DNA-dependent protein kinase complex (DNA-PK) consisting of Ku and DNA-PKcs (catalytic subunit) and homologous

recombination proteins such as RAD51D normally reside at telomeres (Song et al., 2000, Wu et al., 2000, Bailey et al., 2004). DNA damage response proteins such as RAD54 and ERCC1/XPF affect telomere function but do not associate with telomeres directly (Chan and Blackburn, 2002, Blasco and Hahn, 2003) suggesting the functional interplay between telomere function and DNA damage response that goes beyond direct association of individual protein sets. Most of the above-mentioned DNA damage response proteins influence telomere length control, G-rich overhangs structure and telomere function. Their effects on telomeres will be discussed in (section 1.3.1 and 1.3.2).

1.2.2 Telomere maintenance by telomerase

Telomeres may become dysfunctional via a number of mechanisms, some of which have been highlighted above. However, the most common mechanism in this respect is physiological telomere sequence loss resulting from inability of conventional DNA replication enzymes to replicate telomeric DNA in full (see section 1.2). This causes telomere shortening, which contributes to the subsequent replicative cell senescence (O'Sullivan et al., 2002). Replicative cell senescence, or Hayflick limit, refers to the phenomenon first observed by Hayflick and Moorhead (1961) that normal human somatic cells can divide *in vitro* only a limited number of times. In most cases differentiated human somatic cells cease to divide after roughly 50 divisions. However, some cells, in particular germ-line and stem cells, may be able to avoid this replicative senescence. They differ from the most differentiated somatic cells in that they express the enzyme that can prevent telomere sequence loss, the enzyme telomerase (Bryan et al., 1997, Dunham et al., 2000). In this section we will review telomerase structure and function.

As a result of the investigations carried out in biochemistry of DNA replication, it is common knowledge that the 3` ends of linear DNA molecules cannot be entirely replicated by conventional polymerases (Levy et al., 1992) and the only enzyme that can accomplish this is

telomerase. Telomerase, a specialised reverse transcriptase, was initially isolated from the ciliate protozoan *Tetrahymena thermophila* (Greider and Blackburn, 1985). Telomerase, or telomere terminal transferase, is a ribonucleoprotein which adds telomeric (TTAGGG)n repeats onto chromosome ends (Blackburn, 1991, Feng et al., 1995). This event is generally conserved in eukaryotes, as it is revealed by phylogenetic comparison. For a very long period of time since the first report on telomerase activity in cancer (Kim et al., 1994) it was assumed that normal human somatic cells lack telomerase activity completely. However, subsequent studies suggested that some human somatic cells such as fibroblasts have low telomerase activity levels as revealed by immunological detection of telomerase catalytic component known as hTERT (Masutomi et al., 2003). Still, it is safe to conclude that most human somatic cells lack robust telomerase activity.

On the contrary, high telomerase activity has been observed in most human cancers (Kim and Wu, 1997, Dhaene et al., 2000), suggesting that telomerase is essential in providing a proliferative capacity to cells for the progression towards malignancy. Telomerase activity can easily be detected in various embryonic cells during development, in adult stem cells (Ulaner and Giudice, 1997, Ulaner et al., 1998) and adult germ-line tissues (Weinrich et al., 1997). It has been theorized that cell senescence may probably be overcome via upregulation of telomerase (Blackburn, 1991, Feng et al., 1995, Kim and Wu, 1997). A formal proof for this has been provided by the over-expression of hTERT in somatic human cells resulting in by-passes of replicative senescence or immortalization (Takano et al., 2008).

The length of telomeres, the length of G-rich overhangs and also expression levels of telomerase subunits play the role of indirect indicators of the enzyme function. Telomeres are also assumed to control the expression of subtelomeric genes, a phenomenon acknowledged as telomere position effect (Baur et al., 2001), and therefore paradoxically this may have an effect on the expression of telomerase itself which in humans, is positioned at the extreme end of

chromosome 5p (Meyerson et al., 1997, Kilian et al., 1997). Most investigations have linked telomerase to the maintenance of stable telomere length, even though telomere length has the ability to be maintained in the absence of telomerase via alternative mechanisms. These mechanisms are known as alternative lengthening of telomerase (ALT).

1.2.3 Telomerase components

Human telomerase has a molecular mass of over 1000 kDa containing two major components: an RNA component (hTERC) and a catalytic component (hTERT) and several smaller components (Blackburn, 2000a) (see

Figure **1.3**). hTERC is widely expressed in normal human cells, while hTERT is, according to some studies, low and even absent in the same cells (Dhaene et al., 2000, Kanaya et al., 1998, Artandi, 2006).

However, this is a controversial issue as a good quality antibody can detect hTERT in human primary fibroblast (Masutomi et al., 2003). Telomerase plays an important role in cancer (Zhou et al., 2013) as a correlation exists between the over-expression of hTERT and an increase in telomerase in tumours. hTERC and hTERT are indispensable for telomerase activity, and expression of these subunits in *vitro* leads to the formation of a functional telomerase enzyme (Weinrich et al., 1997, Chen and Huang, 2012).

1.2.3.1 Human Telomerase Reverse Transcriptase (hTERT)

Presence of hTERT, the catalytic subunit of telomerase that also harbours the reverse transcriptase activity, was first identified in 1989 in crude nuclear HeLa fractions (Morin, 1989). A single copy hTERT gene consists of 16 exons and 15 introns spanning more than 40 kb. The hTERT gene was localised, using the FISH probes, on human chromosome 5p15.33, very close to the telomere (Bryce et al., 2000). The hTERT gene encodes a 127kDa protein consisting of 1132 amino acids (Meyerson et al., 1997), which is almost entirely localised in

the nucleus (Harrington et al., 1997). Phylogenetic studies found that the TERT subunit is very well conserved from protozoa to humans, including plants. It is interesting that TERT motifs are shared by viruses and retroelements (Nakayama et al., 1998). These motifs are significant for the reverse transcriptase activity as mutations in amino acids in the motifs prevent telomerase activity (Nakayama et al., 1998, Weinrich et al., 1997, Wojtyla et al., 2011). They also aid in telomere elongation because through these motifs the hTERT protein recognises the RNA template and reversibly transcribes the telmeric motif, leading to the elongation of telomere.

In the actual process of telomeric DNA synthesis telomerase positions itself on the edge of the 3' end of the leading DNA strand (Figure 1.3). The hTERC sub-unit of the telomerase enzyme is located near the template region and elongation is carried out by hTERT, the catalytic sub-unit of telomerase. Subsequently, the complex is translocated and repositioned on the newly synthesised DNA to continue telomere elongation. Eventually, the lagging strand is replicated by DNA polymerases. The region containing the TERT motifs has also been shown to bind hTP1 protein, independent of the hTERT binding (Wojtyla et al., 2011).

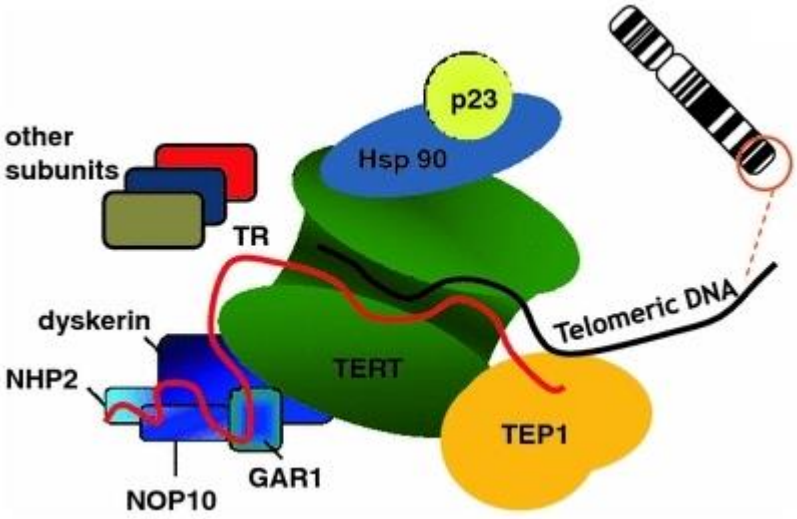

Figure 1.3 Human telomerase complex and binding proteins. Adapted from (Wojtyla et al., 2011). The assembly of human telomerase occurs by a complex mechanism, which depends on energy and it involves, first of all, stabilisation of hTERC and its subsequent association with the hTERT protein (Aisner et al., 2002, Collins, 2008). To demonstrate telomerase activity in *vitro*, only two components are required: TERT protein and TERC (Nakayama et al., 1998, Kilian et al., 1997). On the other hand, assembly of the active telomerase complex in *vivo* requires additional components that facilitate the enzyme function (McEachern et al., 2000).

1.2.3.2 Human Telomerase RNA Component (hTERC)

hTERC is one of telomerase's subunits and serves as a template during telomere elongation. In order to demonstrate telomerase activity in *vitro* hTERC was one of the two necessary components (Weinrich et al., 1997). The gene encoding hTERC was localised on the human chromosome 3q26.3 (Feng et al., 1995). Biochemical analysis of hTERC expression revealed that this component is widely expressed in both tumour and non-tumour tissues (Yi et al., 2001, Feng et al., 1995). Given that telomerase is required for the immortalization step in malignant transformation hTERC may be used to distinguish between precancerous lesion and high grade cancer lesions in relevant tissues (Heselmeyer-Haddad et al., 2003, Heselmeyer-Haddad et al., 2005). This is in line with observations that the hTERC expression is up-regulated in tumour

tissues (Soder et al., 1998). However, the hTERC is not essential for telomerase reactivation (Weinrich et al., 1997), in contrast to hTERT.

The mature hTERC transcript is 451 nucleotides long and lacks a polyA tail. The RNA contains a template region of 11 nucleotides 5'-CUAACCCUAAC-3' located in the 5' extremity (Chen et al., 2000). Although hTERC RNA sequences are phylogenetically divergent, their secondary structures have been found to be similar form ciliates to vertebrates (Chen et al., 2000).

1.3 Telomeres and DNA damage response

A number of DNA damage response proteins are physically present at telomeres (see above) suggesting a functional interplay between mechanisms responsible for telomere maintenance and DNA damage response mechanisms. In this section we review functional links between the above two sets of molecular mechanisms.

DNA damage response may be described as a network of mechanisms that:

A) sense, signal and repair DNA damage which can be caused by various external and internal agents;

B) control cell-cycle progression and cell death via apoptosis.

It is becoming more evident that telomeres are involved in DNA damage response. For instance, mice that lack functional telomerase are radiosensitive (Goytisolo et al., 2000). Radio-sensitivity is usually a sign of defective DNA damage response. For example, exposure to ionizing radiation (IR) results in induction of numerous DNA damage lesions including DNA double strand breaks (DSBs) (Ward, 2000). Sensitivity to IR is an indication that cell repair mechanisms cannot effectively repair IR induced DNA lesions such as DSBs.

Therefore, even though telomerase is not directly involved in DSB repair its absence is sufficient to affect this pathway thus confirming the functional interplay between DNA damage response and telomere maintenance. Furthermore, a number of studies have shown that the loss

of telomere function activates DNA damage response (Longhese, 2008). This is the consequence of chromosome end deprotection resulting in them being recognized as pathological DSBs by cellular the DNA damage response mechanisms.

In addition, research carried out within the last 10-15 years revealed that cells defective in proteins regulating different aspects of DNA damage response show a variety of telomere dysfunction phenotypes (see below). Therefore, it is considered that these DNA damage response proteins are also needed in the maintenance of telomeres and their deficiency gives rise to deprotected or dysfunctional telomeres. A number of reviews have been published in recent years summarizing these proteins and pathways they regulate (Longhese, 2008). They range from the DNA damage signalling proteins such as ATM (Polo and Jackson, 2011), to DNA damage sensors such the MRN complex (Polo and Jackson, 2011) to proteins involved in repair of DNA DSBs (Karran, 2000), UV induced DNA lesions (Sinha and Hader, 2002) and DNA cross-links (Sinha and Hader, 2002). It is striking that the role of DSB repair proteins in telomere maintenance is best characterized.

DSBs are thought to be the most severe form of DNA damage. They are usually caused by exposure of cells to IR, chemotherapeutic or radiomimetic agents for example bleomycin, mitomycin C, cisplatinum, methylmethanesulfonate, etc. as well as to endogenous free radicals, the by-products of oxidative metabolism.

If DSBs are not repaired before the DNA replication process starts (or mitosis), DSBs would be able to induce cell death. More dangerously, if they misrepair, DSBs could potentially lead to chromosome translocations as well as genomic instability and cancer predisposition. The mechanisms which respond to DSBs include three different categories; pathways of DNA repair, cell-cycle checkpoint arrest and apoptosis (Buscemi et al., 2006).

Cell-cycle checkpoint controls prevent progression through the cell cycle as DNA replication and mitosis in the presence of DSBs would destabilise the genome. In order to repair DSBs in mammalian cells there are two major pathways: homologous recombination (HR) and non-homologous end joining (NHEJ). HR requires DNA sequence homology resulting in DSB repair by recovering genetic information from intact sister chromatids. Therefore, HR is an error free repair mechanism. On the other hand, NHEJ rejoins DNA by directly joining DNA ends without any requirement for sequence homology and as a result may not be error free. Moreover, the relative contribution of HR and NHEJ in the cell cycle is differential; it is widely accepted that mammalian cells predominantly use HR in the G2 phase of the cell cycle and NHEJ mostly in the G1 phase of the cell cycle (Haber, 2000, Rothkamm et al., 2003, Jeggo et al., 2005).

Telomere maintenance is linked to both pathways as it is shown by telomere dysfunction phenotypes in the absence of functional HR and NHEJ (see below).

1.3.1 Non-homologous end joining (NHEJ)

Although NHEJ shows the highest level of activity in G1 phase biochemical studies indicate that it remains active throughout the cell cycle, including late S and G2 (O'Driscoll and Jeggo, 2006). Several proteins have been implicated in NHEJ in higher organisms (Pasta and Blasiak, 2003). Three of them comprise the complex called DNA dependent protein kinase (DNA-PK), namely Ku 70 and Ku 80 which are the two subunits of the heterodimeric Ku protein and also a large catalytic subunit which is known as DNA-dependent protein kinase catalytic subunit (DNA-PKcs) (Buck et al., 2006, Ahnesorg et al., 2006). DNA DSBs are recognised in mammalian cells via the sensor molecule, MRN complex and this signal is mediated by the key DNA damage signalling molecule ATM. As a result the DSB repair will be activated starting with binding of Ku to the end of the broken DNA molecules. Subsequently, the Ku protein recruits the DNA-dependent protein kinase catalytic subunit (DNA-PKcs), which sequesters the

DNA ends. The DNA ligase complex (including XRCC4, XLF and DNA ligase IV) then catalyses phosphodiester bond formation.

Moreover, XRCC4 known as the X-ray cross linking protein and the XLF protein may be used to bridge XRCC4 and Ligase IV proteins. The only remaining NHEJ molecule, Artemis, is regulated by DNA-PKcs through phosphorylation (Miller and Cooper, 2003). Figure 1.4 shows an outline of the NHEJ process. It is interesting that XRCC4 and Ligase 4, which are required for the subsequent rejoining stages (Figure 1.4) co-associate in undamaged cells but, surprisingly, do not associate with DNA-PK in the same cells (Lees-Miller and Meek, 2003). They are also involved in V(D)J recombination and this indicates that NHEJ is also vital for this process (Ma et al., 2002).

It is interesting that a protein involved in HR, namely BRCA1, has been suspected to indirectly contribute to NHEJ (Zhong et al., 1999). However, the exact biochemical function of BRCA1 in NHEJ has not been uncovered yet. It has been hypothesised that BRCA1 interacts with the RAD50 protein which is a part of the MRN complex (Ahnesorg et al., 2006). The MRN complex most likely acts as a sensor for DSBs (Lee and Dunphy, 2013). BRCA1 may also act in a fashion similar to that of DNA-PKcs, namely to provide a bridge between adjacent DNA breaks, or it may be able to inhibit the nucleolytic processing capability of the MRN complex (Paull et al., 2001). This indicates that BRCA1 is the regulator for the function of the MRN complex, which prevents extensive DNA end processing.

The loss of the Ku protein in mice causes telomere dysfunction in the form of chromosome fusions (Espejel and Blasco, 2002, Samper et al., 2000, Yasaei et al., 2013). Biochemical studies have shown that Ku is present at telomeres (d'Adda di Fagagna et al., 2001) and that interacts with both TRF1 and TRF2 (De Lange, 2002). It has been assumed that Ku is one of the negative regulators of telomerase. For example, Ku defective cells have elongated

telomeres (Samper et al., 2000). Hence, it is hypothesised that Ku works to block access of telomerase to telomeres (Slijepcevic and Al-Wahiby, 2005).

Furthermore, defective DNA-PKcs causes a similar phenotype to the one described in the case of defective Ku: telomere elongation and telomeric fusions (Yasaei et al., 2013). Biochemical studies have confirmed that similarly to Ku, DNA-PKcs also interacts with shelterin components TRF1 and TRF2 (de Lange, 2002, Chakhparonian and Wellinger, 2003). Therefore, two key components of NHEJ, Ku and DNA-PKcs, are strongly associated with regulating telomere length and function.

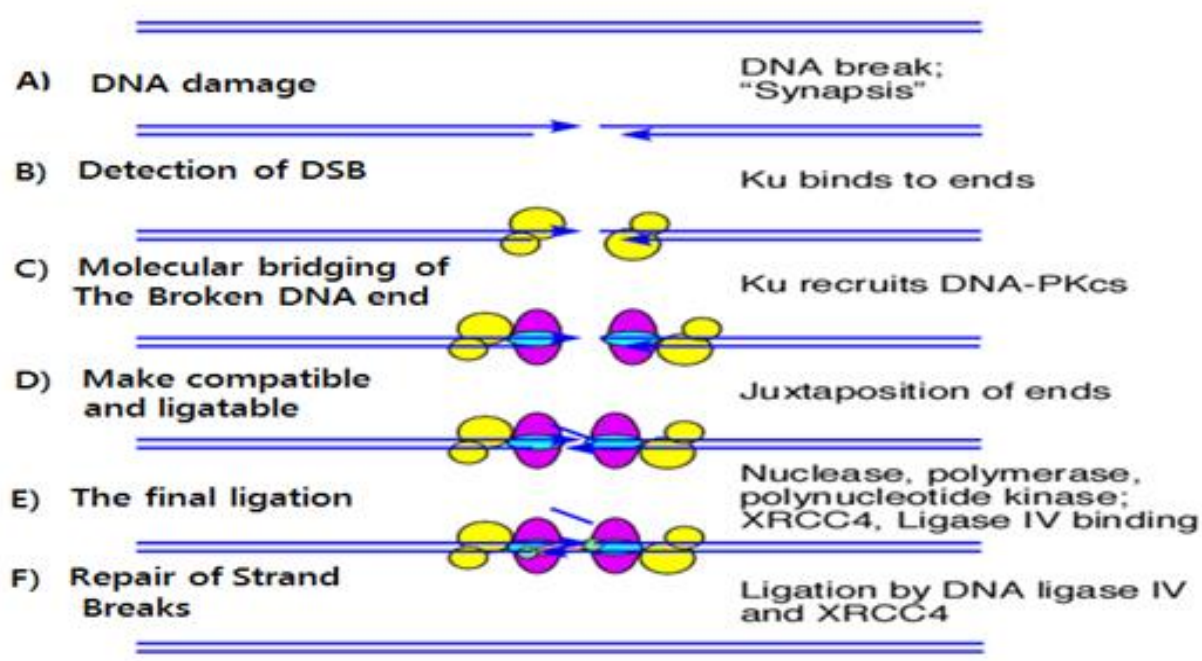

Figure 1.4 Schematic representation of NHEJ (Griffin and Thacker, 2004).

The only other NHEJ protein that plays a role in telomere maintenance is Artemis, a member of the SNM1 family of proteins, which has nucleolytic activity. However, its effects on telomere function are much less severe than the effects exerted by the loss of Ku and DNA-PKcs. It has been shown that cells from Artemis defective patients display a mild telomere dysfunction and more severe telomere shortening in comparison to normal cells (Yasaei et al. 2010). Interestingly, another member of the SNM1, Apollo, is a nuclease similar to Artemis. Apollo interacts with TRF2 and its absence causes a severe telomere dysfunction phenotype (van Overbeek and de Lange 2006; Lenain et al., 2006).

Two more NHEJ proteins have been investigated with respect to their effects on telomeres, XRCC4 and Ligase 4. None of them shows any effect on telomere maintenance (see for example Nijnik et al. 2007). At present it is unknown if XLF has any role in telomere maintenance.

1.3.2 Homologous recombination (HR)

The HR pathway for DSB repair is based on using the intact sister chromatid as the repair template**,** operating mainly in late S and G2 phases of a cell cycle. Therefore the coding information lost at the location of the break is retrieved as shown in (Figure 1.5). HR is therefore potentially an extremely accurate and efficient DSB repair pathway in contrast to NHEJ. In the initial steps of DSB processing the MRN heterotrimeric complex, which has exonuclease and endonuclease function, plays a significant role in order to produce and expose single stranded DNA tail as shown in (Figure 1.5) (Griffin and Thacker, 2004).

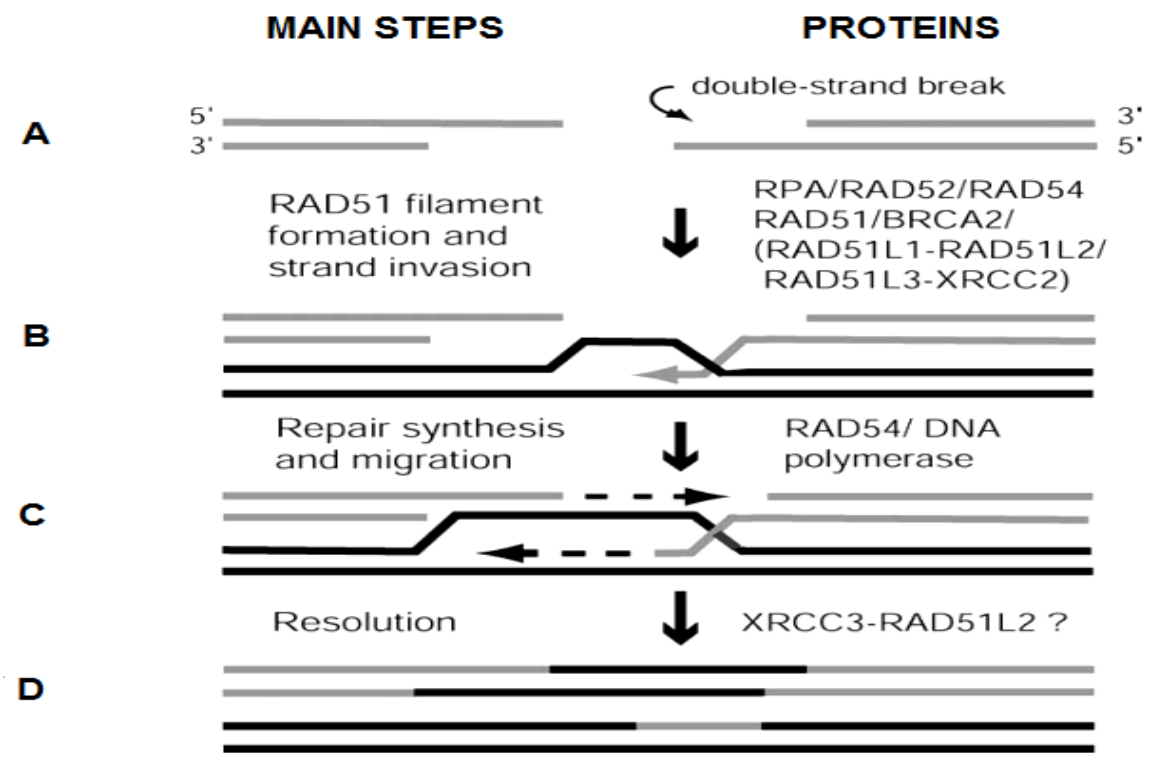

Figure 1.5 Schematic representation of the HR pathway.

A) DSBs recognised and the ends which are nucleolytically processed by the MRN complex. Formation of 3` single-stranded tails by resection of break ends which are layered with RAD51. B) Displacement of single-stranded binding replication protein A (RPA) with the assistance of RAD52 and RAD51. A 3` end molecule (grey colour) invades an unbroken molecule (black colour), displacing a strand (D-loop) that is considered to be a repair template. C) RAD54 has both pre- and post-invasion roles in order to facilitate the launching of DNA. D) The cross stranded structures will be determined by XRCC3 and a RAD51 like heterodimer (adapted from Griffin and Thacker 2004).

The next stage of HR processing involved RAD51 in cooperation with BRCA2 and RAD54 to bind the exposed single stranded DNA and**,** following that**,** to invade the broken DNA into the neighbouring sister chromatid, in order to search for homologous sequences (Yang et al., 2002). By this invasion, the non-matching intact strand is displaced, forming a D-loop, which expands as new DNA synthesis progresses over the break location. As soon as these neighbouring DNA strands get paired at the homologous sequence, the DNA polymerases will

be activated in order to fill the damaged gap. The resulting Holliday junction will be formed which will then complete the process (Thompson, 2005).

At least five HR proteins have been shown to affect telomere maintenance: RAD51D, RAD54, RAD50, BRCA1 and BRCA2. The effects of RAD51D, RAD54, RAD50, BRCA1 on telomeres will be discussed in this section. The effects of BRCA2 dysfunction on telomere maintenance will be discussed in the next section.

One of RAD51 paralogs, RAD51D, interacts with the shelterin component, TRF2, and it is present at telomeres in both somatic and meiotic cells (Tarsounas et al., 2004). Furthermore, MEFs (mouse embryonic fibroblasts) from RAD51D defective mice exhibited telomeric fusions and telomere shortening suggesting that RAD51D is important for telomere maintenance (Tarsounsa et al., 2004). Therefore, RAD51D plays a dual role. It is involved in (i) DSB repair via HR and (ii) telomere maintenance. Similarly to RAD51D, cells from RAD54 defective mice show telomere shortening and telomeric fusions (Jaco et al. 2003). However, there is no evidence that RAD54 interacts with any of the telomeric proteins.

A yeast study revealed that Rad50 mutants show telomere shortening and cell senescence (Kironmai and Muniapa 1997). Subsequent studies in mammalian cells revealed that RAD50, which is part of the MRN complex, interacts directly with TRF2 and telomeres (Zhu et al., 2000). A study using cells from a plant species, *Arabidopsis thaliana*, has shown that RAD50 mutants suffer from dramatic telomere shortening resulting in cell crisis and subsequent cell death (Gallego and White 2000). Rare surviving mutant cells show elongated telomeres suggesting activation of alternative mechanism(s) for telomere maintenance. Interestingly, RAD50 defective mice did not show any effects on telomere maintenance (Adelman et al., 2009). In contrast to this, a human squamous carcinoma cell line containing the RAD50

dominant negative vector displayed tumor cytotoxicity and telomere shortening (Abuzaid et al., 2009).

Finally, several studies investigated effects of BRCA1 on telomeres. It has been shown that BRCA1 suppresses telomerase activity by down-regulating hTERT (Xiong et al., 2003). This mechanism appears to be mediated by the c-Myc oncoprotein. Consistent with this, BRCA1 knock-down resulted in elevated telomerase activity and telomere elongation in tumor cells (Billal et al., 2009). Furthermore, it has been shown that BRCA1 interacts with TRF1 and TRF2 (Billal et al., 2009). This interaction is most likely mediated by one of the MRN complex components, namely RAD50. Therefore, BRCA1 may exert its effects on telomeres via the MRN complex. Analysis of cell lines from BRCA1 carriers revealed chromosomal abnormalities consistent with telomere dysfunction phenotypes (Cabuy et al. 2008, McPherson et al., 2006, Al-Wahiby and Slijepcevic, 2005).

It is important to stress that apart from NHEJ and HR proteins some other proteins involved in DNA damage response play a role in telomere maintenance. It is clear from the above outlines that the MRN complex plays a role on telomere maintenance. Apart from RAD50, the remaining two members of the complex, NBS1 and MRE11, are both found to associate with telomeres and exert effects on telomere function (for review see Lamarche et al. 2010).

One of the key DNA damage signalling proteins, ATM, is also implicated in telomere maintenance. The first study to describe effects of ATM on telomeres was that of (Pandita et al., 1995). Mice lacking functional ATM show accelerated telomere sequence loss, telomeric fusions and extra-chromosomal telomeric fragments (Hande et al., 2001). ATM phosphorylates both TRF1 and TRF2 as part of its DNA damage signalling role (Bradshaw et al., 2005). Some other DNA damage response proteins play a role at telomere maintenance (for a recent review

see Diotti and Loayza 2011). Because of space limitations it would not be appropriate to discuss them further.

1.4 Telomeres, BRCA2 and the ALT pathway

The significance of telomeres in human pathology is becoming increasingly crucial because of their vital role in cellular senescence and carcinogenesis (Blasco and Hahn, 2003). In addition, dysfunctional telomeres are a common feature in increasing number of cancer predisposition syndromes. A few base pairs (50–200 bp) of telomeric DNA sequence are lost with each cell division. This progressive reduction could be compensated for by telomerase, which becomes activated in the majority of tumours. Hence, telomerase reactivation allows tumour cells to proliferate indefinitely and this at the same time allows mutation accumulation (Chan and Blackburn, 2004).

Most human cancer cases appear to have short telomeres and high levels of telomerase, whereas telomerase is absent in most normal somatic tissues (Walne et al., 2007). Based on this observation, telomerase is a potentially sensitive biomarker for screening, early cancer detection, prognosis and also in monitoring as an indication of residual disease (Kiyono et al., 1998).

All this evidence indicates that telomere dysfunction would lead to two outcomes in somatic cells depending upon the integrity of checkpoint mechanisms: 1) responding to checkpoints with senescence / apoptosis or 2) proliferating which would result in genomic instability. The rare cells that continue to proliferate and emerge from crisis which would accumulate additional mutations, genetic lesions and inactivate tumour suppressor checkpoints**,** are the ones that will eventually develop cancer in the environment that favours positive selection (Figure 1.6).

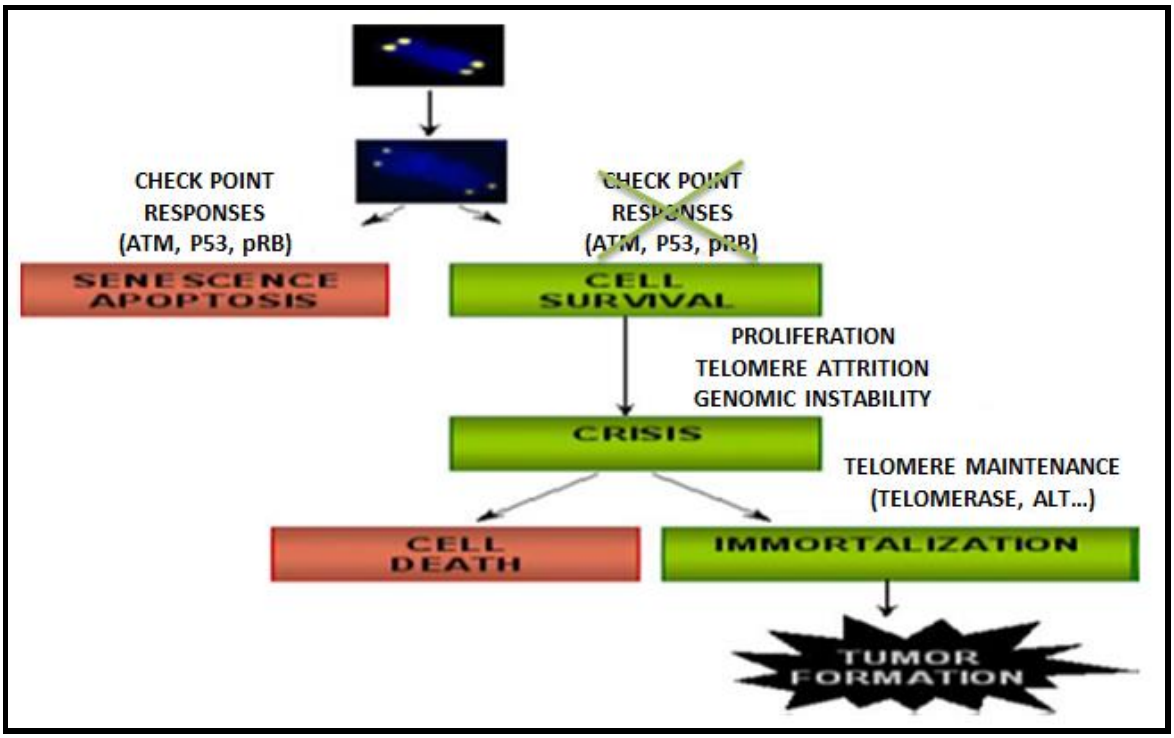

Figure 1.6 Cellular responses to telomere shortening.

Once telomeres become shorter below a critical length, and if cell-cycle checkpoints are integral, cells activate apoptosis. On the contrary, if cell-cycle checkpoints are avoided, then cells will survive and continue proliferating; telomeric attrition therefore leads up to level of crisis. Then, if the mechanism of telomere maintenance activates, cells might acquire the everlasting but genetically unstable status and continue dividing**,** gives rise to a tumour. The diagram was adapted from (Callen and Surralles, 2004).

Development of cancer is considered to be one of the most important organismal consequences of telomere dysfunction (Artandi and DePinho, 2000b). Dysfunctional telomeres primarily cause cancer by fuelling the genomic instability that allows the emergence of progressive malignant phenotypes. As malignant tumours develop, the resident cancer cells will eventually have to employ mechanisms to stabilise telomeres and prevent their erosion in order to survive (Levy et al., 1992). Consequently, cancer cells reactivate telomerase on a regular basis (Kim et al., 1994) or acquire an alternative mechanism for maintaining telomeres known as ALT (Alternative Lengthening of Telomeres) (Dunham et al., 2000) most likely based on recombination mechanisms (Reddel et al., 2001).

The main aim of this study is to examine the effects of BRCA2, a well-known tumor suppressor, on telomeres. Therefore, in the reminder of this section we will focus on the role of BRCA2 in various molecular pathways.

1.5 BRCA2 structure and function

The *BRCA2* gene has a complex genomic structure. It is a compound of 27 exons, which generate a large nuclear protein consisting of 3418 amino acids with a predicted molecular weight of 384 kDa (Collins et al., 1995). Although BRCA2 shows no strong sequence similarity to any other known human protein, certain regions are highly conserved and demonstrate a functional importance of BRCA2 in mammalian cells (Warren et al., 2002). In humans, eight BRC repeats are known that were located within exon 11, residing in the central portion of the protein. The BRC repeats extend over 1200 amino acids, while each BRC repeat is approximately 70 amino acids in length with the core sequence comprised of 26 amino acids (Bignell et al., 1997). Each of the eight BRC repeats in human BRCA2 have been shown to have the ability of binding RAD51 recombinase, the homolog of the bacterial RecA and yeast Rad51 (Sung et al., 2003) (see Fig 1.7).

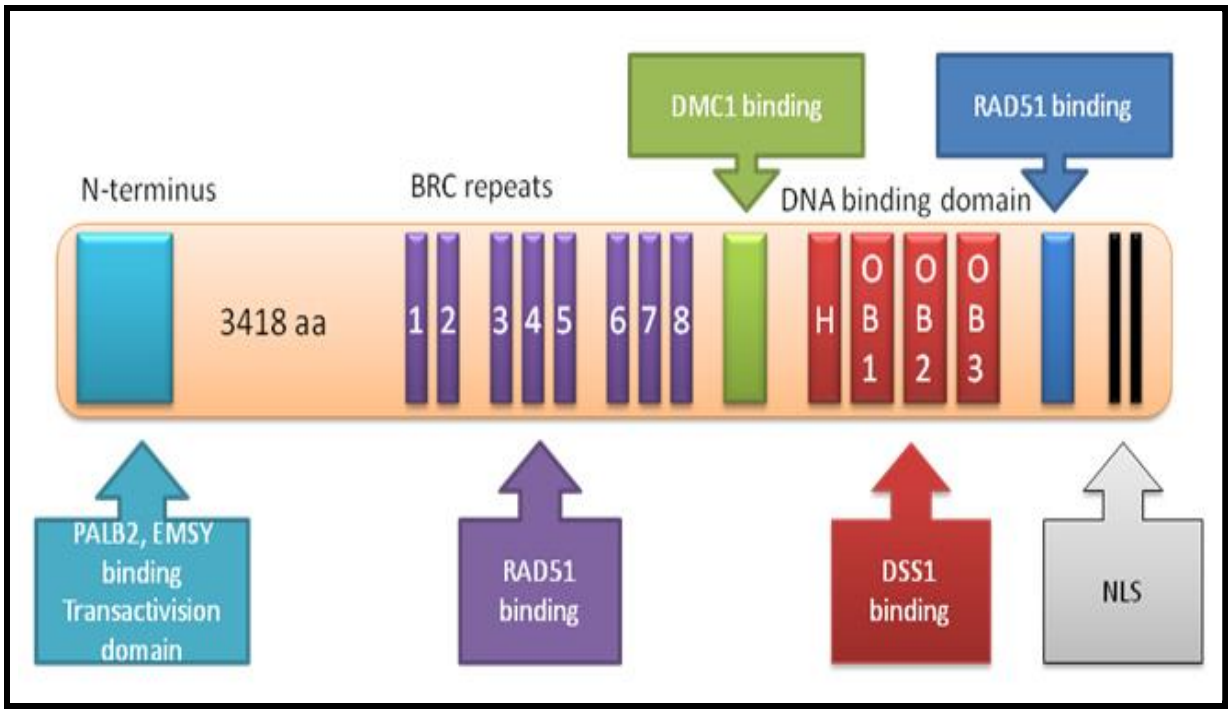

Figure 1.7 Schematic diagram of the BRCA2 protein.

N-terminus interacting region (pale blue), eight BRC repeat motifs (purple), H, helical domain (light red), OB oligonucleotide binding fold (red), RAD51 binding site at the c-terminus (blue) and NLS nuclear localization signal (black). At the extreme C-terminus, there are at least two nuclear localization signals (NLS) that are important for BRCA2's function as a nuclear protein (gray). These and other observations suggest that BRCA2, through cooperation between the BRC repeats and the OB domains, can target RAD51 to dsDNA/ssDNA junction at double strand breaks in order to promote repair through HR. The diagram was adapted from (Powell and Kachnic, 2003).

However each repeat exhibits a varying affinity for RAD51, such that the four BRC repeats located at the 5' region of exon 11 bind RAD51 more strongly than the four repeats at the 3' end of the exon (Chen et al., 1998b). This interaction points to the critical role of BRCA2 in HR. HR mechanism is involved in many core reactions in cells such as mitosis, meiosis (Helleday, 2003) DSB repair (Lundin et al., 2002; see also previous section) and restarting stalled DNA replication fork (Liang et al., 1998), suggesting the involvement of BRCA2 in these pathways (see Figure **1**.8). In addition, HR has been demonstrated to be the mechanism behind ALT (Roth et al., 1997).

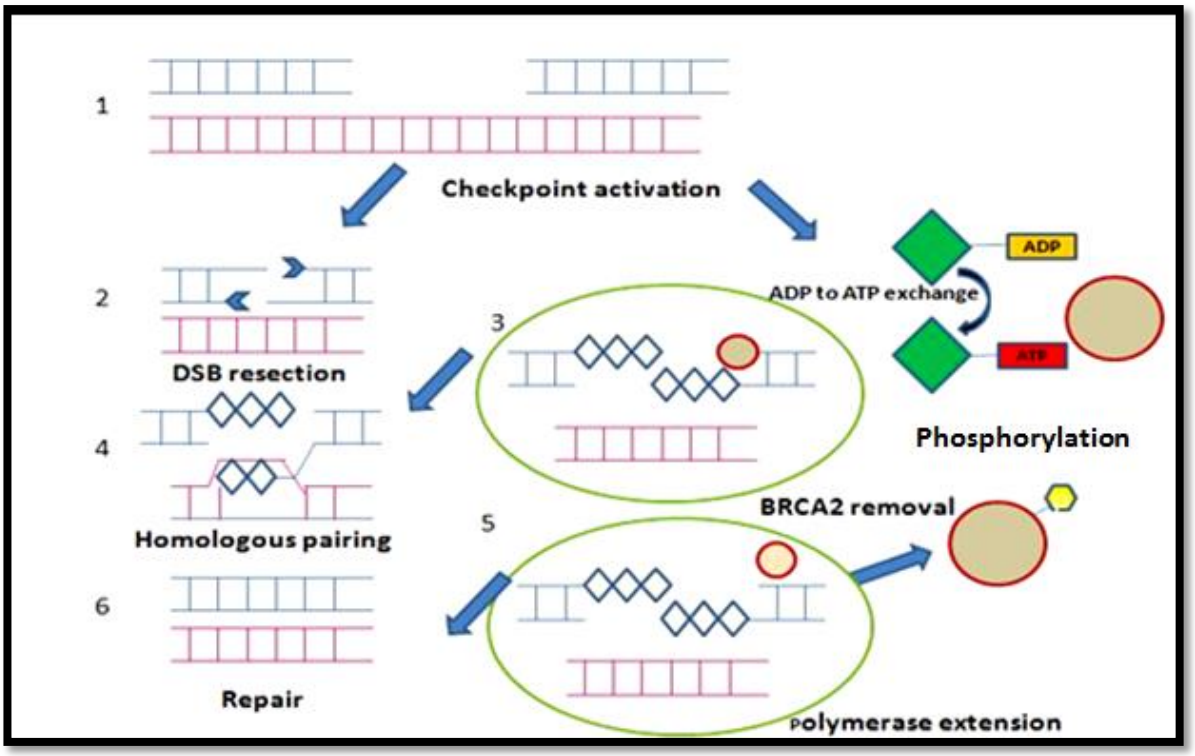

Figure 1.8 Model for BRCA2 function in HR.

DNA damage or replication arrest cause DSBs that activate signalling mechanisms 1) DSBs are resected 2) by exonuclease activity (as shown by ») to generate single strand (ss) DNA tracts. Following activation of RAD51 (marked by green diamond) a nucleoprotein filament will be formed on ssDNA that mediates homologous pairing 4) followed by strand extension 5) exchange and repair 6) Phosphorylation of BRCA2 (gray circle) may permit the removal of RAD51 from the DNA. Diagram adapted from (Venkitaraman, 2002).

1.5.1 Interacting partners of BRCA2

Fanconi anaemia (FA) is a rare autosomal recessive disorder characterised by cancer susceptibility and cellular hypersensitivity to DNA cross linking agents, such as mitomycin C (MMC) and cisplatin (Grompe and D'Andrea, 2001). At least 13 genes are known to be responsible for FA (FANCA, FANCB, FANCC, FANCD1, FANCD2, FANCE, FANCF, FANCG, FANCI, FANCJ, FANCL, FANCM and FANCN) and mutation in each one of them can cause this genetic disease (Howlett et al., 2002). An improvement in understanding BRCA2 function came from the realisation that BRCA2 is actually one of the FA proteins, known as

FANCD1 (Alter et al., 2007). Howlett et al have shown that cell lines derived from FANCD1 patients had biallelic mutations in BRCA2 and that reintroduction of BRCA2 cDNA into these cell lines rescued MMC hypersensitivity (Howlett et al., 2002). In line with these findings, BRCA2 (-/-) tumour cells display MMC hypersensitivity and chromosome instability, similar to the phenotype observed in cells from FA patients (Patel et al., 1998).

The murine *Brca2* gene disruption has resulted in mice exhibiting FA-like phenotype (Connor et al., 1997). It is suggested that BRCA2 and other FA proteins co-operate in a common DNA damage response pathway (Kennedy and D'Andrea, 2005), thus explaining the similarity in clinical features between FA patients bearring BRCA2 mutations and other subtypes of FA patients. The FANCD1/BRCA2 pathway for DNA repair is based on the co-localisation and interaction between the monoubiquitinated FANCD2 and FANCD1/BRCA2 in DNA damage foci (Wang et al., 2004).

The N-terminal region in BRCA2 harbours interaction sites for two proteins, partner and localiser of BRCA2 (PALB2 also known as FANCN) (Xia et al., 2006, Sy et al., 2009), and EMSY, the putative oncogene (Hughes-Davies et al., 2003). PALB2 has been proven to be a nuclear partner of BRCA2 while creating strong and stable associations with certain nuclear structures. PALB2 enables BRCA2 localisation, accumulation and function in the nucleus, as it allows BRCA2 to escape from proteasome-mediated degradation. Moreover, PALB2 has been shown to have a role in HR repair through its ability to recruit BRCA2 and RAD51 to DNA breaks (Xia et al., 2006). Sy et al., (2009) have further expanded PALB2's role by showing that PALB2 precipitates with BRCA1 and BRCA2 and forms a functional complex *in vivo*, which is targeted to DNA damage sites. This study has also revealed that PALB2 functions as a molecular scaffold in the formation of BRCA1-PALB2-BRCA2 complex that is involved in HR repair and cell survival.

The data from this study suggested that PALB2, via direct interaction with BRCA1, can influence BRCA2-RAD51 function in HR, thereby contributing to genomic stability. In line with this suggestion, various germ-line BRCA2 missense mutations were identified in breast cancer that demonstrated disability of binding PALB2, as well as a failure to exert functional HR. Furthermore, cells containing mutation that interfered with BRCA1-PALB2 interaction showed defective HR repair (Sy et al., 2009).

The EMSY protein is capable of binding BRCA2 within exon 3 that contains the transactivation domain (Hughes-Davies et al., 2003). This interaction has been shown to silence the activation role of BRCA2 through association with chromatin remodelling proteins. An especially interesting finding shows that EMSY is amplified in many cases of sporadic breast cancer and high-grade ovarian cancer (Hughes-Davies et al., 2003). This finding suggests a possible mechanism for BRCA2 inactivation without the requirement for BRCA2 mutation and may explain the infrequent BRCA2 somatic mutations in sporadic cancers (Hughes-Davies et al., 2003). Linking BRCA2 and EMSY to DNA repair, both proteins were shown to localise to DNA damaged sites; however the EMSY role in the repair mechanism is still unclear.

An interesting relationship was reported between P63/P73 and BRCA2. P63 and P73 could bind to the promoter region of BRCA2 gene (as well as RAD51) and transactivate its transcription (Lin et al., 2009). In addition, mouse cells lacking P63 or P73 were unable to repair DNA damage resulting in reduced survival. Moreover, P63+/- and P73+/- mice developed mammary tumours while losing their wild type allelic expression (Lin et al., 2009). These results suggest that P63 and P73 function as tumour suppressors and this function may be related to their ability to transcriptionally regulate genes that are involved in the DNA repair pathway.

1.5.2 BRCA2 function during cell cycle

Cancer is a genetic disease characterised by accumulating mutations and chromosomal instability. Chromosomal aberrations may include numerical changes, such as aneuploidy, and structural changes, such as translocations, amplifications and deletions. Therefore, it is essential to understand the relationship between chromosome aberration and cancer, which may offer diagnostic and therapeutic tools in the future. Cells with mutant BRCA2 protein, similarly to most cancer cells, are genetically unstable, presenting high frequencies of chromosomal rearrangements (Yu et al., 2000). BRCA2 homozygous mutant mouse embryo fibroblasts undergo spontaneous chromosome breaks while in some cells centrosome amplification and aneuploidy have been observed (Yu et al., 2000, Tutt et al., 1999).

Additionally, dividing cells with defective BRCA2 give rise to random chromosomal translocations that promote genetic instability due to the accumulation of DSBs (Scully and Livingston, 2000). The main explanation of these phenomena may be the essential role of BRCA2 in HR, an error-free DSB repair mechanism, which becomes 100-fold reduced when BRCA2 is dysfunctional (Connor et al., 1997, Chen et al., 1998b, Moynahan et al., 2001). The importance of BRCA2 in HR and genomic integrity is further supported by a study conducted by (Tutt et al., 2001), which have illustrated that the loss of BRCA2 increased error-prone DSB repair pathways, such as gene conversion with unequal cross-over or single strand annealing, as well as increasing intra-strand cross-linking. This leads to a considerable genomic instability and contributes to tumourigenesis.

Several lines of evidence indicate that stalling of replication forks is a regular event at sites of DNA lesions (Cox et al., 2000). Normally, this stalling does not generate DNA breaks, due to a mechanism that stabilises stalled replication forks. HR is required to restart blocked replication. The high incidence of DSBs in cells containing impaired BRCA2 is suggested to be due to BRCA2 involvement in the stabilization of stalled DNA replication forks and HR (Lomonosov

et al., 2003). BRCA2 has been shown to co-localise with BRCA1 in dividing cells (Chen et al., 1998a). These two proteins physically interact with each other through a region in BRCA1, ranging from residues 1314 to 1863. This interaction appears to be involved only a minor fraction of the total BRCA2 pool (Wang et al., 2000).

Chromosomal stability and segregation are monitored and maintained by mitotic checkpoint proteins that can arrest mitosis and repair damaged spindles when necessary (Paulovich et al., 1997). Defects in these proteins lead to genomic instability and the promotion of cancer development (Paulovich et al., 1997, Roberts et al., 1994). The yeast two-hybrid system has revealed an interaction between BRCA2 and the mitotic checkpoint protein, hBUBR1, which regulates the transition from metaphase to anaphase (Powell and Kachnic, 2003). Furthermore, BRCA2 is phosphorylated by hBUBR1 *in vitro*. Following co-transfection of both proteins into the cos7 cell line and nuclear staining, both proteins were found in the nuclei of cells whose spindle fibres were disrupted, but not in undamaged cells (Futamura et al., 2000). These results suggest that BRCA2 might be involved in a mitotic checkpoint.

Moreover, BRCA2 has been shown to take part in the formation of high molecular weight protein complex together with the evolutionary conserved protein BRCA2-Associated Factor 35 (BRAF35) (Marmorstein et al., 2001). BRAF35 is a DNA binding protein with a similar pattern of expression as BRCA2 during embryogenesis. The highest level of its expression is found in rapidly dividing cells during the early stage of chromosome condensation. An analysis of condensed chromosomes and their comparison with mitotic chromosomes, for the presence of BRCA2 and BRAF35, has revealed the co-localisation of both proteins in mitotic chromosomes. In support of this, an antibody against BRCA2 delayed metaphase progression (Marmorstein et al., 2001, Kerr and Ashworth, 2001). These results suggest the BRCA2 role during mitosis.

A proposed role of BRCA2 in meiosis is based on its interaction with DMC1 protein, a meiosis-specific recombinase (Thorslund et al., 2007). This interaction occurs through a highly conserved region in BRCA2 that is comprised of 26 amino acids and is distinct from the RAD51 interaction domain. The existence of two distinct interaction regions for RAD51 and for DMC1 enables the interaction of both recombinases with BRCA2 during meiosis.

1.5.3 BRCA2 mutations

Germline mutations in either BRCA1 or BRCA2 account for 20-60% of familial breast cancer cases (Nathanson et al., 2001). Mutations in these genes are highly penetrant, thus increasing the life-time risk for cancer onset to 30-70% (Ford et al., 1998). Over 100 different germline mutations in BRCA2, which are associated with cancer susceptibility, have been identified. These mutations are spread throughout the BRCA2 coding sequence, with a tendency to concentrate in the 3' half of the BRCA2 gene that might be associated with increased disease onset (Rahman and Stratton, 1998).

Most BRCA2 mutations result in truncated BRCA2 protein due to small deletions or insertions that generate a translation frameshift, or faulty splice sites. More than 70% of these mutations involve one or two nucleotides that are located within a repetitive sequence, suggesting that their generation is caused by DNA polymerase slippage during DNA replication. In addition, many missense and nonsense alterations have been described. However, only a few mutations that result in amino acid substitution have been reported (Rahman and Stratton, 1998, Gudmundsson et al., 1995).

Some BRCA2 mutations are very common in specific populations. For example in Ashkenazi Jews, the germline 6174delt mutation that results in truncated BRCA2 protein due to insertion of premature stop codon is estimated to be present in 1% of the population and is reported to correlate with breast, ovarian and prostate cancer (Oddoux et al., 1996).

In the Icelandic population the BRCA2 mutation 999del5, accounts for 40% of male breast cancer and approximately 8% of female breast cancer (Thorlacius et al., 1997, Mikaelsdottir et al., 2004). This mutation is found in more than 75% of families with more than four breast cancer cases (Thorlacius et al., 1997). It has been suggested that 999del5 mutation that generates unstable protein increases the risk of breast cancer, since it causes haploinsufficiency at the BRCA2 locus (Thorlacius et al., 1997, Mikaelsdottir et al., 2004). Additional common BRCA2 mutations in selected populations or groups include Dutch -5579insa (Verhoog et al., 2001), French Canadian and Italian-8765delAG (Tonin et al., 1999, Pisano et al., 2000), Scottish and Northern Irish-6503delTT (Scottish/Northern Irish BRCA1 and BRCA2 Consortium 2003) and Pakistani 3337C>T mutation (Liede et al., 2002).

Tumour suppressor mutations are mainly recessive in nature, since one intact allele is usually sufficient to exert its function, thus a requirement for mutation in both alleles within a single cell is needed for neoplastic transformation to occur. There are several mechanisms which can cause a cell to lose its normal gene and be predisposed to develop into a tumour. These may result in a loss of heterozygosity (LOH). BRCA2 is believed to be a tumour suppressor gene (TSG) and indeed, BRCA2 mutation carriers almost invariably exhibit LOH while retaining the mutant allele.

For example, 30-40% of sporadic breast and ovarian cancers showed LOH on chromosome 13q12-q13 (Cleton-Jansen et al., 1995). Therefore, it is surprising that somatic mutations in BRCA2 are an infrequent event in sporadic breast cancer (Lancaster et al., 1996). However, this does not refute the notion that BRCA2 protein is involved in cellular functions that are impaired in most breast cancers, or that BRCA2 functions as TSG. A possible explanation for this contradiction is that BRCA2 inactivation occurs through mechanisms other than somatic mutation, or more likely that other regulators or proteins functionally linked to BRCA2 are genetically altered, thereby exerting the same effect as the BRCA2 loss. An example would be

the loss of RAD51 or p73 (Kato et al., 2000, Leong et al., 2007, Nowacka-Zawisza et al., 2008).

In addition to breast cancer, BRCA2 is involved in the tumorigenesis of several other cancer types. LOH on chromosome 13q12-q13 in 50 tumours from BRCA2 carriers has been examined and results demonstrated a high frequency of LOH in tumours of the prostate, ovary, cervix, colon, male breast cancer and urethra, thus implicating BRCA2 as TSG in these cancers (Gudmundsson et al., 1995). In addition, BRCA2 mutations may increase the risk of laryngeal, pancreatic, ocular melanoma and perhaps stomach cancer, thyroid cancer, leukaemia, gall-bladder cancer and cancer of the fallopian tube (Rahman and Stratton, 1998, Wooster et al., 1995).

1.5.4 BRCA2 absence for therapy

Most commonly used chemotherapeutic agents, as well as radiotherapy, aim to cause DNA damage and subsequent cell death. Affected cells respond to DNA damage by activating multiple pathways, including DNA repair, cell cycle arrest and apoptosis, depending on the damage extent and the types of DNA damage. It is well understood that cancer is a genetic multistep disease, typically arising due to mutational activation or inactivation of oncogenes and/or TSGs respectively. Some of these mutations result in alteration and dysfunction of proteins involved in DNA repair pathways, a central mechanism of maintaining genomic integrity. Therefore, treatment designed to target cells with a defective repair system may be lethal to cancer cells while sparing normal cells. The absence of error-free DSB repair mechanism due to an impaired BRCA2 gene was proven to be the Achilles' heel of BRCA2 deficient tumours (Sharan et al., 1997). Therapeutic strategies designed to target the DSB repair pathway constitute a useful therapeutic approach (Kelland, 2007, Farmer et al., 2005).

PARP is an enzyme involved in base excision repair (BER), a central pathway in the repair of DNA Single Strand Breaks (SSBs). Inhibition of PARP was shown to sensitise cells containing dysfunctional BRCA2, leading to chromosomal instability and subsequent cell death (Fong et al., 2009, Farmer et al., 2005). The proposed mechanism suggests that PARP inhibition initially leads to the accumulation of DNA SSBs.

When these SSBs encounter the replication fork, the consequence might be the creation of DNA DSBs. Normally these DSBs are repaired by error-free RAD51-dependent HR repair pathway, in which BRCA2 is involved. However, when BRCA2 is absent, the replication fork cannot be restarted and collapses resulting in failed DSB repair. Repair of these breaks then occurs by alternative error-prone mechanisms such as single-strand annealing and/or NHEJ that cause numerous chromosomal aberrations and eventually cell death (Fong et al., 2009) (see Figure **1**.9).

This concept of synthetic lethality, using PARP 1 inhibitor such as AstraZeneca compound AZD2281 (Evers et al., 2008) and the Pfizer compound AGO14699 (Plummer et al., 2008), showed strong effects in BRCA2 deficient cells with no additional toxicity. Moreover, an increased cytotoxicity was observed when combined with different drugs such as cisplatin and temozolomide.

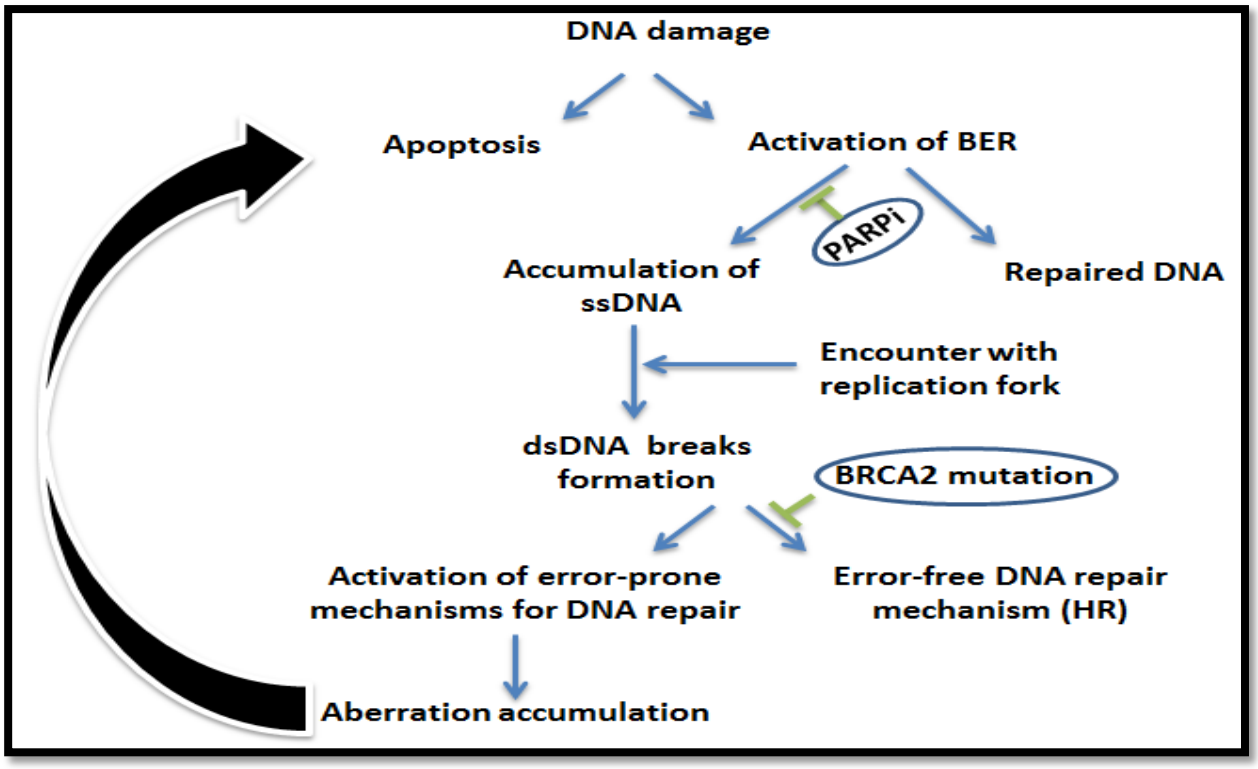

Figure 1.9 Model of therapeutic strategy designed to target the DSB repair pathway.

This diagram demonstrates the sequence of events following DNA damage which can be targeted for the design of therapeutic intervention. After DNA damage, the cell can either die (apoptosis) or subjected to repair by the BER mechanism. As a result of inhibiting PARP enzyme the BER pathway cannot take place and the amount of SSBs increases. When SSBs encounter the replication fork, DSBs are formed and cannot be repaired by HR due to BRCA2 mutation. DSBs will accumulate, leading to chromosomal instability and an elevated number of aberrations causing cell death. The diagrams were adapted from (Fong et al., 2009).

1.6 Role of ALT mechanism for telomeres maintenance

As discussed earlier telomeres cap the end of chromosomes in order to prevent DSB repair mechanisms from activation, hence protecting chromosome integrity (Zakian, 1995, Wai, 2004). It has been demonstrated that telomeres are important in preventing the loss of genomic information in the eukaryotic linear nuclear genome, which cannot be completely replicated by the conventional DNA polymerase (Watson, 1972, Harley et al., 1990). Therefore, in normal human cells, telomeres shorten with each round of DNA replication; a phenomenon described in the 1970s by Olovnikov A.M (Olovnikov, 1971) as well as by James D. Watson and termed

the “end replication problem”. The shortening of telomeres leads to a permanent growth arrest called senescence (Harley et al., 1990). Therefore, cells with extensive replication potential such as germ line, stem cells and tumour cells must overcome the loss of telomeric sequences.

De novo synthesis of telomere at the chromosome’s terminus is mainly carried out by telomerase; an enzymatic ribnucleoprotein complex, which functions as an RNA-dependent DNA polymerase (Greider and Blackburn, 1985). An additional mechanism, known as ALT, was found in cells that do not possess telomerase activity and yet are able to maintain telomere length for many populations doubling (Bryan et al., 1997, Dunham et al., 2000).

Almost all tumour cell lines bypass cellular senescence and DNA damage-signalling pathway leading to extended growth followed by genomic instability and possible activation or upregulation of telomerase (Shay and Keith, 2008). About 85-90% of all human cancers were shown to have increased telomerase activity (Greider and Blackburn, 1996), which implicated telomerase in the pathogenesis of cancer and is therefore the main target for developing anti-cancer therapies. Even though ALT mechanism is not as common as upregulation of telomerase, it has been reported to maintain telomeres in approximately 30-40% of immortalized human cell lines and 10-15% of human tumours (Bryan et al., 1997, Bryan et al., 1995, Bryan and Reddel, 1997). In addition, ALT was shown to be more prevalent in tumours of mesenchymal origin such as glioblastoma multiforme, osteosarcomas and some soft tissue sarcomas (Hakin-Smith et al., 2003, Henson et al., 2005).

An understanding of ALT’s features, mechanism and regulation is very important for the development of anti-cancer drugs for several reasons. First, targeting telomerase as a therapeutic strategy may result in a selective pressure shifting telomere elongation towards the ALT mechanism, which means that an inhibition of both mechanisms would be required for therapeutic effect. Second, repression of ALT in ALT-dependent immortal cell lines has been

shown to result in senescence and subsequent cell death (Perrem et al., 1999). Finally, since ALT is more common than telomerase in specific tumour types (see above) and it is suggested to have good prognosis value (Hakin-Smith et al., 2003), it may offer a strategy for individualised therapy, tailored to the patient's specific tumour features.

1.6.1 Phenotypes of ALT cells

ALT-dependent cells, as opposed to telomerase positive human cancers or non-cancerous immortal cells are characterised by the presence of heterogeneous telomere length (Henson et al., 2002). An analysis of telomeric DNA from ALT cell lines has indicated that, within ALT cell population, the telomeric DNA ranges from <2 to 50 kb in length (mean size 20 kb). In addition, ALT telomeres are highly unstable, demonstrating dynamic changes in telomere length, with both rapid elongation and rapid deletion events, and multiple truncated telomeres (Murnane et al., 1994). A substantial portion of the telomeric repeats in ALT cells are extrachromosomal and may be linear or circular in form, including double-stranded telomeric circles (t-circles) or single-stranded circles (C or G circle) (Lustig, 2009).

A novel form of promyelocytic leukaemia nuclear bodies (PML-NBs) (Yeager et al., 1999) are distinguished from other PML-NBs by the additional ALT-specific content; they are termed ALT-associated PML bodies (APBs). The APBs include telomeric DNA and telomeric binding proteins, TRF1 and TRF2 (Bernardi and Pandolfi, 2007, Yeager et al., 1999).

Moreover, APBs were found to contain and co-localise with proteins involved in DNA recombination, repair and replication, such as the Bloom Syndrome protein (BLM), RAD50, RAD51, RAD52 and RPA (Bernardi and Pandolfi, 2007), some of which are required for telomere maintenance, suggesting that ALT activity may occur in these nuclear structures. High levels of APBs are found, in addition to the S phase, in mitotic cells that are in the G2-M phase (Grobelny et al., 2000), indicating that regulation of APB formation may be co-ordinated

with cell cycle, and further supporting the notion of APB involvement in telomere maintenance via the ALT pathway. In agreement with this, when ALT activity was inhibited, a decrease in APB-containing cells was observed (Zhong et al., 2007).

In contrast, several lines of evidence suggest that APBs are not involved in the ALT mechanism of telomeric maintenance. For example, cell lines that did not express telomerase but still maintained telomere length (presumably by ALT mechanism) had no detectable APBs (Cerone et al., 2005). In addition, it has been shown that large numbers of APBs are formed in ALT negative cells undergoing cell cycle arrest or senescence (Jiang et al., 2009). A possible explanation for the latter may be that in the reported study, drugs were used to induce stress conditions, in order to achieve cell cycle arrest, thus APB formation may be associated with stress conditions, which are not normally present.

A high rate of post-replicative telomeric sister chromatid exchanges (T-SCEs) is another feature of ALT-cells. T-SCEs were reported to occur more frequently in ALT cells compared to telomerase-positive cell lines without an increase in sister chromatid exchange (SCE) rate in other genomic locations (Lundberg et al., 2011). Indeed, when telomerase was inhibited in a human cell line with a mismatch repair defect in order to induce ALT-like telomeric elongation, it was associated with T-SCEs in all examined cells (Henson and Reddel, 2010).

1.6.2 ALT Mechanism

The presence of proteins in APB structures that are involved in HR such as RAD51 and RAD52 (Henson and Reddel, 2010), as well as the presence of RAD50/Mre11/Nbs1-complex (Zhong et al., 2007), which is involved in cell cycle check point control and DNA damage repair, has pointed to the possibility that HR is the central mechanism for telomere elongation in ALT cells.

Even though the precise mechanism of telomere maintenance in ALT cells is not yet fully understood, two mechanisms, both of which are based on HR, have been suggested. Based on the observation of high rate T-SCEs in ALT cells (Londono-Vallejo et al., 2004, Bechter et al., 2004), it was suggested that T-SCEs occur in an unequal manner, resulting in the elongation of one telomere and shortening of the other, hence leading to unlimited cellular proliferation (Bailey et al., 2004). However, no experimental evidence yet exists for this model. Generally, SCE is thought to occur due to the recombinational repair of a broken replication fork (Wilson and Thompson, 2007). A large number of internal gaps and/or nicks that can cause stalling of replication fork and activation of the HR repair pathway were found in the telomeric DNA of ALT cells (Nabetani and Ishikawa, 2009) and thus may result in T-SCEs.

An alternative hypothesis is that the ALT mechanism is based on classical HR that occurs during DNA replication (Henson et al., 2002, Dunham et al., 2000). According to this model, ALT cells are able to elongate their telomeres using telomeric sequences from adjacent chromosomes as a template for newly synthesised telomeric DNA by HR. This suggestion is consistent with the evidence showing that when a DNA tag was placed into the telomere of ALT cells, after several populations doubling, the tagged telomere was copied onto other telomeres, in contrast to telomerase positive cells (Dunham et al., 2000). Two models are shown in (Figure 1.10).

In addition, two proteins (ATRX and DAXX) play multiple cellular roles, including chromatin remodelling at telomeres and localize to telomeres where they are involved with the histone variant H3.3 (Goldberg et al., 2010, Lewis et al., 2010), and mutations in both gene were found to correlated with features in ALT positive cells including paediatric glioblastomas, pancreatic neuroendocrine tumours (PanNETs) and other tumours of the central nervous system, suggesting that these mutations probably contribute to the activation of the ALT mechanism (Lovejoy et al., 2012, Heaphy et al., 2011). The function of histone H3.3 and ATRX/DAXX at

telomeres is still unknown, but diminished ATRX function has been documented to boost telomeric DNA (TTAGGG) repeat containing telomeric transcripts (Azzalin et al., 2007). Furthermore, Law's groups (2010) have shown that chromatin localization of DAXX and ATRX imply that the both proteins specifically bind to G-rich repetitive sequences such as telomeres (Lower et al., 2010).

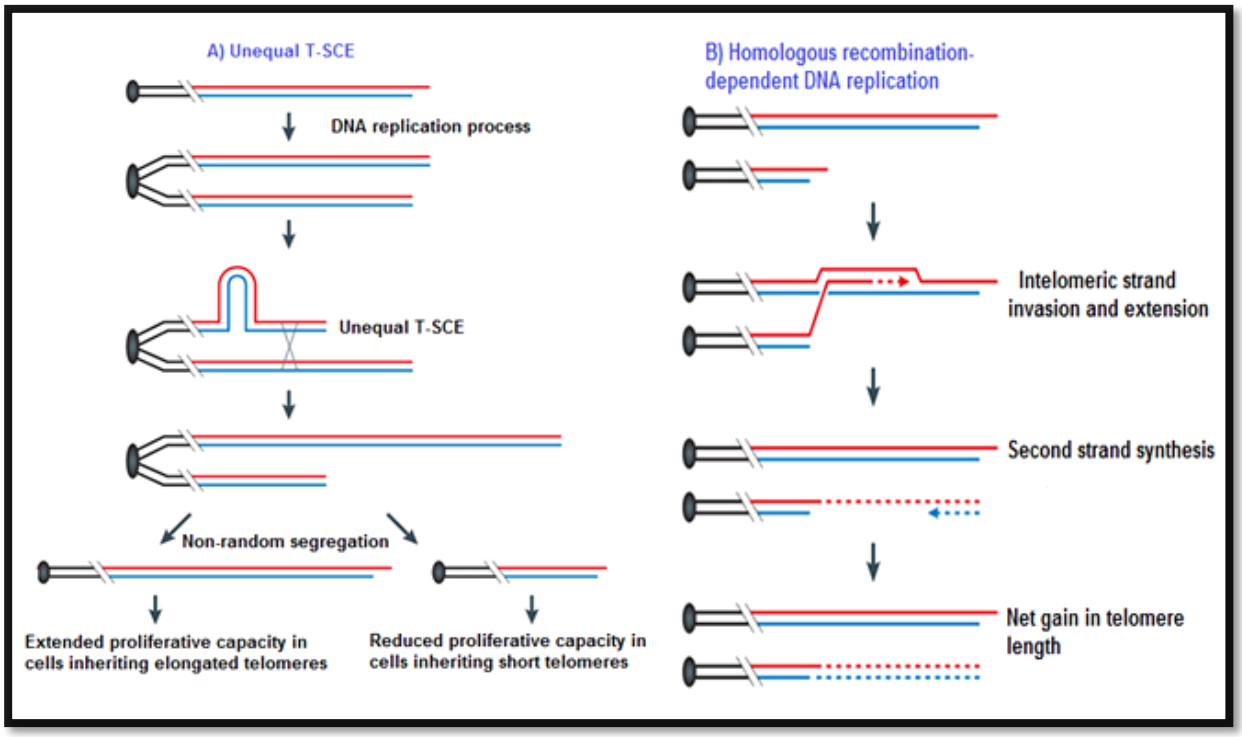

Figure 1.10 Two models of ALT.

A) ALT mechanism is thought to be based on unequal sister chromatic exchanges (SCEs) events. This can result in lengthened telomere of one daughter cell, which prolongs its proliferative ability, and shortened telomere of another daughter cell, decreasing its proliferative ability. B) An alternative mechanism devised for ALT is based on HR during DNA replication. In this mechanism telomeres from adjacent chromosomes can serve as a template for new telomere synthesis. The diagram was adapted from (Cesare and Reddel, 2010).

Alternatively, telomeres can copy themselves via t-loop formation (Figure 1.11 A); the single strand overhang is able to fold back, invade the double-stranded telomeric DNA tract and anneal to the complementary strand (Griffith et al., 1999). Additional options for copy

templates include sister chromatid (Figure 1.11 B) and extrachromosomal telomeric DNA (either linear or circle) (Muntoni et al., 2009) (Figure 1.11 C and D).

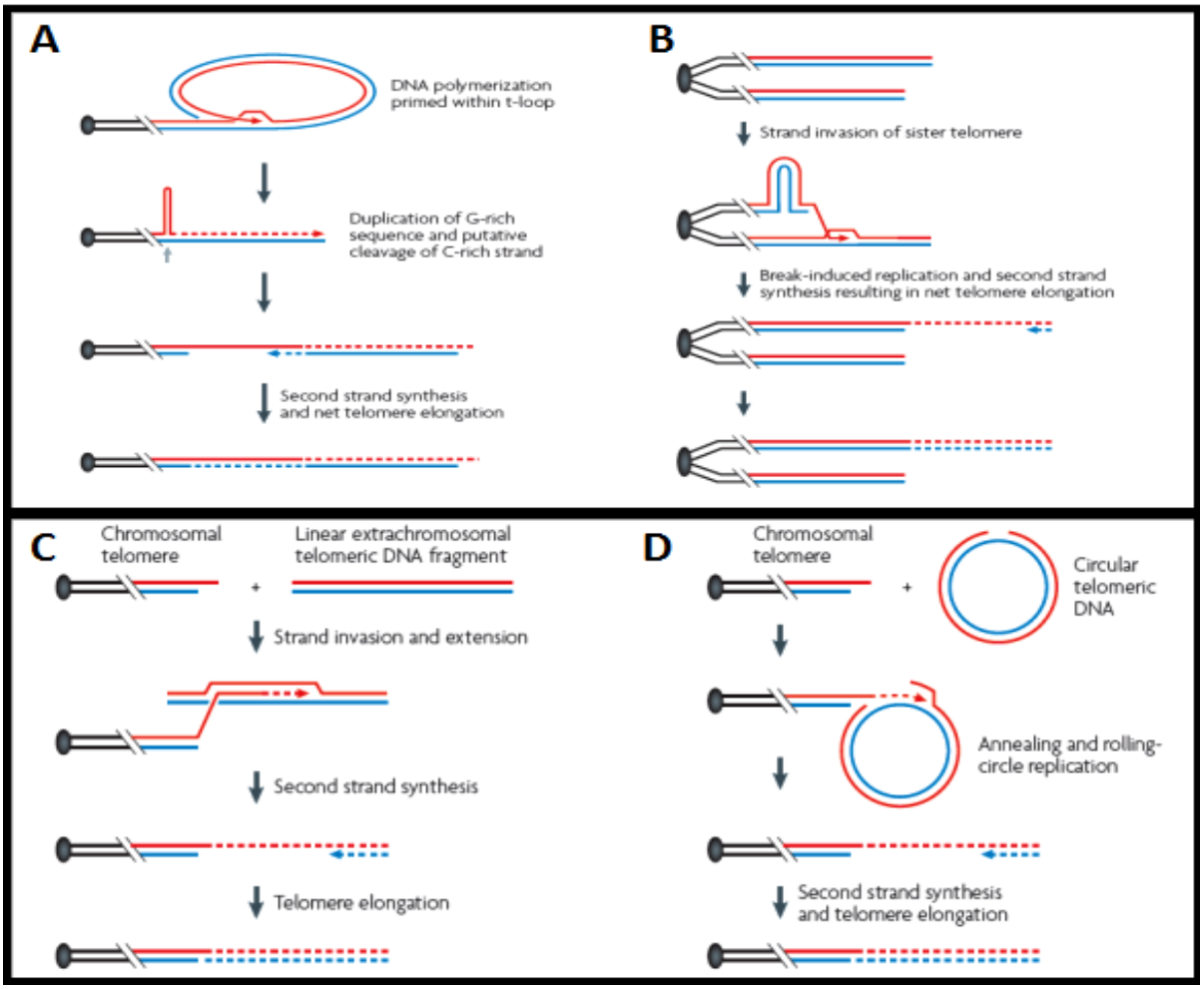

Figure 1.11 Alternative copy templates for recombination-mediated synthesis of telomeric DNA. ALT mechanism based on homologous recombination may utilise, in addition to the adjacent chromosome, alternative templates such as A) t-loop formation B) the telomere of the sister chromatid C) linear extrachromosomal telomeric DNA D) circular extrachromosomal telomeric DNA. The light grey arrow indicates the site of putative cleavage of the C-rich strand. The diagrams were adapted from (Cesare and Reddel, 2010).

1.7 BRCA2 and ALT pathway

Direct evidence that linked BRCA2 and ALT mechanism has been provided by Spardy et al (Spardy et al., 2008), who reported on the presence of BRCA2 in APBs induced by HPV-16 E7 oncoprotein. HPV-16 E7 induced APBs contained ssDNA and proteins that are involved in the response to replication stress including FANCD2 and BRCA2 itself.

Moreover, the presence of RAD51, BRCA2 main interaction protein, in APBs (Yeager et al., 1999) reinforces the idea of BRCA2 involvement in the ALT mechanism. In support, APBs are suggested to be the site in which telomere elongation takes place in ALT positive cells. An additional associative link between BRCA2 and ALT comes from the notion that the ALT mechanism may be based on HR and the fact that BRCA2 plays an important role in HR. Additional evidence obtained in Dr Slijepcevic's laboratory has shown elevated levels of T-SCEs, one of the ALT markers, in a FA patient with biallelic mutation in BRCA2/FANCD1 (Sapir et al., 2012).

Indirect evidence that links BRCA2 to the ALT mechanism has come from a study that examined the localisation and effect of the FA proteins, FANCD2 and FANCA, on the ALT mechanism (Fan et al., 2009). This study has shown that in ALT positive cells, FANCD2 co-localised at nuclear foci with telomeres and PML bodies, but not in cells that expressed telomerase. Moreover, transient knockdown of FANCA or FANCD2 resulted in a sharp decrease of telomere length, as well as in reduced T-SCE frequencies. These results have been obtained only in ALT positive cells and not in telomerase expressing cells.

These works lead us to examine whether indeed there is a relationship between BRCA2 and the ALT mechanism and how this could be exploited for therapeutic intervention.

1.8 Objectives of the study

It has been well documented that dysfunctional BRCA2 leads to chromosomal instability. Given that telomeres serve to maintain chromosomal stability, it is of interest to study whether chromosomal instability triggered by BRCA2 dysfunction will affect telomere maintenance. Therefore, this PhD project has three main aims:

i. To create a BRCA2 defective environment using different human cell lines as a platform and examine subsequent telomere phenotype.

ii. To examine telomere phenotypes in Chinese hamster and human cell lines defective in BRCA2.

iii. To examine effects of BRCA2 dysfunction on the repair of interstitial telomeric sequences.

Chapter -2

Materials and Methods

2.1 Cell lines and tissue culture conditions

A total of fifteen established cell lines have been used in this project (Table 2.1). Most cell lines have been selected for their deficiencies in DNA damage response such as *BRCA2* deficient cell lines. Mouse lymphoma LY-S (radio- sensitive) and LY-R (radio-resistant) cell lines were used as a reference for cytological testing of telomere length measurements using Q-FISH techniques. The proteins from the PC3 cell line were used to set up a calibration curve for the real-time PCR TRAP assay.

Table 2-1 List of cell lines used in this project.

Cell line	Species	Origin	Source
HeLa	Human	Cervical carcinoma; 31 years old female	ATCC (American Tissuce Culture Collection)
U2OS	Human	Osteosarcoma; 15 years old female	ECCC (European Collection of Cell Cultures)
MCF-7	Human	Breast carcinoma	Professor Newbold group (Brunel University)
Capan-1	Human	Pancreatic adenocarcinoma; BRCA2 defective	HTCC
GM00893	Human	Lymphoblastid; 32 year old normal female	Coriell Cell Repositories
GM14170	Human	Lymphoblastoid; 46 years old BRCA2 carrier female	Coriell Cell Repositories
GM14622	Human	Lymphoblastoid; 39 years old BRCA2 carrier female	Coriell Cell Repositories
V79B	Chinese hamster	Lung fibroblasts	Leiden University (Dr. M. Zdzienicka's group)
V-C8	Chinese hamster	Derived from V79B; BRCA2 defective mutant	Leiden University (Dr. M. Zdzienicka's group)
V-C8+ BACA2	Chinese hamster	Transfected with bacterial artificial chromosome (Bac) containing functional mouse *BRCA2* gene	Leiden University (Dr. M. Zdzienicka's group)
V-C8+13#	Chinese hamster	Contains a copy of human chromosome 13 with the functional BRCA2 gene	Leiden University (Dr. M. Zdzienicka's group)
LY-R	Mouse Lymphoma, Normal radiosensitive	Lymphoblastoid	Dr Andrzej Wojcik, University of Warszaw, Poland
LY-S	Mouse Lymphoma, radiosensitive	Derived from LY-R; radiosensitive due to unknown molecular defect	Dr Andrzej Wojcik, University of Warszaw Poland
PC3	Human	Prostate adenocarcinoma	Professor Newbold group (Brunel University)
PC3/hTERT	Human	Derived from PC3; telomerised	Professor Newbold group (Brunel University)

2.2 Cell culture and tissue culture methodology

2.2.1 Human adherent cell lines

The U2OS cell line was grown in McCoy's 5a medium (Fisher), supplemented with 10% foetal bovine serum (Gibco/Sigma) and 2mM glutamine (Sigma) in the atmosphere of 10% CO_2 at 37^{o}C. The HeLa cell line was grown in Dulbecco's modified Eagle medium (DMEM) (Sigma), supplemented with 10% foetal bovine serum (Sigma) at atmosphere of 10% CO_2 at 37^{o}C. The MCF7 cell line was grown in Dulbecco's modified Eagle medium (DMEM) (Sigma), supplemented with 2mM Glutamine, 5µg/ml insulin and 10% foetal bovine serum. The PC-3 cell line was cultured in Ham's F12k medium supplemented with 2 mM L-glutamine adjusted to contain 10% FBS in an atmosphere with 5% $CO_{2.}$ The Capan-1 cell line was established from a hepatic metastasis in a patient with pancreatic adenocarcinoma (Fogh et al., 1977) and completely lacking one BRCA2 allele and containing a truncation (6174 delT) mutation in the other allele leading to a truncated protein product (Goggins et al., 1996). Capan-1 cells were cultured in RPMI 1640 (Gibco/Invitrogen) medium, supplemented with 10% of foetal calf serum and 2% L-glutamine with 5% carbon dioxide in air and cells were sub-cultured every two days. In order to avoid contamination, Streptomycin and Penicillin (1µl per 100 ml medium) were added all media.

2.2.2 Human lymphoblastoid cell lines

All human lymphoblastoid cell lines were grown in RPMI 1640 medium (Gibco/Invitrogen) containing 10% foetal calf serum and 0.1 mg/ml of streptomycin at 37^{o}C in the atmosphere of 5% $CO_{2.}$

2.2.3 Mouse lymphoma cell lines

Mouse lymphoma cell lines were grown in standard tissue culture conditions by using RPMI 1640 medium (Gibco/Sigma) and 10% foetal calf serum with 0.1mg/ml of streptomycin at 37^{o}C in the atmosphere of 5% $CO_{2.}$ Cells were sub-cultured at the ratio 1:5 every 3-4 days.

2.2.4 Chinese Hamster cell lines

All Chinese hamster cell lines were cultured in Ham-F10 medium (Gibco/Sigma), 10% foetal calf serum, 1% of penicillin and streptomycin at 37^{o}C in the atmosphere of 5% $CO_{2.}$ However, cell lines containing human chromosome 13 (V-C8 Chrom) and the BAC with murine Brca2 (V-C8 Bac) were grown in the presence of Geneticin (G418, Sigma) for selection. Cells were subcultured at ratio of 1:3 every 3-4 days. Additionally, all cells were cryopreserved in 90% FBS and 10% DMEM.

2.2.5 Tissue culture procedure

All cell lines were kept frozen in liquid nitrogen. When required vials of frozen cells were thawed and set up in either 25cm^2 or 75cm^2 tissue culture flasks with filter head (Nunc) to avoid any contamination. Cells were incubated in a humidified incubator (Heracell 150) at 37ºC. The confluent state of tissue culture for most cell lines was at the cell concentration of approximately 1x10^6 viable cells/ml. Once cells reached confluency they were subcultured at a ratio of 1:3 – 1:5, depending on the cell line, by gentle trypsinization with trypsin-EDTA (Invitrogen) for three to five minutes. After trypsinisation cells were spun down using a Megafuge 1.0, Heraeus centrifuge for 5 minutes at 12000rpm. A representative image of semi confluent cells is shown in Figure 2.1.

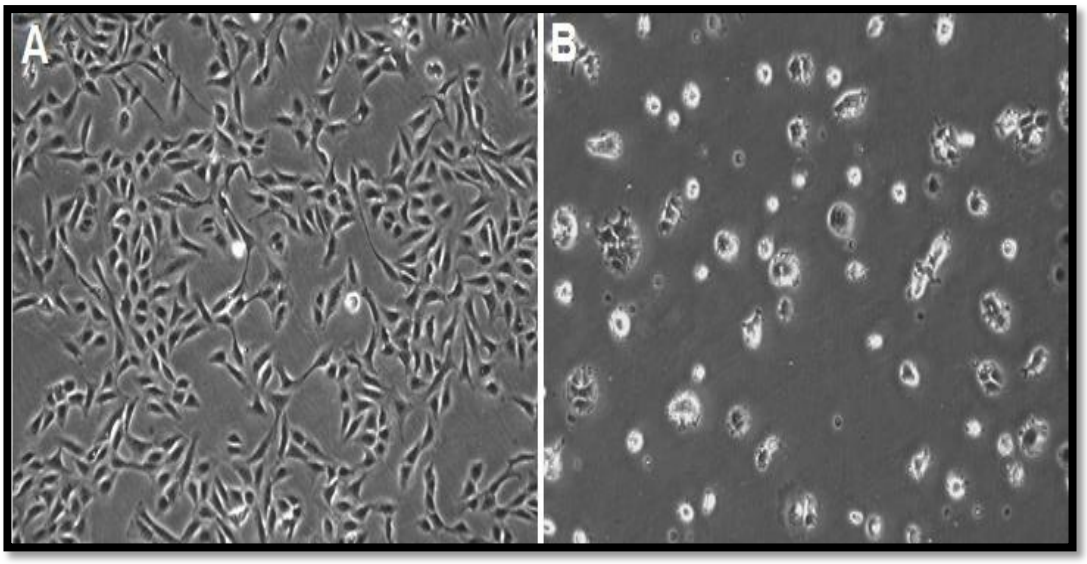

Figure 2.1 A typical morphology of HeLa (A) and MCF-7 (B) cells.

2.2.6 Cell Counting

Cell counting was carried out using both manual and automatic methods. In the manual method an 'Improved Neubauer Haemocytometer' was used. IMS (Industrial Methylated Spirit) was used to clean both the coverslip and the chamber. After drying the coverslip was placed gently on the chamber until the Newton ring (rainbow-like optical phenomenon) appeared. A total of 10µl of thoroughly mixed cell suspension was added into the edge of the chamber and allowed to run under the coverslip. The cells were counted as indicated in Figure 2.2.

The average of the number of sections counted is taken and a formula $C = n \times 10^4$/ml is used to calculate the number of cells. In the above formula C is the concentration and n is the number of cells counted.

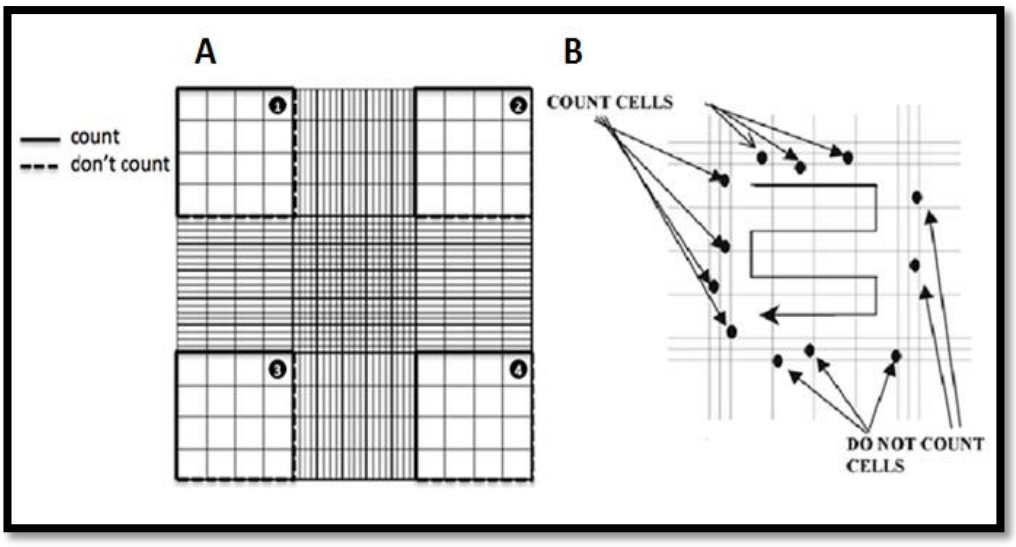

Figure 2.2 Cells within section A; 1, 2, 3 and 4 were counted using the rules as indicated in panel B.

For the automatic method a Countess Automated Cell Counter from Invitrogen was used. A mix of 10µl of Trypan blue and 10µl of cell suspension was prepared. A total of 10µl was taken from the mixture and added on to each side of the slide provided. The slide is then inserted into the allocated slot in the machine and the machine automatically calculates the total number of cells per ml and indicates how many of those are viable and non-viable. This information is displayed on the screen.

Figure 2.3 Image of the countess automated cell counter.

2.2.7 Cell Cryopreservation

Before freezing cells were checked for contamination and then trypsinised according to the methodology described above, depending on the cell type. In the case of lymphoblastoid cell lines trypsonisation was not required.

The cell suspension was then mixed with 1ml of freezing mixture consisting of 90% foetal calf serum (Gibco/Invitrogen) and 10% DMSO (dimethylsulfoxide, Sigma). The cell suspension was aliquoted into 1ml cryogenic vials for storage in liquid nitrogen. Before storing in liquid nitrogen vials with cells were stored at -20ºC for 24 hours in a Nalge Nunc Cooler which contained Isopropyl Alcohol (IPA). The base insulates the container and gives a cooling rate of approximately 1ºC/min in the cryotube.

2.2.8 Thawing of Cryopreserved cells

The cryopreserved cells were taken out of liquid nitrogen, warmed for 2-3 minutes at 37ºC and the contents of the vials were transferred to flasks containing pre-warmed medium. The medium in the flasks was changed after 24 hours so as to wash away any DMSO residual.

2.2.9 Irradiation of cells

Cells were irradiated with ionising radiation using a Cobalt-60 source. Adherent cells were irradiated either in non-filtered tissue culture flasks (Nunc, Fisher) for chromosome analysis, or on polyprep slides (Sigma) for immuno-cytochemical assays for DNA damage detection (see below). At the time of irradiation the cells were at the 80-90% confluence level. Cells were exposed to 0.5Gy, 1.0, 2.0 or 4.0 Gy of radiation which was calculated using datasheets provided by the physicists in charge of the facility.

The formula used to calculate this was:

$$Time\ (Mins) = \frac{\text{Dose Needed (Gy)}}{\text{Dose Rate (Gy min} - 1)}$$

Irradiated cells were incubated for different time intervals to allow recovery.

2.3 Cytogenetic Analysis

2.3.1 Metaphase preparation using adherent cell lines

All adherent cell lines were incubated with 10µg/ml Colcemid (Sigma-Aldrich) for between 1.5-12 hours, depending on the cell line and the purpose of the analysis. Cells were washed with PBS, trypsinised and spun down at 1000rpm for 5 minutes. The cells were then treated with 3ml of hypotonic buffer (75 Mm KCl) for 15 minutes at 37ºC. Cells were then fixed with 1.0 ml of fixative (3 parts Methanol and 1 part Glacial acidic acid). This process was carried out 3 times, 10 minutes for the first three times and 30 minutes for the third time. Cells were then re-suspended in fresh fixative and 20µl of this suspension was dropped on to the microscope slides followed by the addition of 20µl of fresh fixative.

2.3.2 Metaphase preparation using lymphobastoid cell lines

All lymphoblastoid cell lines were cultured with Colcemid as above with the exception that the duration of incubation never exceeded 4.0 hours. These cells grow at a faster rate and therefore do not require colcemid to be added for longer periods of time as described above 2.3.1. The rest of the protocol was followed as per 2.3.1.

2.3.3 Chromosomal Aberration analysis

This protocol was performed to detect any damage in cells at chromosomal level by staining metaphase chromosomes using either DAPI (fluorescence microscopy), or Giemsa (light microscopy). Chromosomes were analysed at G1 and G2 stage of the cell cycle.

Protocols for human and Chinese hamster cells were slightly different. For Chinese hamster cells analysis were done as follows.

For G1 analyses, cells were irradiated as confluent, sub-cultured and incubated for 16.5 hours. Then 10µg/ml colcemid was added for 1.5 hour. The cells were harvested as described in section 2.3.2. The duration of one single cell cycle in the case of Chinese hamster cells is approximately 18 hours and incubation for 16.5 hours plus 1.5 hour colcemid treatment allow capturing of metaphase G1 cells exclusively.

For G2 analysis cells were irradiated as semi-confluent and incubated for 2 hours before adding Colcemid for 1.5 hour. The rest of the protocol was carried out as described in section 2.3.2. The duration of the G2 phase is approximately 4.0 hours. Therefore, all cells that enter metaphase 3.5 hours after irradiation will have been irradiated in the G2 phase of the cell cycle. For human cells the protocol was essentially the same with the only difference that one single cell cycle in human cells is 24 hours. Therefore, for G1 analysis incubation after irradiation and colcemid treatment were adjusted to last exactly 24 hours. There was no difference in the case of the G2 analysis.

2.3.3.1 Chromosomal Aberrations with Giemsa staining

After the metaphase preparation cells were stained with 7% (v/v) Giemsa (Sigma-Aldrich) for 3 mintues in 5ml of PBS. To achieve better staining the Giemsa stain was filtered using standard filter paper (Watman paper). Once the slides were stained with Giemsa they were washed with

ddH_2O and left to air dry. DPX mountant (BDH laborotaries), a Polystyrene Plasticizer in Xylene, was used to mount the cover slips onto the slides. The slides were left for 2 hours to dry and then analysed using light microscopy (Zeiss Axioplan 2) equipped with CCD camera and Metasystems software (Altlussheim, Germany).

2.3.4 Chromosomal Aberrations with telomeric probe

After metaphase preparation the cells were dropped on to slides and hybridised with the telomeric probe as described below (see section 2.4).

2.3.5 Micro-nuclei Assay

Exponentially growing cells were treated with 6µg/ml of Cytochalasin B for 48 hours. The cells were then centrifuged at 800 rpm for 5 minutes and the supernatant was aspirated. A total of 3ml of KCL (75mM) was then added to the cells and left at room temperature for 5 minutes. A few drops of fixative (Methanol: Acetic Acid; 3:1) were added to the cells, and they were centrifuged at 800 rpm for 5mins. After centrifuging the supernatant was aspirated and the cells were re-suspended in 500µl of fixative. A total of 400 µl of this suspension was cyto-spun onto slides at 800rpm for 5 minutes. The slides were then stained with Giemsa as described in section 2.3.3.1.

2.4 Hybridisation with the telomeric probe

This procedure was carried out either to analyse chromosomal aberrations (see above) or to measure telomere length. In the case of telomere length measurement the procedure is usually called Q-FISH (quantitative fluorescence in situ hybridization). We describe below two methods for Q-FISH. One method uses metaphase chromosome preparations and it is known as the conventional Q-FISH. The same method is used for analysis of chromosomal aberrations. The other method uses interphase cells and we named it interphase Q-FISH or IQ-FISH.

2.4.1 Pre-hybridisation washes

Microscope slides containing metaphase or interphase cells were prepared using methods described in 2.3.1 and 2.3.2. Please note that in the case of Q-FISH addition of Colcemide was obligatory. In the case of IQ-FISH addition of Colcemide was not required. The slides were washed in PBS for 5 minutes on the shaking platform. After the PBS treatment the slides were incubated in a 4% formaldehyde solution for 2 minutes and then washed in PBS on the shaking platform 3 times for 5 minutes each time. A total of 500µl of pepsin (10% pepsin; Sigma Co.) mixed in 50ml of acidified dH_2O at pH 2 (49.5ml of deionized water added to 0.5ml HCL) plus 50ml PBS, was used to remove unwanted proteins. Slides were put in a coplin jar containing this solution and were incubated at 37°C for 10 minutes. Slides were washed 2 times in PBS for 2 minutes on the shaking platform. A solution of 4% formaldehyde was used to fix the cells for further 2 minutes. The slides were then washed in PBS solution 3 times for 5 minutes, dehydrated in ethanol series (70%, 90% and 100%) and left to air dry at room temperature.

2.4.2 Hybridisation

A FITC or Cy3 labelled Oligonucleotide PNA $(CCCTAA)_3$, complementary to telomeres was added to slides (20µl). The slides were then placed on a heating block preheated 70-75°C and kept on it for 2 minutes. Slides were removed from the heating block and incubated in a dark humidified chamber for 2 hours to allow hybridisation. A brief outline of this procedure is presented in (Figure 2.4).

2.4.3 Post-hybridisation washes

After hybridisation slides were washed in 70% Formamide solution 2 X 15 minutes, followed by 3 X 5 minute washes in PBS. Slides were then dehydrated in ethanol series (70%, 90% and 100%). Once the slides were air-dried 15µl of Vectashield anti-fade mounting medium

containing DAPI (Vector Laboratories) was added, covered with a cover slip and sealed using clear nail varnish.

2.4.4 Image capture for telomere length analysis

Image capturing depended on the type of Q-FISH. For IQ-FISH we used the Smart Capture imaging software (Digital Scientific, Cambridge, UK) followed by the analysis of telomere fluorescence using the IP-Lab software. For conventional Q-FISH we used the Smart Capture software followed by the analysis of telomere fluorescence using the TFL-TELO software. For chromosomal aberration analysis we used the Metasystems software (Altlussheim, Germany).

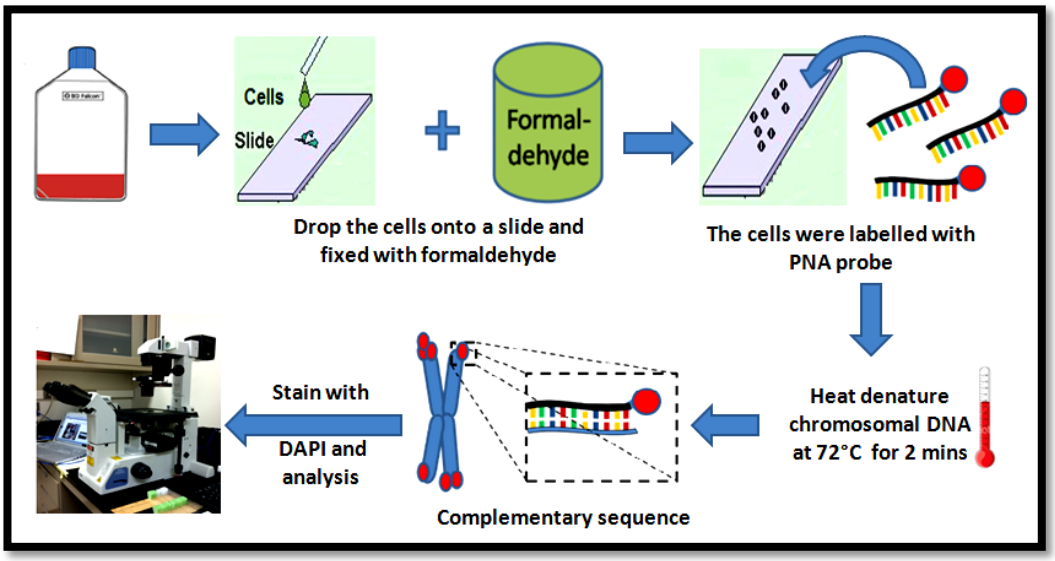

Figure 2.4 A schematic of an overview of Q-FISH (Author's adaptation).

2.4.5 Telomere length analysis by IQ-FISH

A total of 50 interphase cells have been analyzed for each cell line. Each measurement was repeated 3 times. Images of interphase cells were captured using a 63X objective on an Axioplan 2 Zeiss fluorescent microscope equipped with a CCD camera and the Smart capture 2 image acquisition software. Images were used to measure telomere signal intensity which is proportional to telomere length using the IP Lab software. The software produces a combined

image of the detected telomeres and the cell nucleus boundaries which are superimposed onto the telomere image. In order to maintain the accuracy of IQ-FISH methodology it was important to use appropriate controls for the experiment. This is because the fluorescence microscope lamp intensity is not constant. To ensure the accuracy of fluorescence intensity measurement we used two mouse cell lines, LY-R and LY-S, with long and short telomeres respectively, as calibration standards (Mcllrath *et al.*, 2001). In each experiment we captured images of LY-R and LY-S cells together with the test samples (human cells). After capturing images of interphase cells in the Smart Capture 2 software, the information was imported to the IPLab program in which telomere fluorescence intensities were measured. The procedure for IQ-FISH was described in detail in a PhD thesis by another student working in Dr Slijepcevic laboratory (Ojani 2012).

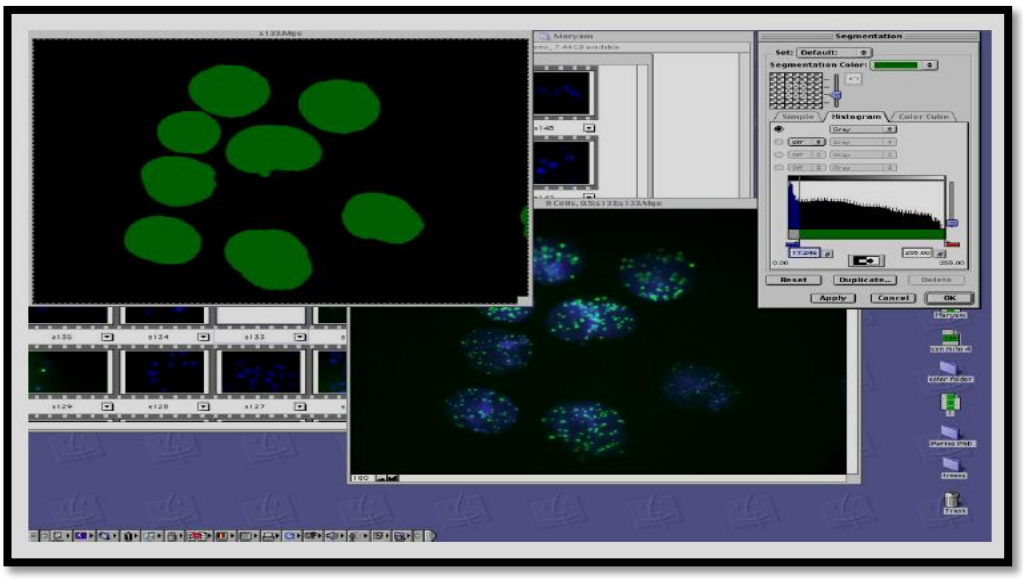

Figure 2.5 Image displays a typical segmented image with cell nuclei stained in green.

The other options of the software include: the "background removal" option, "measurement" options and display of results, which were also assessed. The "background removal" option is very important and key, as it allows subtracting the fluorescence background noise from the actual fluorescence values, so it is clear what is happening inside the plates. This process is performed using the "Pixel arithmetic" procedure which is shown below (Figure 2.6).

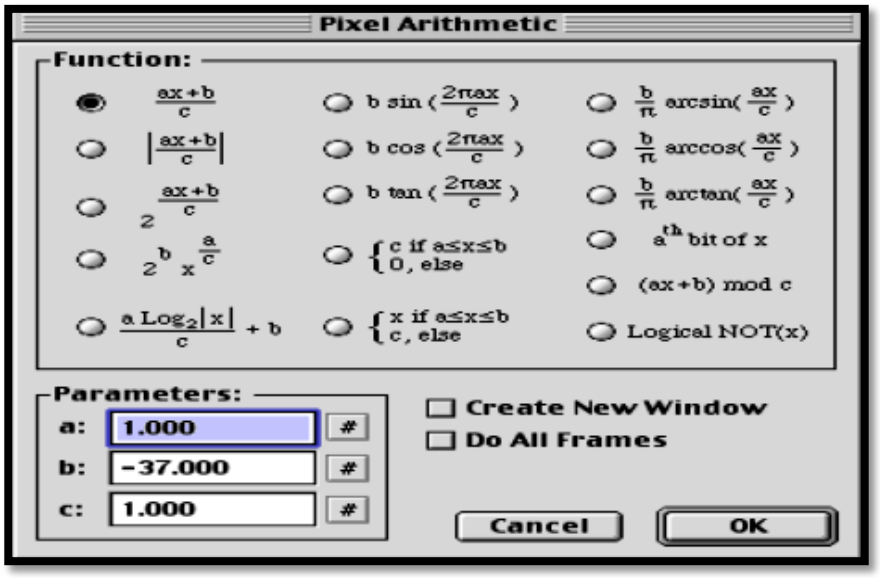

Figure 2.6 Image displays a snap-shot of the mathematical manipulations behind the process of telomere fluorescence intensity measurement.

Figure 2.5 and Figure 2.6 demonstrate the procedures behind telomere fluorescence measurement. This involves steps like cell image segmentation to determine nuclear boundaries, background removal to eliminate non-specific fluorescence, and measurement of telomere fluorescence intensity. At the end of the procedure a table is generated that shows the average fluorescence intensity for each cell.

2.5 Conventional Q-FISH

For conventional Q-FISH, cells were prepared using the metaphase protocol as described in 2.3.1 or 2.3.2, depending on the cell type.

Images of the metaphase cells were captured using the Smart Capture Software (Digital Scientific, Cambridge, UK) and the telomere fluorescence analysed using the TFL-Telo software (Flintbox, online). This software is developed by the Lansdorp group (University of British Columbia, Vancouver) and it is extensively described in numerous publications. Briefly, the software generates the image of chromosomes and telomeres in which each individual telomere (T1-T4) is recognized by a different colour (see Figure 2.7). For example, T1 is recognised by the blue colour etc. (Figure 2.7). The software has various editing function which allows separation of chromosomes that overlap, or telomeres that overlap. Also, occasionally a single telomere may be displayed as two telomeres (hence T5 in the table in Figure 2.7). The editing function of the software allows merging two artificially split telomeres.

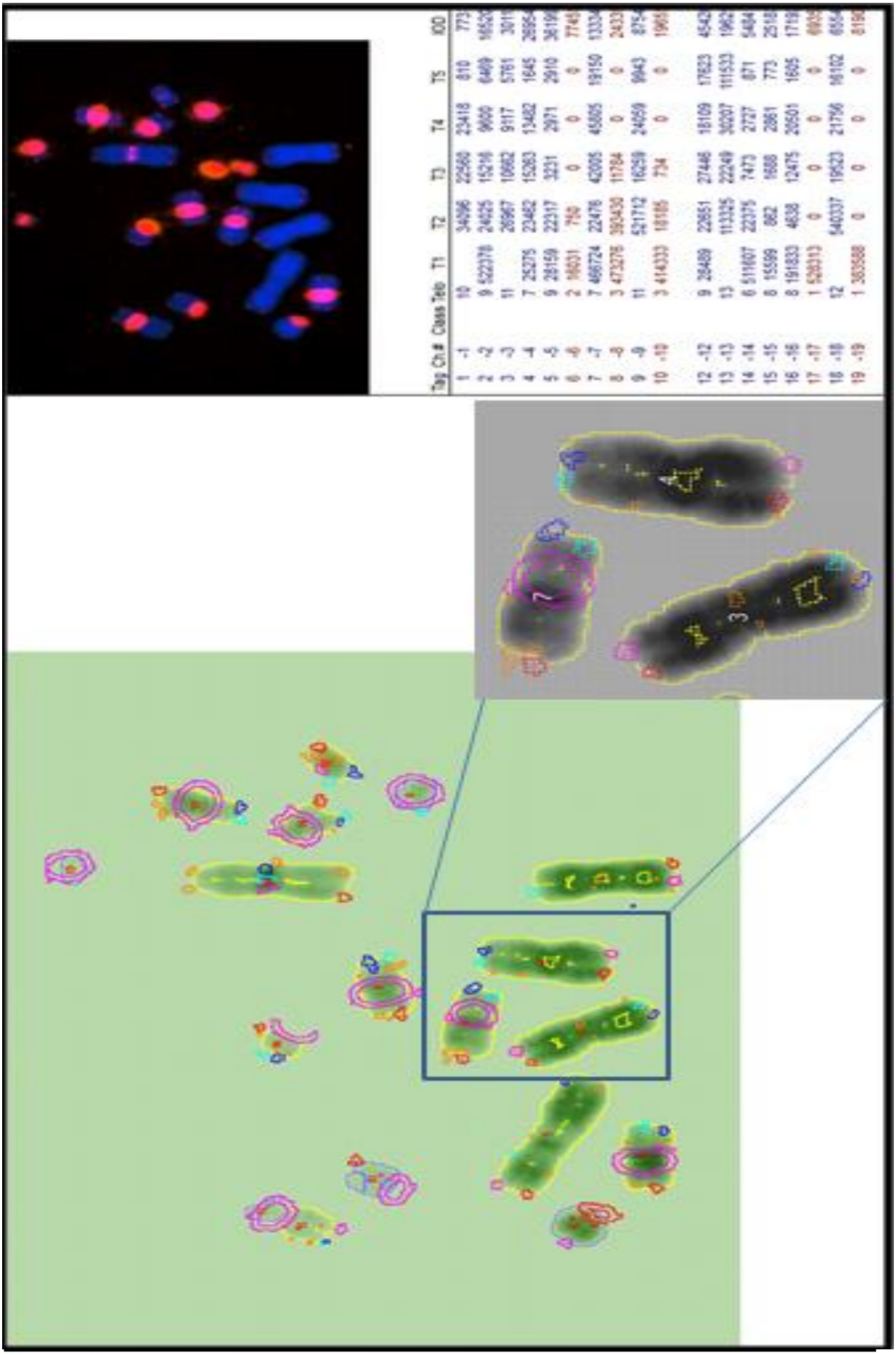

Tag	Ch #	Class	Telo	T1	T2	T3	T4	T5	IOD
1	-1		10		34596	22560	23418	810	773
2	-2		9	5223378	24625	15218	9600	6469	16520
3	-3		11		26967	10662	9117	5761	3618
4	-4		7	25275	23462	15263	13482	1645	2895
5	-5		6	29159	22317	3231	2971	2910	3619
6	-6		2	16031	750	0	0	0	7745
7	-7		7	466724	22478	42005	45805	19150	13334
8	-8		3	473278	393430	11784	0	0	2433
9	-9		11		521712	16259	24659	9943	8754
10	-10		3	414333	18185	734	0	0	1961
12	-12		9	39489	22851	27446	18109	17823	4542
13	-13		13		113325	22249	30007	111533	1962
14	-14		6	511607	22375	7473	2727	871	5484
15	-15		8	15599	862	1688	2861	773	2518
16	-16		8	191833	4638	12475	29501	1605	1719
17	-17		1	526313	0	0	0	0	8026
18	-18		12		5403337	19523	21756	16102	6554
19	-19		1	383588	0	0	0	0	8196

Figure 2.7 Shows the outcome from TFL-Telo software.

For the analysis images of metaphase cells with well-separated chromosomes and clear telomeric signals were chosen. Results can be presented either as telomere fluorescence values for each individual telomere (see table in Figure 2.7). For this approach histograms were generated using all the telomere lengths produced by the software. Alternatively, the average telomere fluorescence intensity can be expressed by calculating the average value of telomere fluorescence intensity.

2.6 Chromosome Orientation Fluorescence in situ Hybridisation (CO-FISH)

CO-FISH is a technique that is able to determine the absolute 5' to 3' orientation of DNA sequence relative to short arm to long arm of the chromosome. The technique is based on standard FISH principles, which allows hybridisation of a single stranded probe to only one chromatid of a metaphase chromosome (Goodwin et al 1993). The main principles of this technique are highlighted in (Figure 2.8).

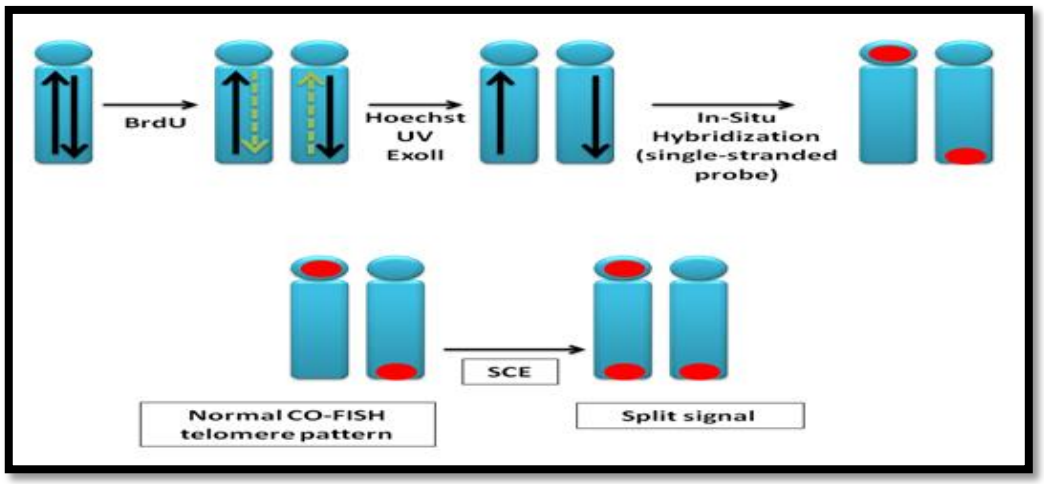

Figure 2.8 Schematic presentation of the CO-FISH method.

CO-FISH is used to detect telomeric sister chromatid exchanges (T-SCEs) which can be seen above. The split signal shown in the image shows a T-SCE. This image was adapted and adjusted from (Bailey et al 2004).

After cells were sub-cultured, 3µl of 5'-bromo-2-deoxyuridine at the concentration of $1x10^{-5}$M (Sigma Co.) was added to the cells for 20 hours. After this incubation period metaphase preparation was carried out as described in 2.3.1 and 2.3.2, depending on the cell line. Cells were then incubated overnight at the heating block pre-heated to 54°C to allow better preservation of chromosomes after subsequent DNA denaturing.

2.6.1 Washing, Digestion and Fixation

Slides were then washed with PBS for 15 minutes and stained with 2.5 µl of Hoescht 33258 (0.5µl/ml) which was mixed gently with standard saline citrate (2x SSC) for 15 minutes. A total of 100µl of Exonuclease III (Promega Co.) (1.5µl Exonuclease III + 10 µl buffer + 88.5µl H2O) was added to each slide covered with a cover slip and left at room temperature for 10 minutes. The slides are then exposed to 365nm UV light for 30 minutes. Samples were then washed with PBS twice for 5 minutes on the shaking platform. The slides were then treated with Ethanol series (70%, 90% and 100%) for 5 minutes each and left to air dry. Hybridisation and posthybridization washes are carried out as described in sections 2.4.2.

2.6.2 Image Analysis

A Zeiss fluorescence microscope equipped with a CCD camera and ISIS (in *situ* imaging system, Meta Systems, Altlusshim, Germany) capture software was used to acquire digital images.

2.7 Immuno-cytochemical detection of DNA damage (the γ-H2AX assay)

One of the most popular methods of detecting DNA double strand breaks is γ-H2AX assay. It detects damage in interphase cells using a monoclonal anti-body against the γ-H2AX protein. For γ-H2AX assay on adherent cells, they must be grown on poly-prep slides (Sigma- Aldrich) for 24 hours before treatment with DNA damaging agents (in our case ionizing radiation). After

irradiation cells were fixed using 4% formaldehyde in PBS for 15 minutes. Cells were pearmeabilised using 0.2% Triton-X solution (Sigma-Aldrich) in dH_2O for 10 minutes at 4°C.

Non-specific sites on the cell were then blocked using blocking buffer (0.1gram Milk powder + 50µl Triton-X solution + 50ml PBS). A total of 100µl of blocking buffer was added to each slide, slides covered with parafilm and placed in a humidified dark box. After 1 hour incubation the primary anti-body (γ-H2AX, Millipore) was added to the slides at a concentration of 1:1000 following manufacturer's instructions. The slides were covered with parafilm and are placed in a humidified dark box for 1 hour.

After 1 hour the slides were washed 3 X 5 minutes with TBST solution (8.8.grams of NaCl + 0.2 grams of KCL + 3 grams of tris base + 500µl tween 20 in 1 litre of dH_2O. pH 7.4). The secondary antibody (FITC labelled anti-mouse, Invitrogen) was added at a dilution rate of 1:1000. A total of 100µl of diluted antibody was added to the slides, covered with parafilm and placed in a humidified chamber for 1 hour.

The slides were then washed 3 X 5 minutes in TBST and then 3 X 5 minutes in PBS. The slides were de-hydrated in ethanol series (70%, 90% and 100%) for 5 minutes each time. Once the slides were air dry a total of 15µl of mounting medium containing DAPI (Vector Laboratories) was added to each slide and covered with a cover slip and sealed using clear nail varnish.

2.7.1 γ-H2AX assay using cytospin

The protocol for DNA damage detection in lymphoblastoid cell lines required the use of cytospin. In contrast to adherent cells, which can be grown on pre-coated microscope slides, lymphoblastoid cells cannot as they grow in suspension. The alternative method for spreading these cells on to microscope slides employs the cytospin procedure. Cells were irradiated in flasks or tubes as cell suspension. This cell suspension was then used to attach cells to

microscope slides using a cytospin at 800rpm for 5 minutes. After this the same procedure as the adherent cells described in 2.7 can be used for the immunocytochemical detection of DNA damage.

2.7.2 Telomere Dysfunction-Induced Foci (TIF) Assay

TIF is immuno-FISH protocol that combines the γ-H2AX assay with synthetic telomeric PNA probe hybridisation in order to detect DNA damage at telomeres. First, the γ-H2AX assay protocol as described in section 2.7 is performed on the slides. After the de-hydration as described in section 2.7 DAPI is not added to the slides. Instead slides were incubated overnight in a dark container at room temperature. This incubation allows better preservation of antibodies and enables them to remain intact after the subsequent hybridization procedure. On the next day, the hybridisation procedure was carried out as described in sections 2.4.2.

2.8 Reverse Transcriptase Polymerase Chain Reaction (RT-PCR) analysis

2.8.1 RNA extraction

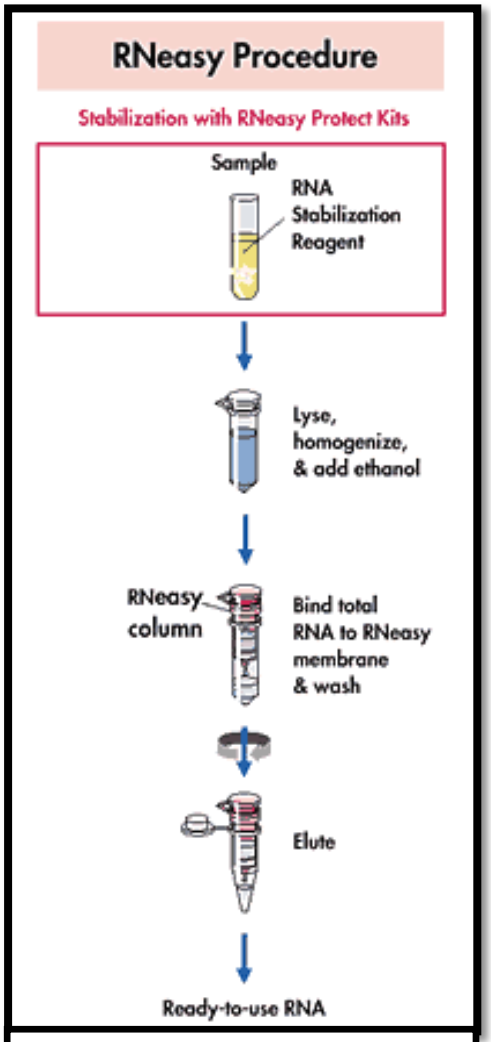

Figure 2.9 Shows a summary of the RNA Extraction procedure as per Qiagen kit.

RNA extraction was performed using the RNeasy Plus Kit (Qiagen) following manufacturer's instructions. A brief outline of this procedure can be seen in Figure 2.9. A total of 1 x10^7 cells is recommended for this procedure. Adherent cells were trypsinised and centrifuged at 1500rpm for 5 minutes. The supernatant was aspirated and the cell pellet washed with PBS 3 times.

After flicking the pellet to loosen it 600µl of RLT buffer (guanidium thiocyanate lysis buffer) was added to the eppendorf tube containing the cell pellet and the cells were homogenised using a syringe. One volume of 70% RNA free ethanol was added to the cells and mixed well using the pipette technique. A total of 700µl of the homogenised lysate was transferred on to an RNeasy spin column and centrifuged for 15 seconds at 10000rpm. The flow through was thrown away and 700 µl Buffer RW1 was added to the RNeasy spin column. The spin column was then centrifuged for 15 seconds at 10000 rpm. The flow through used was then discarded. 500µl of Buffer RPE was added to the RNeasy spin column and the column was centrifuged for 15 seconds at 10000 rpm. The flow through used was thrown away. Another 500µl of buffer RPE was added to the spin column and the column was centrifuged for 2 minutes at 10000rpm. The spin column is

then placed in a 1.5ml collection tube and 30-50µl of RNase–free water is added to its membrane. The 1.5ml collection tube is then centrifuged for 1 minute at 10000rpm to elute the RNA.

The quality of the RNA was measured using a Nano Drop 2000C (Thermo Fisher Scientific). The spectrophotometer was blanked using the reference RNA free solution that was placed on to the measurement pedestal, and the reading was taken at 260nm wavelength. An example of RNA measured can be seen in (Table 2.2).

Table 2-2 Sample readings of RNA concentration from Nano Drop.

Cell Line	A260/280 nm ratio	A260/230 ratio	RNA concentration (ng/µl)
U2OS	2.05	2.08	1536.4
MCF-7	2.03	2.07	1352.5

2.8.2 First- strand cDNA synthesis with Superscript III

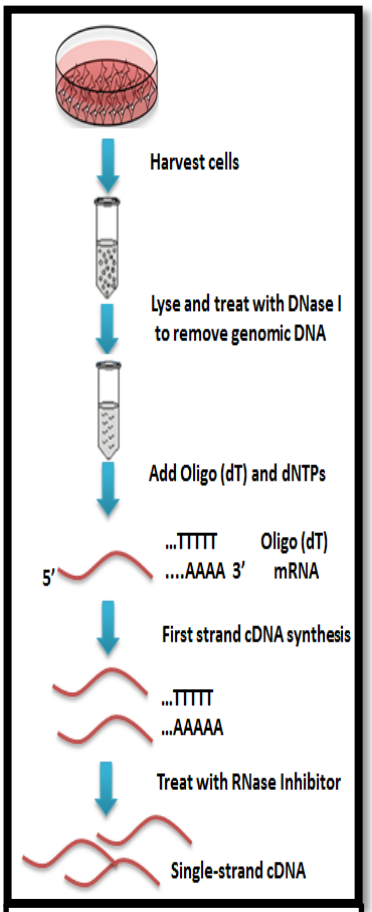

Figure 2.10 Shows the procedure used to synthesis first-strand cDNA using Superscript III.

cDNA was extracted using the superscript method (Life Technologies) (Figure 2-10). For each sample 1µg of total RNA extracted as per the method described in 2.8.1 was added to a tube followed by 1µl of DNAse I reaction buffer, 1 µl of DNAse 1 Amp grade and RNA-free water according to how much total RNA was added to make the total volume of the solution 10µl reaction mix.

The 10µl final mixture was incubated at room temperature for 15 minutes. A total of 1µl of EDTA was added to each sample, which made the volume of the mixture 11µl. This was heated to 65ºC for 10 minutes using a thermal cycler (PTC-225 Peltier). 1µl of random primer and 1µl of dNTP was then added to each sample, which made the final volume of the mixture 13µl. This was then heated to 65ºC for 5 minutes.

Once this was heated, 4µl of first strand buffer, 1µl of 0.1M DTT (Dithiothreitol), 1µl of RNaseOUTM recombinant RNase Inhibitor (40units/µl) and 1µl of superscriptTM III RT (200 units/µl) was added to the mixture. This made the final volume of the mixture 20µl.

The 20µl mixture was mixed gently and heated at 25ºC for 5 minutes, followed by 60 minutes incubation at 50ºC for the random primer and then 15 minutes incubation at 70ºC to inactivate the reaction.

2.9 Primer Design

The primers that were used were previously designed by a MSc student (E. Sapir with Dr Predrag Slijepcevic). The primers used can be seen in Table 2-3.

Table 2-3 Represents the human primers that were used for RT-PCR and Real-time PCR.

Gene Name	Orientation	GC%	Tm C°	Length bp	Sequence
GAPDH (house keeping gene)	Forward	55	55	18	5'-GAAGGTGAAGGTCGGAGT-3'
GPDH (house keeping gene)	Reverse	45	53	20	5'-GAAGATGGTGATGGGATTTC-3'
BRCA2	Forward	53	59	19	5'-AATGCCCCATCGATTGGTC-3'
BRCA2	Reverse	52	60	21	5'-AGCCCCTAAACCCCACTTCAT-3'

2.9.1 RT-PCR

Both the forward and reverse primers were optimised using three different concentrations 10µM, 5µM and 2.5µM, using a conventional PCR reaction. Between 1 to 5µl of cDNA were used for PCR amplification using PCR Master Mix (Thermo Scientific, 15mM $MgCl_2$). A total of 21µl of reaction mixture was used which consisted of: 1µl of cDNA + 1 µl of forward primer according to the gene of interest + 1 µl of reverse primers according to the gene of interest +18 µl of master mix.

The thermal cycler machine was configured with settings as per (Table 2-4).

Table 2-4 Shows the different settings that were used for the thermal cycler machine.

	Temperature (˚c)	**Time**	**Cycles number**
Enzyme activation	95	5 minutes	1 cycle
Denaturation	95	45 seconds	30- 40 cycles
Annealing (variable)	53/55/57/59	45 seconds	
Initial extention	72	45 seconds	
Extension	72	10 minutes	1 cycle

2.9.2 Agarose Gel Electrophoresis

In order to make 2% agarose gel a solution consisting of 1x Tris acetate EDTA (TAE) buffer (Sigma-Aldrich) was used. A total of 5µl ethidium bromide (10mg/ml) was added to the molten gel just before it was set in the tank. The gel was covered with 1x TAE and the PCR samples were loaded into the gel wells. A 1kb ladder was added to the gel to determine the PCR product size accurately. The gel was then run at 65 V for approximately 1.5 hours. An Alphaimager under U.V. light was used to visualise the PCR products.

2.9.3 Real-Time quantitative RT-PCR (Real-Time qRT-PCR)

The primer concentration was measured after optimisation using qRT-PCR. The technique amplified cDNA and simultaneously quantified the cDNA products using the Syber green I dye. The amount of DNA produced was quantified by measuring the fluorescence intensity produced by the binding of Syber Green to the DNA.

The optimal concentration yields the lowest threshold cycle (Ct), determined by the intersection between the amplification curve and the threshold line, and maximum run, which is the

reported signal of normalised fluorescence. Both MCF-7 and U20S cell lines were used to test for BRCA2 optimal primers. Three different primer concentrations were examined (20 µM, 10µM, 5 µM and 2.5 µM). Some of the results that were obtained while testing the GAPDH and BRCA2 primers optimal concentrations can be seen in (Figure 2.11).

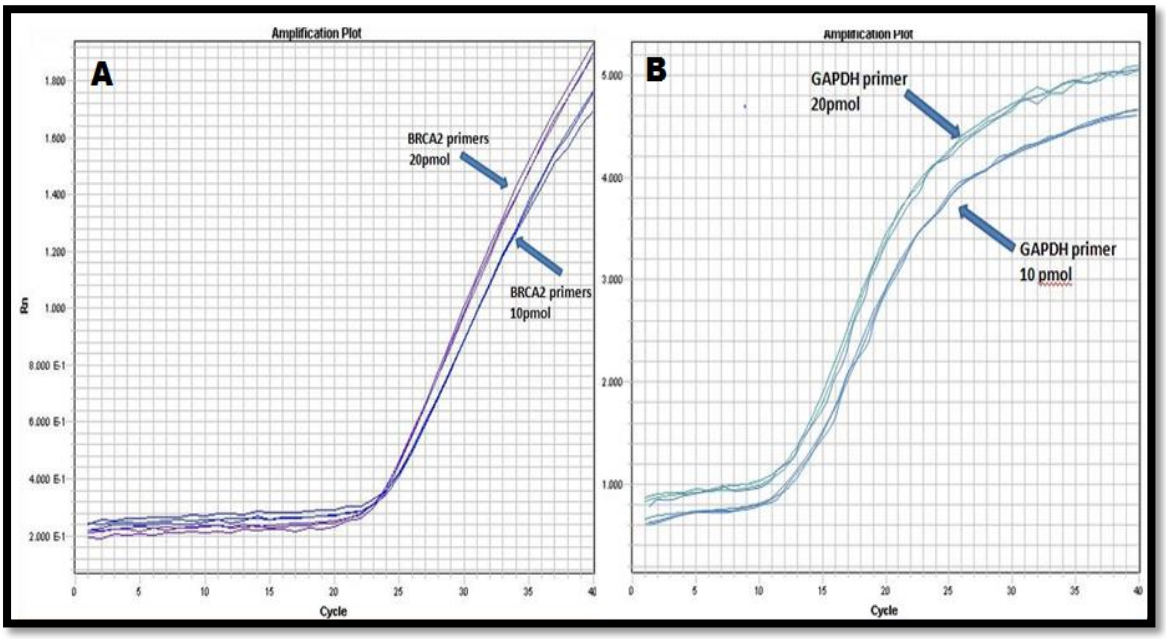

Figure 2.11 Real-time PCR amplification curves obtained at different concentrations of BRCA2 and GAPDH primers. A) Amplification curve for BRCA2 primers at two concentrations 10pmol and 20mol using U2OS cell line. Concentration of 10pmol reduced the amplification efficiency, as seen as an increase of Ct (from 24 to 25). B) amplification curve for GAPDH primers at 10pmol and 20pmol using U2OS cell line. Similar to BRCA2 primers concentration of 10pmol reduced amplification efficiency.

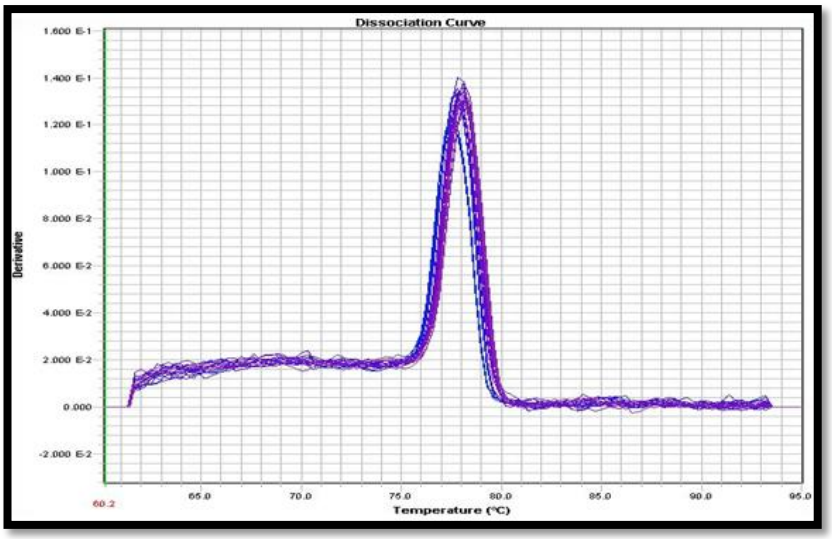

Figure 2.12 Dissociation curve analysis of BRCA2 showing only one amplification product without any non-specific amplification or primer dimmer.

2.10 Small Interfering RNA (siRNA)

In 2001 it was observed that the RNAi technique was very effective in mammalian somatic cells, and since then it has been used in gene function analysis (Elbashir et al., 2001). Over the years siRNA oligonucleotides have been tested in various disease models, and clinical trials have shown the effective treatment of some malignant tumours, such as hepatic cancer (Brower, 2010), suggesting that siRNAs could possibly be used as therapeutic drugs. siRNA is a class of double-stranded RNA molecules that interferes with the expression of a specific gene, 21-23 bases in length. The main purpose of this technique is to knock-down the expression of desired protein. We used ON-TARGET plus SMARTpool (Thermo Scientific Dharmacon) siRNA oligonucleotides. This product is designed to enhance target specificity and reduce undesirable effects. The pool was composed from four individual siRNA sequences to ensure a specific and high level of gene silencing. The siRNA was delivered to the cells using jetPRIME^{TM} transfection reagent (Polyplus-transfection). This powerful product is based on a non-liposomal formula that ensures effective delivery of oligonucleotides into mammalian

cells. Several controls (Table 2-5) were selected in order to ensure reliable and efficient results. The selected controls were as follows:

Table 2-5 Summary of controls in RNA inhibition process.

Type of control	Function	Features	Product
Positive control	Monitor the efficiency of siRNA delivery	Targets a housekeeping gene characterises by an abundance expression in a large number of different cell types. This control should not affect cell viability and phenotype	ON-TARGET GAPD Control pool (silencing GAPDH)
Negative control	Distinguish between sequence-specific silencing to non-specific effect	Does not target any known gene in the cell with a minimal effect on cell viability and phenotype.	ON-TARGET Non-targeting pool. Also Known as scrambled RNA
Transfection control	Ensure that the transfection procedure itself does not affect any gene expression	Does not target any gene in the cell with no effect on cell viability and phenotype	Transfection reagents only
Basic control	Determine the base level of gene expression as well as viability and phenotype	—	Untreated cells

2.10.1 siRNA Procedure

Adherent cells were seeded in a T25 flask by adding 5ml medium containing approximately 400,000 cells. siRNA buffer (Thermo Scientific Dharmacon) was diluted with RNase free water from 5x concentration to 1x concentration. The siRNA concentration was verified using the spectrophotometer NanoDrop 2000C (Thermo Fisher Scientific). 24 hours after seeding (allowing the cells to adhere), the medium was replaced by 4ml of new medium. A mixture containing 210µl of 50nM siRNA, 8µl of transfection reagent (jetPRIME™ reagent) and 200µl of transgection buffer (jetPRIME™ buffer) was added. The mixture was vortexed, briefly spun down and incubated at room temperature for 15 minutes prior to its addition. Schematic description of the knockdown procedure are shown in (Figure 2.13).

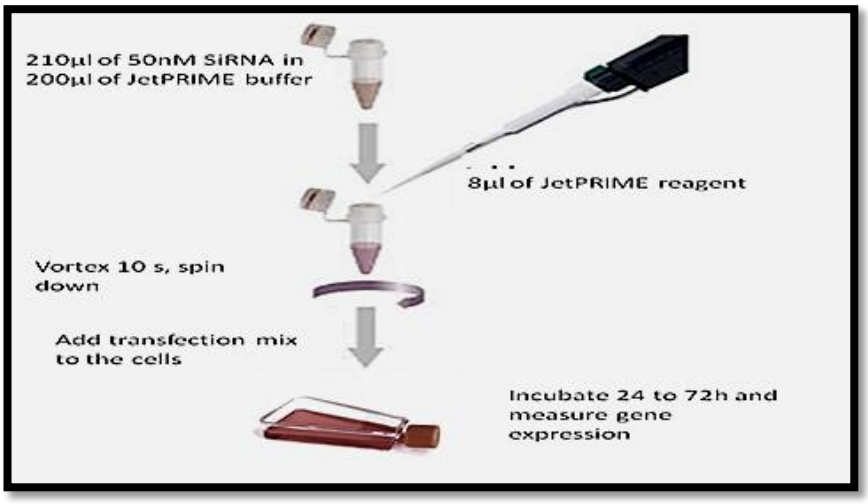

Figure 2.13 Schematic representation of the siRNA experimental procedure.

2.10.2 siRNA experiment design

Cells were seeded for 24 hours prior to siRNA oligonucleotide addition. After 24 hours, the medium was replaced. Cells were harvested 48h, 72h, 96h and 7 days after treatment. This was followed by RNA extraction, cDNA synthesis and knock-down measurement using real-time qRT –PCR. The procedure was performed twice. When BRCA2 expression was at its lowest

level, CO-FISH, H2AX and TIF was performed. Schematic presentation of the experimental design is shown in (Figure 2.14).

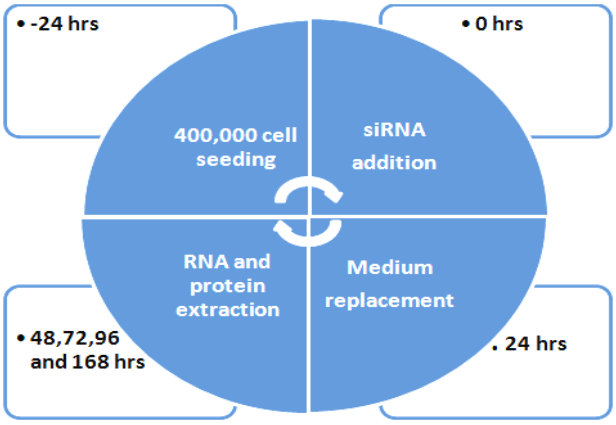

Figure 2.14 Schematic representation of the RNA inhibition experimental procedure.

2.11 Short hairpin RNA (shRNA)

Short-hairpin RNAs (shRNAs) (Paddison et al., 2002) as opposed to siRNAs, are synthesized in the nucleus of cells. Using appropriate vectors hairpin constructs can be introduced into the genome resulting in their stable expression (Paddison et al., 2002).

The expressed hairpins are processed by Drosha (RNase III enzyme) and transferred to the cytoplasm, where Dicer turns on them to create siRNAs, which then get incorporated into the RNA interfering silencing complex (RISC).

shRNAs can also be chemically synthesized and introduced into the cytoplasm (Siolas et al., 2005), but in this case it is essential to mimic the product of Drosha, which has a 2-30 nt overhang. Both siRNAs and shRNAs operate through the same pathways of gene silencing.

To create stable BRCA2 knockdown in different cell lines we used the shRNA approach: SMART vector 2.0 Lentiviral shRNA Particles (Thermo Scientific Dharmacon) containing unique BRCA2 sequences. This product is designed to enhance target specificity and reduce undesirable effects.

2.11.1 shRNA experiment design

The starting aim was to identify a set of conditions that provide maximal transduction efficiencies and gene silencing with minimal toxicity. Finding such conditions can be done in a single multi-parameter optimization experiment.

2.11.2 Puromycin selection condition

Puromycin (Fisher # ICN10055225) is an antibiotic, derived from the streptomyces alboniger bacterium. Puromycin resistance gene (PuroR) is a feature of all SMARTvector 2.0 constructs designed for mammalian cells. It allows selection by inhibition of protein synthesis through ribosomal binding (Brooks et al., 2003) and isolation of clonal populations when generating stable cell lines.

Therefore, all cells that did not take up the shRNA vector will be killed if cells are grown in the medium containing puromycin. The amount of puromycin needed to allow gradual cell death before introducing the shRNA vector must be optimized. It is known that high doses of puromycin can be toxic to cells whether or not they have vectors. Therefore, it was necessary to optimise the amount of puromycin used in normal cells without vectors as these are less resistant compared to shRNA transfected cells. Puromycin kill curves were generated as follows.

Six by six-well plates (Fisher # 08-757-214) were used to seed 50,000 cells/well. Each six-well plate represented one time point (20, 28, 48, 60, 68 and 75 hours). This was done for two different cell lines (MCF-7 and U20S cells). On the first day 50,000 cells were seeded in each of the wells of the 6X6-well plates. On the second day the medium was changed with a range of different puromycin concentrations (0.0 – 2.0 µg/ml) (see Figure 2.15). Therefore, in each of the six-well plates 6 different puromycin concentrations were used. In the first well of all the

six-well plates no puromycin was added. This was the control sample. In the second well of the six well plates 0.5 µg/ml, in the third well 0.8 µg/ml, in the fourth well 1.0 µg/ml, in the fifth well 1.5 µg/ml and in the sixth well 2.0 µg/ml of puromycin was added (Figure 2.15). The number of cells were counted using the countess automated cell counter as described previously, at the different time points and a puromycin kill curve (Figure 2.15) was generated for each of the cell lines. From this curve the minimum antibiotic concentration that killed 100% of the cells in 1-3 days was selected.

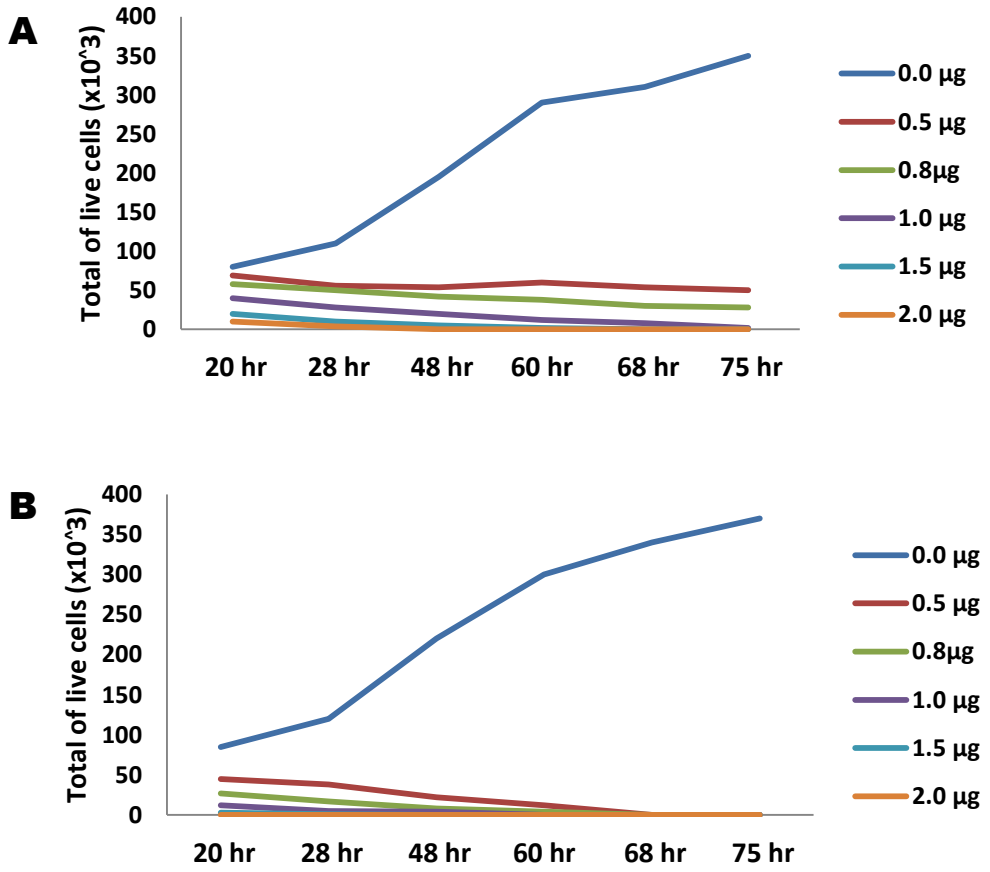

Figure 2.15 Puromycin kill curve: illustrating cell death in relative to increasing doses of puromycin over time. A) shows the puromycin kill curve in MCF-7 cells. 1.0µg/ml of puromycin concentration was selected for this cell line. B) shows the puromycin kill curve in U2OS cells and 0.5 µg/ml was selected as the optimum puromycin concentration for this cell line. These concentrations for both the cell lines were selected because they gradually killed 100% of the cells in 3 days, as seen in the graphs above.

2.11.3 **Polybrene selection condition**

Polybrene (Hexadimethrine bromide – Sigma #H9268) enhances the efficiency of retroviral transfection in mammalian cells by 2-10 fold by binding to the cell surface and neutralising the cell surface charge. Polybrene acts by neutralizing high doses of heparin and sialic acid on the cells surface (Rong et al., 2013).

The optimal transduction conditions are different for each cell type and should be determined empirically. Polybrene can be toxic to certain cell types. To optimize Polybrene concentrations for transduction the following procedure was carried out.

One six-well plate was seeded with 50,000 cells/well and was incubated overnight. The following day the medium was changed and a range of Polybrene concentrations were added to the wells to determine cell viability. After 24 hours incubation cells were examined for viability using the countess automated cell counter as described previously. The highest concentration of Polybrene that does not cause toxicity to the cells is chosen for the different cell types (Fig 2.16). (Note: If Polybrene is toxic to the cells, DEAE-Dextran [1-10 ug/mL] may be substituted.)

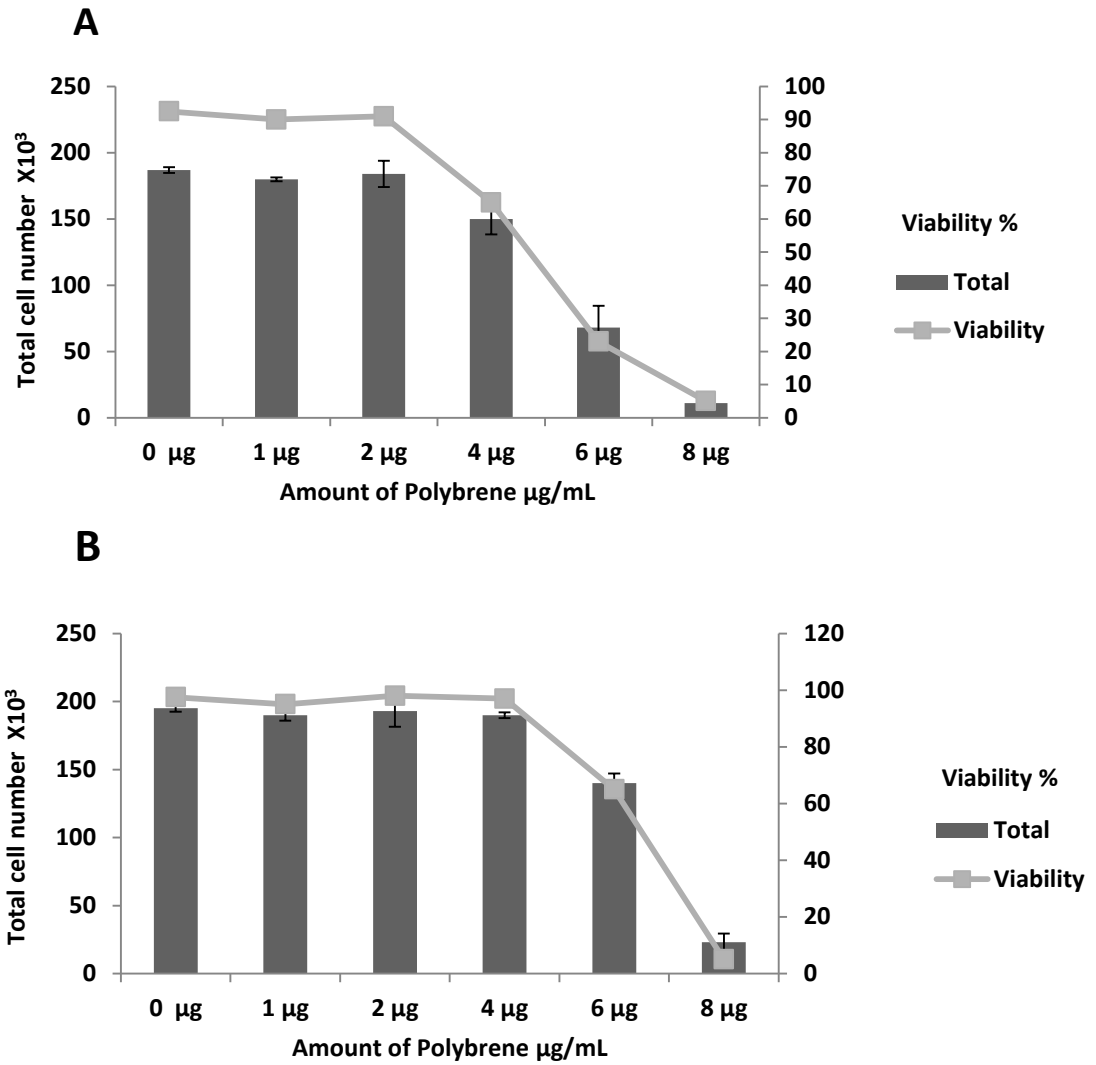

Figure 2.16 Shows the optimisation of polybrene concentrations and cell viability.

A) Viability of MCF-7 cells. The optimum polybrene concentration for MCF-7 cells is 2µg/ml.
B) Viability of U2OS cells. The optimum polybrene concentration for U20S cells is 4 µg/ml.

2.11.4 Determining optimal cell density and Multiplicities Of Infection (MOI)

For transduction to take place effectively the optimum number of viruses per cell needs to be determined. The number of viruses per cell is expressed in units called MOI. Therefore, 5 MOI means 5 viruses per cell. To determine the optimum MOI an experiment was carried out whereby a range of MOI's were tested.

A six-well plate was used, seeded with 6 x 10^4 cell/well and incubated overnight. The next day the number of SMART vector 2.0 human GAPDH was calculated using the formula:

$$\frac{MOI\ X\ \ CN}{VT} = Volume$$

in which CN and VT are defined as:

CN = number of the cells in the well

VT = stock viral titer in TU/µl (Transducing Unit).

For example for an MOI of 5 the calculation is as follow:

$$\frac{5\ X\ 66{,}000}{100{,}000} = 3.3\ \mu l$$

Therefore 3.3µl from the stock 1 x 10^5 TU/µl is used.

Table 2-6 The range of MOI used for GAPDH in MCF7 and U2OS cell lines.

MOI	**Volume required from stock**
MOI 20	13.2 µl
MOI 10	6.6 µl
MOI 5	3.3 µl
MOI 2.5	1.65 µl

In the six-well plate the concentrations mentioned in (Table 2-6) were added to 1ml of serum-free medium and appropriate amounts of polybrene as determined previously (Figure 2.16). These mixtures were added to 4 separate wells containing cells. In the fifth well only 1ml of serum free medium was added to the cells. This acted as the control well. In the sixth well 1ml

of serum free medium and polybrene were added. This experiment was carried out for both U2OS and MCF-7 cells.

After 24 hours the six-well plate was washed with PBS two times and fresh media containing serum and appropriate amounts of puromycin (optimum levels determined as described previously) was added to the wells. The six-well plate was incubated for another 24 hours and the GFP expression in these cells was checked using a fluorescence microscope. After 96 hours cells were trypsinised, RNA extracted and gene expression of gene of interest measured using real-time quantitative PCR.

For long-term time points (>96 hours) cells were washed every 2 to 3 days and new media containing serum and appropriate amounts of Puromycin were added to the wells.

2.12 Western Blot

2.12.1 Protein sample preparation

Cells were grown to 80-90% confluence and plates were rinsed 3 X with PBS. Excess liquid was removed and 200µl of a 5 X sample buffer (SB) containing 10% (v/v) sodium dodecyl sulfate (SDS), 250mM Tris pH 8.0, 50% (v/v) glycerol and 0.01% (w/v) bromophenol blue plus 10µl of protease Inhibitor (x7) and 10µl of beta-mercaptoethanol (BME) were added for at least one minute on to the plate. Cells were then scraped off using a cell scraper. Samples were collected into an Eppendorf tube and mechanically sheared 10 X using a 1ml syringe and a 23g needle. The samples were kept on ice at this stage at all times to prevent protein denaturing. The samples were then spun at 13,000rpm for five minutes, supernatants aliquoted in to clean Eppendorf tubes and stored at -20°C. Repeated thawing and freezing of the protein sample was avoided.

2.12.2 Protein Quantification

Each protein sample was quantified using a RC DC-protein assay (Biorad). This assay was used since it was compatible with reagents in the sample buffer and had a high concentration of SDS and a strong reducing agent such as beta-mercaptoethanol. The assay was performed according to manufacturer's instructions. In short, a serial dilution of 0.2 mg/ml – 1.6mg/ml of protein standard was made using bovine serum albumin (BSA). This was used to construct a standard curve where all unknown sample protein concentrations were measured against the standard curve. A total of 125 µl of reagent I was added to 25µl of each protein standard and protein sample vortexed and left for one minute. A total of 125 µl of reagent II was added to the sample tube vortexed briefly and centrifuged at 15,000xg (13,000rpm) for five minutes at room temperature.

The supernatant was discarded by tipping it on to a dry paper tissue. 127µl of reagent A', made earlier by 5µl of DC reagent S to 250µl of DC reagent A, was added to the tube and left for five minutes after a brief vortexing. It normally takes longer than five minutes for all the proteins to dissolve completely, as some surface membrane proteins are insoluble and difficult to dissolve. With a regular vortexing for 15 minutes all proteins were dissolved. At this point 1ml of DC reagent B was added to the tube, vortexed, and left for 15 minutes to incubate at room temperature. After 15 minutes absorbance was read at 595nm wavelength using Nano drop. The absorbance of protein standard was recorded first and a standard curve of protein concentration in mg/ml against absorbance was constructed. Absorbance of each protein sample was read using the spectrophotometer and the concentration of each protein sample was calculated from the standard curve.

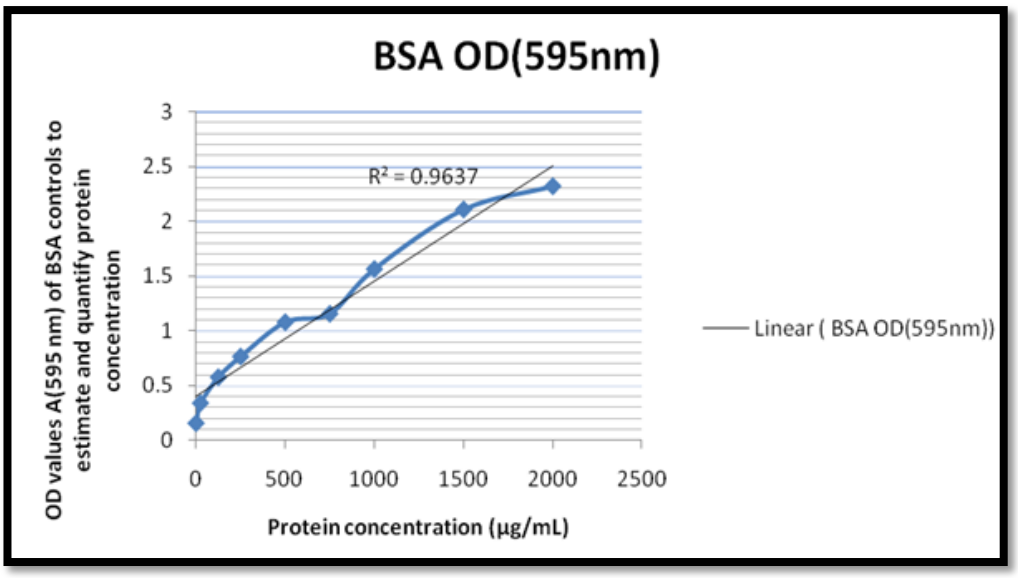

Figure 2.17 Standard curve used in protein quantification analysis.

2.12.3 Protein Gel electrophoresis

A total of 10µg of each protein sample was transferred to Eppendorf tubes. The lid of each tube was pierced and the protein sample was heated up to 95°C for 5-7 minutes to denature the proteins. Then the samples and 10µl of a high molecular weight protein marker (Invitrogen) was added to first well of 6% gel. The lower the molecular weight of a protein of interest, the higher the percentage of gel that is required. In our experiments where heavy proteins such as BRCA2 (molecular weight of 384kDa) were involved, a 6% gel was used. The gel was made using the following ingredients:

- 5.3ml distilled water (DW)
- 2.0ml 30 percent acrylamide mix (protogel EC890)
- 2.5ml 1.5M Tris pH 8.8 (36.3g Tris/200ml)
- 100µl 10% SDS
- 100µl 10% ammonium persulphate (APS) freshly made
- 8µl TEMED.

The above formula will give a 6% gel that is poured into the gel tank plate. The gel tank plate was set up following the manufacturer's protocol. The above gel was loaded immediately onto the gel plate, topped with water for even distribution, and left for 20-30 minutes to set. The stacking gel was then made with the following reagents:

- 2.7ml DW
- 670µl 30% Acrylamide mix
- 500µl 1M Tris pH 6.8 (24.2g Tris/200ml)
- 40µl 10% SDS
- 40µl 10% APS
- 4µl TEMED.

The stacking gel was poured onto the gel (the excess water was blotted off first) and left to set for at least 15 minutes with a separation comb in place. Eventually the comb was removed and the protein samples were loaded carefully onto each well. The protein marker was normally loaded on the first wells. The interior and exterior of the tank was filled with 1x running buffer made with 3.0g (w/v) of Tris base, 14.4g (w/v) of glycine, 1g of SDS, distilled water to 1 liter. The samples were initially run at 100V until proteins were evenly located in the gel and the power was switched to 150V for approximately 45 minutes. The samples were checked regularly to prevent running off of the protein samples.

2.12.4 Blotting and transfer

Once proteins were separated based on their size and mobility (heavier proteins move slower and hence were at the top of the gel, whereas smaller proteins move faster and were found near the bottom of the gel), proteins were transferred onto a blotting paper. Polyvinylidine fluoride (PVDF) is a non-reactive membrane that has a non-specific affinity to amino acids. PVDF was activated by soaking in 100% methanol for 10 seconds. A sandwich of filter pad, 3mm filter

paper, activated PVDF membrane, gel, 3mm filter paper, and filter pad was assembled according to the manufacturer's protocol (Bio-Rad) (Figure 2.18).

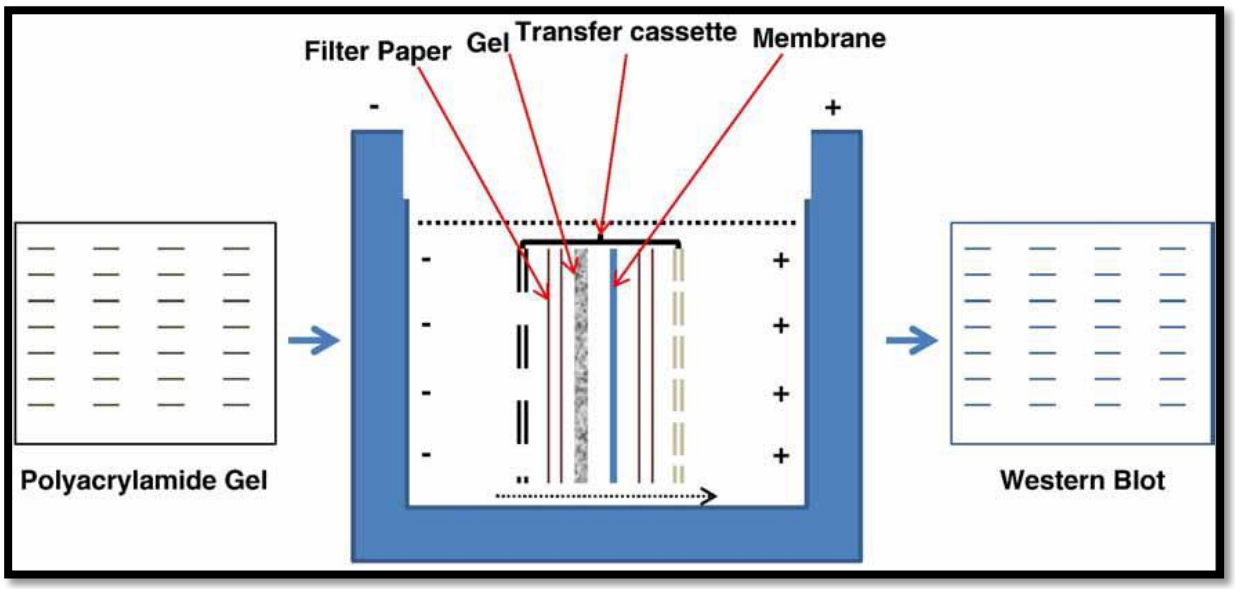

Figure 2.18 A schematic of the electro blot transfer process using an immersion procedure. Arrow at the bottom of the tank indicates transfer direction.

A small magnetic stirrer was placed in the tank, topped with 1 X transfer buffer made with 11.25g (w/v) of glycine, 2.42g (w/v) of tris base, 100ml (v/v) of methanol and distilled water to 1 litter. The blotter was placed inside the tank and the tank was run at 100V for at least 2.30 hours on a magnetic stirrer to create an even distribution of the electrolysis. An ice pack was also placed inside the tank to prevent over-heating of the buffer solution.

2.12.5 Blocking and antibody incubation

Once the transfer of protein from gel onto the PVDF membrane was complete the proteins were blocked with 5% blocking reagent containing 5g (w/v) of semi skimmed milk (Marvel) in 100ml of Tris buffer saline-Tween (TBST) made with 16g (w/v) of NaCl, 0.2g (w/v) KCl, 3g (w/v) of Tris base, 0.1% (v/v) Tween- 20 added to 800ml of distilled water adjusted pH to 7.6,

and distilled water added to 1 liter. The membrane was left in 30ml of blocking solution for about one hour on a shaking platform at room temperature. The milk mixture blocks unspecific binding of an antibody with the membrane. After one hour of blocking, the membrane was rinsed with TSBT and the primary antibody (anti BRCA2 (Ab-1) mouse (Calbiochem), diluted 1/300) was diluted in a one in five dilution of 5 % blocking buffer in 1x TBST and added onto the membrane overnight on a shaker set at medium pace (200rpm/minute) at 4°C. The following day the membrane was washed twice with 1x TBST for 15 minutes each and incubated with a secondary antibody, which is anti-mouse IgG in rabbit (Sigma), diluted 1/2000) diluted in one in five dilution of 5% blocking buffer on a shaker at RT for a minimum of one hour.

Table 2-7 Antibodies used in western blot experiments.

Antibody	Company	Source	Clonality	Dilution
BRCA2 Primary	Calbiochem	Mouse	Monoclonal	1:300
BRCA2 Secondary	Sigma	Mouse	Monoclonal	1:2000
GAPDH Primary	Abcam	Mouse	Monoclonal	1:5000
GAPDH Secondary	Abcam	Rabbit	Polyclonal	1:5000
Beta-actin Primary	Sigma	Rabbit	Polyclonal	1:1000
Beta-actin Secondary	DAKO	Rabbit	Polyclonal	1:2000

2.12.6 Protein detection with chemiluminescence

After one hour incubation with a secondary antibody the membrane was washed as before. Meanwhile, ECL plus (Enhanced chemiluminescence) kit (GE Healthcare) was taken out of the fridge and left at RT to warm up. The amount of ECL required for detection was based on the

size of the membrane and it was recommended by the manufacturer to be of a final volume of 0.125m/cm2 of membrane. The manufacturer's protocol was consulted for the exact mixture of chemicals A and B. As a rule of thumb, 2ml of reagent A was mixed with 50µl of reagent B. That is 1 part of reagent A mixed with 40 parts of reagent B. The ECL mixture was added onto the membrane and covered with saran wrap for five minutes in a dark room. The excess of the ECL was tipped off onto a paper towel, wrapped in the membrane facing down onto a piece of clean Saran wrap and placed in an x-ray cassette.

Unexposed ECL plus hyperfilm (GE healthcare) was put on top of the membrane and the cassette closed and left for exposure for five minutes. The x-ray films were developed either manually in developer first (Kodak) and fixer (Kodak), or using an automatic machine (Xograph). The exposure time was assessed accordingly depending on the size of the exposed bands. If the protein bands were faint and could not be visualized then a second film was exposed for a longer period. The ECL chemiluminescence was active for at least one hour.

2.13 TRAP (Telomere Repeat Amplification Protocol) Assay

Two sets of primers were used to do the TRAP, ACX (5' – GCGCGGCTTACCCTTACCCTTACCCTAACC - 3') and TS (5' – AATCCGTCGAGCAGAGTT- 3') (Life Technology). The TRAP assay was performed as per protocol published in (Wege et al, 2003).

Protein extract was made using 200 µl of CHAPS buffer (Millipore 220201-1GM Calbiochem, Millipore) and a total of 250ng of the extracted proteins were used in the assay. Samples were kept on ice at all times and homogenised using a needle syringe. The protein concentration of the unknown samples was measured on a Nano Drap, using the Pierce BCA Protein Assay Kit from Thermo Scientific. The products of the reaction were stained using 1x Syber Green (4309155 Applied Biosystem PCR Master Mix) which helped in quantification.

Each well contains a total of 25µl reaction mixture. This reaction mixture consists of 1µl ACX primer (0.05µg/µl), 1µl TS Primer (0.1µg/µl), 12.5µl of 1x Standard Syber Green, 1-4µl containing 250ng of protein) sample depending on the concentration of the protein needs to be added and (9.5µl – 6.5) DEPC water depending on the amount of protein added.

Each 96 well plate contains samples to make the standard curve (PC-3 hTERT), non-template control, heat inactivated sample and all the unknown samples (proteins extracted for cells in question). Each one of these samples is repeated in a minimum of 3 wells to give an average value. To make a negative control 6.5 µl DEPC water was added to master mix.

The standard curve was generated using the PC-3 hTERT cell line (Provided by Dr Terry Roberts, Brunel University). A new standard curve was generated each time a TRAP experiment was performed. The standard curve was made using serial dilutions of PC-3 hTERT cells (10^8 - 10^3). Heat inactivated samples contained 10^5 cell/µl of PC-3 hTERT cells concentration. The PC-3 hTERT sample were added to the DEPC water and heated to 85°C for 10 minutes. This was then added to the rest of the reagents (Syber Green, ACX Primer and TS primer). This sample also acts as a control and does not produce telomerase as the heat kills the enzyme.

The 96 well plate is then taken to the Q-PCR machine and the reaction is first incubated at 25°C for 20 minutes allowing the telomerase in the protein extracts to elongate the TS primer by adding TTAGGG repeat sequences. PCR is was then started at 95°C for 10 minutes to activate Taq polymerase followed by a two-step PCR amplification of 35 cycles at 95°C for 30 seconds and 60°C for 90 seconds.

2.14 Effects of 5-aza-CdR

The U2OS and MCF-7 cell lines were cultured at 370^{0}C, 5% CO2 as previously described. Briefly, 8x104 cells were seeded into 6-well plate to a total volume of 3ml media per well. Each experiment was carried out in duplicate with concentration of 5µM 5-aza-CdR (Sigma, St. Louis, MO) (Dr H. Yasaei, personal communication). Twenty four hours after cell plating, the cells were randomly assigned into, untreated, GFP (empty vector), MOI-10 and 5-aza-CdR groups (schematic Figure 2.19).

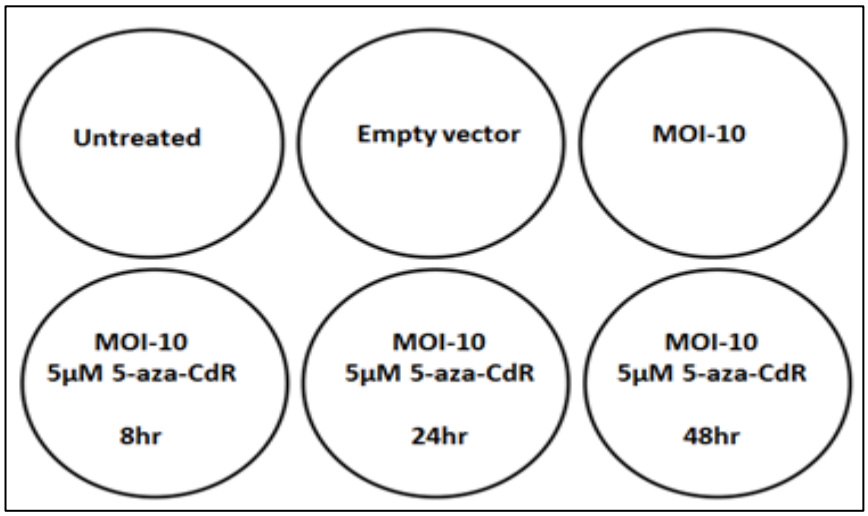

Figure 2.19 Schematic representation of the 5-aza-CdR experimental procedure.

The culture medium was replaced with fresh medium containing 5µM 5-aza-CdR. Based on time points (8, 24, 48 hours) the culture medium was replaced with fresh medium. The purpose of these treatments was based on the published data (Krishnan et al., 2006, Jin et al., 2012, He et al., 2005, Brooks et al., 2004). Then cell were left for one week. This was followed by RNA extraction, cDNA synthesis and knockdown measurement using real-time qRT –PCR.

Table 2-8 Represents U2OS and MCF-7 transfected cells treated with 5µM of 5-aza-CdR at different time points.

No of experiment	5-aza-CdR concentration (µM)	Time in culture treated with 5-aza-CdR	Total time in culture
1	5	8 hours	7 days
2		24 hours	
3		48 hours	

2.15 GFP expression determination by flow-cytometry

Cells were grown as described and $5x10^5$ cells were collected in suspension, washed in PBS once, and spun down at 1,500 rpm for 5 minutes. Supernatant was discarded carefully and the cells were then fixed in a solution containing methanol and Acetone (1:1 V/V) solutions. The cells were left at room temperature for 5 minutes.

Thereafter, the cells were centrifuged at 1,500 rpm for 5 minutes, and then supernatant was discarded. The cell pellets were washed twice by adding one ml of PBS, centrifuged, and then the supernatant was discarded carefully. Finally, the cell pellets were re-suspended in 1 ml of PBS. All samples were stored on ice until analysis by flow cytometry.

Flow cytometric analysis was performed on fresh samples using a Beckman coulter EPICS XL equipped with a single laser and a 4 colour (FITC, PE, ECD/PI and PeCy5) detection system (Becton Dickinson, USA). The expression of GFP (green) was measured in U2OS and MCF-7 cell lines. GFP, when excited by a 488 nm laser emits fluorescence that can be detected in the FL1 channel. A total of 20,000 cells were counted and perentage of cells gated with FL1 channel were calculated as GFP-positive cells.

2.16 Statistical Analysis

Basic statistical analysis such as descriptive measurements and graphical display were done using Microsoft Excel 2007 software. All t-tests were done at 95 percent significance with α set at 0.05.

Chapter -3

Telomere analysis in BRCA2 defective cell lines

3.1 Introduction

Chromosomal instability is a hallmark of breast cancer. For example, at least mild karyotypic changes are detectable in majority of breast tumours, whereas about one third is expected to harbour the severe chromosomal instability phenotype, a feature characterized by major and persistent karyotype changes. These changes include translocations, deletions and insertions, losses and gains of entire chromosomes, or chromosome arms, and finally changes in chromosome number (Teixeira et al., 2002). The mechanisms behind this instability are varied but can be classified broadly into two categories: mechanisms that affect chromosome structure and mechanisms that affect chromosome number (Venkitaraman, 2004). The key to preservation of chromosome structure is the network of molecular pathways collectively known as DNA damage response. These pathways sense, signal and repair DNA damage thus maintaining chromosome integrity (van Heek et al., 2002, Blackburn, 1991). The key to preserving the chromosome number are processes that ensure accurate segregation of chromosomes between daughter cells.

We are interested in mechanisms that affect preservation of chromosome structure. Research has shown that two genes of particular importance to understanding genetic forms of breast cancer, namely the breast cancer susceptibility genes, *BRCA1* and *BRCA2*, are tumor suppressor genes that affect chromosome structure by virtue of their involvement in the repair of DNA double strand breaks (DSBs) through homologous recombination (HR). Murine cells deficient in the BRCA2 homolog and human breast tumors with *BRCA2* mutations have been shown to have various chromosomal abnormalities (Gretarsdottir et al., 1998, Patel et al., 1998). Biochemical and molecular studies have revealed that *BRCA2* is involved in regulating HR, also known as homology directed repair (HDR), by cooperating with the recombinase Rad51 (Moynahan et al., 2001, Pellegrini and Venkitaraman, 2004). HDR, an error free DSB repair pathway, takes place during the S or G2 phases of the cell cycle. It is initiated when a

damaged DNA strand overrun the intact duplex of its sister chromatid DNA strand, which is then used as a template for restoring the damaged DNA strand (Venkitaraman, 2009). Moreover, HDR is involved in resolving stalled replication forks (Petermann et al., 2010). In deficient BRCA2 cells, during normal cell growth when the replication fork pauses or arrests, spontaneous DNA breakages lead to mutations and cancer (Lomonosov et al., 2003)

Numerous studies indicate that cells lacking functional DNA damage response genes frequently exhibit various deficiencies in maintaining specialized structures at chromosome ends, known as telomeres. Telomeres act as protective caps that prevent chromosomes from fusing with one another most likely by preventing cellular mechanisms that recognize DSBs to interpret natural chromosomal ends as pathogenic DSBs. This is achieved by the specific DNA structure that is only found at telomeres, the so called T (telomeric)-loop (Griffith et al., 1999). The T-loop structure is facilitated by a set of proteins known as shelterin, some of which bind either single or double stranded telomeric DNA (Blackburn, 2000, de Lange, 2004). Therefore, it is not surprising that this telomere capping function is closely linked with mechanisms that repair DNA DSBs. For example, key proteins involved the repair of DSBs through non-homologous end joining (NHEJ), Ku and DNA-PKcs, interact with some shelterin members (de Lange 2005) and their dysfunction leads to telomere dysfunction (Wong and Slijepcevic, 2004).

It is therefore possible that cells lacking functional BRCA2 may also show some form of telomere dysfunction phenotype. In line with this prediction recent studies indicate that this is the case. The first clear indication that BRCA2 affects telomere maintenance was provided by Badie et al. (2010). This study revealed that BRCA2 associates with telomeres in S and G2 phases of the cell cycle and helps Rad51 recombinase access telomeres. Furthermore, the study has shown that lack of functional BRCA2 leads to telomere shortening in mouse cells and human tumor samples. The finding that telomeres may be abnormal in human breast cancer samples originating from BRCA2 affected individuals was replicated by another study

(Bodvarsdottir et al., 2012). Therefore, genomic instability in BRCA2 defective cells may be caused, at least in part, by telomere dysfunction.

In this chapter we wanted to expand on the initial findings and examine more closely the nature of telomeric abnormalities caused by dysfunctional BRCA2 using cytological methods. To this end we employed 3 sets of human and Chinese hamster cell lines defective in BRCA2 and several cytological techniques for assessing telomere function and chromosome sensitivity to ionizing radiation.

3.2 Results

3.2.1 Cell lines and rationale

In order to assess the extent to which dysfunctional BRCA2 contributes to genomic instability through causing telomere dysfunction it is important to have suitable cell lines and accompanying controls. Studies published so far used exclusively murine BRCA2-/- cells reported previously to have unstable karyotypes (Patel et al 1998; Badie et al. 2010) and human BRCA2 defective tumours exhibiting chromosomal instability (Badie et al. 2010; Bodvarsdottir et al., 2012). Our approach was to use different BRCA2 defective cell models that have not been explored before with a view to (i) expanding the initial findings implicating BRCA2 in telomere maintenance and (ii) uncovering any potentially novel phenotype that was not observed in murine cells or human tumors.

The sets of BRCA2 defective cell lines at our disposal included:

- A Chinese hamster cell line defective in BRCA2 with the accompanying normal control cell line and two cell lines in which the BRCA2 defect has been corrected.
- Two human lymphoblastoid cell lines from BRCA2 carriers and a control cell line;
- The Capan1 human carcinoma cell line and accompanying control line.

The Chinese hamster cell line, V-C8, carries two mutations in exons 15 and 16 of BRCA2 resulting in truncated proteins (Wiegant et al., 2006). The cell line is derived from the normal Chinese hamster cell line V79B which is used as a control. Two additional cell lines have been generated by Wiegant et al. (2006) from the V-C8 cells by correcting the BRCA2 defect by either introducing a BAC containing the normal mouse BRCA2 gene (V-C8+BRCA2) or human chromosome 13 that contains the normal human BRCA2 gene (V-C8 #13).

Lymphoblastoid cell lines, GM14622 and GM14170, have been derived from BRCA2 mutation carriers. The cell line GM14622 was from a patient with a frameshift mutation, 6503delTT, in exon 11, leading to a truncation at codon 2099 (Coriell 2009). The cell line GM14170 was derived from a patient with a 1 bp deletion at nucleotide 6174 in exon 11 resulting in a frameshift starting at codon 1982 and terminating at codon 2003 (Coriell 2009).

Capan-1 is the pancreatic carcinoma cell line lacking one BRCA2 allele. The other BRCA2 allele contains a truncation (6174delT) mutation resulting in the production of a truncated protein product (Goggins et al., 1996). MCF-7 was selected as the control line because it has normal BRCA2.

We analysed the above cell lines with the aim of (i) expanding the initial finding that BRCA2 causes telomere dysfunction and (ii) uncovering any potentially novel telomere dysfunction features. The usual indicators of telomere dysfunction in any cell type are changes in telomere length and/or increased frequencies of end-to-end chromosome fusions (ECFs). We started by analysing telomere length and monitoring ECFs frequencies in all cell lines. Results of our analysis are shown in the next section.

3.2.2 Telomere length analysis

There are several methods for measuring telomere length including Southern blot, Q-FISH (quantitative fluorescence in situ hybridization), flow-FISH, real-time PCR and STELA (Lansdorp et al., 1996, Rufer et al., 1998, Baird et al., 2003). Each method has advantages and disadvantages. The choice of the measurement method is critically dependent upon the material to be analysed. Chinese hamster chromosomes are known to have large blocks of interstitial telomeric sequences in centromeric regions of most chromosomes (McIlrath et al., 2001). This poses a major problem for measuring telomere length in cells from Chinese hamster as these interstitial telomeric sequences mask real telomeric sequences. The only method that is suitable for measuring telomere length in Chinese hamster chromosomes is Q-FISH as it is able to make a clear distinction between interstitial telomeric sequences and real telomeres. Using this method it has been shown that primary fibroblast cell cultures established from 4 Chinese hamster female animals had average telomere length in the region of 38 kb (Slijepcevic and Hande, 1999). This is similar to the average telomere length observed in mouse chromosomes (McIlrath et al., 2001).

Therefore, we used the Q-FISH method to measure telomere length in the set of four Chinese hamster cell lines described above. As can be seen, most Chinese hamster chromosomes have large blocks of interstitial telomeric sequences around their centromeres apart from two longest chromosomes 1 and 2 (Figure 3.1). Terminal telomeric sequences are visible as small size signals in most chromosomes (Figure 3.1). It is unlikely that the size of these signals is equivalent to 38 kb as observed in primary Chinese hamster cell cultures (Slijepcevic and Hande, 1999).

Most established immortalized Chinese hamster cell lines, such as CHO-K1 and V79 cell lines, have very short telomeres estimated to be in the region of 1 kb (Slijepcevic and Hande, 1999). The mechanisms behind this dramatic telomere loss from 38 kb to 1 kb are not completely clear

given that Chinese hamster cells express telomerase activity throughout their replicative history. It has been speculated that this loss could be due to extra-strong exonuclease activity required for producing G-strand overhangs, tight control of telomerase access to telomeres, or lack of telomerase-independent mechanisms in these cells (Slijepcevic and Hande, 1999).

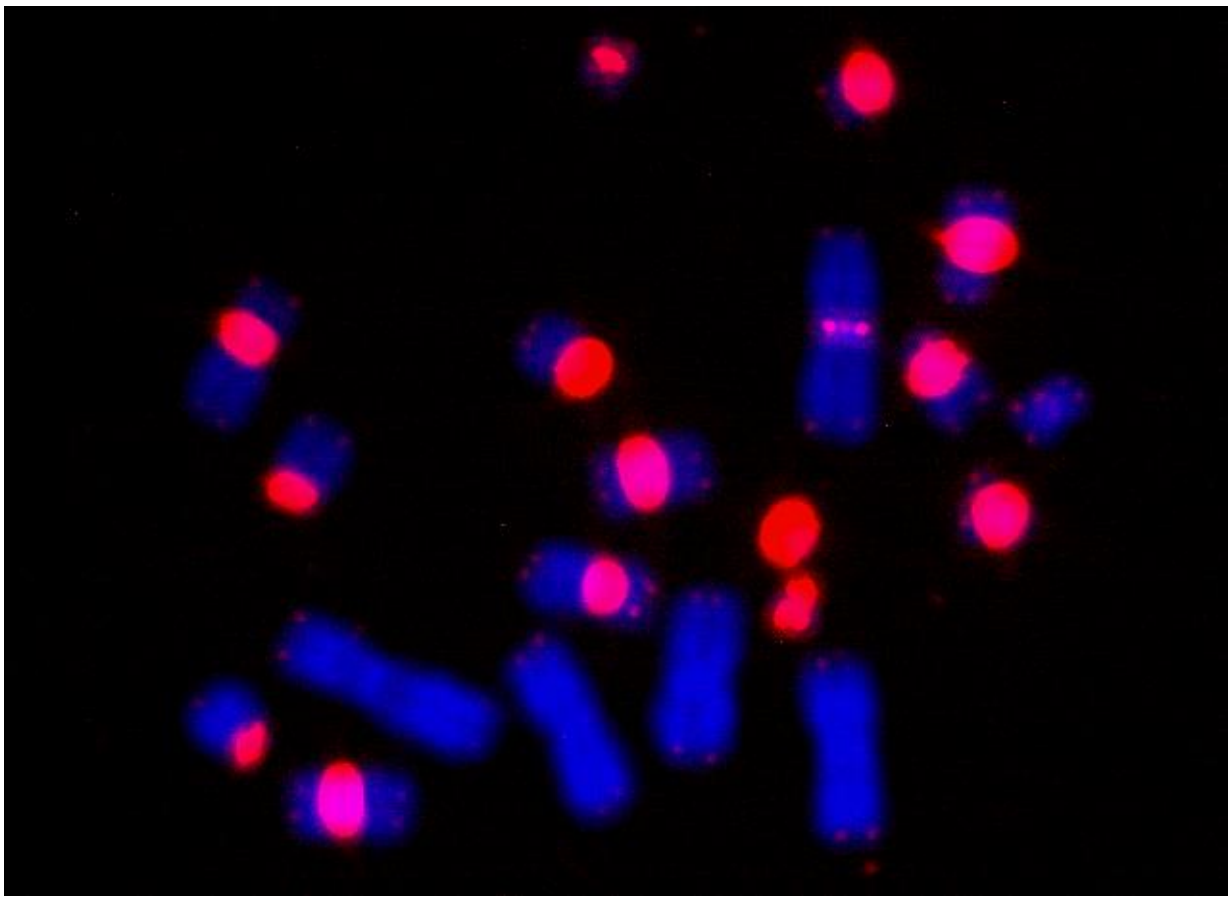

Figure 3.1 A metaphase cell from the V79B cell line after hybridization with the telomeric PNA probe. Note the weakness of terminal telomeric signals.

The presence of the weak terminal telomeric signal in the V79B cell line (Figure 3.1) is consistent with the reported short telomeres in Chinese hamster immortalized cell lines (Slijepcevic and Bryant 1995). The remaining cell lines, V-C8+BRCA2, V-C8 #13and V-C8 had similarly weak telomeric signals (not shown). The Q-FISH analysis of telomere length (TFU – telomere fluorescence units are arbitrary) in these cell lines is shown in (Figure 3.2).

Based on this analysis average telomere lengths have been calculated for each cell line as shown in Figure 3.3. Statistical analysis has revealed that V79B cells have significantly longer telomeres than V-C8 cells ($P<0.01$).

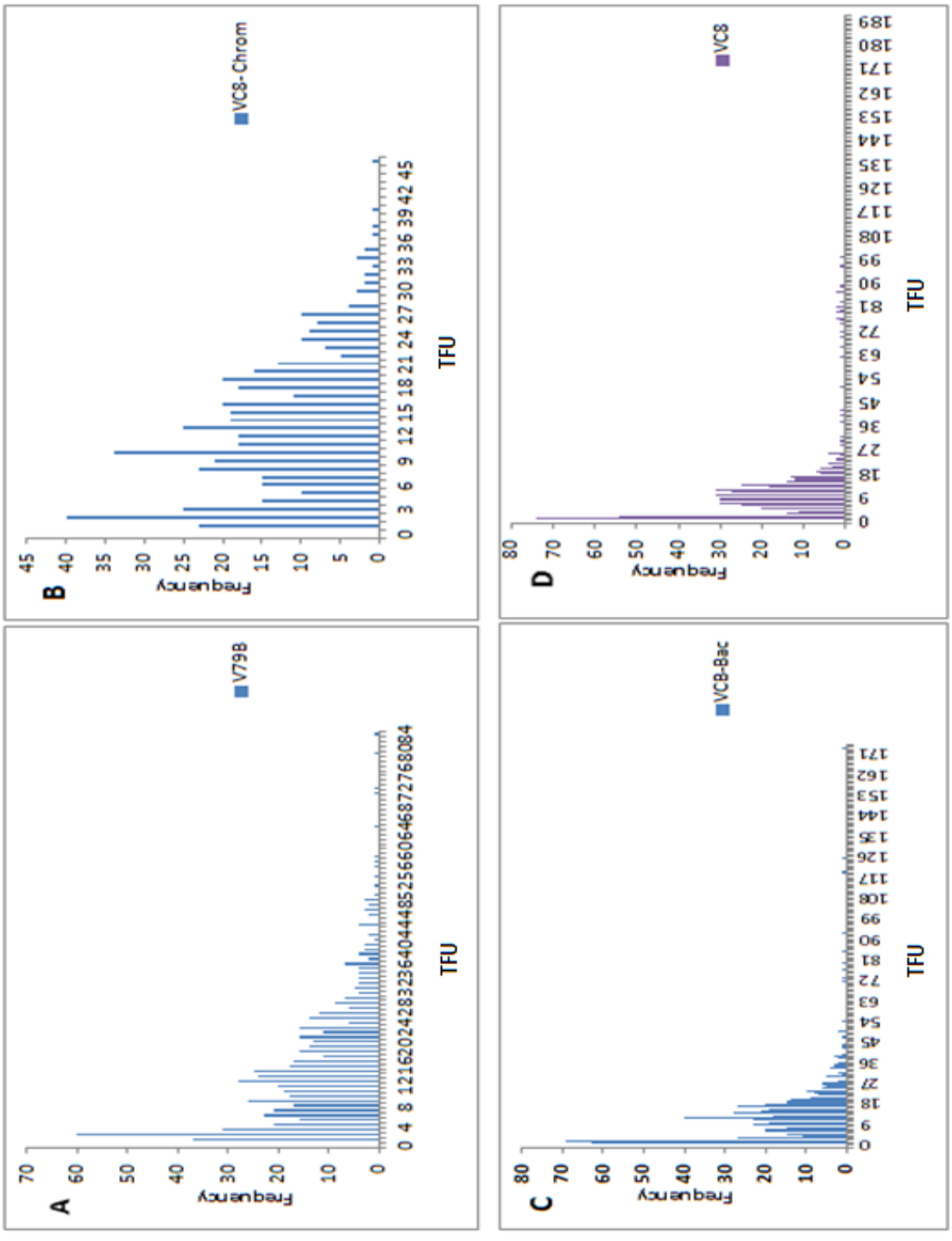

Figure 3.2 Telomere length measured by Q-FISH telomere frequency in four Chinese hamster cell lines. Graph A) V79B, B)VC8-Chrom, C)VCB-Bac, D)VC8. A total of 10 intact metaphases were analysed. TFU – telomere fluorescence units are arbitrary units.

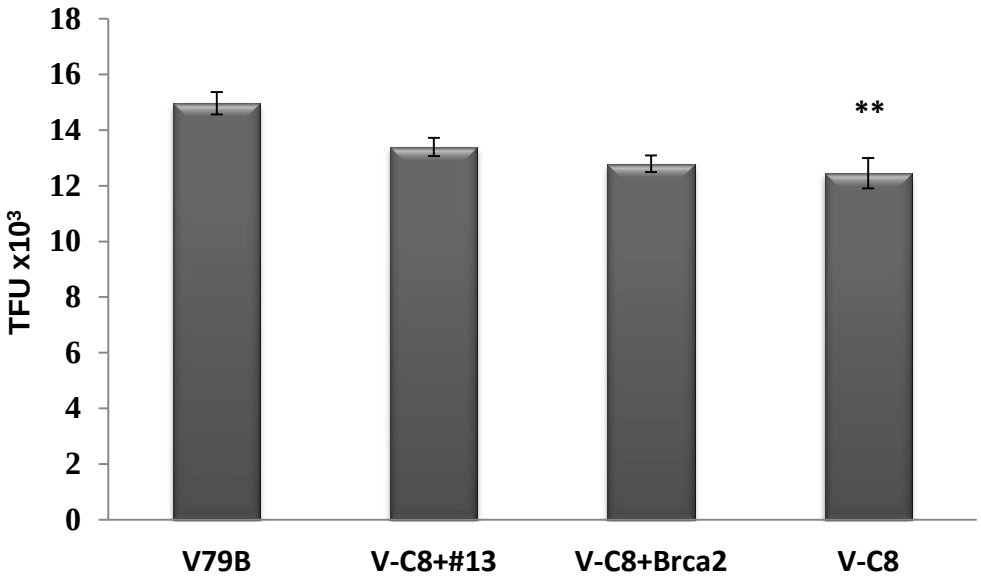

Figure 3.3 Average telomere length in four Chinese hamster cell lines. Statistical analysis has revealed that V-C8 cells have significantly shorter telomeres than V79B cells **=P<0.01, Error bars represent SEM.

Next, we measured telomere length in lymphoblastoid cell lines from BRCA2 mutation carriers. For this purpose we used our recently developed method, IQ-FISH (interphase Q-FISH) (Ojani 2012). This method is a fast and reliable estimate of the average telomere length in interphase cells. It relies on using mouse cell lines, LY-R and LY-S, as calibration standards. The telomere fluorescence is expressed in arbitrary units as CCFL (Corrected Calibrated FLuorescence) following the calibration method using the LY-R and LY-S cell lines as described in Ojani (2012). It is important to stress that this method is suitable for DNA damage response defective cell lines, which are usually impaired in cell proliferation as a result of cell cycle checkpoint blocks, thus making metaphase chromosome preparations, which require fast proliferating cells, impractical. Both BRCA2 defective lines showed poor proliferation properties. As a result, we have not been able to obtain good quality chromosome preparations from these cell lines that are required for Q-FISH. Therefore, we resorted to the IQ-FISH method.

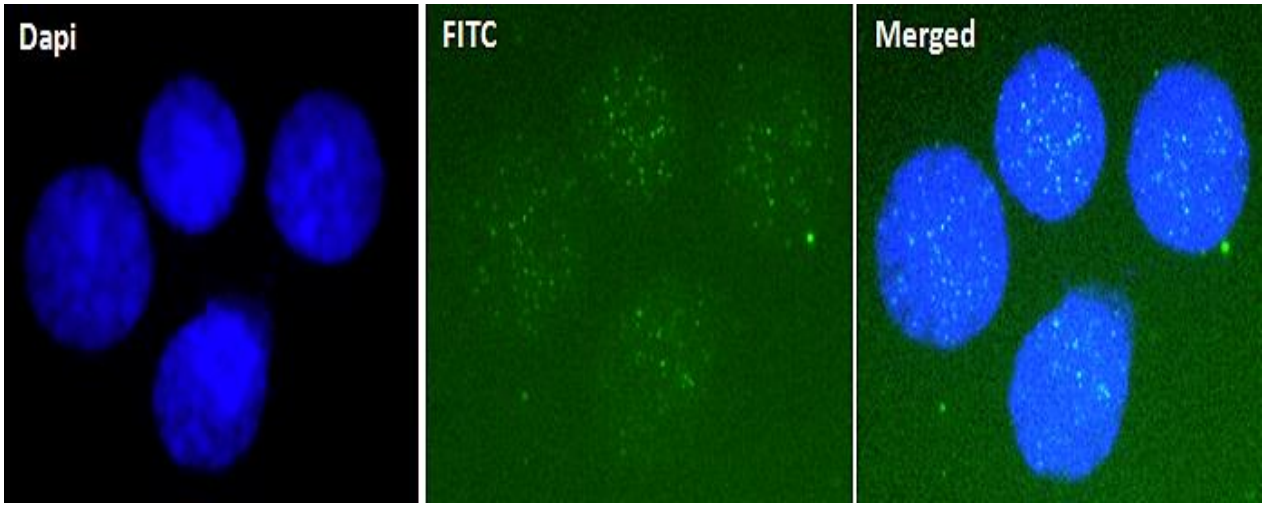

Figure 3.4 Example of digital images of GM00893 human lymphoblastoid cells in interphase after hybridization with telomeric PNA oligonucleotides.

A representative example of the hybridization pattern after hybridization with telomeric PNA probe seen in the control cell lines is shown in (Figure 3.4). Our IQ-FISH results indicate that both cell lines from BRCA2 mutation carriers (GM14622 and GM14170) showed shorter telomeres than the normal cell line (GM00893) (Figure 3.5). GM14170 cells showed almost three times shorter telomere relative to the control GM00893 cell line ($P<0.001$). The extent of telomere loss in the GM14622 cell line was smaller but still significant (*** = $P<0.001$, Error bars represent SEM) (Figure 3.5).

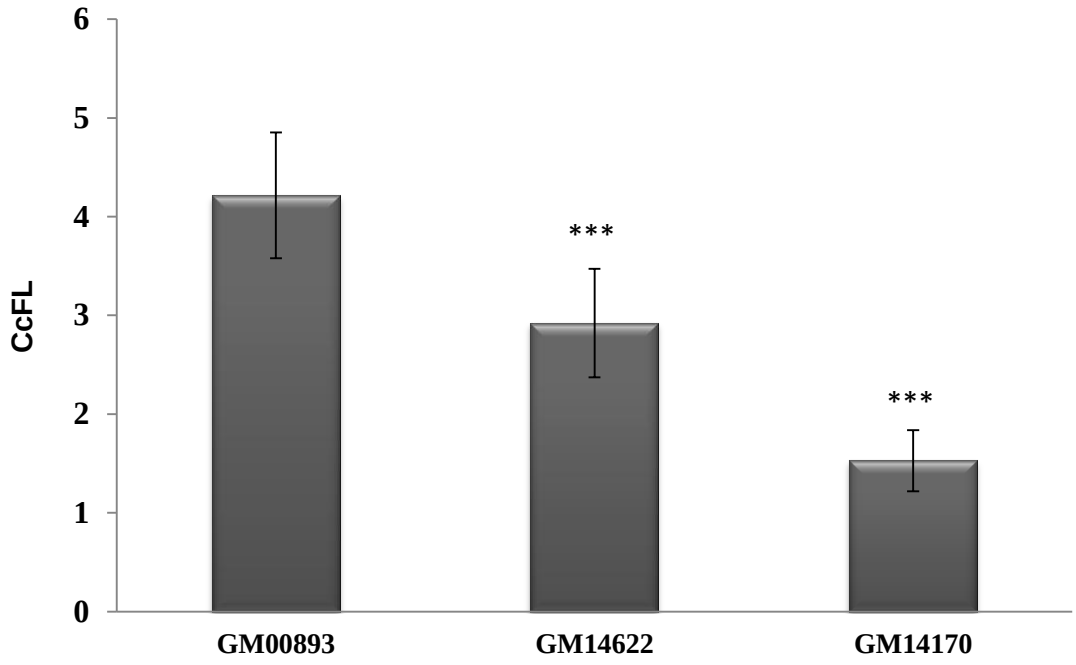

Figure 3.5 Corrected calibrated fluorescence (CcFl) in BRCA2 defective cell lines relative to the control cell line. GM14170 cells showed approximately 3x shorter telomere compared to the control cell line and GM14622 cells showed almost 1.5x shorter telomeres relative to the control cell line. The GM14170 cell line had shortest telomeres. ***=P<0.001, Error bars represent SEM.

Next, we measured telomere length in the CAPAN-1 cell line and the MCF-7 control cell line using the IQ-FISH method. The BRCA2 defective CAPAN-1 cell line showed significantly shorter telomeres than the control MCF-7 cell line (*** = P<0.001, Error bars represent SEM (Figure 3.6).

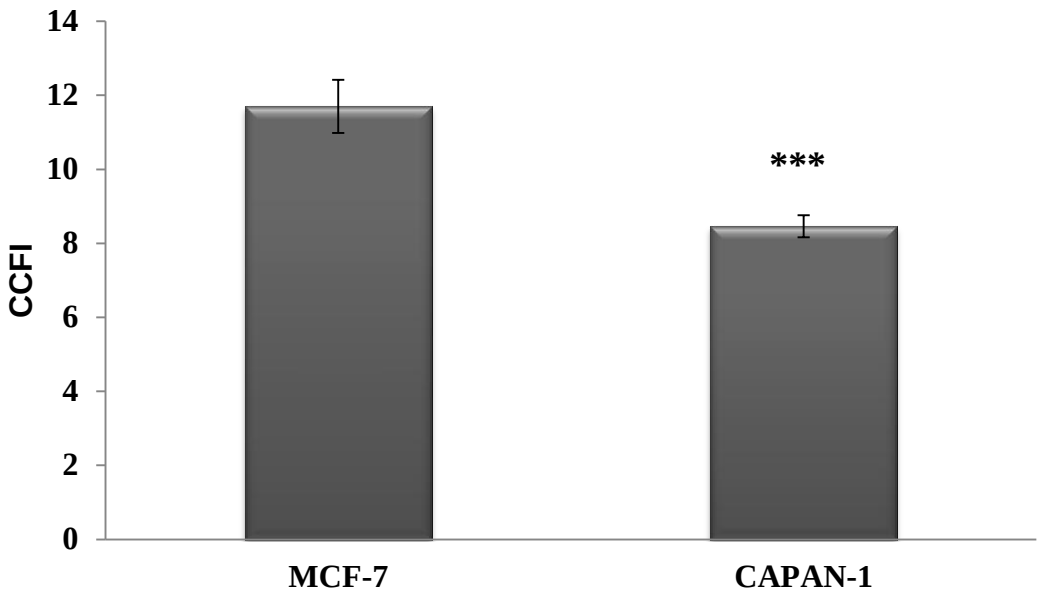

Figure 3.6 Corrected calibrated fluorescence (CcFl) in *BRCA2* defective cell line relative to the control cell line. *** = P<0.001, Error bars represent SEM.

Based on the analysis of telomere length in the above sets of cell lines we can conclude that, in line with the initial findings (see above) the BRCA2 deficiency leads to significant telomere shortening in human and Chinese hamster cell lines. However, introduction of functional BRCA2 did not restore telomere length in Chinese hamster cells.

3.2.3 Telomere function analysis

Next, we measured frequencies of ECFs in metaphase cells. For this purpose we prepared metaphase chromosome spreads using standard methods and measured frequencies of spontaneous ECFs on Giemsa stained chromosome preparations. Results of this analysis are shown below.

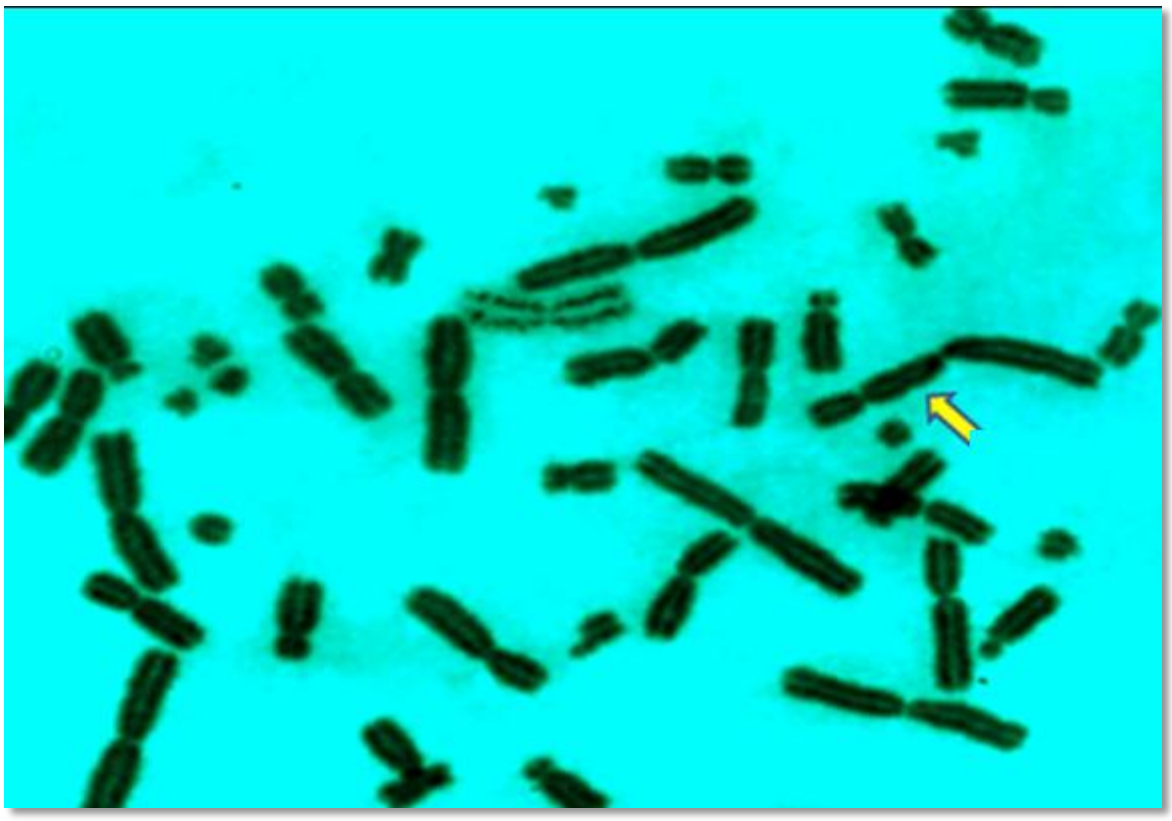

Figure 3.7 An ECF in the V-C8 cell line. Chromosomal abnormalities in VC8 Chinese hamster BRCA2 defective cell. An example shows Giemsa stained chromosome from VC8 with dicentric chromosome (arrowhead) as consequence of chromosome end-to-end fusions (CEFs).

A representative example of an ECF observed in the V-C8 cell line is shown in (Figure 3.7). As expected this cell line showed the highest frequency of ECFs (Figure 3.8). This is consistent with the previously reported results that BRCA2 defects lead to telomere dysfunction. Introduction of functional BRCA2 caused either a complete disappearance of ECFs or their significant reduction (Figure 3.8). The normal control cell line, V79, lacked ECFs completely (Figure 3.8).

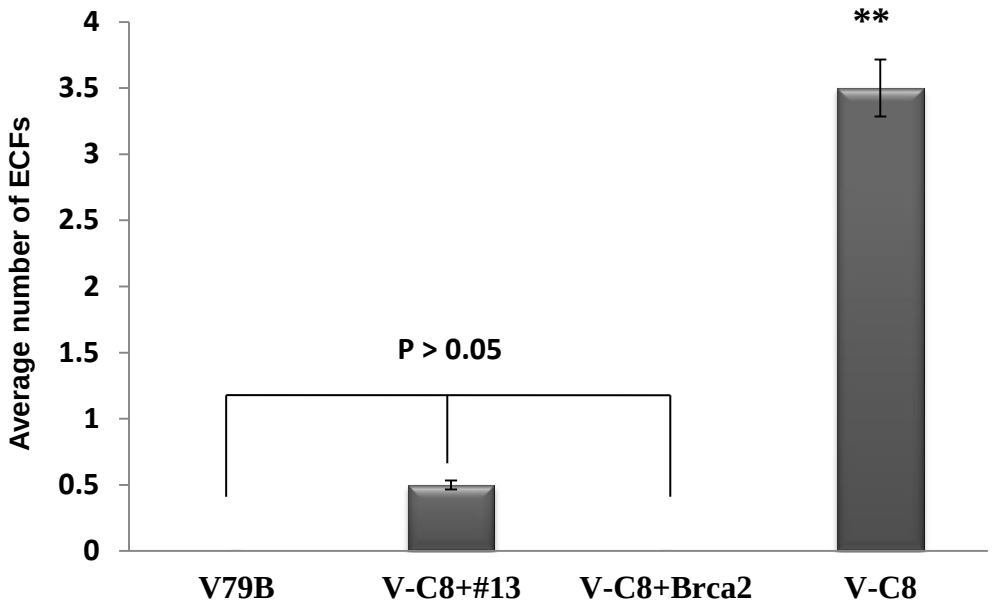

Figure 3.8 Frequencies of ECFs in Chinese hamster cell lines. A total of 60 cells have been analysed in two different experiments and the average values presented. Error bars represent standard error of the mean (SEM). ** Significantly higher than wild type (P< 0.01).

Next, we measured ECF frequencies in human lymphoblastoid cell lines. Similarly to the Chinese hamster cells both cell lines from BRCA2 carriers showed higher frequencies of ECFs relative to the control cell line (Figure 3.9). However, ECF values were significantly higher relative to control cells in only one cell line. When these results are combined with the telomere length measurement in the same cell lines (Figure 3.5) this points to the evidence of haploinsufficiency. One functional copy of BRCA2 in cell lines from BRCA2 carriers is not capable of maintaining telomere length and function at the normal level.

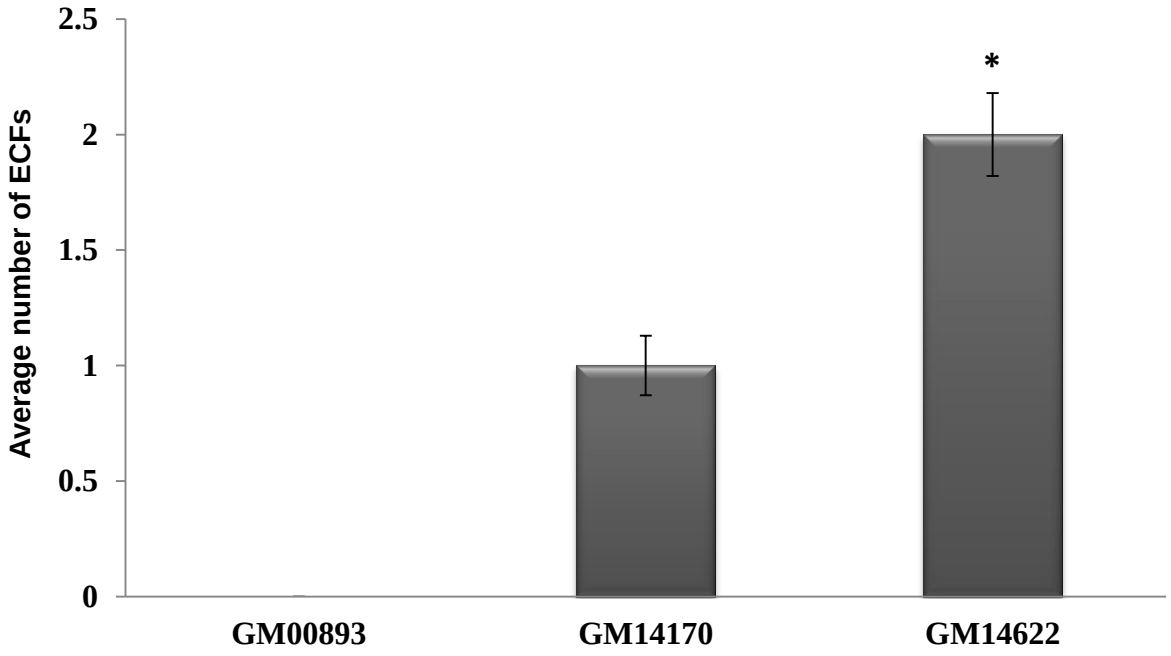

Figure 3.9 Frequencies of ECFs in human lymphoblastoid cell lines.

A total of 30 metaphases in two separate experiments have been analysed. Error bars represent standard error of the mean (SEM). * Significantly higher than wild type (P< 0.05).

We could not monitor ECFs in CAPAN-1 and MCF7 cells accurately because of the complex karyoptypes in both cell lines which precluded identification of true ECFs.

Therefore, based on the analysis of ECF frequencies of Chinese hamster cell lines and human lymphoblastoid cell lines we can conclude that mutations in BRCA2 lead to telomere dysfunction. This confirms initial findings reported by Badie et al. (2010) and Bodvarsdottir et al. (2012).

3.2.4 Analysis of recombination frequencies at telomeres

An important question is whether any other telomere dysfunction phenotype, apart from changes in telomere length or frequencies of ECFs, exists in BRCA2 defective cells. Other types of telomere dysfunction abnormalities in BRCA2 defective cells including telomere fragility and telomere dysfunction induce foci (TIF) have been reported (Badie et al., 2010,

Bodvarsdottir et al., 2012). However, abnormalities that result directly from defects in HR have not been investigated extensively.

Given the involvement of BRCA2 in HR it is possible that its effects on telomeres may be recombination related. The CO-FISH technique, commonly used to detect the orientation of DNA sequences along the chromosomes (Meyne et al., 1994), can detect recombination events at telomeres in the form of sister chromatid exchanges (SCEs) (Bailey et al., 2004). When CO-FISH is carried out using the telomeric PNA probe, it is expected to yield only two telomeric signals per chromosome (present at 2 out of 4 chromatids) as opposed to four telomeric signals (present at 4 out of 4 chromatids) generated by conventional FISH (for full details of the CO-FISH procedure see material and methods). The presence of >2 signals/chromosome after CO-FISH is indicative of genetic recombination events, or exchanges of telomeric sequences between sister chromatids (Londono-Vallejo et al., 2004), events known as T-SCEs (Telomeric SCEs). Frequencies of T-SCEs can be efficiently assessed in each cell line under investigation using CO-FISH.

Therefore, we analysed T-SCE frequencies in our set of cell lines. Examples of T-SCEs observed in Chinese hamster cells are shown in (Figure 3.10). The hybridization pattern observed at chromosomal ends is typical of CO-FISH i.e. one signal/2 sister chromatids (Figure 3.10 A and B). However, the signal visible at centromeres is still very strong, probably reflecting the large quantity of interstitial telomeric sequences present in Chinese hamster chromosomes (Figure 3.10 A and B). Furthermore, in order to identify telomeric signals with no ambiguity we enhanced terminal telomeric signals digitally which resulted in the enhancement of the centromeric signal as well. Nevertheless, the presence of strong centromeric signal did not interfere with our analysis. It was clear that the BRCA2 defective cell line, V-C8, exhibited a significantly higher frequency of T-SCEs relative to the control

V79 cell line (P< 0.05) (Figure 3.10 C). It was interesting that the introduction of functional human BRCA2 rescued the abnormal T-SCE frequency phenotype in full (Figure 3.10 C).

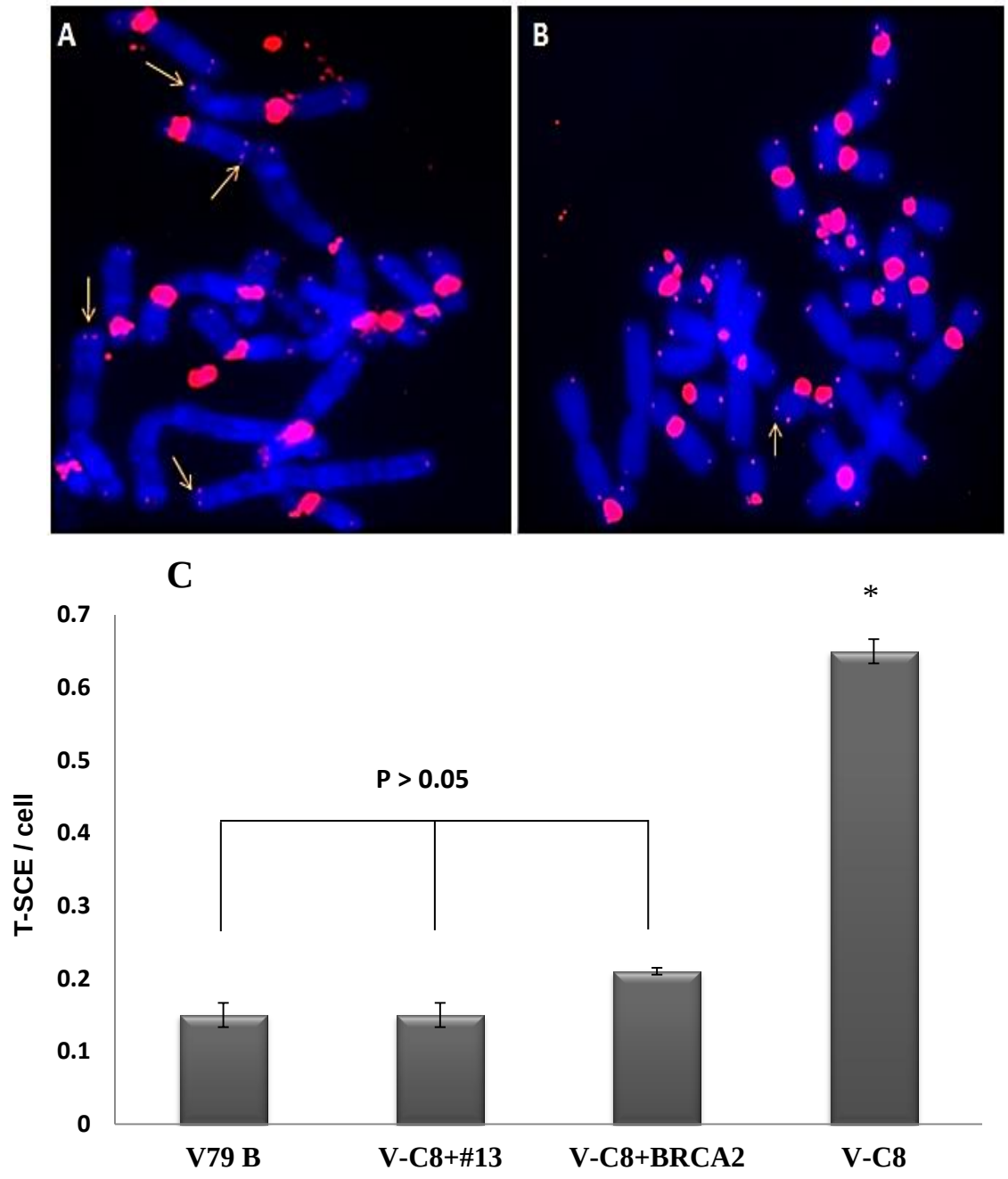

Figure 3.10 Frequency of T-SCEs in Chinese hamster cell lines.

A) V-C8 and B) V79B Chinese hamster cell lines indicated by arrows. C) Average frequencies of T-SCEs in four cell lines. Error bars represent standard error of the mean (SEM). * Significantly higher than wild type (P< 0.05).

We next analysed T-SCEs frequency in human lymphoblastoid cell lines. Examples of T-SCEs in human chromosomes are shown in (Figure 3.11 A-C). Our analysis revealed that both cell lines from BRCA2 mutation carriers showed significantly higher frequencies of T-SCEs relative to the control cell line ($P < 0.0001$) (Figure 3.11 D). Similarly to telomere length/function analysis in the same cell lines (Figure 3.5 and Figure 3.9) the finding of elevated T-SCE rates is consistent with haploinsuficiency i.e. one functional copy of BRCA2 is not sufficient to maintain the normal level of T-SCEs.

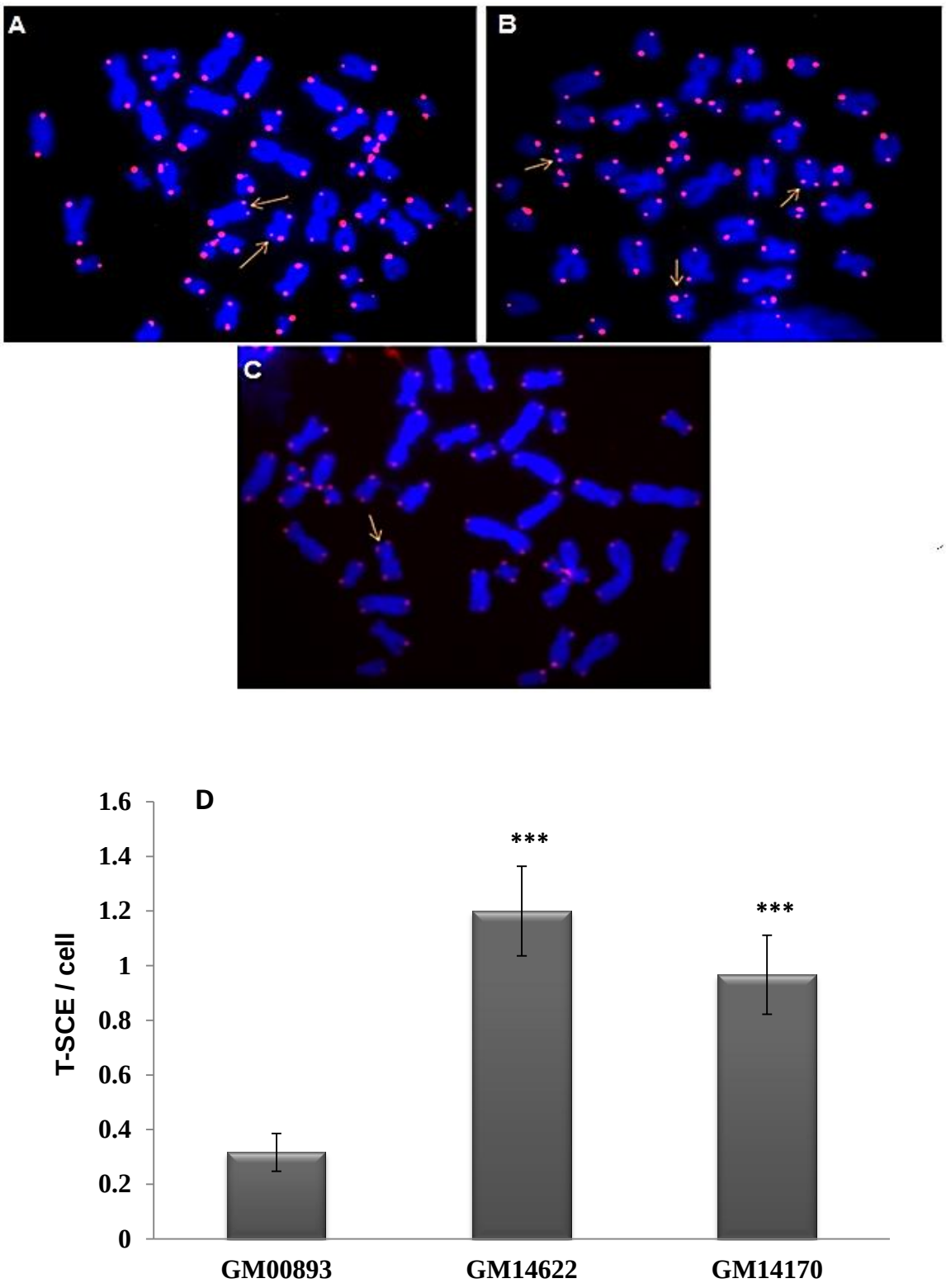

Figure 3.11 Frequency of T-SCEs in human lymphoblastoid cell lines. A) GM14170, B) GM14622 C) GM00893 and D) Frequencies of T-SCE/cell in three lymphoblastoid cell lines. Error bars represent standard error of the mean (SEM). *** Significantly higher than wild type (P< 0.0001).

Finally, we analysed T-SCE frequencies in Capan-1, the pancreatic carcinoma cell line, and the MCF7 control cell line. Examples of T-SCEs observed in these cell lines are shown in Figure 3.12 A and B. Our analysis revealed significantly higher frequencies of T-SCEs in the Capan-1 cell line relative to the control MCF7 cell line (Figure 3.12 C).

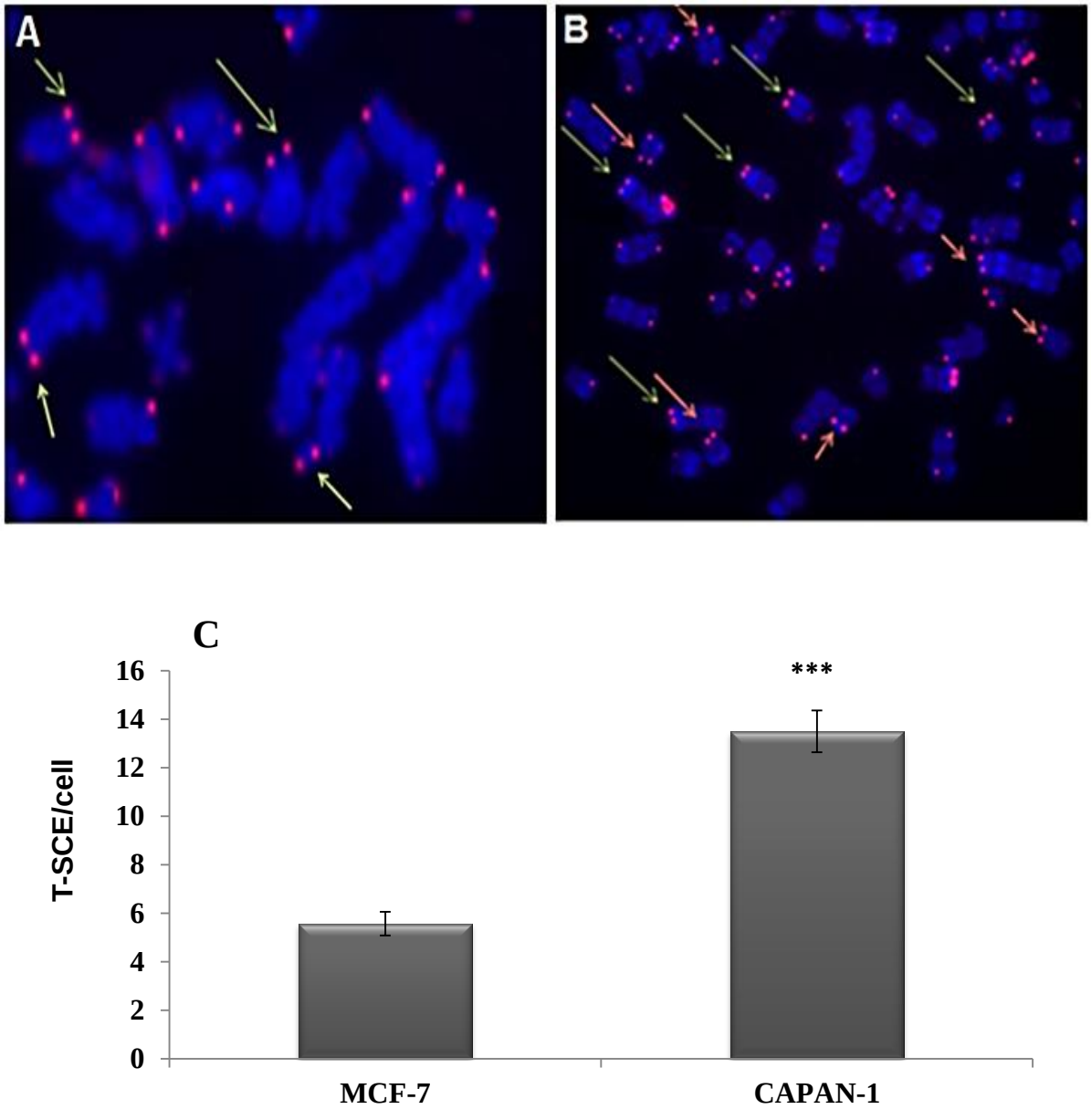

Figure 3.12 Frequency of T-SCEs in MCF-7 and Capan-1. A) MCF-7 and B) Capan-1 cell lines. C) Average T-SCE frequencies in two cell lines. Error bars represent standard error of the mean (SEM). *** Significantly higher than wild type (P< 0.0001).

Taken together, our CO-FISH analysis revealed a novel phenotypic feature associated with dysfunctional BRCA2: increased frequencies of T-SCEs. This is directly in line with the BRCA2 role in HR. Given that elevated levels of T-SCEs indicate hyper-recombinant telomeres it is possible that the function of BRCA2 is to suppress recombination at telomeres.

3.2.5 Radiation induced chromosomal abnormalities

Defects in HR, including defects in BRCA2, cause chromosomal instability, which becomes more pronounced when cells are exposed to DSB inducing agents such as ionizing radiation (IR) (Crespan et al., 2010). In order to assess telomere function in Chinese hamster and human lymphoblastoid cells further we monitored frequencies of radiation-induced chromosome aberrations (CAs) using two approaches: (i) standard methods based on Giemsa staining and (ii) FISH based methods. Giemsa staining can detect CAs induced by IR either in the G2 phase of the cell cycle, or in the G1 phase of the cell cycle.

Furthermore, Giemsa staining can be used to detect micronuclei (MN) resulting from radiation induced chromosome breaks. These breaks cannot attach to mitotic spindle and remain detached from the main nucleus in the form of a much smaller nucleus or MN (Kirsch-Volders et al., 2011). It is important to stress that Giemsa-based methods cannot make distinction between CAs involving telomeric or non-telomeric sequences. However, they are still useful because they can detect whether dysfunctional BRCA2 causes chromosome sensitivity to IR or not in our set of cell lines. However, the FISH-based approach is capable of detecting specifically radiation-induced CAs involving telomeric sequences. The CO-FISH method detects exclusively radiation-induced chromosome breaks or exchanges involving telomeres as described (Bailey 2004, Goggins et al., 1996). The rationale behind this approach is shown diagrammatically in (Figure 3.13).

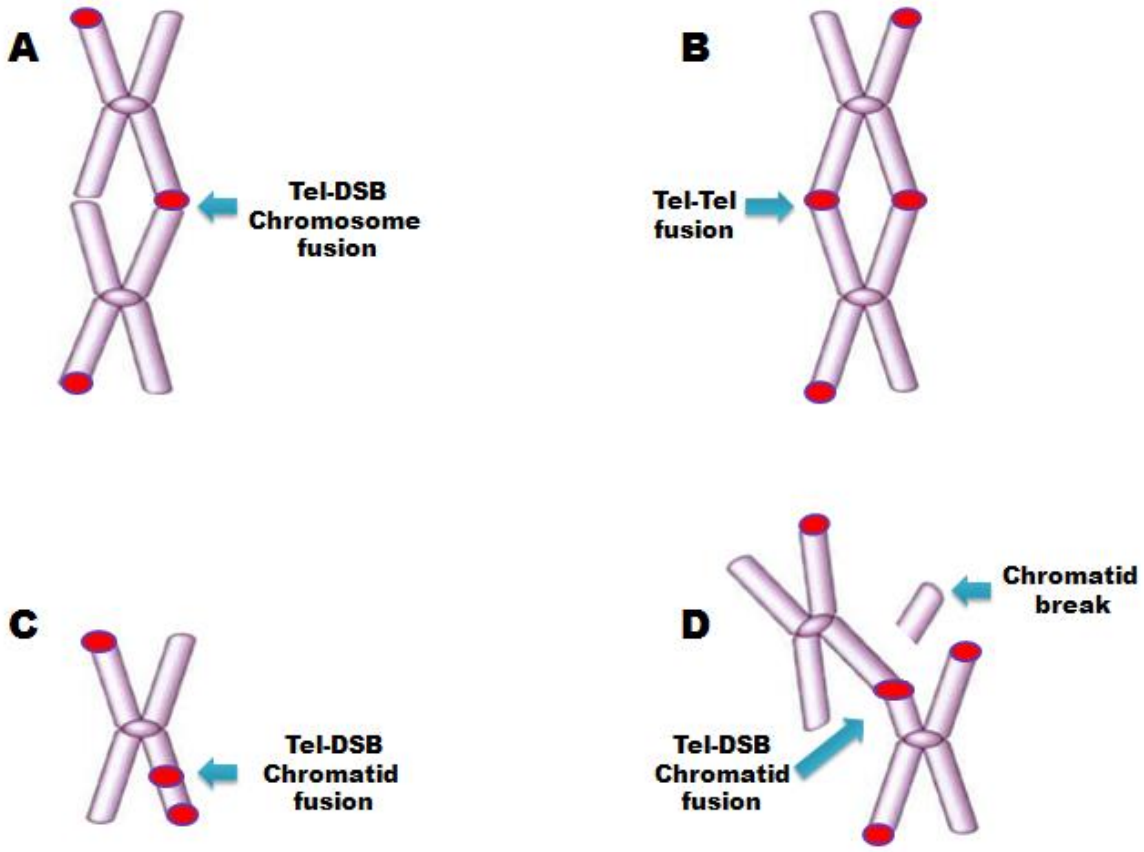

Figure 3.13 Diagram shows telomere dysfunction detected by CO-FISH. A)Tel-DSB fusion between a broken chromosome end and telomere. B) Telomere-Telomere fusion between two telomeres (telomeric signals at the point of fusion). C and D) Telomere DSB fusion between a telomere and a broken chromatid. The diagram was adapted from (Bailey et al., 2004).

We started by analysing radiation-induced CAs in a set of Chinese hamster cell lines using Giemsa staining. Examples of radiation-induced CAs, either in G2 or in the G1 phase of the cell cycle are shown in (Figure 3.14). For the G2 assay we treated cells with 0.5 Gy of gamma rays and for the G1 induced CAs we used a dose of 2.0 Gy. As expected BRCA2 defective cells showed significantly higher frequencies of CAs, relative to control cells, in both cases.

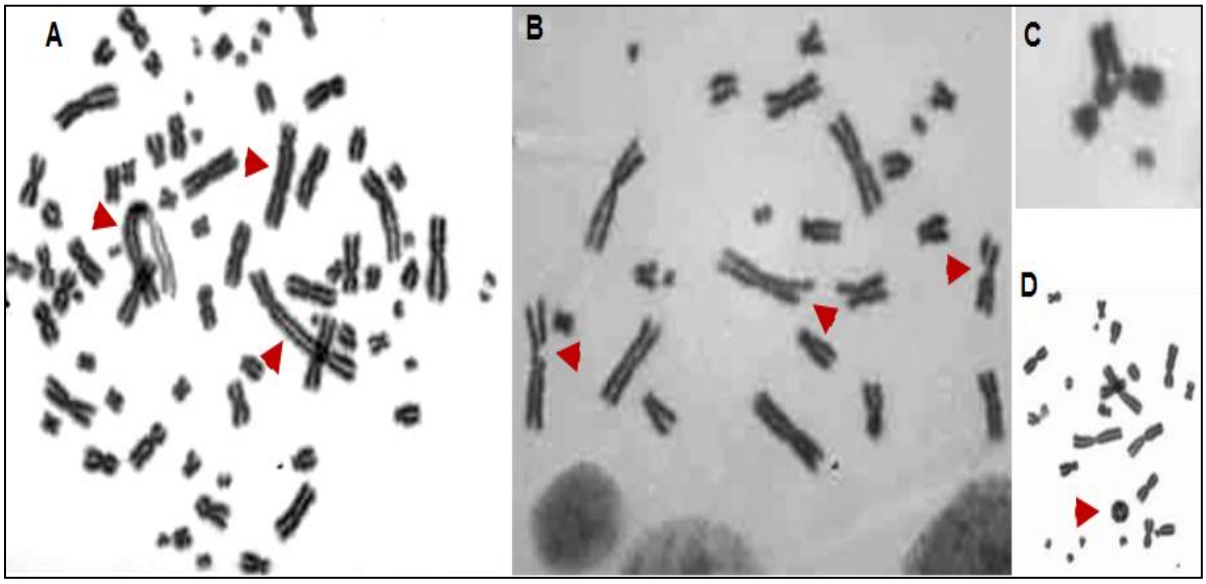

Figure 3.14 Examples of chromosomal abnormalities in Chinese hamster cells. A) dicentric chromosomes, B) chromatid breaks, C) triradial structures and D) a ring chromosome.

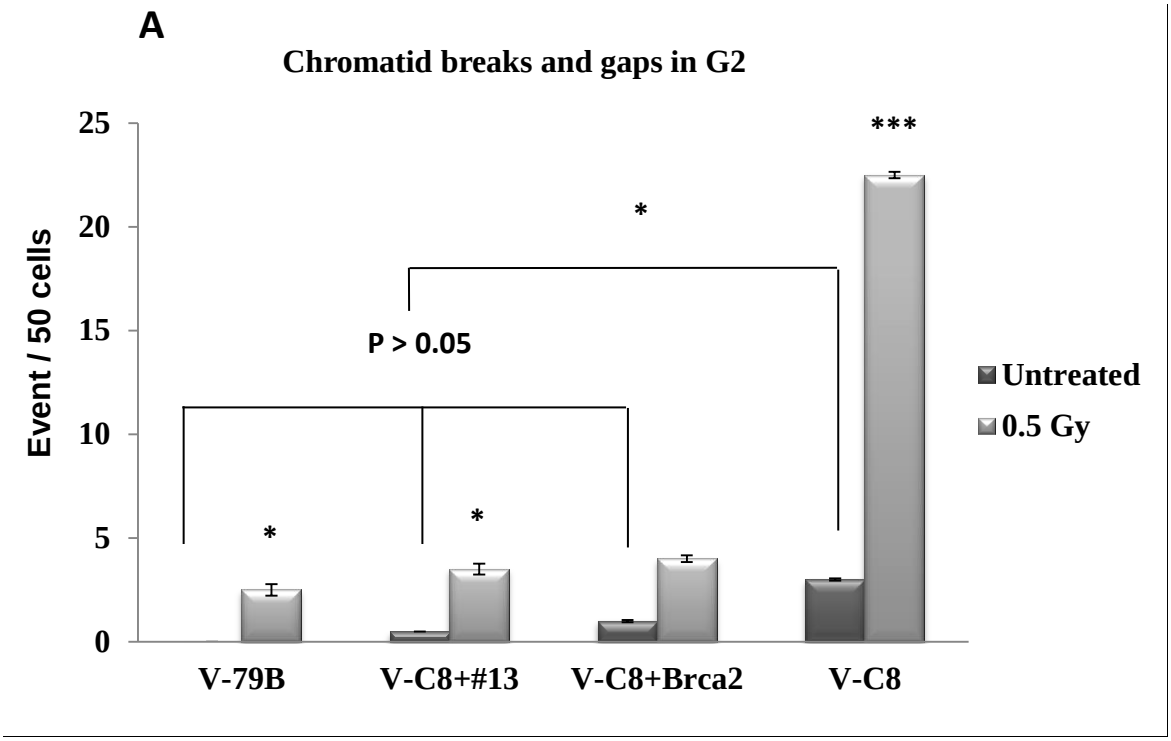

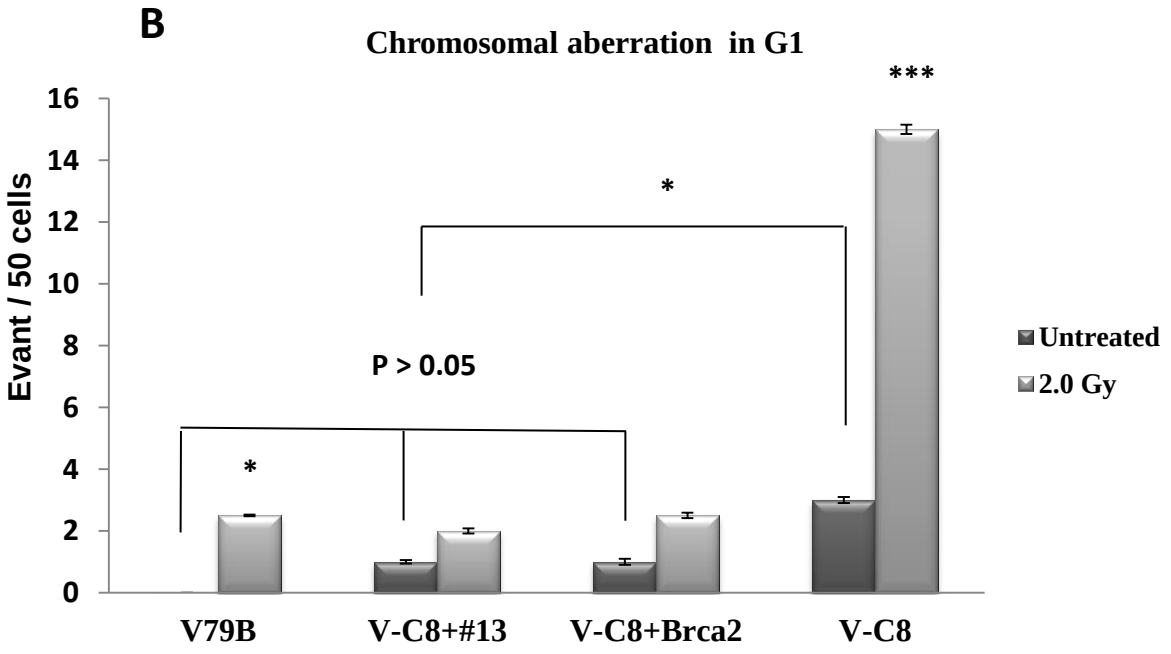

Figure 3.15 Frequency of Chromosomal abnormalities in Chinese hamster cells. A) Frequencies of radiation-induced induced chromatid breaks (G2 assay). B) Frequencies radiation induced CAs in G1 phase. *=P<0.05, **=P<0.01, ***=P<0.001, Error bars represent SEM.

These results show that BRCA2 defect leads to increased chromosomal sensitivity to IR. However, the contribution of telomeres to this sensitivity cannot be assessed based on Giemsa staining.

In order to assess whether telomeric sequences contribute to radiation-induced chromosome sensitivity we used CO-FISH. The cell lines were exposed to 2.0 Gy of gamma radiation. A total of 50 metaphases in each cell line were analysed. Results of this analysis are shown in (Table 3.1). Examples of CAs involving telomeric sequences are shown in (Figure 3.16).

It was clear from this investigation (Table 3-1) that BRCA2 defective cells (V-C8) are significantly more sensitive to radiation-induced damage that involves telomeres than all other cell lines. *significantly higher at $P<0.05$.

Table 3-1 Frequencies of radiation-induced CAs after CO-FISH.

	Cell line	Telo-telo fusion	Chromosome exchange	Breaks	Total CAs
Non-Treated	**V-79B**	0	0	0	0
	V-C8+#13	0	1 ± 0.17	0	1
	V-C8+BAC	0	2 ± 0.19	0	2
	V-C8	4 ± 0.25*	22 ± 0.75 *	1 ± 0.17	27
Treated	**V-79B**	1 ± 0.17	1 ± 0.17	1 ± 0.17	3
	V-C8+#13	0	4 ± 0.27	1 ± 0.17	5
	V-C8+BAC	0	5 ± 0.30	2 ± 0.19	8
	V-C8	5 ± 0.32*	25 ± 0.79*	8 ± 0.36*	38

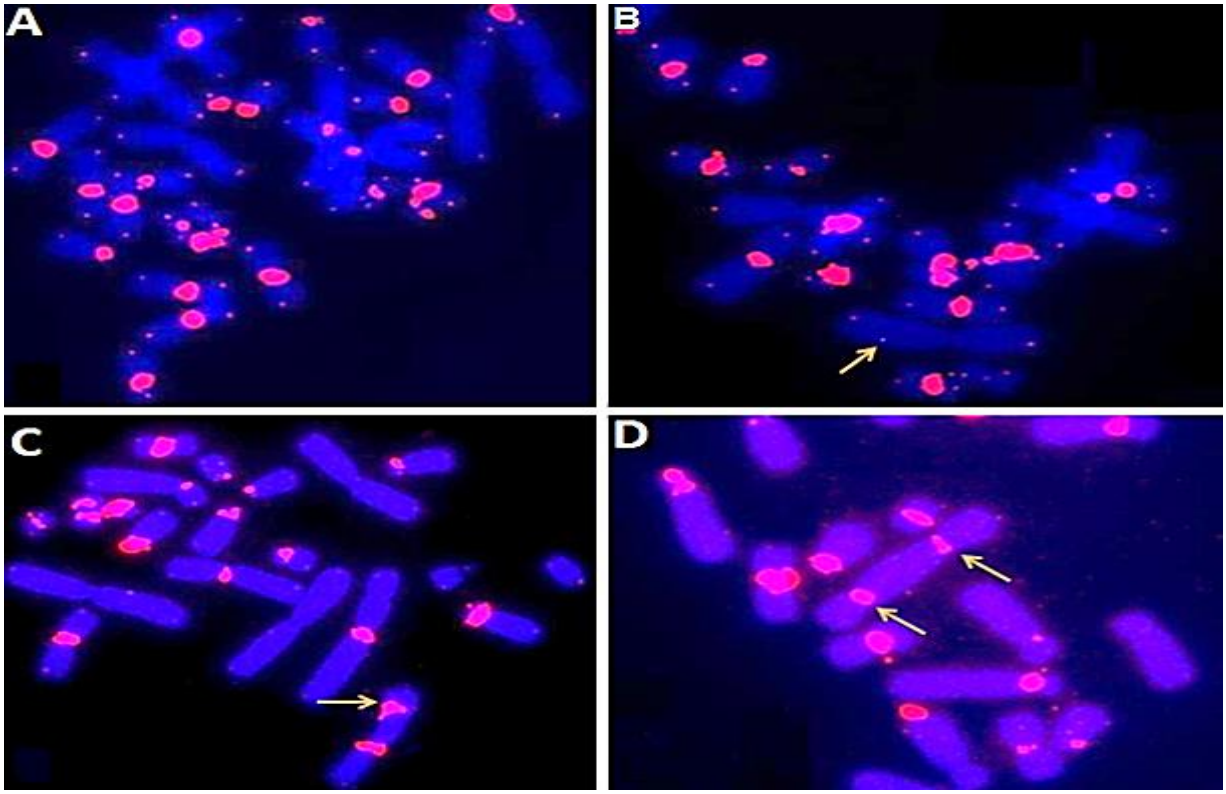

Figure 3.16 Digital images show chromosomal aberrations in Chinese hamster cells after CO-FISH. A) A normal cell with no aberrations. B) Tel-DSB chromatid fusion. C) Chromosome exchange. D) Tel-Tel fusion (containing two centromeres).

3.2.6 Radiation induced CAs in human cells

Next, we analysed CA frequencies in human lymphoblastoid cell lines by either Giemsa staining or CO-FISH. All the cell lines were exposed to 0.5 Gy of gamma radiation for the G2 assay which detects chromatid breaks and gaps. The cells were also exposed to 2.0 Gy radiation for G1 assay where cells were analysed for the presence of dicentric chromosomes, ring chromosomes and chromosome fragments. Examples of G1 and G2 type CAs are shown in (Figure 3.17).

After exposure to 0.5 Gy for the G2 assay it was noted that the BRCA2 defective cells lines, GM14622 and GM14170, had a higher incidence of chromatid breaks and gaps compared to the control GM00893 cell line (Figure 3.19). It was also noted that the exposure to 2.0 Gy of

gamma radiation resulted in higher frequencies of dicentric and ring chromomes and chromosome fragments in BRCA2 defective cells in comparison to the normal control cell line (Figure 3.18). Therefore, our results indicate that human BRCA2 defective cell lines show increased incidence of radiation-induced chromosome damage relative to the control cell line. This is another example of haploinsuficiency.

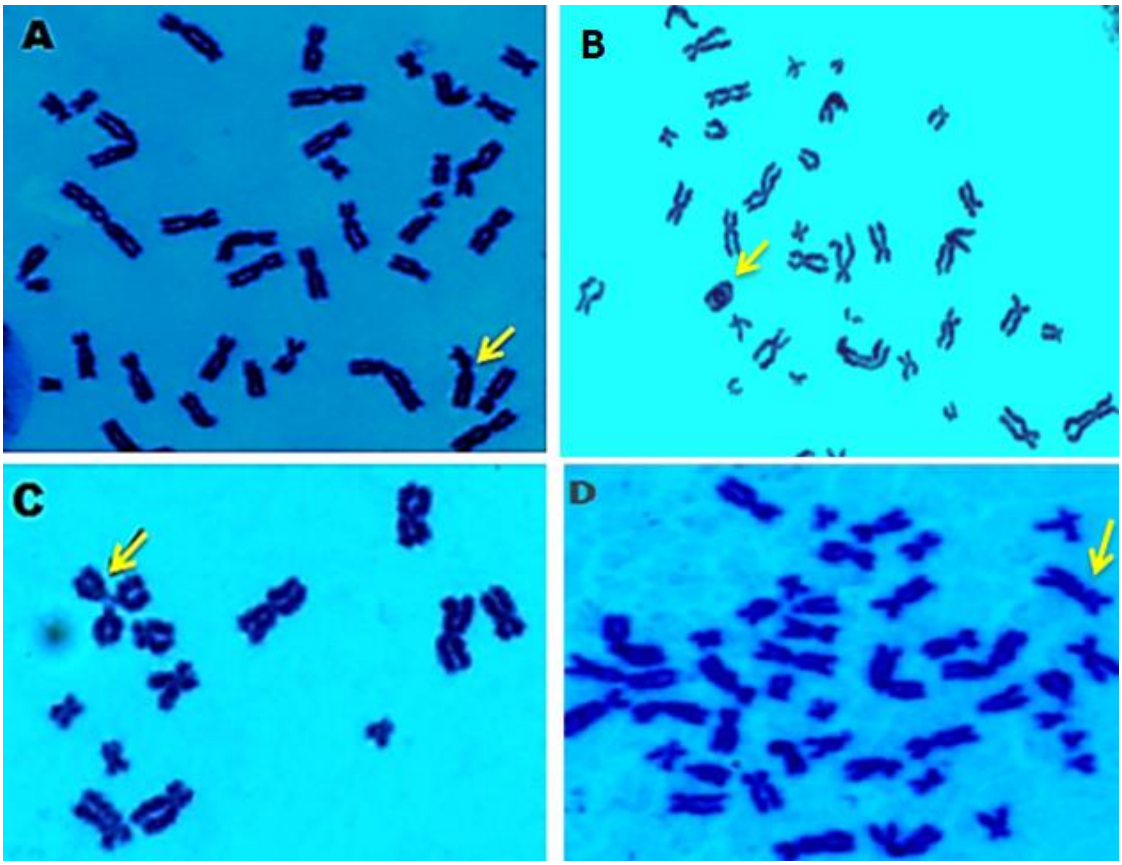

Figure 3.17 Chromosomal abnormalities in human lyphoblastoid cells lines indicated by arrows. A) Dicentric chromosome. B) a ring chromosome. C) Triradial. D) Chromatid breaks.

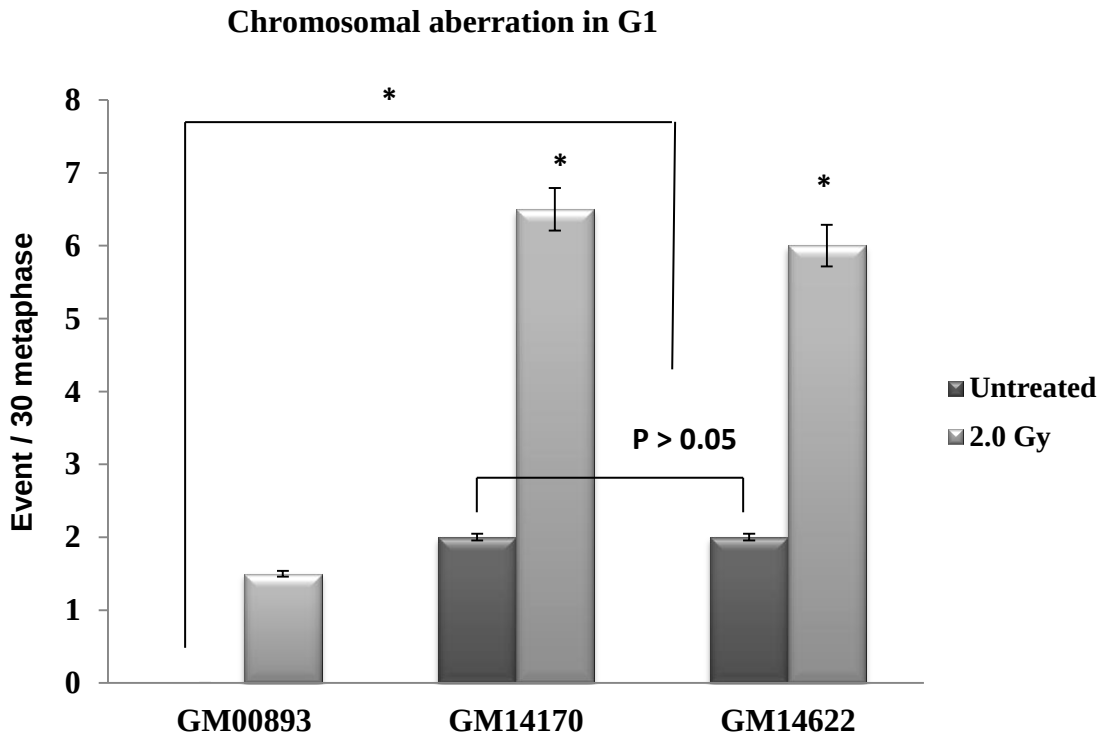

Figure 3.18 Frequencies of G1 induced CAs in human cell lines. *=P<0.05, the error bars represent SEM.

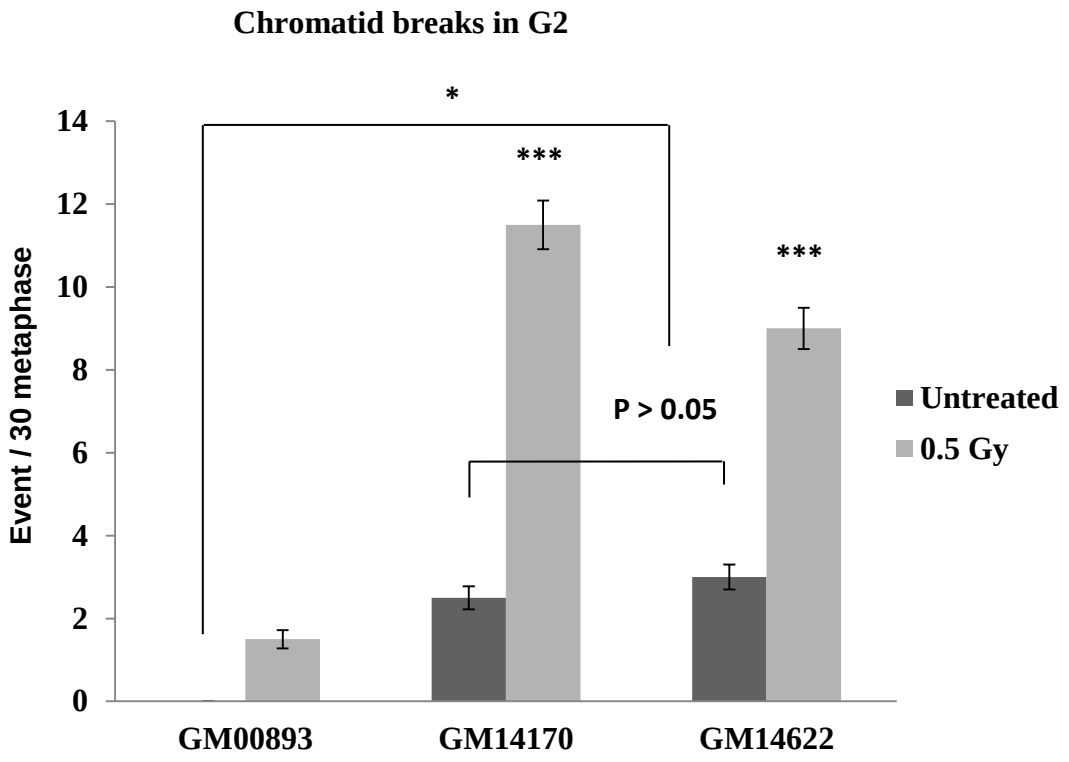

Figure 3.19 Frequencies of G2 induced chromatid breaks. *=P<0.05, **=P<0.01, ***=P<0.001, Error bars represent SEM.

In order to confirm this haploinsuficiency with a different method we used the Cytochalasin B MN test. It is now accepted that micronuclei are derived from acentric chromatid fragments, acentric chromosome fragments or whole chromosomes that fail to segregate properly in anaphase (Fenech, 2010). Representative examples of MN observed are presented in (Figure 3.20).

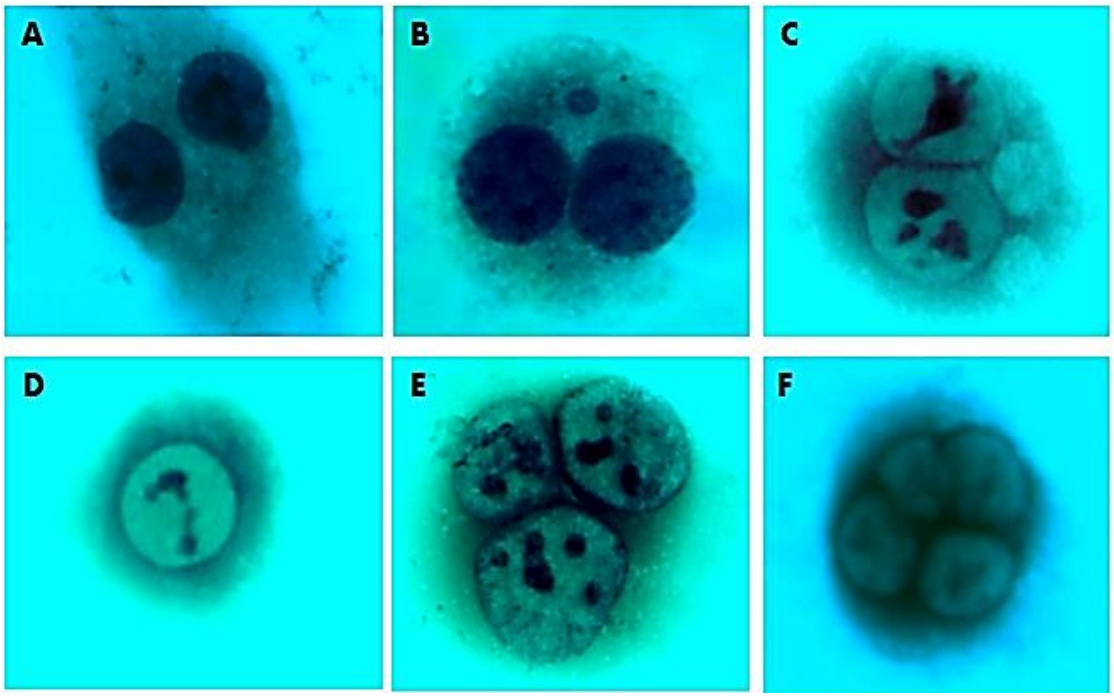

Figure 3.20 Scoring binucleated cells in human lymphoblastoid cell lines. A) A normal binucleated cell after the cytokinesis block MN assay. B) an example of a MN; C) a binucleated cell with two MN that are lightly stained most likely due to extensive chromatin decondensation; D,E and F) viable mono-, tri- and quadrinuclear cells that are excluded from analysis.

Our analysis revealed a clear distinction the spontaneous level of micronucleus frequencies in the un-irradiated and irradiated human lymphoblastoid cell lines treated with Cyt-B is shown in (Figure 3.21). The level of MN formed following IR is higher in the BRCA2 defective cell lines compared to the normal cell line. The highest level of MN was seen 24 hours after exposure to 2Gy and 4Gy radiation in both BRCA2 defective cell lines comparison of control. It is important to note that statistical analysis has been carried out in two different ways. Results of this analysis at each radiation dose (0.5, 1.0, 2.0 and 4Gy) are represented by stars above the bars, which were calculated relative to the BRCA2 control cell lines. The table above the graphs shows the results of the statistical comparison between each sample at different doses of radiation. *=P<0.05, **=P<0.01, ***=P<0.001, Error bars represent SEM.

Cell lines	0.5 Gy	1.0 Gy	2.0 Gy	4.0 Gy
GM00893	P > 0.05	P > 0.05	**	***
GM14622	P > 0.05	P > 0.05	***	***
GM14170	P > 0.05	P > 0.05	***	***

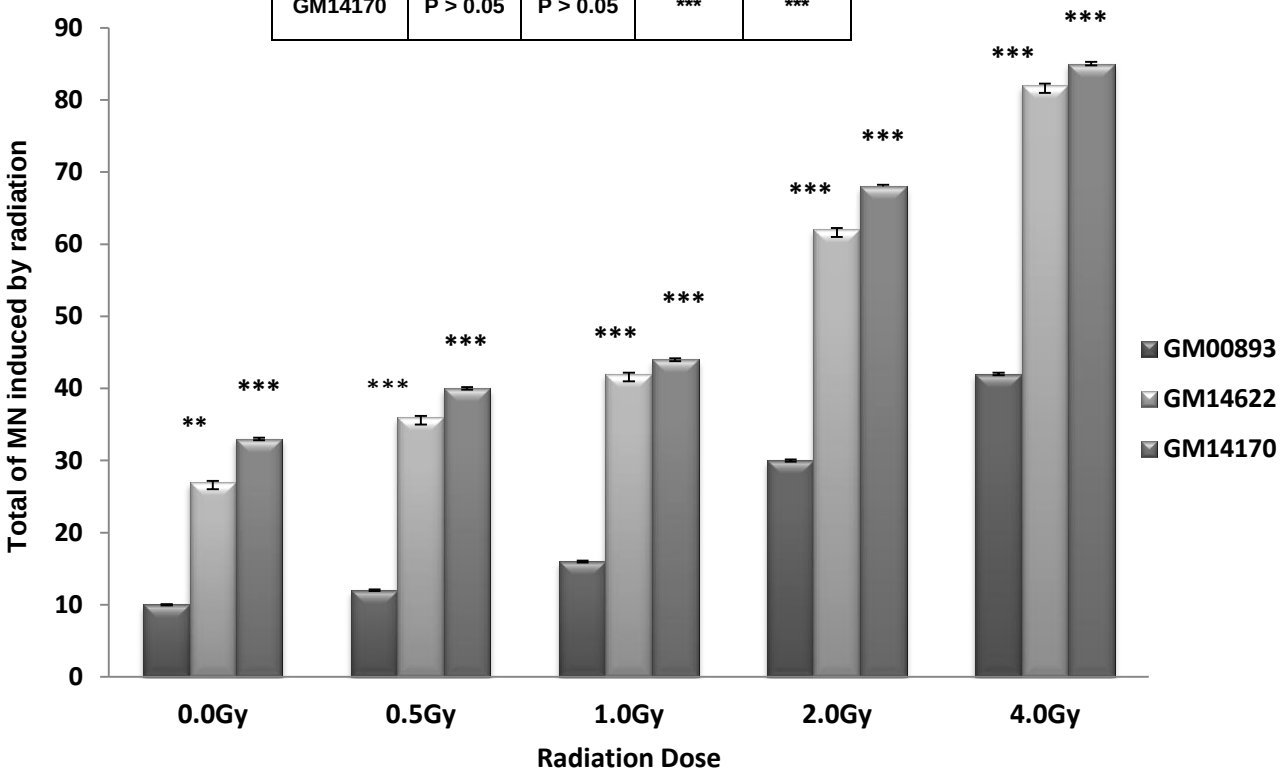

Figure 3.21 Frequencies of MN after irradiation in human Lymphoblastoid cell lines. MN induced by IR 24 h after exposure to different Gy in cultures of one BRCA2 normal (GM00893) and two BRCA2 defective cell lines (GM14622 and GM14170) treated with 6 µg/ml of Cyt-B. Mean ± S.E. from 500 scored binucleated cells.

3.2.7 Telomere function in human BRCA2 defective lymphoblastoid cells

Next, we analysed CAs in lymphoblastoid cell lines after CO-FISH. Similarly to hamster cells we used a dose of 2.0 Gy to induce CAs. Examples of Tel-tel fusions and Tel-DSB fusions are presented in (Figure 3.22).

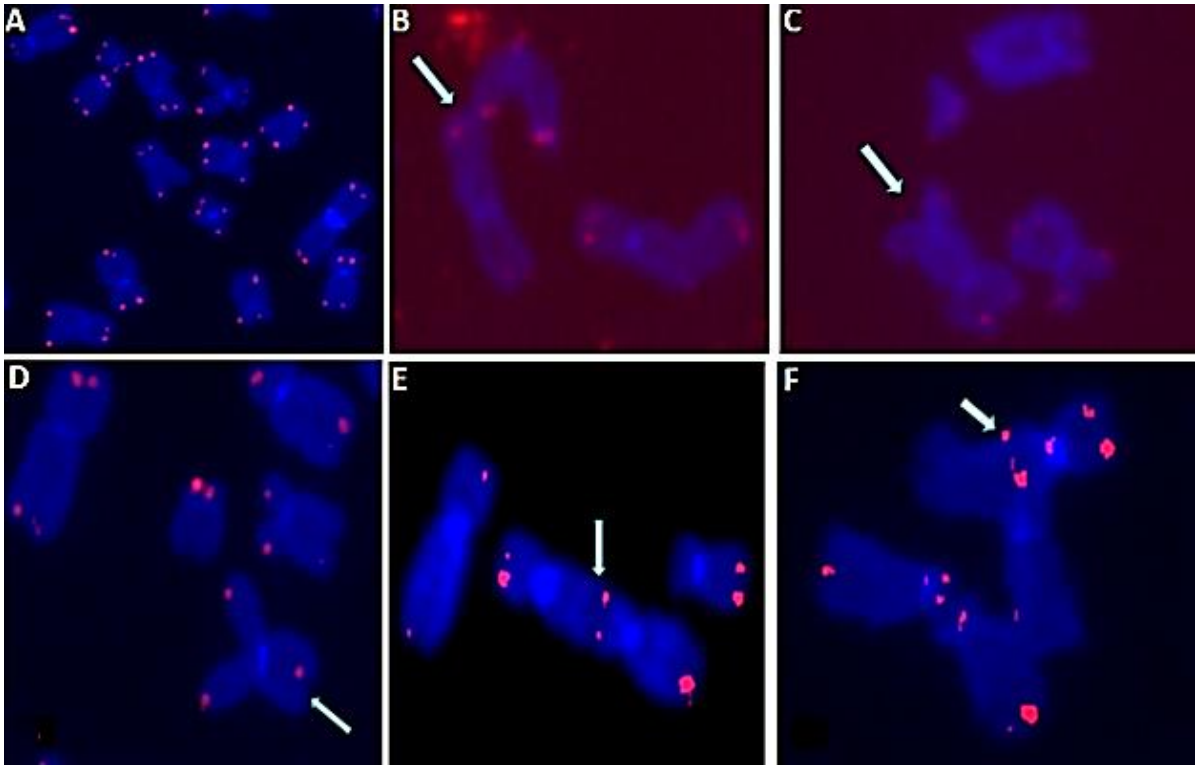

Figure 3.22 Examples of CAs detected after CO-FISH. A) Partial metaphase with standard FISH and no aberrations. B) Fusion beetwen a telomere and a broken chromosome end. C) Dicentric chromosome. D) Sister chromatid fusion. E) fusion between two telomeres (two telomeric signals at the point of the fusion). F) tri-radial (telomeric signal at the point of fusion).

Results of our analysis are shown in (Table 3-2). Similarly to Chinese hamster cells this kind of analysis detects CAs that involves telomeric sequences. It was clear that both BRCA2 defective cell lines showed some spontaneous CAs. Following exposure to IR CAs frequencies become elevated significantly in BRCA2 defective cells relative to the control cell line, further supporting the notion of haploisufficiency.

Table 3-2 Frequencies of radiation-induced CAs in human cell lines after CO-FISH. Cells have been irradiated with the dose of 2.0 Gy. A total of 50 metaphases in each cell lines in G1 phases were analyzed. *P>0.05.

	Cell line	Sister Chromatid Fusion	Telomere-Telomere fusion	Dicentric	Chromatid breaks	Telomeric fusion	Tri-radial
Non-Treated	GM00893	0	0	1 ± 0.17	0	0	0
	GM14170	0	2 ± 0.16	3± 0.22	0	1 ± 0.17	0
	GM14622	0	1 ± 0.17	2 ± 0.16	0	0	1 ± 0.17
Treated	GM00893	0	1 ± 0.17	2 ± 0.16	0	0	0
	GM14170	2± 0.16	5± 0.18*	4 ± 0.14	1 ± 0.17	1 ± 0.17	3 ± 0.22*
	GM14622	1 ± 0.17	4 ± 0.14*	3± 0.22	0	1 ± 0.17	1 ± 0.17

3.3 Discussion

Taken together, results presented in this chapter indicate that BRCA2 defective cells show abnormalities in telomere maintenance. First, telomere length measurements indicate significant telomere shortening (Figure 3.5 and Figure 3.6). Second, telomere function analysis revealed elevated ECF frequencies (Figure 3.8 and Figure 3.9). Third, CO-FISH analysis revealed elevated T-SCE frequencies. Finally, exposure to IR revealed involvement of telomeric sequences in CAs (Figure 3.14). Interestingly, we have found evidence of haploinsufficiency in the case of human lymphoblastoid cell lines. This haploinsufficiency was evident from telomere length measurements, telomere function analysis, CO-FISH analysis and analysis of IR induced CAs (Figure 3.9, Figure 3.11 and Figure 3.18). However, the notion of haploinsufficiency was not supported by MN analysis.

In familial breast tumours with BRCA1 and BRCA2 mutations genomic alterations are more common than in sporadic tumours and show a distinct genomic profile (Holstege et al., 2010). Also, research has shown that both BRCA1 and BRCA2 are involved in the repair of DNA DSBs via the HR pathway (O'Donovan and Livingston, 2010). As a result, chromosomal rearrangements in BRCA2 defective tumors are extensive (Lewis et al., 2006). Therefore, involvement of BRCA2 in telomere protection presented above, but also reported by other investigators (see below) links telomere homeostasis with the well-defined BRCA2 tumour suppressor function. Our results are in line with recent publications reporting telomere length and function abnormalities in human and mouse cell lines defective in BRCA2. For example, telomere length and CAs in human mammary epithelial cell lines derived from tumor breast tissue, BRCA2-999del5-2T, BRCA2-999del5-1N and HME348 were significantly different than in cells which do not carry mutations in BRCA2 (Bodvarsdottir et al., 2012). Moreover, Badie et al., (2010) showed that BRCA2 directly associates with telomeres during the G2 and S phases of cell cycle and acts as a RAD51

loader to facilitate telomere capping and replication. Furthermore, they provide evidence of telomere length/function abnormalities in BRCA2 defective tumor cells.

However, our results also revealed a novel phenotypic feature of BRCA2 defective cells: elevated recombination frequencies at telomeres as evidenced by the analysis of T-SCE frequencies after CO-FISH. This was particularly clear in the set of 4 Chinese hamster cell lines. The BRCA2 defective V-C8 cell line showed several fold higher frequencies of T-SCEs relative to the control V79B cell line (Figure 3.10). However, the correction of BRCA2 in both VC-8+#13 and V-C8+BRCA2 detect resulted in significant reduction of T-SCE frequencies (Figure 3.10). Also the CO-FISH analysis revealed several fold higher T-SCE frequencies in the Capan-1 cell line than in the control MCF-7 cell line (Figure 3.12).

Similarly, T-SCE frequencies were several times higher in the two lymphoblastoid cell lines from BRCA2 carriers in comparison with the control cell line (Figure 3.9). These results based on three different sets of cell lines are consistent with the notion that BRCA2 may normally suppress recombination at telomeres. In line with our results (Bodvarsdottir et al., 2012) reported elevated frequencies of T-SCEs in BRCA2 defective tumor cell lines.

It is interesting that high frequencies of T-SCEs at telomeres are reported in human ALT positive cells lines (Hakin-Smith et al., 2003). As a matter of fact, elevated frequencies of T-SCEs are one of the markers of ALT positive cells (Bechter et al., 2004). An important question is whether BRCA2 is involved in the ALT pathway. Judging by a study that focused on the role of FANCD2 in ALT this may be the case (Spardy et al. 2008). This study has shown that the well characterized DNA damage response protein, FANCD2, a participant in the so called Fanconi anemia molecular pathway responsible for the repair of DNA cross-links, associated with PML bodies in ALT positive cells.

Moreover, it was shown that several more DNA damage response proteins, including BRCA2, interact with FANCD2 in this process. Interestingly, BRCA2 is also known as FANCD1 (Howlett et al., 2002), another player in the FANC pathway opening an interesting possibility that this pathway may be important for the ALT mechanism. It is known that approximately 10% tumors that have been tested for telomerase activity were negative. The assumption is that these tumors maintain their telomeres by the ALT pathway. Better understanding the mechanisms underlying ALT could lead to potential improvement in cancer therapy given that telomeres are required for the survival of any cell type including cancer cells.

In conclusion, our cytogenetic analysis in this chapter showed that cells with defective BRCA2 had clear abnormalities in telomere length and function.

Chapter-4

Effects of *BRCA2* knock-down on ALT positive cell lines

4.1 Introduction

In the previous chapter we have shown that BRCA2 defective cell lines show a range of telomere maintenance abnormalities. This finding suggests a direct involvement of BRCA2 in telomere maintenance. The mechanism(s) behind this involvement appear(s) to be related to the BRCA2 role in HR. Two lines of evidence support this view. First, it has been shown that BRCA2 associates with telomeres in S and G2 phases of the cell cycle and this association facilitates access to telomeres of another HR protein, RAD51 (Badie et al. 2010). Second, our own results show that BRCA2 may act as a suppressor of recombination at telomeres (Figure 4.4 and Figure 4.12). Taken together, these findings are of interest because BRCA2 is a protein directly involved in human cancer and it has a clear role in telomere maintenance. As a result, the findings may be relevant for both developing novel therapeutic approaches and understanding the role of BRCA2 in tumourigenesis.

In this chapter we investigated effects of BRCA2 on recombination rates at telomeres in both non-ALT (Alternative Lengthening of Telomeres) and ALT positive cell lines by examining T-SCE (Telomere Sister Chromatid Exchange) frequencies.

The majority of somatic human tissues do not express telomerase activity. The result is that a continued cell proliferation will lead to replicative senescence due to critically short telomeres (Greider and Blackburn, 1985). The formation and development of tumours usually requires extensive cell proliferation and consequently an avoidance of telomere shortening and replicative senescence (Opresko et al., 2005). Roughly, 85% of all human cancers achieve this through enhanced activity of telomerase (Cheung and Deng, 2008), which is currently a prime target for developing anti-cancer therapies. The remaining 15% tumours are able to maintain their telomere length by the ALT mechanism (Bryan et al., 1997).

The ALT mechanism is prevalent in tumours of mesenchymal origin (Decker et al., 2009). The reasons for this are still unknown but human mesenchymal stem cells may have a specific tendency to activate the ALT pathway (Hills et al., 2009). ALT positive cells contain so called ALT-associated PML (promyelocytic leukaemia) nuclear bodies (APBs) (Yeager et al., 1999) characterized by the presence of telomere-associated proteins, telomeric DNA and DNA damage response proteins. Other hallmarks of ALT include extreme heterogeneity in telomere length (Bryan et al., 1995), elevated level of recombination at telomeres in the form of high frequencies of T-SCEs (Londono-Vallejo et al., 2004) and rapidly changing telomere length (Perrem et al., 2001). It has been reported that BRCA2 associates directly with APBs together with other DNA damage response proteins such as FANCD2 and RAD51 (Spardy et al., 2008).

The presence of two HR interacting partners, BRCA2 and RAD51 in APBs (Yeager et al., 1999) supports the idea that BRCA2 may be involved in the ALT pathway. Our own finding of elevated frequencies of T-SCEs, one of the ALT markers (Bodvarsdottir et al., 2012, Badie et al., 2010), in BRCA2 defective Chinese hamster cells and lymphoblastoid cell lines from BRCA2 mutation carriers (Figure 3.9, Figure 3.11 and Figure 3.18 from chapter 3) is in line with this possibility. Furthermore, it has been shown by Dr Slijepcevic's group that cells from a patient with bi-allelic mutation in BRCA2 had elevated frequencies of T-SCEs (Sapir et al. 2011).

Finally, the main function of BRCA2 in the HR mechanism is regulation of RAD51 (Sharan et al., 1997). Other proteins involved in HR also affect the ALT pathway including the RAD51 (Yeager et al., 1999) and MRE11/RAD50/NSB1-recombination complex (Zhong et al., 2007). Therefore, based on either direct or indirect association of BRCA2 with two ALT markers, namely T-SCEs and APBs, we hypothesise that BRCA2 may be involved in the ALT pathway.

In this chapter we knocked-down BRCA2 using siRNA oligonucleotides in ALT positive and ALT negative cell lines and examined the effects of this procedure on T-SCE frequencies and DNA damage response with a view to testing the above hypothesis.

4.2 Results

4.2.1 High frequencies of T-SCEs in the ALT positive cell line

T-SCE frequencies are regularly elevated in ALT positive cells which makes them one of the accepted ALT markers (Londono-Vallejo et al., 2004). As a result, the CO-FISH method that detects T-SCEs (see previous chapter) has been used as an assay for confirming ALT positive cell lines (Liu et al., 2007). For example, ALT positive cell lines, such as Saos-2, U2OS and W138, have dramatically higher frequencies of T-SCEs compared to control telomerase positive cells (Bechter et al., 2004).

Several ALT positive cell lines, namely U2-OS, WI38 Va13/2RA, SK LU1 and G-292, have been screened for telomerase activity, telomere length and APB bodies in Dr Slijepcevic's laboratory to confirm that they are indeed ALT positive cell lines (Cabuy, PhD thesis, 2005). Our first task was to select an ALT positive cell line most suitable for knock-down experiments. Based on previous publications from Dr Slijepcevic's laboratory (Cabuy et al. 2004) we selected the U2-OS cell line as this line had the best *in vitro* growth characteristics. Given that BRCA2 is a DNA damage response protein which affects cell cycle progression it is essential to use a cell line with good *in vitro* growth characteristics in order to allow timely examination of the subsequent phenotype.

We started by analysing T-SCEs in the U2OS cell line. We used the telomerase positive HeLa cell line as a control non-ALT cell line. Examples of T-SCEs observed in these two cell lines are shown in (Figure 4.1). It was obvious that these two cell lines have a different range

of telomere lengths in individual chromosomes. For example, all chromosomes in HeLa cells had telomeric signals of uniform strength (Figure 4.1 A) whereas many chromosomes in U2OS cells completely lacked telomeric signals and signal intensity in the rest of chromosomes was heterogeneous (Figure 4.1 B). Telomere length heterogeneity is a hallmark of ALT positive cells.

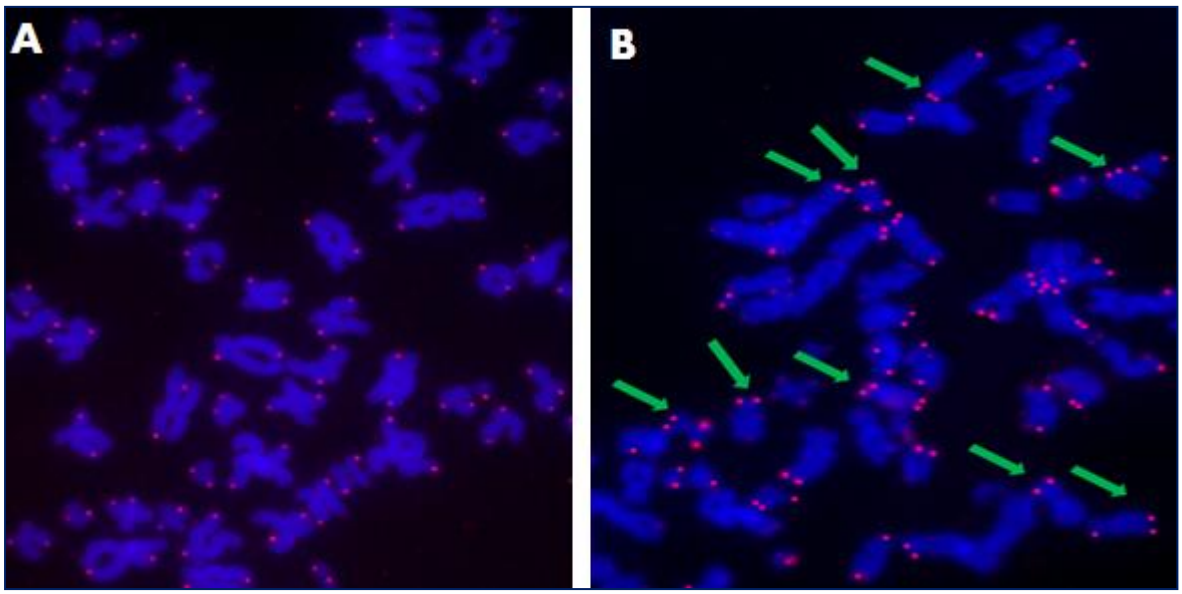

Figure 4.1 Examples of T-SCEs in ALT and non-ALT cell lines. A) A metaphase from the HeLa cell lines with no T-SCEs. B) A metaphase from the U2OS cell line with multiple T-SCEs (arrows). Please also note telomere length heterogeneity in these two lines with some chromosomes completely lacking the signal.

To confirm this heterogeneity we carried out the IQ-FISH procedure. Our results show that U2-OS cells have a greater heterogeneity of telomere length in individual cells compared to the control HeLa cells (Figure 4.3). As expected, telomeres were, on average, significantly longer in U2-OS cells (Figure 4.3).

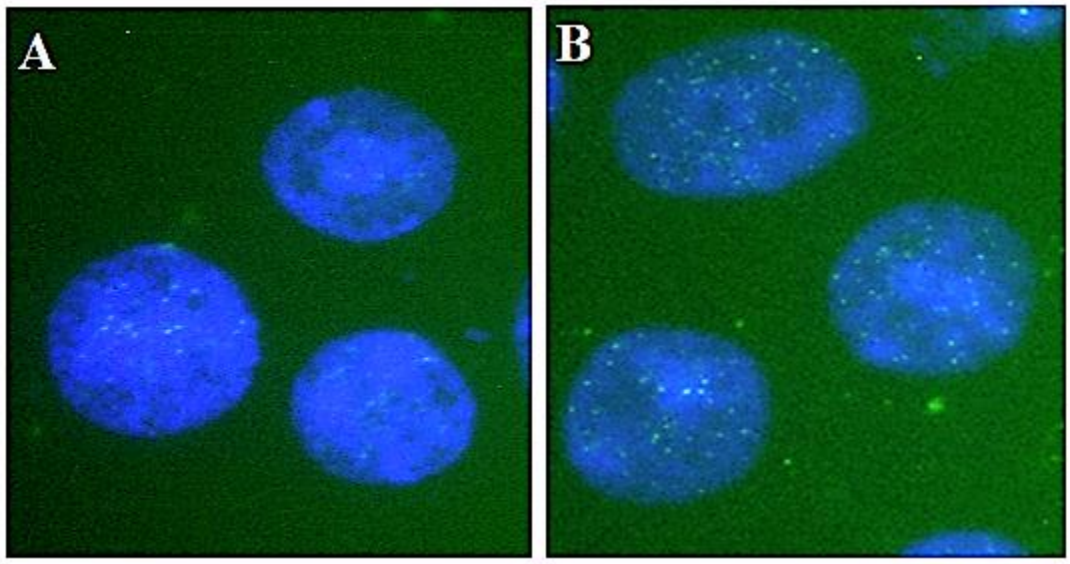

Figure 4.2 Examples of digital images of Q-FISH. A) HeLa and B) U2OS cells in interphase after hybridization with telomeric PNA Oligonucleotides. As can be seen above, there is a clear difference in the strength of fluorescence signals between U2OS and Hela cells with U2OS (B) showing stronger signals than HeLa (A).

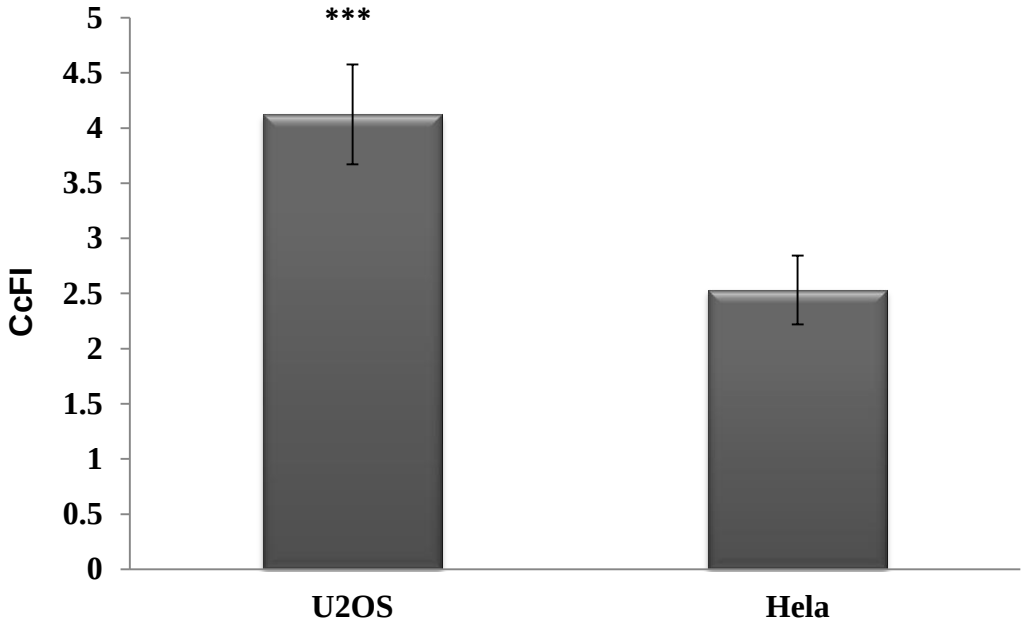

Figure 4.3 Telomere length analysis of U2OS and HeLa cell lines. As expected, U2OS cells showed significantly greater telomere fluorescence than HeLa cells. HeLa cells showed approximately 1.5x shorter telomeres relative to the U2OS cells. CcFl - Corrected calibrated Fluorescence. ***=P<0.001, Error bars represent SEM.

Our analysis of T-SCE frequencies in the two cell lines is shown in (Figure 4.4). As expected, U2-OS cells showed much higher frequencies of T-SCEs relative to HeLa cells. On average, we found ~ 9 T-SCEs in each U2OS metaphase cell, relative to ~ 1 T-SCE per cell observed in the HeLa cell line (Figure 4.4).

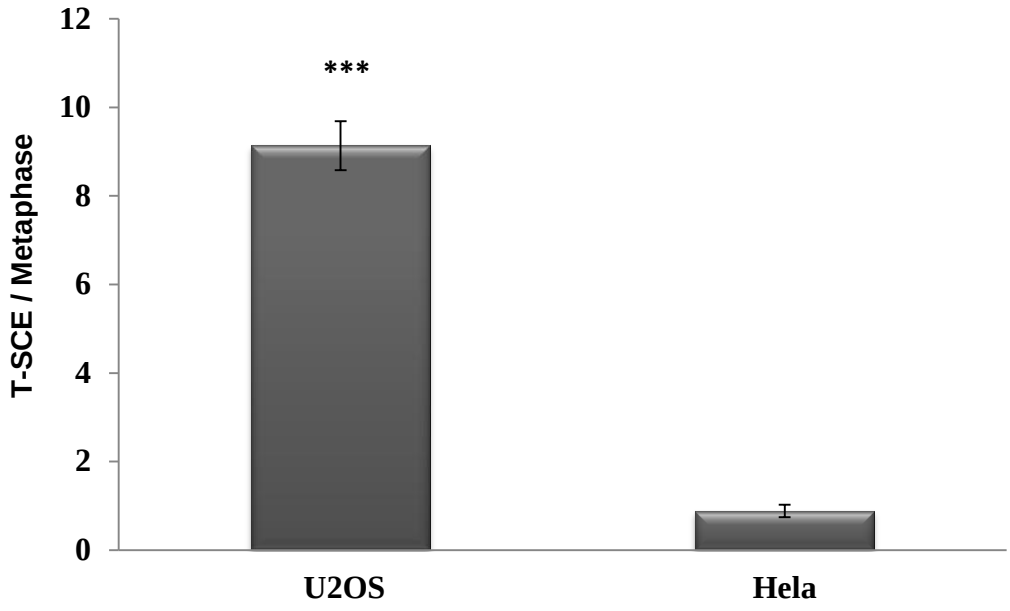

Figure 4.4 Frequencies of T-SCEs in U20S and HeLa cell line. This difference was statistically significant (P<0.001), Therefore, the U2OS cell line is clearly an ALT positive cell line as judged by the frequencies of T-SCEs. Error bars represent SEM. *** = P<0.001.

4.2.2 BRCA2 transient knockdown

Given that defective BRCA2 causes increased recombination at telomeres in non-ALT cells (see chapter 3) the next question for us was to examine the effect of BRCA2 deficiency in ALT positive cells. ALT relies on recombination (Cesare and Reddel, 2010) and it has been shown that BRCA2 associates with APBs (Spardy et al., 2008). Interestingly, the knock-down of FANCD2 and FANCA proteins, which are involved in the same pathway as BRCA2

(also known as FANCD1), caused reductions in T-SCE frequencies in ALT positive cells (Fan et al., 2009).

Therefore, we set out to investigate effects of BRCA2 depletion in ALT positive cells, in particular the effect on T-SCE frequencies which represent a surrogate for recombination rates at telomeres. To create BRCA2 deficiency in U2-OS cells we used siRNA oligonucleotides. The procedure of knocking-down BRCA2 and verifying this by quantitative RT-PCR was carried out. We started by designing primers for BRCA2 and optimising their annealing temperatures and optimal concentrations by RT-PCR and Real-time PCR respectively. As a control, we used the house keeping gene, GAPDH. The primers for GAPDH were kindly provided by Dr. Terry Roberts from Professor Newbold's group, together with data for the optimal concentration and temperature. The procedure for BRCA2 primer optimisation, RT-PCR and Real-time PCR was carried out by MSc student (Ester Sapir), in Dr Slijepcevic's laboratory. Her results are shown in (Figure 4.5, Figure 4.6, Figure 4.7 and Figure 4.8). My responsibility was to carry out independent Real-time PCR, Western blot to confirm the knock-down and also examine the subsequent phenotype in transfected cells. My results are shown in (Figure 4.9 and Figure 4.10) onwards.

The first step was to determine optimal annealing temperature for BRCA2 and GAPDH primers as shown in (Figure 4.5). In addition to U2OS and HeLa cell lines an additional cell line, W138, was used for this procedure. Bands were clearer at 57°C than at 60^{o}C (Figure 4.5). Therefore, this temperature was used in the rest of our experiments.

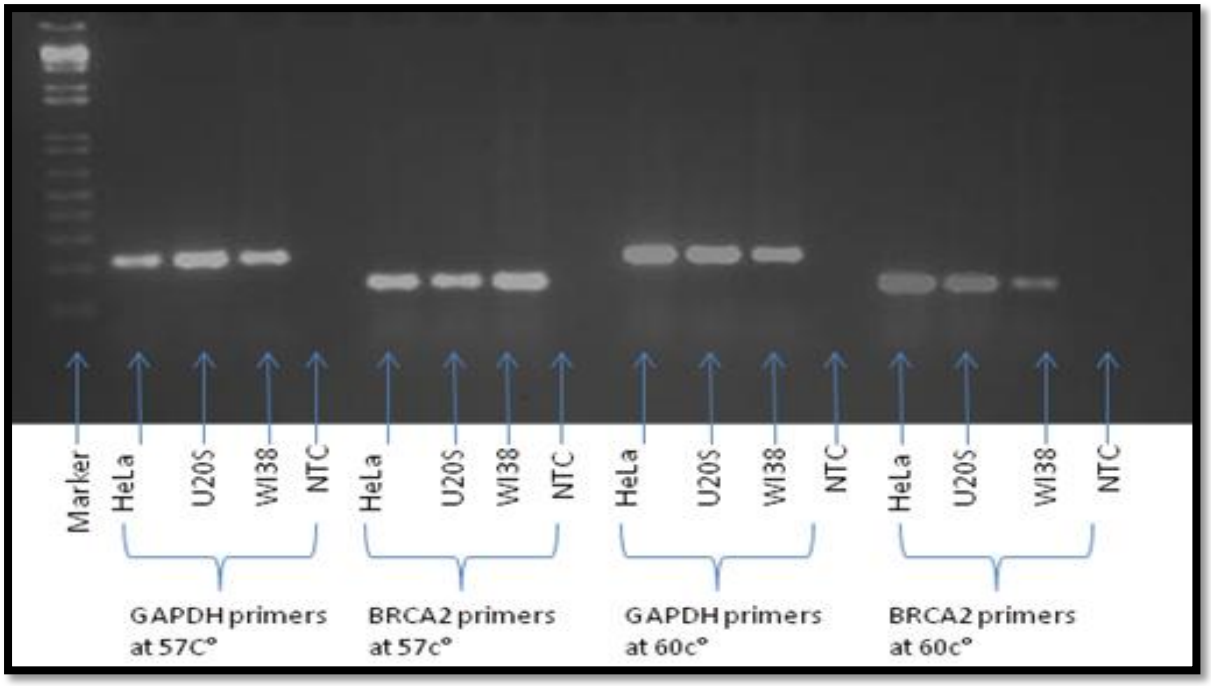

Figure 4.5 Optimisation of primers annealing temperature.

The image shows the running of cDNA obtained from three cell lines, HeLa, U2OS and WI38 in order to determine the annealing efficiency of GAPDH and BRCA2 primers at two temperatures, 57°C and 59°C. From the results it is possible to see clearer bands at 57°C.

The next step was to optimise primers' concentration in HeLa and U2OS cell lines using Real-Time PCR. The results obtained for both cell lines when comparing three different concentrations for BRCA2 primers are shown in (Figure 4.6 A and B). Based on the graphs both cell lines showed that the 5 pmol concentration reduced the amplification efficiency dramatically, while the concentration of 20 pmol increased the amplification effectiveness. Therefore, in subsequent experiments we used the 20 pmol concentration.

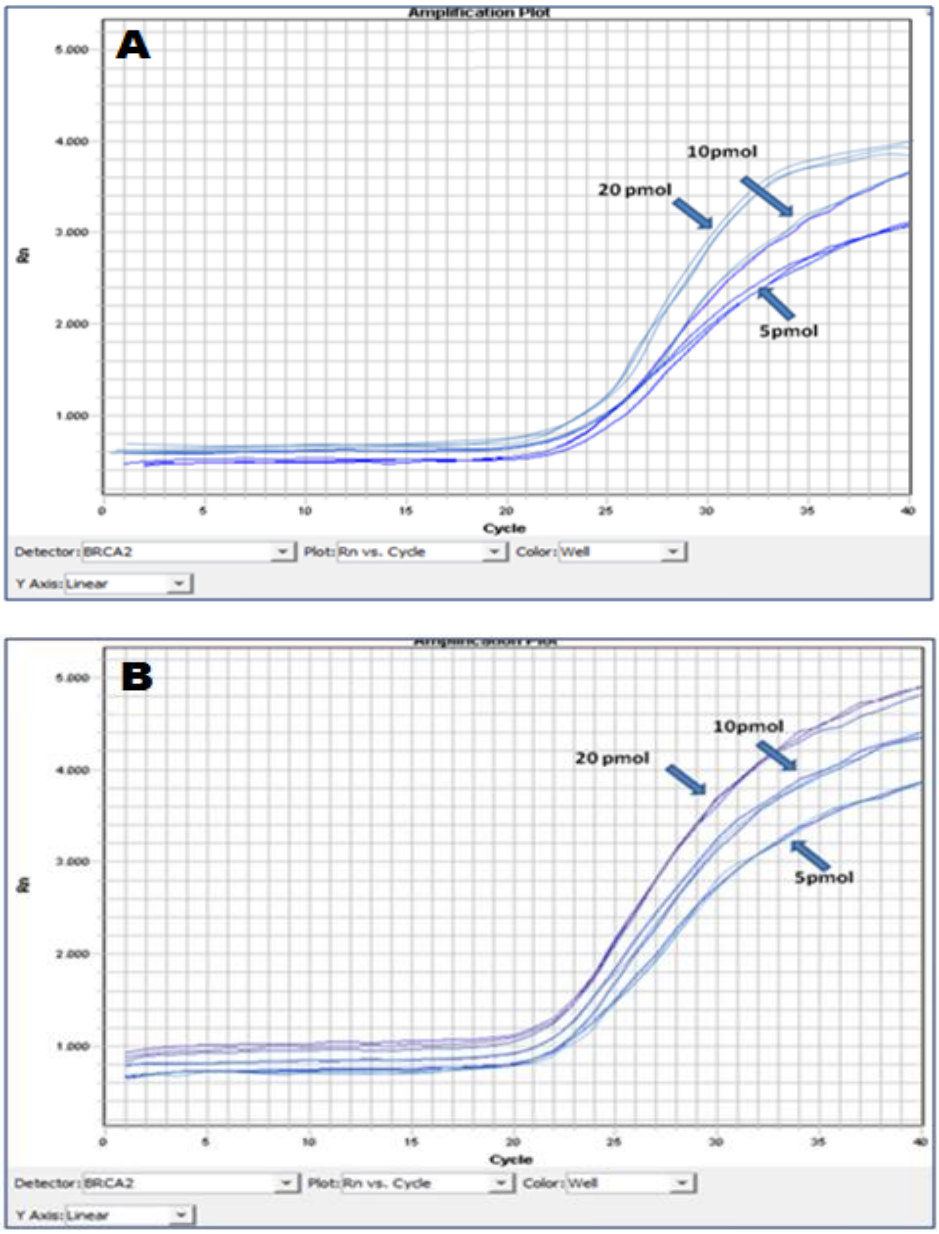

Figure 4.6 BRCA2 primers optimisation at different concentrations. The graphs shows the amplification curves obtained at three concentrations of BRCA2 primers: 5pmol, 10pmol and 20pmol. A) HeLa cell line amplification curve B) U2OS cell line amplification curve.

Having optimized primer concentrations and annealing temperatures the next step was to start the RNAi procedure and introduce Si (small interfering) RNA oligonucleotides into cells. For this protocol we used ON-TARGET plus SMARTpool (Thermo Scientific Dharmacon) siRNA oligonucleotides. The product is designed to enhance target specificity and reduce

undesirable effects. Each oligonucleotide pool provided by the manufacturer consists of four individual siRNA sequences which exert a specific and high level of gene silencing. The siRNA oligonucleotides were delivered to the cells using the jetPRIME™ transfection reagent (Polyplus-transfection). This product is based on a non-liposomal formula that ensures effective delivery of oligonucleotides into mammalian cells. Details of the protocols for gene silencing are described in Material and methods.

We started by knocking-down our control house-keeping gene GAPDH in order to show that the delivery of siRNA oligonucleotides is effective and that the whole procedure works in our hands. Figure 4.7 shows the results of GAPDH knockdown when the Real-time products were run on an agarose gel. The results confirm the reduced amount of GAPDH in U2OS cells after transfection, mainly after 48h, as well as the gradual increase in its expression with the time progression. At 7 days the GAPDH expression was fully recovered as seen by comparing with the band obtained from U2OS untreated cells.

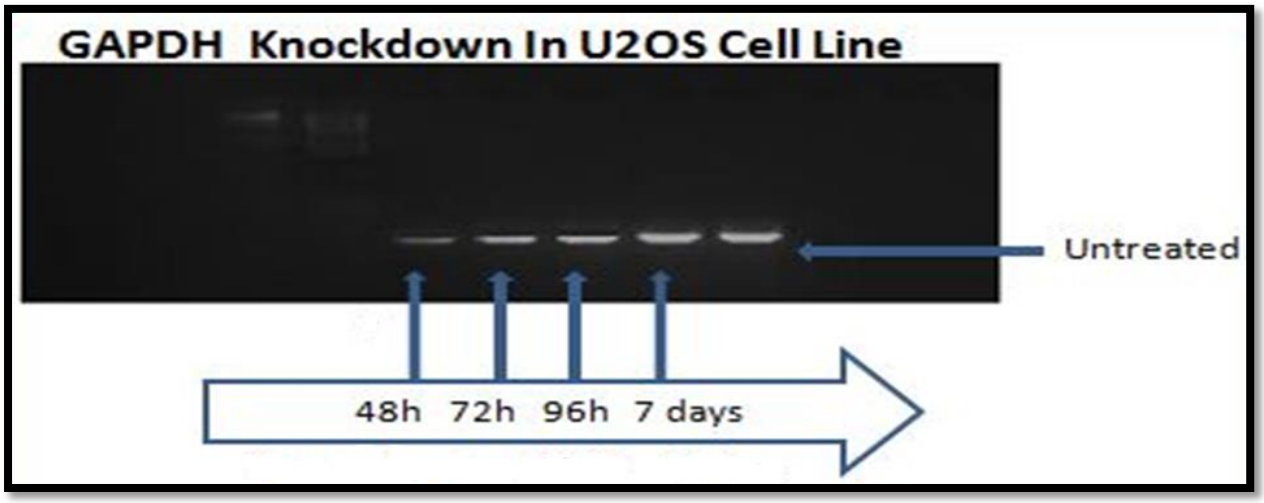

Figure 4.7 GAPDH knock-down as seen by agarose gel electrophoresis. Time in hours (h) after transfection shown at the bottom. Note the weaker staining of the 48h post-transfection point.

GAPDH knockdown was also confirmed by the increase of the Ct value at different times after transfection with GAPDH siRNA Oligonucleotides (Figure 4.8 A nad B). As the Ct value increases there is a need for more PCR cycles in order to get a fluorescence signal. The interpretation is that less GAPDH cDNA template is available for amplification to begin with. In the untreated cells the Ct value was around 15, which points to a very high GAPDH amount when comparing to the Ct values of 96h, 72h and 48h which were 19, 21 and 29 respectively. At 7 days the Ct value was the same as that of the untreated cells points to a full recovery of GAPDH expression. Therefore, these results suggest that the knock-down of the house-keeping gene, GAPDH, was successful.

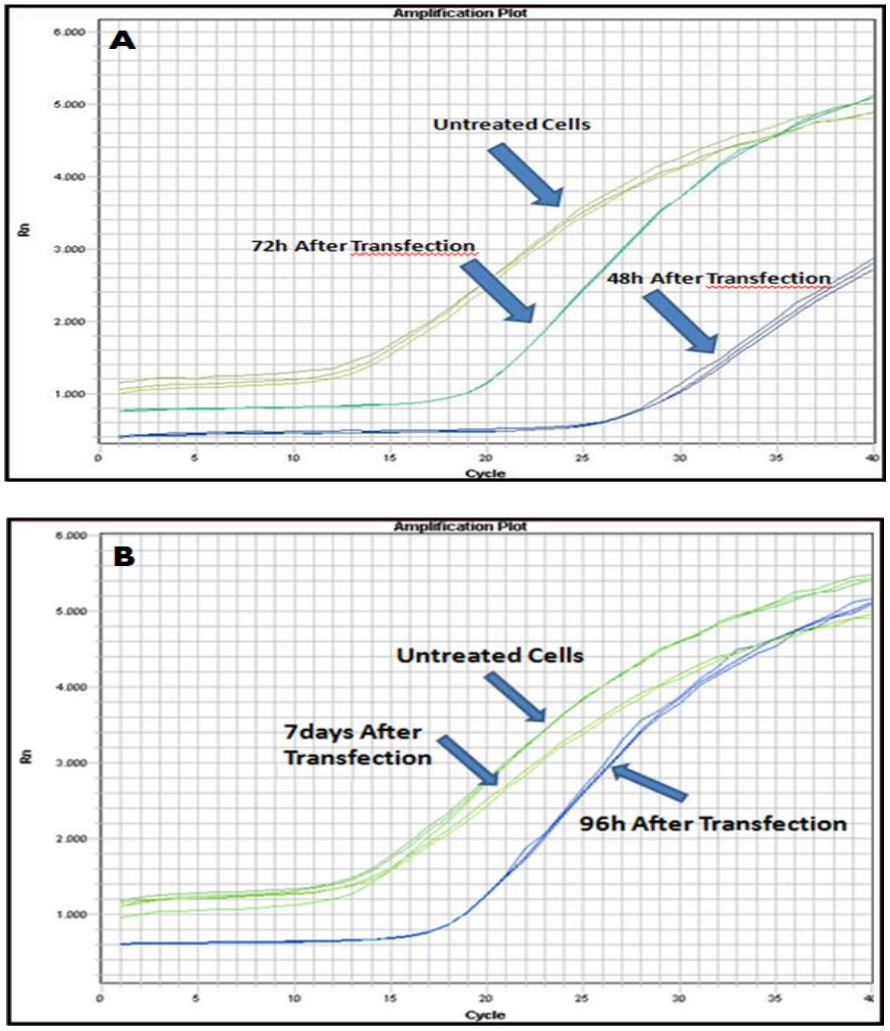

Figure 4.8 GAPDH amplification curves after transfection.

Next, using the same methodology as above we started the procedure for knocking down BRCA2. BRCA2 expression was measured by Real-Time PCR at 4 different time points after transfection (the experiment designed presented in material and methods). The experiment was performed twice in order to ensure reproducibility of results. Figure 4.9 demonstrates the average results from two experiments. In both cell lines the lowest expression of BRCA2 was obtained 48h after transfection and as the time progressed the expression started to recover (Figure 4.9). Full recovery was reached 7 days after transfection. The efficiency of knock-down varied between cell lines. In the case of U2-OS cells the expression of BRCA2 was reduced 90% 48h after transfection and 80% 72 h after transfection. In the case of HeLa cells these figures were 80% and 70% at the same time intervals. Overall, these results show expected knock-down rates in both cell lines.

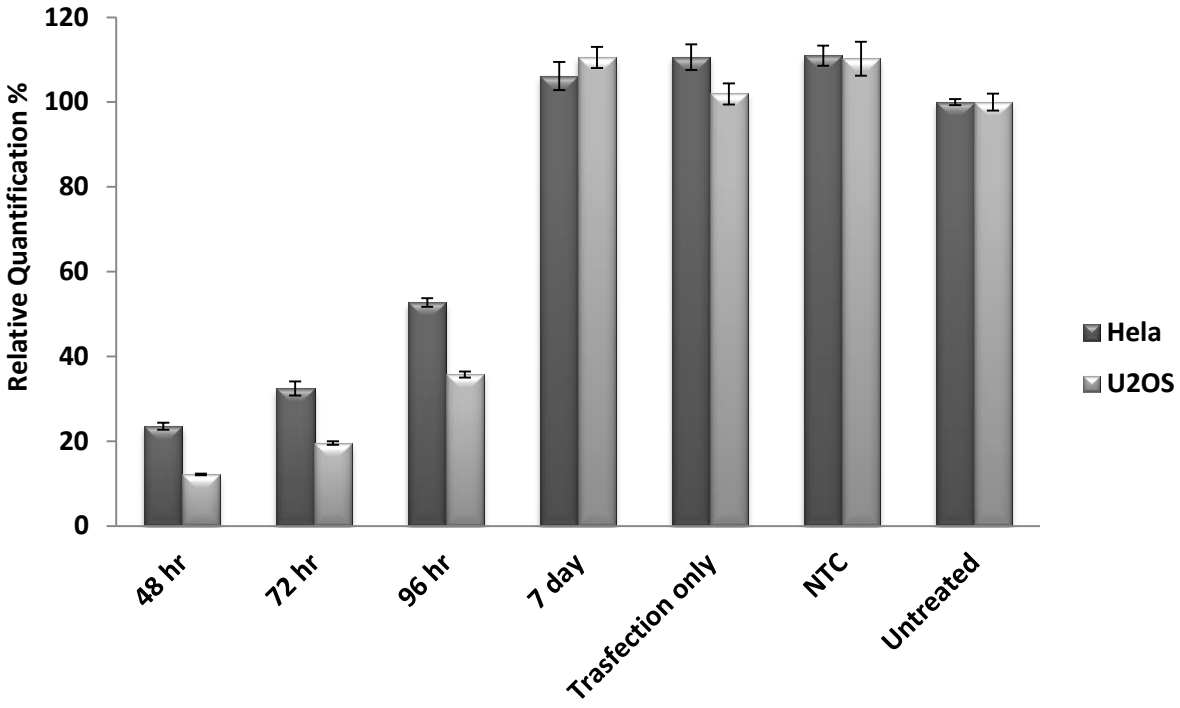

Figure 4.9 BRCA2 expression at different time points after transfection. Relative quantities (RQ) of BRCA2 mRNA assessed by quantitative real time PCR after various times following transfection with siRNA oligonucleotides specific for BRCA2. Additional controls, ensuring reliable results, were cells treated with only transfection reagent and cells treated with non-targeting siRNA. NTC-non targeting control; Transfection only – transfection reagent with no siRNA oligonucleotides; Error bars represent SE.

To confirm the knock-down at the protein level we used Western blot (Figure 4.10). The signal intensities of BRCA2 bands were weaker at 48 h and 72 h in U2-OS cells and at 72h in HeLa cells (Figure 4.10). Some discrepancies were observed between Real-time PCR results (Figure 4.9) and Western blot results (Figure 4.10). The lack of correlation between protein and mRNA levels could be due to post-trancriptional modifications such as phosphorylation, methylation, etc. (Vogel and Marcotte, 2012). In addition, the half-life of different proteins can vary from minutes to days. Research indicates that the degradation rate of mRNA may fall within a much tighter range from 2 to 7 hours for mammalian mRNA and 48 hours for proteins (Vogel and Marcotte, 2012). The relationship described between mRNA and protein

is also evident in our results; mRNA levels and protein levels in both samples different, for example, 72 hours post transfection, suggesting more stable mRNA compared to protein.

Taken together, our results show that BRCA2 expression was significantly reduced 48 and 72 hrs post-transfection in both cell lines. The expression recovered to control levels 7 days from transfection.

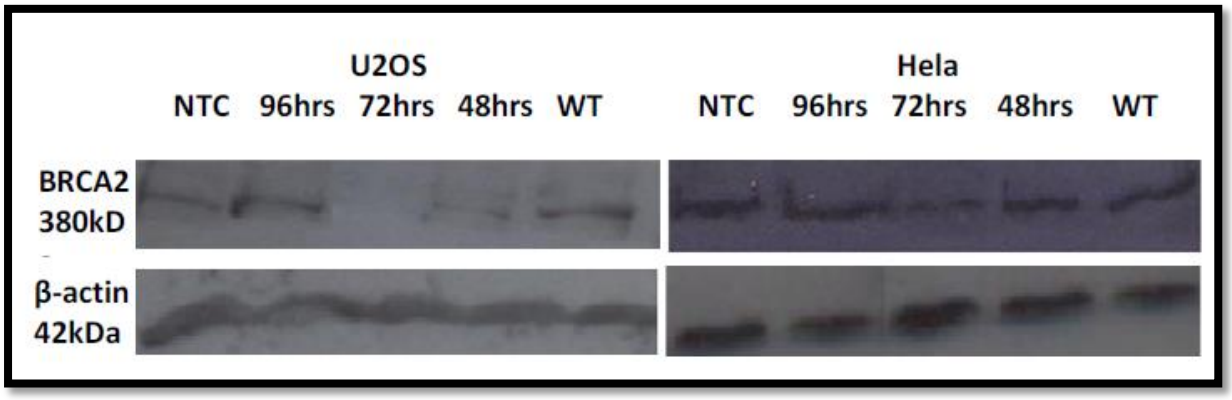

Figure 4.10 Western blot analysis of BRCA2 expression following transfection with siRNA oligonucleotides. The level of β-actin protein expression confirms equal protein loading in both cell types. Additional controls, ensuring reliable results, were cells treated with only transfection reagent (WT) and cells treated with non-targeting siRNA (NTC).

4.2.3 Effects of BRCA2 deficiency on telomere recombination in non-ALT and ALT cells

Since the above results were consistent with the significant reduction in BRCA2 expression levels in both cell lines 48 and 72 h after transfection with siRNA oligonucleotides the next step in the study was the examination of the phenotype of transfected cells. We carried out two types of phenotype examination: measuring T-SCE frequencies by CO-FISH and assessing DNA damage response by immunocytochemical methods.

We started with the CO-FISH procedure. The idea was to carry out CO-FISH at the post-transfection time intervals showing the lowest level of BRCA2 expression i.e. 48 and 72 h (see Figure 4.9). However, in a pilot experiment we have found that that BRCA2 knock-down

significantly slowed down the cell cycle progression resulting in a low mitotic index incompatible with CO-FISH, which requires good quality metaphase preparation, at the first time point of 48 h (results not shown). As a result, we decided to perform the CO-FISH procedure on U2OS and HeLa cells 72 h following transfection as we observed a slight recovery in cell cycle progression approximately 3 days after initiation of transfection procedure. In addition, a longer time after transfection would ensure that all dividing cells had been transfected with siRNA oligonucleotides resulting in an effective BRCA2 silencing. As a control we used cells transfected with non-targeting siRNA oligonucleotides (scrambled) obtained from the same manufacturer as the BRCA2 specific siRNA oligonucleotides. Examples of U2-OS and HeLa metaphase cells after transfection with two types of siRNA oligonucleotides are shown in (Figure 4.11).

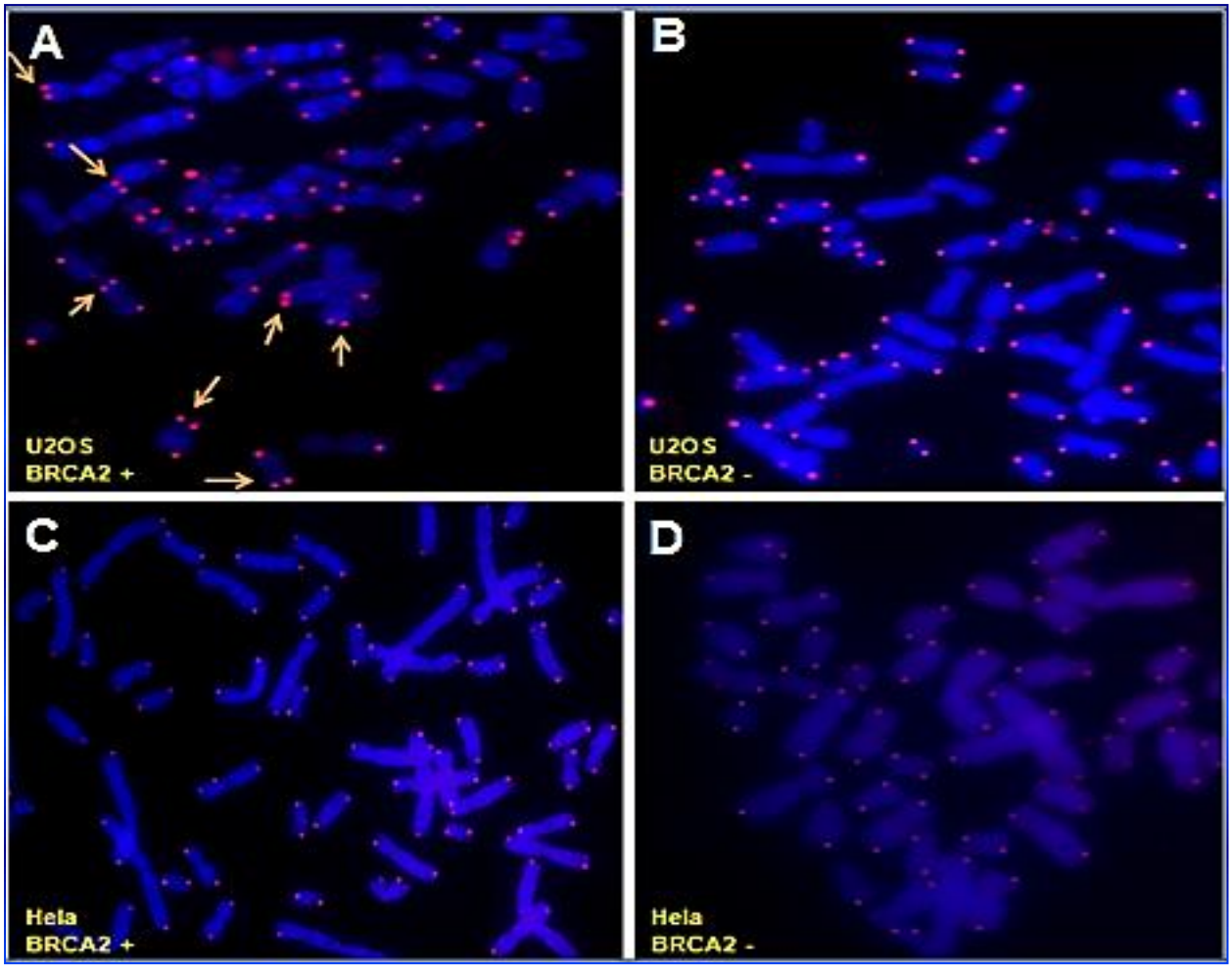

Figure 4.11 Digital images of metaphases cells analysed by CO-FISH after BRCA2 transfection.

A) U2OS metaphase cell that expressed the BRCA2 gene and was treated with scrambled Si-RNA oligonucleotides. T-SCEs are marked by arrows. B) A U2OS metaphase cell treated with Si-RNA oligonucleotides targeting the BRCA2 gene. Please note lack of T-SCE events. C) A HeLa metaphase cell treated with scrambled Si-RNA oligonucleotides (no T-SCEs). D) A HeLa metaphase cell treated with Si-RNA targeting the BRCA2 gene (no T-SCEs).

As expected, cells transfected with BRCA2 specific siRNA oligonucleotides had a lower mitotic index 72h after transfection relative to cells transfected with control scrambled siRNA oligonucleotides (results not shown). Still, the mitotic index was sufficiently high to obtain enough good-quality metaphase cells to carry out the CO-FISH procedure. Results of the analysis of T-SCE frequencies in both cell lines are shown in (Figure 4.12). This analysis revealed a significant reduction in T-SCE frequencies in U2-OS cells following BRCA2

knockdown relative to control cells (Figure 4.12). We have also noticed that HeLa cells show similar effect but because of low numbers of T-SCEs observed the difference was not statistically significant. We would like to note that frequencies of T-SCEs in control untreated U2-OS and HeLa cells (Figure 4.4) were similar to those observed after transfection with scrambled siRNA oligonucleotides (Figure 4.12). Therefore, these results show that BRCA2 knock-down has resulted in a dramatic, ~9-fold reduction of T-SCE frequencies in ALT positive cells, but no significant effect in cells that maintain telomeres by telomerase.

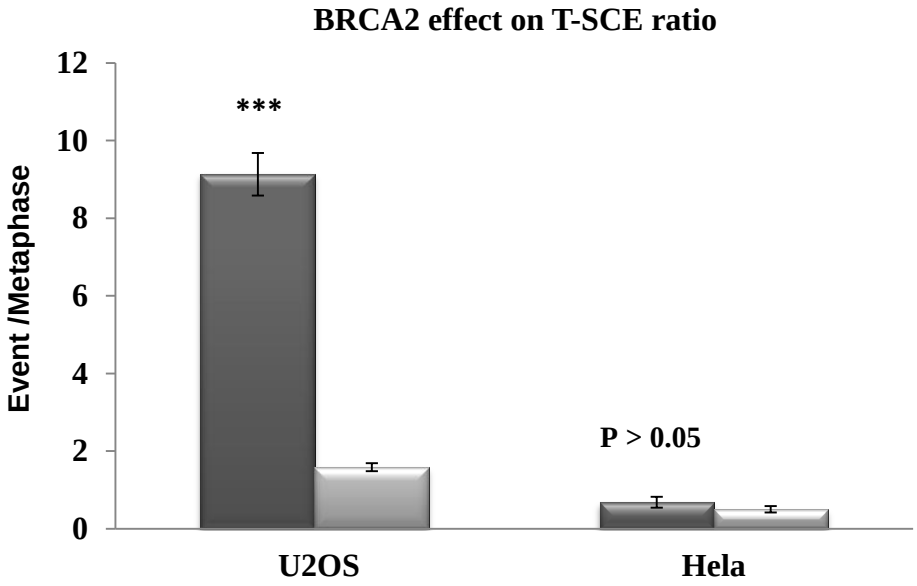

Figure 4.12 T-SCE frequencies after BRCA2 knock-down (72 h post-transfection). Dark grey bars – cells transfected with scrambled Oligonucleotides. Light gray bars – cells transfected with BRCA2 specific siRNA oligonucleotides. ***=P<0.001, Error bars represent SEM.

4.2.4 Immunofluorescence detection of γ-H2AX at telomere after BRCA2 depletion in human cell lines

Apart from effects of BRCA2 on T-SCE frequencies we found that BRCA2 deficiency also causes increased frequencies of CAs (see Chapter 3). CAs are usually elevated when DDR is defective. Therefore, we next examined effects of BRCA2 depletion on DDR response using immunocytochemical analysis based on detecting the phosphorylated form of histone H2AX (γ-H2AX), which is considered a good DNA damage marker. Furthermore, by combining γ-H2AX detection with detection of telomeric repeat sequences, DNA damage can be observed exclusively at telomeres. This assay is also known as the TIF (Telomere dysfunction Induced Foci) assay (Takai et al, 2003). We carried out both tests, namely imunocytological detection of γ-H2AX foci and the TIF assay.

To this end U2-OS and HeLa cells have been transfected with BRCA2 specific and control siRNA oligonucleotides. Frequencies of DNA damage foci and TIFs were monitored at a single time point post-transfection, 72 hours. Representative examples of γ-H2AX foci and TIFs observed are shown in (Figure 4.13). Analysis of γ-H2AX foci and TIF frequencies are shown in (Figure 4.14).

As expected, both U2-OS and HeLa cells showed some increase in frequencies of γ-H2AX foci and TIFs after BRCA2 depletion (Figure 4.14). This is consistent with the view that BRCA2 deficiency affects DDR (Venkitaraman, 2001). However, statistical analysis indicated that the increase was significant only in the case of the U2-OS cell line, but not in the case of the HeLa cell line.

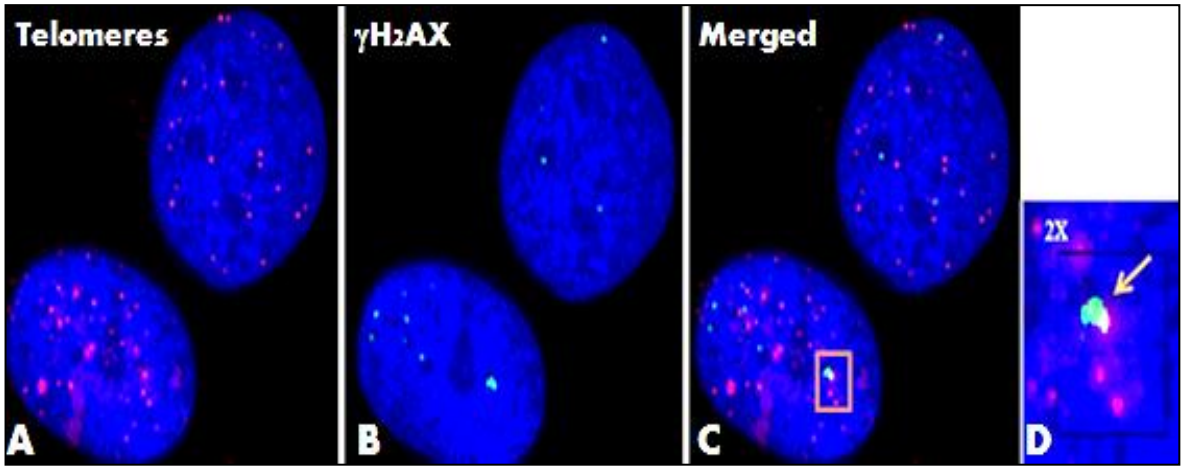

Figure 4.13 Examples of images generated by TIF. A and B, HeLa cells were incubated with γ-H2AX antibodies (green) and hybridyzed with synthetic Peptide Nucleic Acid (PNA) telomeric sequence $(CCCTAA)_3$ conjugated with a Cy-3 fluorescence label (red). C) Co-localization of the γ-H2AX foci and telomeres represent a TIF. D) Represent larger magnification of the squared areas, and TIF are visualized as yellow spots. Please note that only complete overlaps between two colours have been scored as TIFs.

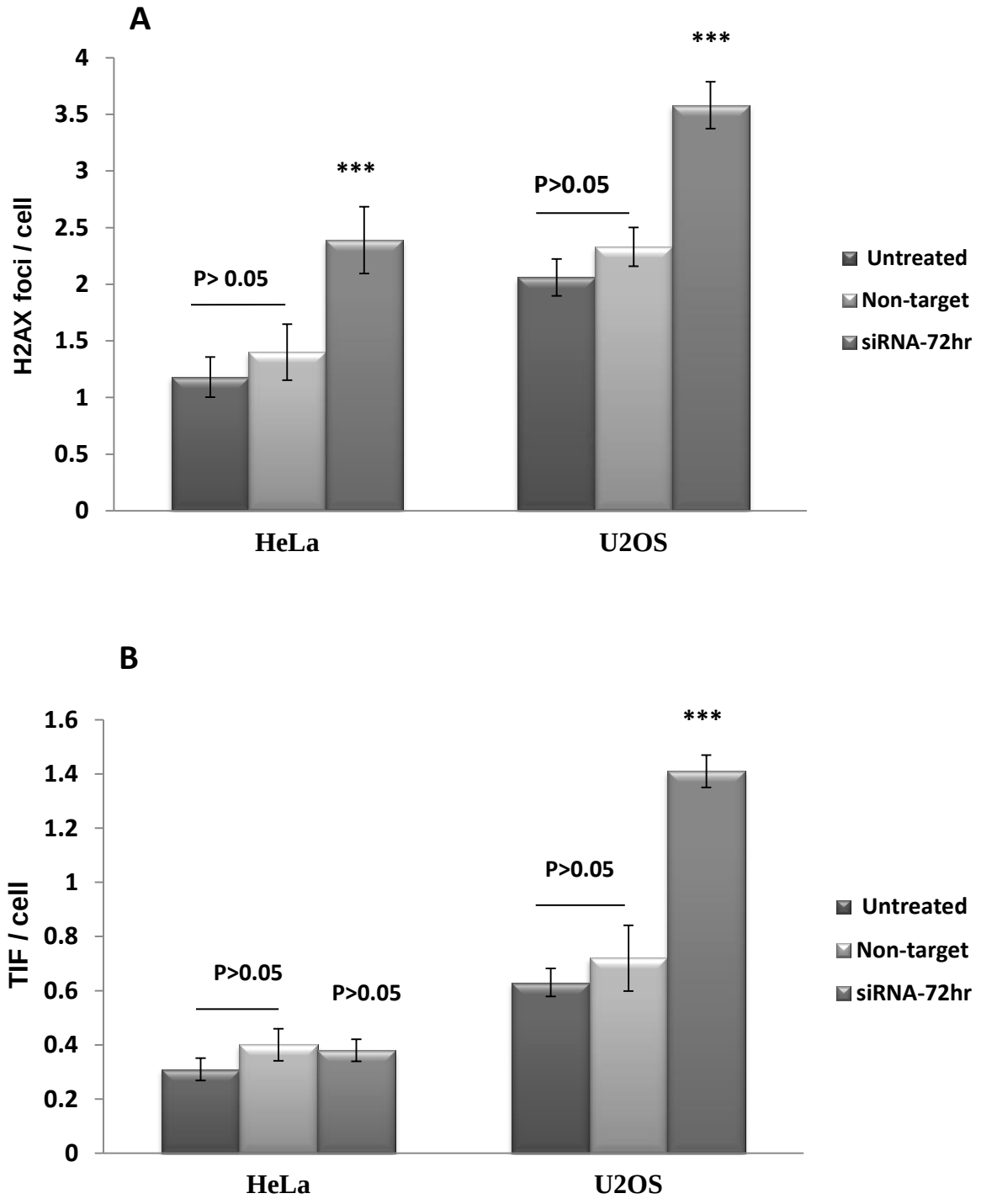

Figure 4.14 Frequencies of γH2AX positive foci (A) and TIFs (B) 72 hours after transfection. A total of 100 cells were analysed per point in two independent experiments. NTC (non-template control) represent scrambled siRNA. ***=P<0.001, Error bars represent SEM.

4.3 Discussion

It is well documented that deficiencies in both BRCA2 and telomere maintenance affect genome stability. For example, examination of mouse cells in which a BRCA2 deficiency was artificially engineered revealed increase in chromosome abnormalities indicative of genome instability. Similarly, loss of telomere function as a result of replicative senescence, or defects in genes encoding components of shelterin leads to increased frequencies of DNA damage foci in the nuclei of affected cells, a scenario consistent with genome instability (Bailey et al., 2004).

Our results (see Chapter 3), and results of others (Bodvarsdottir et al., 2012, Badie et al., 2010) suggest that when BRCA2 is defective, telomere maintenance is also affected raising an interesting possibility that there is a functional interaction between BRCA2 and telomere maintenance aimed at preserving genome stability. In this chapter we examined effects of BRCA2 depletion in cells that maintain telomeres by the ALT pathway.

A study by Spardy et al., (2008) established that BRCA2 associates with APBs in ALT positive cells. Moreover, APBs are particularly enriched with BRCA2 during S/G2/M phases of the cell cycle (Lansdorp, 2009). Interestingly, several proteins that are involved in HR and DNA repair were found to co-localise with APBs including MRE11/RAD50/NBS1 (MRN) recombination protein complex (Zhong et al., 2007), RAD52 (Yeager et al., 1999), RPA (Bernardi and Pandolfi, 2007) and RAD51 recombinase (Yeager et al., 1999). It is important to note that BRCA2 is also a part of the so called Fanconi Anaemia (FA) pathway. FA is a rare autosomal recessive disease that is linked to a defect in the cellular response to DNA damage (Thompson, 2005). A total of thirteen genes have been identified in FA including FANC A,B,C,D1,D2,E,F,G,I,J,L,M and N (Thompson, 2005, Venkitaraman, 2002). FANCD1 has been identified as BRCA2 (Howlett et al., 2002). The majority of FANC

proteins form the so called FANC core complex which is comprised from eight proteins (A, B, C, E, F, G, L and M) and is required for the monoubiquitination of FANCD2 and FANCI (Thompson, 2005, Venkitaraman, 2002). The third group consists of BRCA2/FANCD1, FANCN/PALB2 and FANCJ/BRIP1. Upon DNA damage, monoubiquitinated FANCD2 is targeted to chromatin where it interacts, through its C terminal region, with BRCA2/FANCD1 in order to promote its loading on to chromatin (Wang, 2007). BRCA2 in turn functions, together with RAD51, to repair the damage through HR.

Two members of the FA pathway, FANCD2 and FANCA, are also involved in the ALT mechanism (Fan et al., 2009). For example, FANCD2 co-localises with APBs in ALT positive cells (Fan et al., 2009). In addition, transient depletion of either FANCD2 or FANCA has caused acute reduction in telomere length and even lost of detectable telomeres. Moreover, depletion of these FA proteins has resulted in decreased T-SCE frequencies. We have shown in this chapter that BRCA2 depletion has similar effects in ALT cells, namely reduction in T-SCE frequencies (Figure 4.12). This reduction was approximately 9-fold in ALT positive cells but non-existent in ALT negative cells (Figure 4.12).

An important question is how these results can be reconciled with our hypothesis from Chapter 3, namely that BRCA2 acts as a suppressor of recombination at telomeres. We have shown that defective BRCA2 causes elevated recombination at telomeres in non-ALT cells including Capan-1, two lymphoblastiod cell lines from BRCA2 carriers and BRCA2 defective Chinese hamster cell lines (see Chapter 3). However, depletion of BRCA2 in ALT positive cells has the opposite effect on T-SCE frequencies (Figure 4.12). It is tempting to speculate that ALT positive and ALT negative cells represent two different environments from the perspective of DDR and these differences may eventually lead to different effects of BRCA2 on T-SCE frequencies. This scenario is supported by the observation that ALT positive cell lines show a range of genomic instability signs including: extensive genomic

rearrangements, DSB repair defects, defects in cell cycle checkpoint control etc. (Lovejoy et al., 2012). In such an environment DDR proteins, including BRCA2, may be regulated differently and their functions applicable to the telomerase positive environment may not be applicable to the radically different DDR environment such as the ALT environment. Interestingly, most ALT positive cell lines tested showed lack of the chromatin remodelling protein ATRX/DAXX (Lovejoy et al., 2012). Given the involvement of ATRX and DAXX at telomeres, this led researchers to investigate the telomere status of a panel of pancreatic neuroendocrine tumours. Interestingly, the results have shown that all samples containing mutations for either DAXX or ATRX shows that heterogeneous telomere length are characteristic of ALT positive cells and contain deletion of exons 2 through 19 in ATRX (Heaphy et al., 2011). Furthermore, ALT positive cell lines have not been able to repair DSBs effectively 24h post-irradiation, in contrast to ALT positive cells (Lovejoy et al., 2012). Our observation of elevated rates of DNA damage foci in untreated U2-OS cells relative to untreated HeLa cells (Figure 4.14) is in line with the view that DSB repair mechanisms are not effective in ALT positive cell.

It is important to note that not all the proteins that are involved in HR are necessary for the ALT pathway. A good example may be RAD54 that despite its involvement in HR and even telomere elongation was shown to be unnecessary for ALT (Akiyama et al., 2006). Since our findings indicate that BRCA2 is specifically involved in the maintenance of telomeres in ALT cells, it is expected that patients harbouring BRCA2 mutation, such as patients with hereditary breast cancer, will express telomerase and rely on its activity, rather than be based on the ALT for telomere maintenance. Indeed, ALT mechanism is more common in certain sarcomas and germ cell tumours while it is relatively rare in carcinomas (Hakin-Smith et al., 2003).

During this study additional events were noticed (data not shown), when BRCA2 was transiently silenced by siRNA and shRNA the cells' ability to divide dramatically decreases; pointing to the possibility that BRCA2 depletion in ALT positive cells may induce cell senescence. Therefore, in order to achieve a sufficient amount of dividing cells for analysis, we needed to change the cell growth conditions and to perform the experiments on a larger amount of cells in order to get sufficient number of mitotic cells for T-SCE analysis.

To sum up, the data obtained in this study point to the role of BRCA2 in ALT. However, further investigation is required to confirm this and also explore the importance of these results for cancer therapy.

Chapter 5

Generating stable knock-down of BRCA2 in ALT-positive cells

5.1 Introduction

In the previous Chapter we have shown that a transient BRCA2 knock-down mediated by siRNA oligonucleotides in ALT positive cells leads to a reduction in the frequency of one of the ALT markers, namely T-SCEs. A similar effect was observed when another protein involved in the FANC pathway, FANCD2, was knocked-down (Spardy et al., 2008). These findings suggest that the FANC proteins may be involved in regulating the ALT pathway. The question that is highly relevant for us is whether BRCA2 is critically important in the ALT pathway. If so, this may open up an interesting avenue for further investigation. For example, if BRCA2 plays an important role in the ALT pathway then its deficiency could in turn make this pathway defective. This scenario is relevant for cancer therapeutics based on anti-telomerase drugs. The problem with inhibiting telomerase as a way of cancer therapy is a potential reactivation of the ALT pathway (Bechter et al., 2004). Therefore, combining anti-telomerase drugs with treatments that inhibit the ALT pathway at the same time, for example by inducing BRCA2 deficiency, may be an effective way to render the telomere maintenance machinery, which is vital for survival of cancer cells, ineffective.

In this Chapter we focused on investigating long term effects of BRCA2 deficiency on ALT positive cells. In order to achieve the long term BRCA2 knock-down we used the short hairpin RNA (shRNA) approach.

5.2 Long term knock-down of BRCA2 using shRNA

5.2.1 Establishing shRNA protocol and generation of stable lines

RNAi is an endogenous post transcriptional gene silencing pathway that uses either short interfering (siRNA) or shRNA approaches. The siRNA based approach relies on introducing ~21-25 long nucleotides using artificial means such as transfection and is usually a temporary form of gene silencing (see previous Chapter). On the other hand the shRNA based approach

involves targeting specific transcripts for degradation using plasmids or lentiviral vectors, which stably integrate into the host genome making this a more permanent form of gene silencing. Both gene silencing pathways use the endogenous RNAi pathway in eukaryotic cells to degrade their target gene mRNA (Rao et al., 2009, Pecot et al., 2011).

This pathway is carried out in the cytoplasm through the RNA-interfering silencing complex (RISC) (Cullen, 2005) (see also Figure 5.1). The difference between the siRNA and shRNA based approaches is in the mode of transfection and the ability to produce either transient or long-term stable knock-down of target RNA transcript. Since shRNAs are carried by a vector, they are permanently integrated into the host genome and constantly produce siRNA. This allows for selection of cells that constitutively expresses low amount of the target gene of interest. There are several advantages for using shRNA instead of siRNA. For instance the loading process for siRNA is ten times less efficient in comparison to shRNA (Rao et al., 2009). However its efficiency can be improved by increasing the length of one side of the siRNA duplex to 29-30 nucleotide with a 2 nucleotide 3' over hang (Rao et al., 2009).

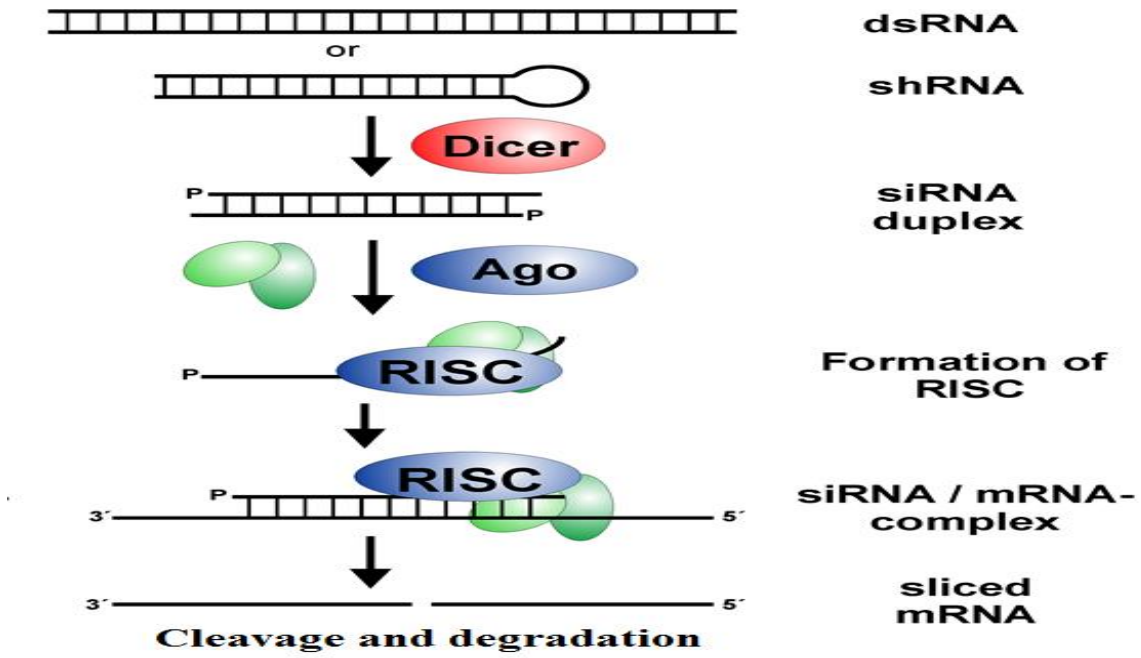

Figure 5.1 Schematic of the RNA interference pathway.

After transfer of the shRNA expression vector into the cytoplasm, the vector for transcription should be delivered into the nucleus. Then by Drosh/DGCR8 complex the primary transcripts are processed and form pre shRNAs. After loading onto the Dicer complex where they are further processed to mature shRNA. The mature shRNA in the Dicer are associated with Argonaute protein including RISC and provide RNA interference function through mRNA cleavage and degradation. This diagram was adjusted and modified from (Rao et al., 2009).

On the other hand the shRNA approach is more efficient than its siRNA counterpart as it incorporates into the endogenous miRNA pathway (Rao et al., 2009).

We used SMARTvector 2.0 Lentiviral shRNA particles (Thermo Scientific Dharmacon) to generate a permanent knock down of BRCA2 in ALT-positive and ALT–negative cell lines. We used the U2OS cell line as the ALT-positive cell line. The primary reason for this is that we used the same cell line for the transient knock-out (see previous Chapter). However, instead of the HeLa cell line that has been used as a control non-ALT cell line in the previous Chapter we decided to use the breast carcinoma cell line MCF7. The main reason for

selecting this cell line is its origin, namely the breast epithelium. This may be important at a later stage in this project. For example, if we are able to knock-down BRCA2 permanently in the above cell lines the next stage would be to treat them with anti-telomerase drugs to test whether telomere maintenance can be disabled completely. Having a breast cancer cell line as one of the test cell lines is important as this is the cellular environment in which BRCA2 exerts its cancer inducing properties.

The SMARTvector 2.0 Lentviral system (Figure 5.2) produces shRNA under the control of the human cytomegalovirus (hCMV) promoter with a drug-selection marker (puromycin) and turboGFP (Evrogen, Moscow, Russia) reporter gene for easy selection of infected cells. It also has a VSVg envelope protein for a broad tropism of infection of mammalian cell type. The structure of the vector is shown in Figure 5.2.

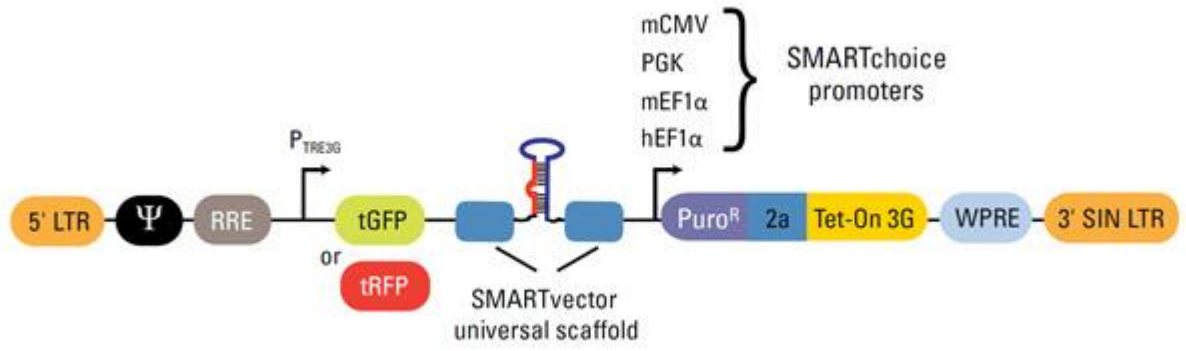

Key:

Vector Element	Utility
5' LTR	5' Long Terminal Repeat necessary for lentiviral particle production and integration of the construct into the host cell genome
ψ	Psi packaging sequence allows viral genome packaging using lentiviral packaging systems
P_{TRE3G}	Inducible promoter with Tetracycline Response Element is activated by the Tet-On® 3G protein in the presence of dox
tGFP or tRP	TurboGFP or TurboRFP reporter for visual tracking expression upon doxycycline induction
SMARTvector universal scaffold	Optimized proprietary scaffold based on native primary microRNA in which gene-targeting sequence is embedded
$Puro^R$	Puromycin resistance permits antibiotic selection of transduced cells
2a	Self-cleaving peptide enables the expression of both PuroR and Tet-On® 3G transactivator from a single RNA pol II promoter
Tet-On® 3G	Encodes the doxycycline-regulated transactivator protein, which binds to *pTRE3G* only in the presence of doxycycline
WPRE	Woodchuck Hepatitis Post-transcriptional Regulatory Element enhances transgene expression in target cells
3' SIN LTR	3' Self-inactivating Long Terminal Repeat for generation of replication-incompetent lentiviral particles

Figure5.2 Elements of the SMARTvector inducible shRNA backbone (adapted from thermoscientificbio.com).

In order to carry out planned knock-down experiments using the SMARTvector 2.0 system some preparatory work was required to establish: (i) the optimum concentration of Puromycin for selection and (ii) the optimum concentration of Polybrene, a chemical that enhances retroviral infection of mammalian cells, which is also the integral part of the SMARTvector 2.0 system. Details of this preparatory work are presented in material and methods (2.11.1).

Having established optimal concentrations of the above two chemicals our next step was to assess transduction efficiency of the SMART vector 2.0 in our two cell lines, MCF-7 and U2OS, using the house keeping gene, GAPDH, before we move on to the BRCA2 knock-down. Details of GAPDH knockdown are described next.

Cells have been transfected with SMART vector 2.0 containing GAPDH insert at different MOI. GFP expression in these cells was assessed using fluorescence microscopy 4 days after transduction (Figure 5.3) and gene expression measured using real-time quantitative PCR (Figure 5.6) and Western blot (Figure 5-7) 96 h after transduction.

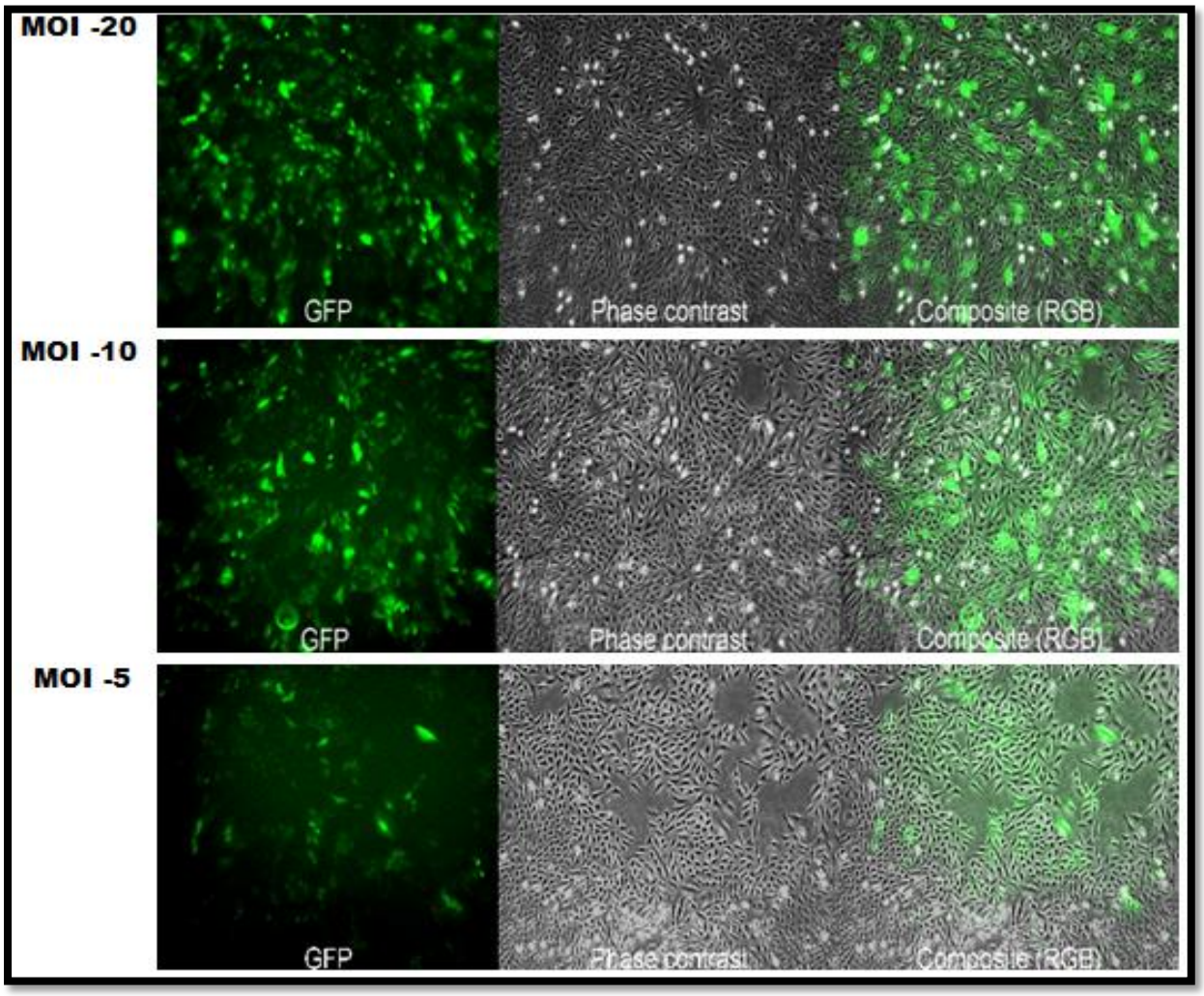

Figure 5.3 Example of GFP expression in U2OS cells. Images show a typical GFP expression in U2OS cells that were transduced with packaged lentiviral vectors expressing shRNA specific GAPDH gene 4 days after transfection. Satisfactory transfection efficiency was seen with both MOI 10 and 20.

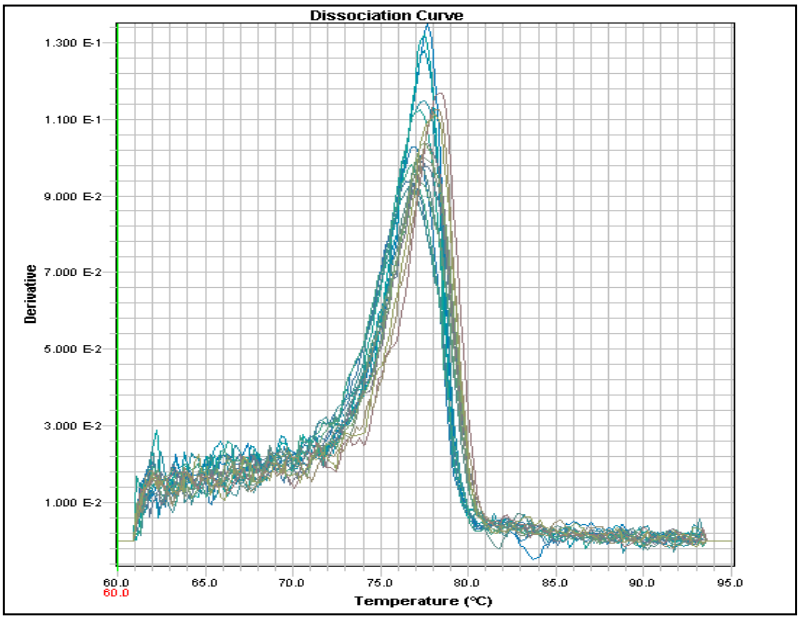

Figure 5.4 Amplification curve for GAPDH primers. GAPDH showing a clean PCR product amplified under real time conditions. There are no signs of primer dimmer formation or secondary products.

Next, the MOI optimization (Figure 5.5) and knock-down verification using endogenous 18s and ACTB genes were carried out. By looking at the changes of the Ct values obtained by Real-time qPCR amplification plots it was concluded that MOI 20 has been most effective.

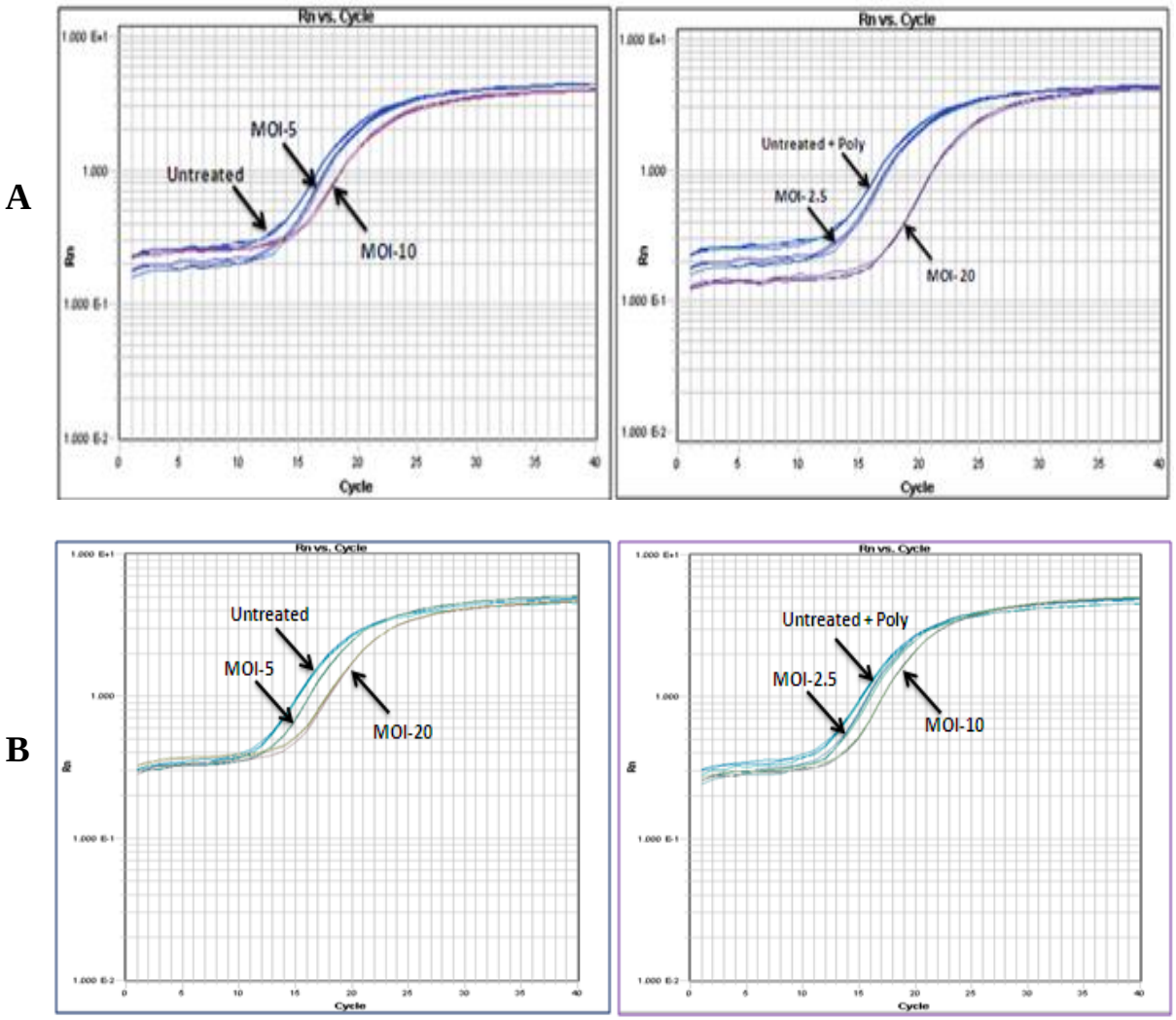

Figure 5.5 Real time PCR amplification curve for GAPDH. A) MCF7 and B) U2OS cell lines at different MOI. MOI-20 was most effective in both cases.

We then normalized GAPDH expression relative to endogenous 18S and ACTB genes (Figure 5.5) in order to assess accurately GAPDH expression following knock-down using the SMARTvector 2.0 system at different MOIs (Figure 5.6). Form Figure 5.6 it was clear that a 90% knock-down was achieved in both cell lines at MOI 20. These results were confirmed by Western blot (Figure 5.7). Therefore, these results indicate that the SMARTvector 2.0 system is capable of knocking-down effectively the expression of GAPDH.

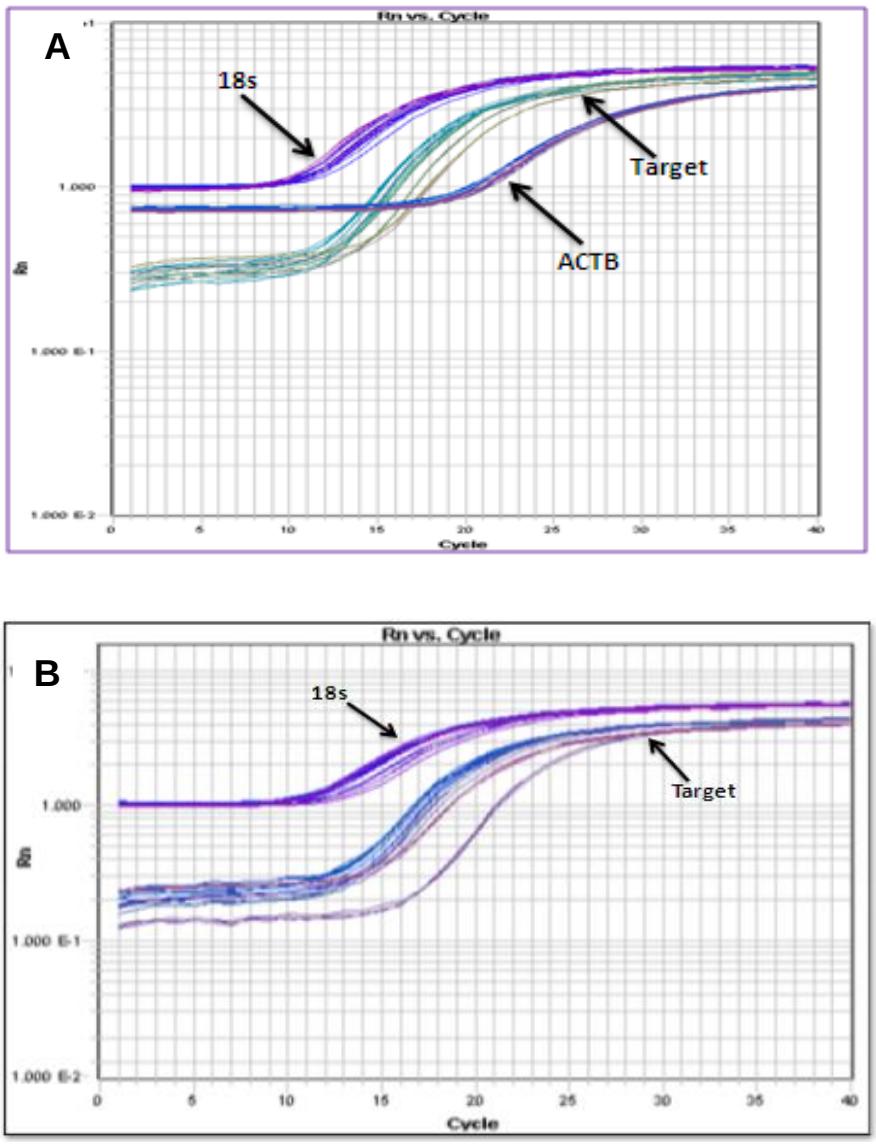

Figure 5.5 Real-Time qPCR amplification curve of GAPDH. A) MCF-7 and B) U2OS cells. The knock-down levels of the target gene (GAPDH) were normalized against endogenous18s (MCF7) or endogenous18s and ACTB genes (U2OS).

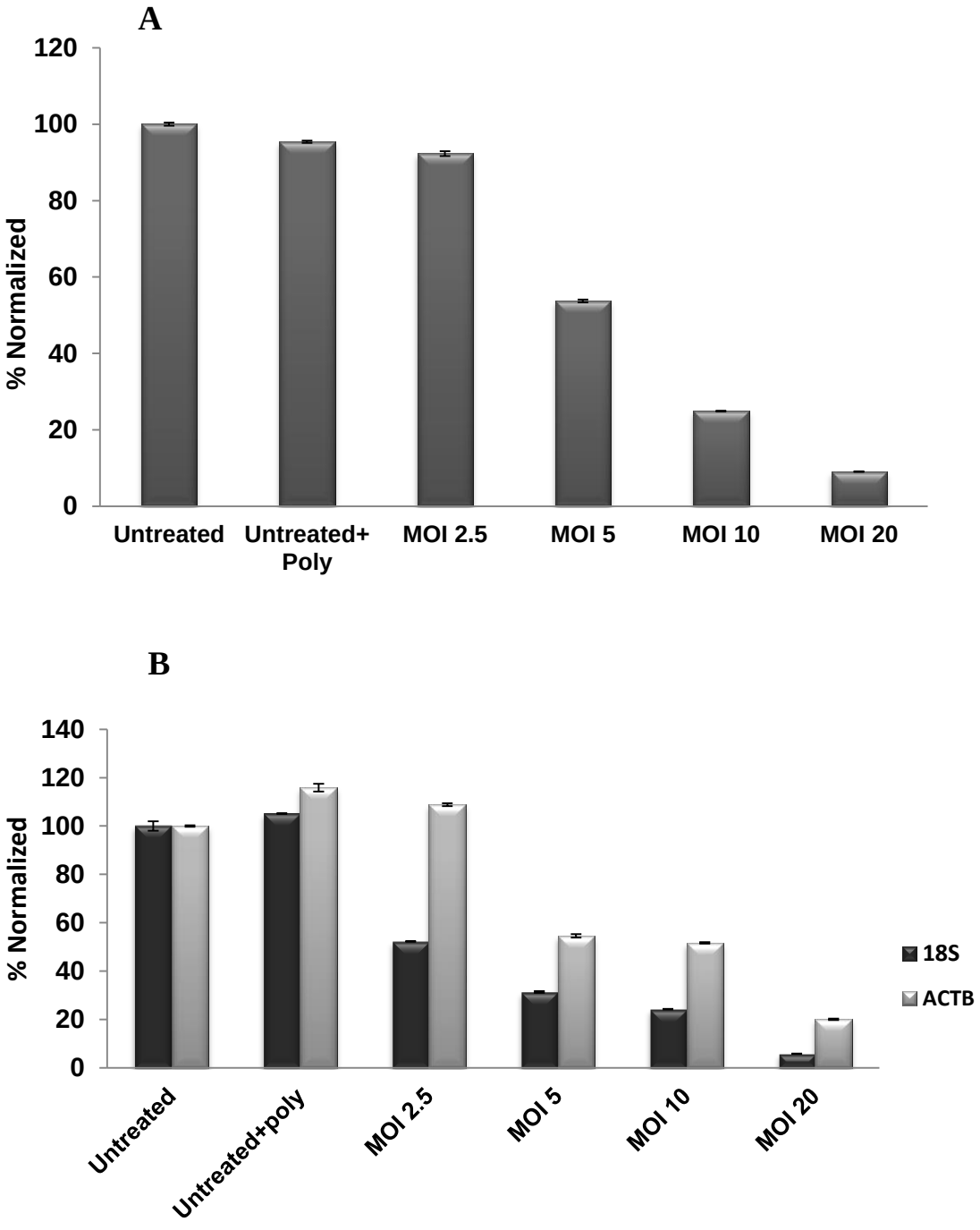

Figure 5.6 GAPDH expression at different MOI after transfection with shRNA. MCF7 (A) and U2OS (B) cell lines. The knock-down levels were normalized against endogenous 18s gene in MCF7 cells and against 18s and ACTB genes in U2OS cells (see Figure 5.5).

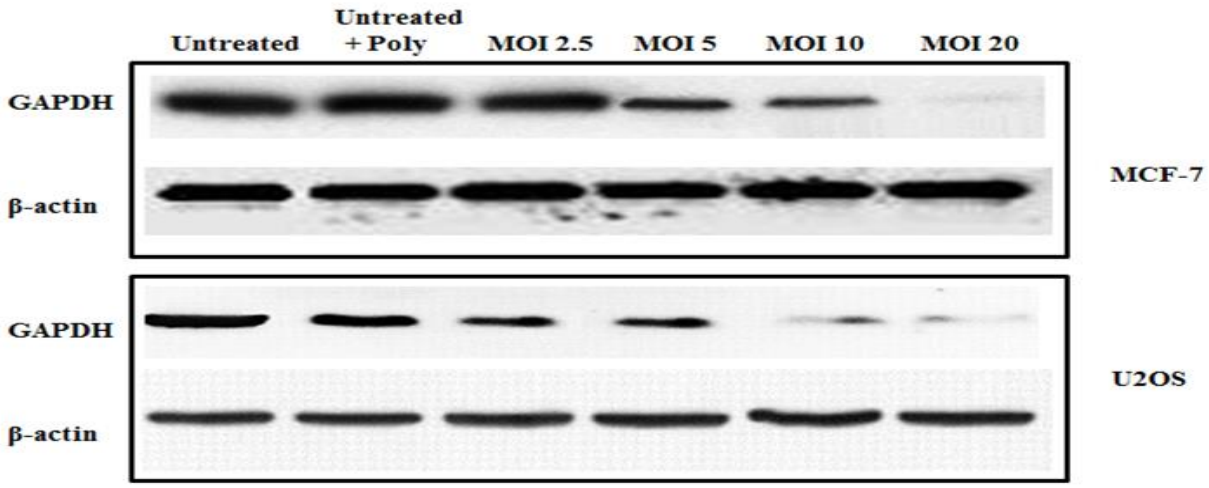

Figure 5.7 Western blot analysis of GAPDH expression. Following transfection with lentiviral shRNA, expression of GAPDH protein levels as detected by Western blotting with control and shRNA tansfected. Equal aliquots from proteins (20µg/lane) were loaded. The level of protein expression in β-actin confirms equal protein loading in both cell types whereas GAPDH bands show different levels of expression in MCF-7 and U2OS after treated with different MOI.

5.3 BRCA2 knock-down using shRNA approach

Given that we optimized the knock-down protocol for the SMARTvector 2.0 system using GAPDH we were confident that the above condition would allow us to replicate the knock-down of BRCA2 in the same cell lines and monitor the long term effect of this knock-down. It is important to note that we have achieved over 90% GAPDH knock-down over the 96 hour period (Figure 5.6). To begin testing on the BRCA2 gene, we identified the optimum MOI as described in materials and method (section 2.11.1).

The SMARTvector 2.0 contained three unique BRCA2 hairpin sequences as shown in (Table 5-1) below. The three sequences were then mixed at equal Titer to generate a pool SMARTvector 2.0. A pool of shRNAs helps to increase the target knock-down efficiency.

Table 5-1 Set of three SMART vector 2.0 human lentiviral shRNA particles.

	Cat.No	Source Clone ID	Vector	Gene Symbol	Gene Target Sequence
1	VSH5417	SH-003462-01-10	hCMV-TurboGFP	BRCA2	GGATTATACATATTTCGCA
2	VSH5417	SH-003462-02-10	hCMV-TurboGFP	BRCA2	ATAAACAGCTGTATACGTA
3	VSH5417	SH-003462-03-10	hCMV-TurboGFP	BRCA2	AATCACTATAGATGGATCA

Three different target sequences of Lentiviral shRNA particles in (Table 5-1) are located between exons 15 and 20. Sequence 1 is located in exon 15 and crosses over to exon 16, sequence 2 is positioned in exon 17 and sequence 3 is located in exon 20 (Figure 5.8).

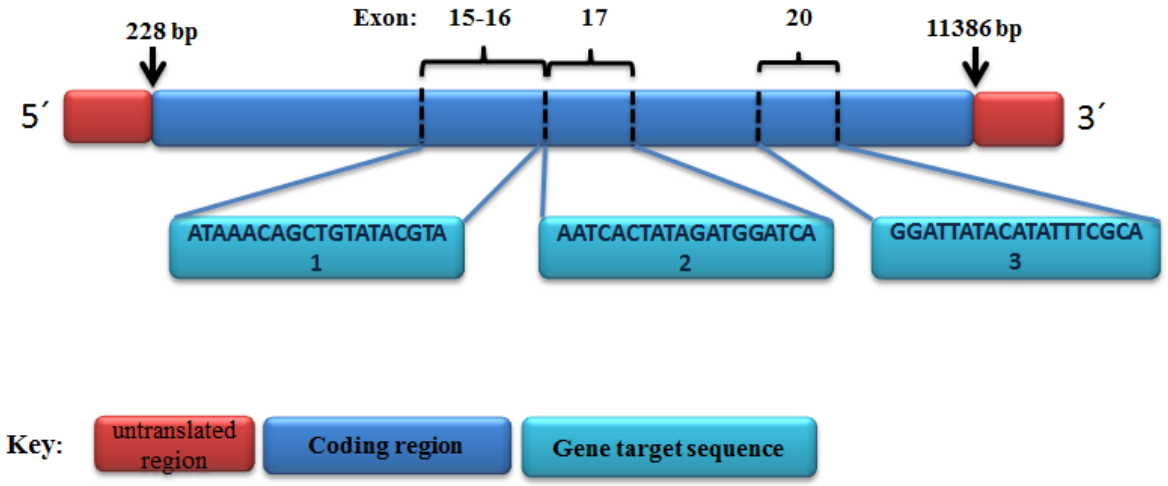

Figure 5.8 Schematic diagram of BRCA2 mRNA which has 11386 bp consisting of 27 exons.

Cells from both cell lines have been transduced with SMARTvector 2.0 particles and incubated for 4 weeks. After 4 weeks we monitored GFP expression in U2OS and MCF7 cell lines by fluorescence microscopy and flow cytometry. A typical profile of cells under the

fluorescent microscope is shown in Figure 5.9. From this Figure it can be seen that MOI 10 has achieved good transduction efficiency as no cells lacking GFP staining were observed.

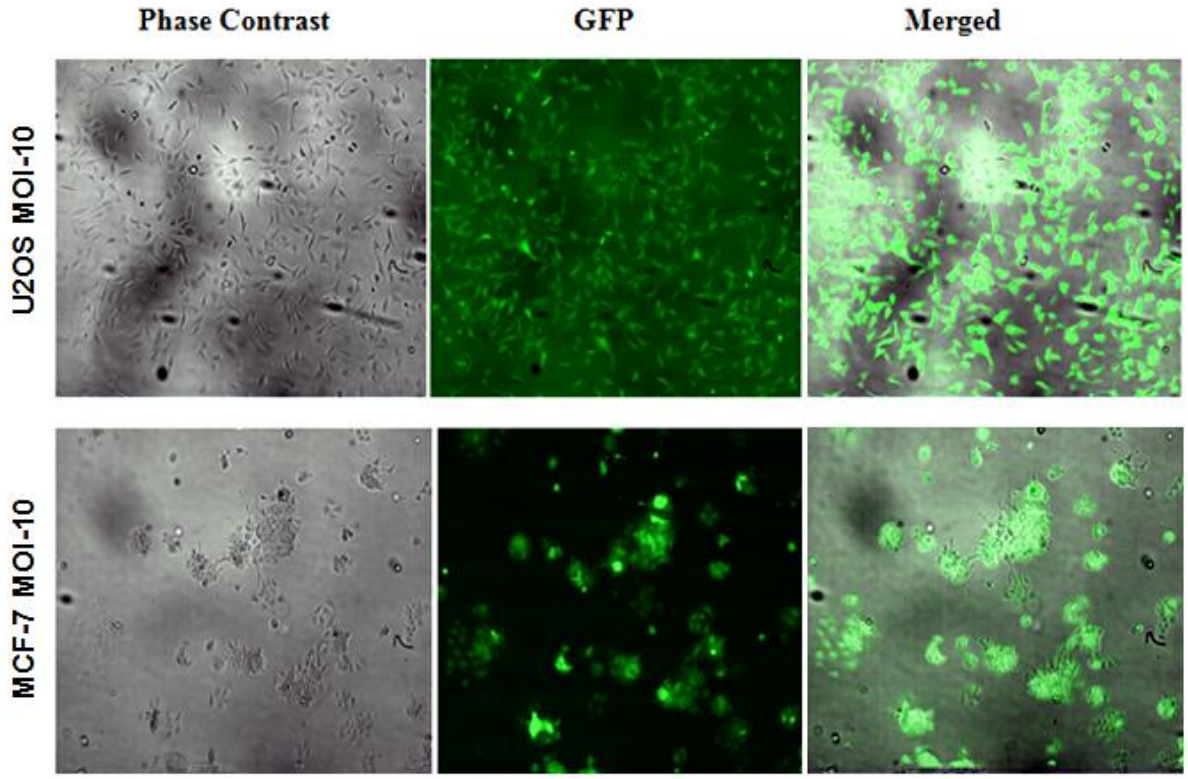

Figure 5.9 GFP expression after four weeks in U2OS and MCF7. Cells that were transduced with packaged lentivirus expressing shRNA specific for the BRCA2 gene. Transfections were performed using MOI-10.

Moreover, the expression of GFP was measured also by Flow Cytometry. As expected, based on Figure 5.9, high levels of GFP (green) fluorescence were obtained in both cell lines using flow cytometry (Figure 5.10).

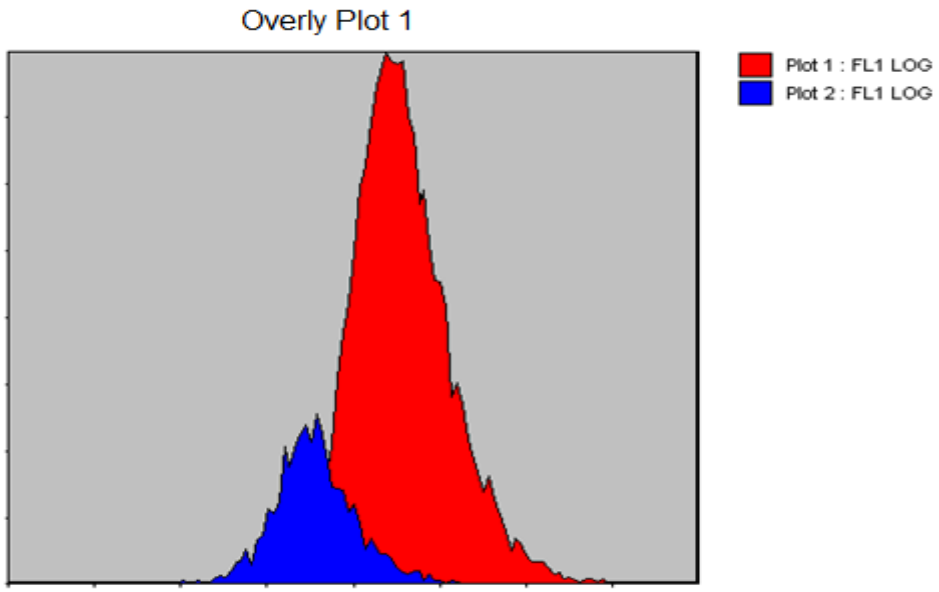

Figure 5.10 A typical Flow Cytometry profile of U2OS cell analysis of subpopulations of cells with BRCA2-shRNA lentivirus. As example the percentage of GFP positive cells was assessed in U2OS cells with flow cytometry. GFP, when excited by a 488 nm laser emits fluorescence that can be detected in the FL1 channel. The blue histogram shows the non-transfected cells, whilst the red histogram shows the cells infected with the GFP contract. Based on FL1 channel analysis over 97% of the infected cells resulted GFP positive, confirming a successful lentiviral vector transduction.

Next, we measured BRCA2 expression by Real-Time PCR at different MOI values. The experiment was performed twice in each cell line in order to ensure reproducibility of results. Figure 5.11 shows average results 20 and 60 days post transduction. It is important to note that the reason for measuring the BRCA2 expression 20 days post transduction was because BRCA2 knockdown caused cell-cycle block resulting in a dramatic decrease in the number of dividing cells in both cell lines. This was similar to what we observed after si-RNA based knock-down in the previous Chapter. Only after 20 days cells began to grow more rapidly and all transfected cells were transferred from 6-well plates to T25 flasks at which stage we had sufficient number of cells for RNA extraction.

Our results were unexpected in comparison to GAPDH results described earlier. Only 15% knock-down was achieved in the U2OS cell line at MOI-10 and 40% in the MCF-7 cell line

at MOI-10 (Figure 5.11 A). Due to this unexpected result, it was hypothesized that a sub-population of cells may have survived puromycin selection after 20 days, therefore both cell lines were maintained in culture in the presence of puromycin for a further 40 days for further investigation. However, when we monitored BRCA2 expression 60 days post transduction there was no major differences (Figure 5.11 B). Almost complete lack of BRCA2 knock-down was evident.

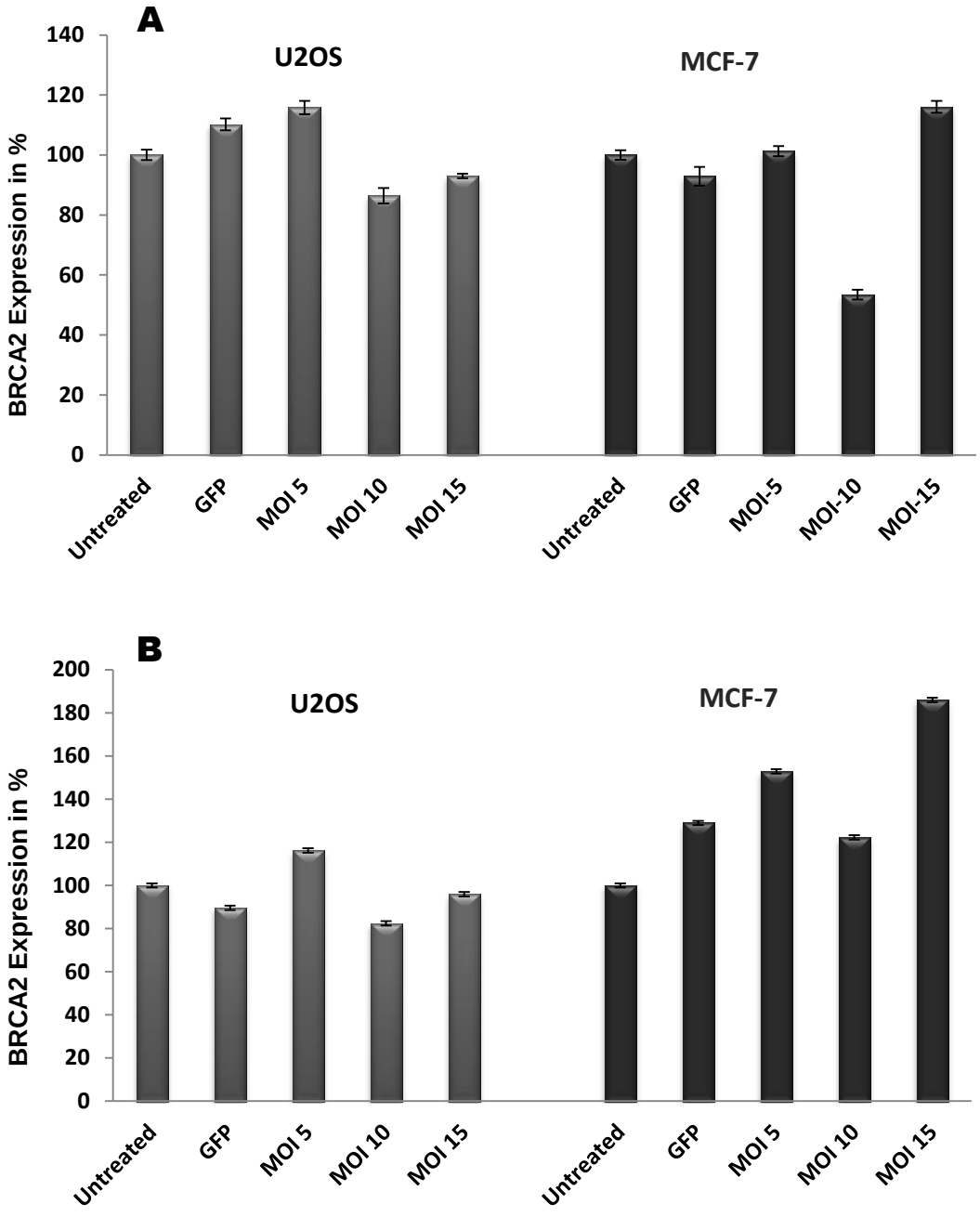

Figure 5.11 BRCA2 expression at different MOI. MOI values after transduction with SMART vector 2.0 human lentiviral shRNA in U2OS and MCF-7 cells 20 days (A) or 60 days (B) following transduction. Relative quantities of BRCA2 mRNA assessed by quantitative real time PCR. shows the relative percentage of BRCA2 mRNA in the two cell lines.

A similar pattern was observed by Western blot, which showed a non-significant BRCA2 expression reduction in the both cell lines following transduction.

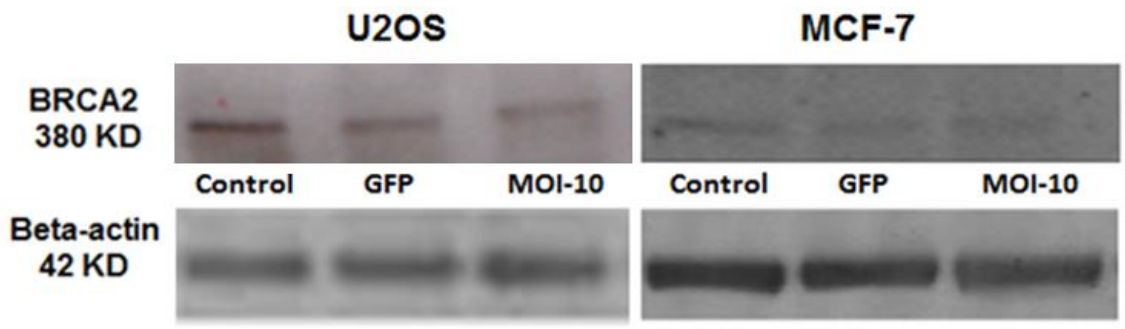

Figure 5.12 Expression of BRCA2 protein levels as detected by Western blot. Expression of BRCA2 proteins, 60 days post-transduction. Equal aliquots of total cell protein (40 µg/lane) were electrophoresed and the protein bands were detected by enhanced chemiluminescence. The expression of ß-actin ratio levels shows equal protein loading in both cell line lanes.

A similar problem of inefficient knock-down using a lenti-virus transduction approach was reported by colleagues in the Division of Biosciences from Professor Newbold's group, Dr Terry Roberts and Dr Hemad Yasaei. They have been able to show that the cause of this poor knock-down was the promoter hypermethylation in transduced cells as reported earlier (Prosch et al., 1996). Therefore, it could be argued that the promoter region in the SMARTvector 2.0 was hypermethylated in transduced cells thus leading to a poor BRCA2 knock-down observed in our cells.

5.3.1 Investigating the causes of poor BRCA2 knock-down

To gain insight into the potential cause of the poor BRCA2 knock-down in our cell lines we treated them with a DNA methyltransferase inhibitor 5-aza-deoxycytidine (5-aza-CdR) (He et al., 2005, Brooks et al., 2004, Ghoshal et al., 2005). The reasoning behind this was that the hCMV promoter in the SMARTvector 2.0 system (see Figure 5.2) could have been silenced by methylation based on: (i) an earlier report (Prosch et al., 1996) and (ii) experience of colleagues in our Division (Roberts and Yasaei, personal communication). If this is the case, then de-methylation by 5-aza-CdR can reverse the effect. Therefore, 5-aza-CdR was used to

treat our cell lines at different time points followed by the assessment of BRCA2 expression levels by qRT-PCR (Figures 5.13 and 5.14).

From Figure 5.13 it can be seen that the number of cells in both cell lines went down with time after treatment with 5-aza-CdR. It has been shown in several studies that 5-aza-CdR has therapeutic value for cancer treatment (Venturelli et al., 2007). Therefore, 5-aza-CdR causes cell death via induction of apoptosis pathways (Jin et al., 2012). It seems after 48 hours treatments a significant reduction in both cell numbers was observed relative to untreated cells.

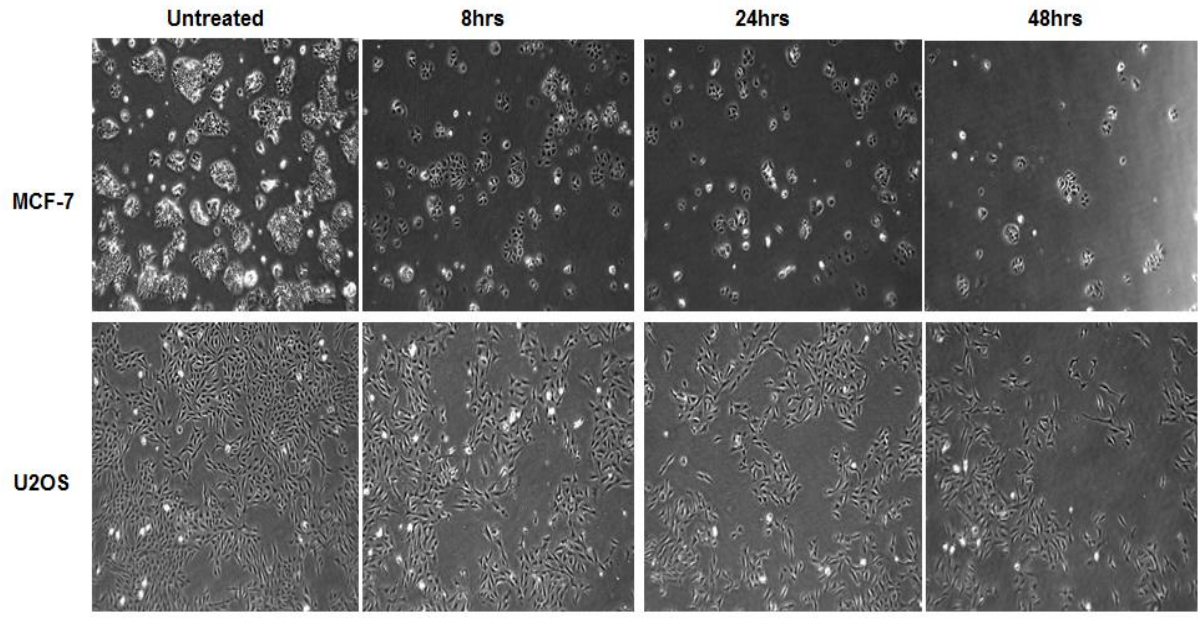

Figure 5.13 Effects of 5-aza-CdR on MCF-7 and U2OS cell lines. MCF-7 and U2OS cell lines were treated with 5μM 5-aza-CdR for 8, 24 and 48 hours.

We then monitored BRCA2 expression relative to the expression observed after transduction with SMARTvector 2.0 at the MOI value of 10 (Figure 5.14). Additional controls included cells transfected with an empty vector (GFP) and untreated cells. In MCF-7 cells the lowest expression of BRCA2 was observed 24 hrs after treatment (Figure 5.14 A). In U2OS cells the lowest expression of BRCA2 was obtained 8hrs after treatment (Figure 5.14 B). Dissociation

curve analysis confirms only one amplification product without any non-specific amplification or primer dimer (Figure 5.14 A).

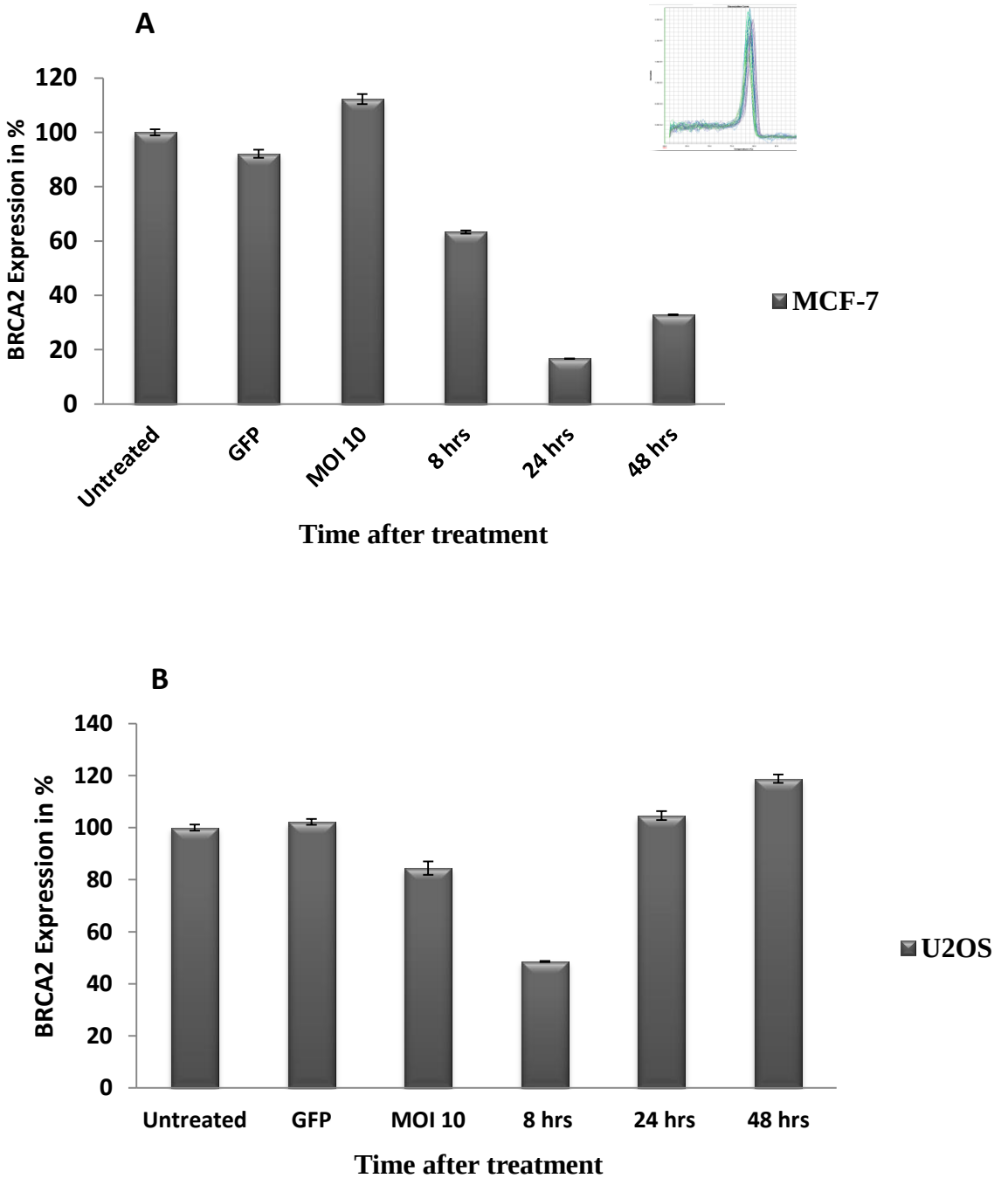

Figure 5.14 BRCA2 expression at different time points after treatment with 5-aza-CdR (5µM). A) MCF7 and B) U2OS cells. Error bars represent SE.

The fact that the expression of *BRCA2* went down following treatment with 5-aza-CdR suggest that indeed hyper-methylation of the hCMV promoter may have been responsible for the poor BRCA2 knock-down observed in our cells.

5.4 Determination of telomerase activity by conventional TRAP assay

We have also measured telomerase activity in both cell lines. The reason behind this was to assess telomerase activity in cells with long-term *BRCA2* knock-down as we suspected that BRCA2 could be associated with the ALT pathway. Telomerase and ALT rarely operate at the same levels in the single cell type. Therefore, expression of telomerase activity was assessed by the q-PCR-based telomerase activity detection method, Telomeric Repeat Amplification Protocol (TRAP). As controls we used two cell lines, PC3 and PC3/hTERT, known to have robust telomerase activity.

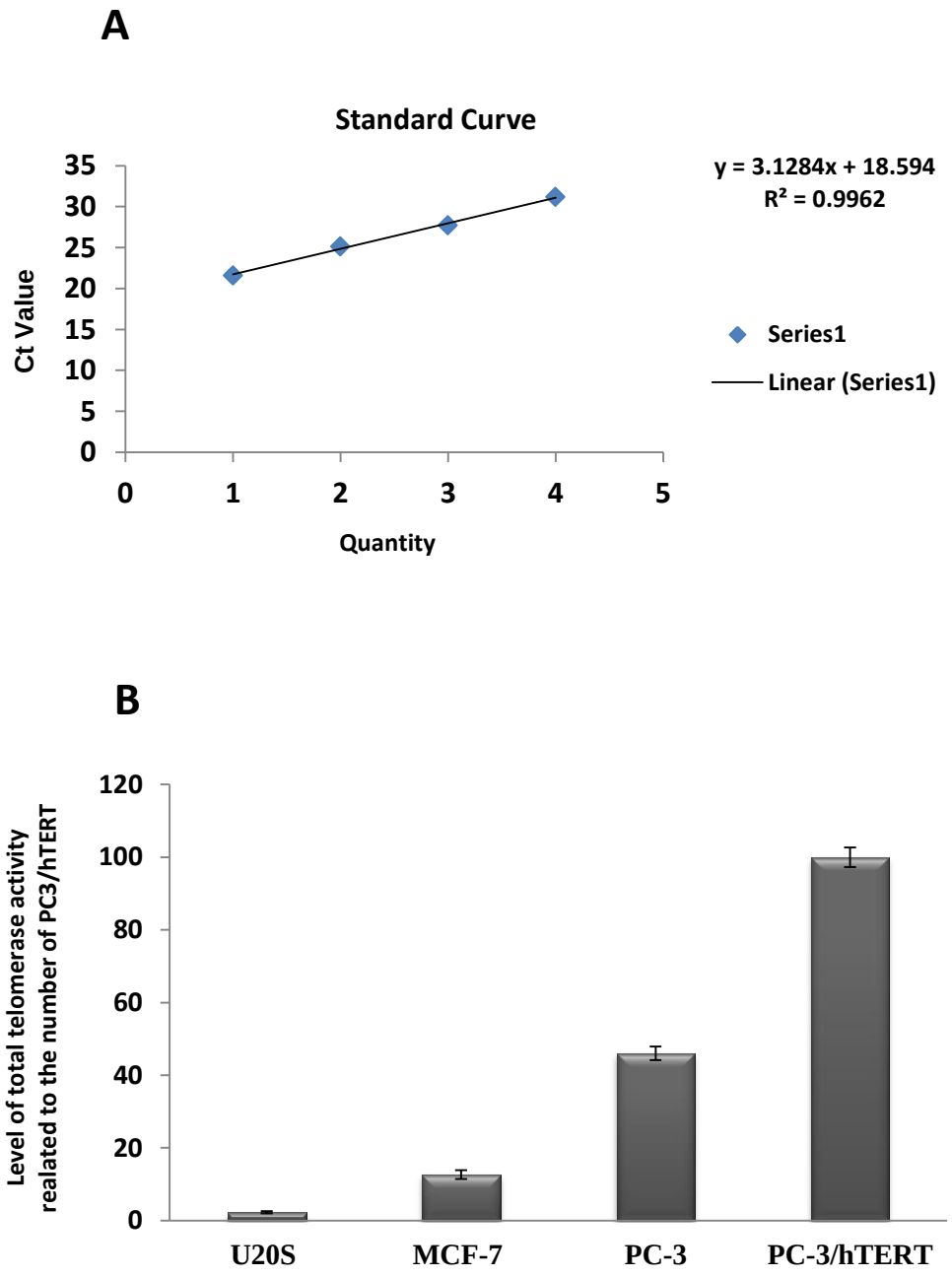

Figure 5.15 Telomerase activity as measured by RTQ-TRAP. A) Serial dilution of PC-3/hTERT cell extract versus Ct with linear trendline for regression analysis. B) Quantitation of telomerase activity in different cell lines.

Our results revealed a low telomerase activity in U2OS cells and a medium activity in MCF7 cells (Figure 5.15). Both PC-3 and PC-3/hTERT cells showed robust telomerase activity as expected.

5.5 Discussion

The initial aim of this part of the work was to generate a long-term BRCA2 knock-down in ALT positive and ALT-negative cell lines. It was planned that once this long-term knock-down was achieved the next step should be monitoring phenotypic features of resulting clones with a view to selecting suitable clones for treatment with anti-telomerase drugs. The thinking behind this was that BRCA2 deficiency could potentially affect the ALT pathway (see Chapter 4) and that it could create conditions for greater telomerase expression in ALT positive cells in which telomerase is down-regulated or absent. Indeed our results of telomerase activity assessment in ALT-positive U2OS cells revealed much lower telomerase activity than in non-ALT MCF7 and P-C3 cells (Figure 5.15). Therefore, this work was aimed at exploring the strategy for telomere maintenance manipulation in the ALT-positive cell line U2OS.

Unfortunately, we encountered problems with the long-term *BRCA2* knock-down (Figure 5.11) using SMARTvector 2.0 Lentiviral shRNA particles (Thermo Scientific Dharmacon). It seems likely that the problems are caused by the hypermetylation of the promoter in the vector system as the treatment of cells with 5-aza-CdR resulted in the increase of BRCA2 expression (Figure 5.14).

In eukaryotic genomes, epigenetic alterations such as methylation of DNA and histone modifications by specific enzymes play an important role in regulating gene expression. In vertebrates, many lines of evidence indicate that aberrant DNA methylation can alter the expression of genes that play an essential role in preventing tumorigenesis (Das and Singal, 2004). DNA methylation is carried out by DNA methyltransferase (DNMTs) enzymes that transfer a covalent methyl group to the position 5 of cytosine at CpG dinucleotides (Momparler et al., 2000). The DNMT family consists of five members: DNMT1, DNMT2,

DNMT3A, DNMT3B and DNMT3L (Okano et al., 1998). DNMT1 is the main enzyme that responsible to methylate hemi-methylated DNA during replication (Pradhan et al., 1999). Gene expression can be inhibited by the methylation of DNA via preventing transcription factors. This process is carried out by protruding out methyl group to the major groove of the DNA helix (Maldonado et al., 1999). A DNA methyltransferase inhibitor, such as 5-aza-CdR demethylates DNA to induce the re-expression of silenced genes (Ghoshal et al., 2005). Re-expression of BRCA2 following 5-aza-CdR treatment (Figure 5.14) is in line with this possibility.

Alternatively, the cause of poor BRCA2 knock-down could have been alterations in the RNAi silencing machinery, in particular alterations in Dicer and Drosha levels. It has been shown that there is a down-regulation of mRNA expression in cancer cells in general but it is not known whether this is due to low dicer levels or due to shortened 3' untranslated regions with fewer miRNA-binding sites (Lu et al., 2005). Both cell lines used, MCF7 and U2OS, are cancer cell lines. Interestingly, a reduced Dicer expression was observed in patients with ovarian cancer (Merritt et al., 2008). Also poor silencing using the shRNA approach has occurred in ovarian cancer cell lines due to low versus high Dicer levels (Schmitter et al., 2006). This shows that the levels of Drosha and Dicer mRNA can disrupt effective knock-down.

Because of the failure to generate a long-term BRCA2 knock-down the rest of the planned experiments, such as phenotype assessment of generated clones and treatment of the resulting clones with telomerase inhibitors were not performed.

Chapter-6

BRCA2 involvement in interstitial telomeric maintenance

6.1 BRCA2 may be involved in interstitial telomeric maintenance in Chinese hamster

6.2 Introduction

In the last part of the project we examined repair kinetics of DNA damage in the set of Chinese hamster BRCA2 deficient and proficient cell lines described in Chapter 3. This introductory section explains the rationale behind this part of the study.

The Chinese hamster genome (2n=22) contains a total of 18 interstitial telomeric sites (ITSs) consisting of large blocks of $(TTAGGG)_n$ sequences located in the centromeric or pericentromeric regions of most chromosomes (Slijepcevic and Hande, 1999). A number of studies carried out in the last 20 years revealed that these ITSs are preferential sites of radiation-induced chromosome breakage (Bolzan, 2012 and 2001, Slijepcevic et al., 1996, Rivero et al., 2004). All these studies used classical cytogenetic approaches to study radiation-induced chromosomal aberrations following FISH with telomeric probe. The exact reasons for the increased incidence of radiation-induced chromosome breakage within ITSs in the Chinese hamster genome remain unknown.

The occurrence of ITSs has been assumed to be the consequence of tandem chromosome fusion (telomere-telomere fusion) during the insertion of telomeric DNA within unstable sites during the repair of DSBs (Azzalin et al., 2001) or during evolution (Meyne et al., 1990, Hastie and Allshire, 1989). ITSs often co-localise with preferential sites of breakage, DNA amplification and chromosomal recombination (Bolzan and Bianchi, 2006, Lin and Yan, 2008, Ruiz-Herrera et al., 2008). It is important to note that so far only a few studies examined the role of ITSs in the long term clastogenicity (Marder and Morgan, 1993, Day et al., 1998).

It has been postulated that ITSs may behave as classical fragile sites (Bolzan, 2012). Fragile sites are physiologically occurring regions in chromosomes that show predisposition to

breakage after treatment with folate reducing chemicals. Interestingly, it has been suggested that not only ITSs, but also terminal telomeric sequences may behave as fragile sites (Sfeir et al., 2009; Bosco and de Lange, 2012). According to this scenario telomeric DNA sequences pose a problem for DNA replication machinery as exemplified by frequent replication-related problems within these sequences that resemble aphidicolin-induced fragile sites (Sfeir et al., 2009). A combination of telomeric proteins such as TRF1 and various helicases such as BLM is required to resolve the resulting fragility. More recently, it has been shown that interstitial telomeric sequences at the human chromosome 2q14 constitute an aphidicolin-induced common fragile site (Bosco and de Lange 2012). TRF1 binds this fragile site in the same manner as it binds terminal telomeric sequences (Bosco and de Lange 2012).

In order to gain further insight into the mechanisms of ITS fragility we monitored DNA damage in ITSs using the TIF assay and total genomic DNA damage using the standard gamma-H2AX assay. Furthermore, we employed additional methods to assess radiation-induced damage in the set of 4 Chinese hamster cell lines. Given the role of BRCA2 at telomeres reported in Chapter 3 the question is whether the aberrant telomere maintenance phenotype resulting from dysfunctional BRCA2 could also affect DNA repair kinetics within ITSs relative to the rest of the genome. To the best of our knowledge this is the first study that uses TIF and gamma-H2AX assays to assess radiation-induced damage at ITSs.

6.3 Results

We used the same set of Chinese hamster cell lines described in Chapter 3. As a reminder, V79B is a BRCA2 proficient control cell line. The V-C8 cell line is BRCA2 defective. The remaining two cell lines are V-C8 isogenic which the BRCA2 defect was corrected either as a result of introducing a BAC with a functional copy of the murine Brca2 gene (V-C8+Brca2),

or human chromosome 13 containing functional BRCA2 (V-C8+#13) (Kraakman-van der Zwet et al., 2002).

6.3.1 Study of ITSs dysfunction in untreated Chinese hamster cell lines at interphase using γ-H2AXand TIF assay

We started by analysing spontaneous DNA damage in Chinese hamster cell lines using the γ-H2AX and TIF assays. As explained in previous chapters these methods detect either global DNA damage in the genome (γ-H2AX assay) or a fraction of DNA damage that localizes within telomeric sequences (TIF assay) (dAdda di Fagagna et al., 2003 and Takai et al., 2003).

It is important to note that Chinese hamster chromosomes contain large number of ITSs (see introduction) and that telomeres in these cells are very short and hardly detectable by FISH (see Chapter 3). Therefore, it is likely that the large majority of telomeric sequences that can be detected by TIF will represent ITSs. A cell was considered TIF positive if at least one telomeric signal co-localized with a γ-H2AX signal (Figure 6.1).

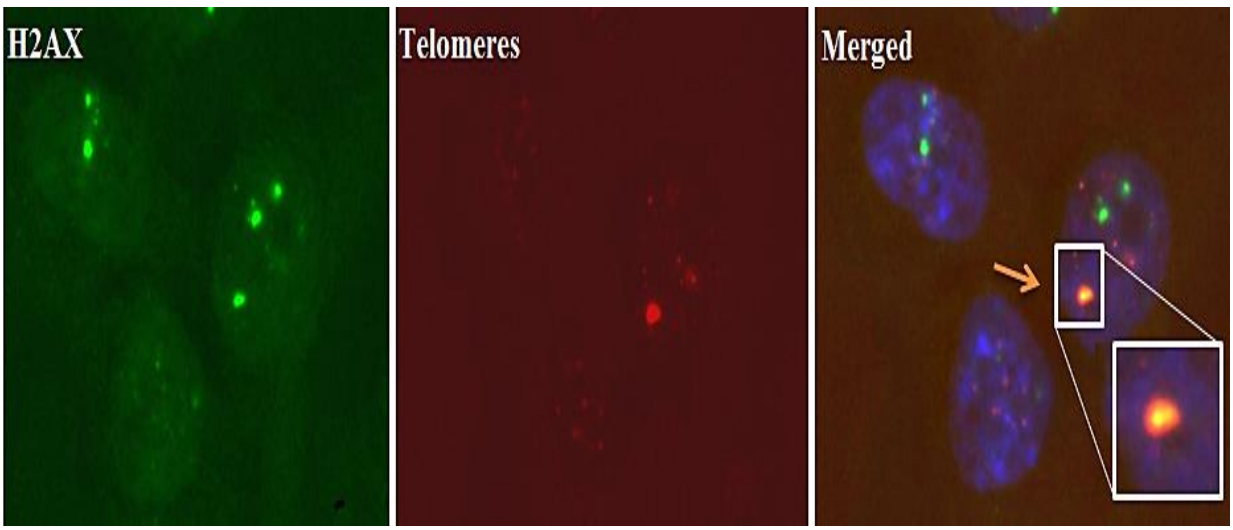

Figure 6.1 An example of Chinese hamster cells images generated by γ-H2AX and TIF assays. Cells were incubated with primary γ-H2AX and hybridyzed with PNA telomeric sequence $(CCCTAA)_3$ conjugated with a Cy-3 fluorescence label (middle image). Co-localization of the γ-H2AX and telomeres represent a TIF (labelled by arrowed).

Results of our analysis are presented in (Figure 6.2). The frequency of γ-H2AX foci/cell ranged from ~ 3 in BRCA2 proficient cells to ~ 8 in BRCA2 deficient cells (Figure 6.2 A). Therefore, these values represent the total DNA damage in the genome. The results of TIF analysis (Figure 6.2 B) allow us to estimate the proportion of DNA damage occurring within telomeric sequences including ITSs and terminal telomeric sequences. Given that terminal telomeric sequences are short in Chinese hamster cells and almost undetectable by FISH (see Chapter 3) it is safe to assume that the large majority of telomeric sequences detected by the TIF assay will be due to ITSs. Our results of TIF analysis suggest that ~10% of DNA damage occurs within telomeric sequences in BRCA2 proficient cells (Figure 6.2 B). This proportion is higher in BRCA2 deficient cells (~17%) (Figure 6.2 B). We would like to note that the frequency of spontaneous DNA damage is somewhat higher in normal Chinese hamster cells (V79B-3 foci/cell) relative to most normal human cell lines used in our laboratory that show on average 1-2 foci/cell.

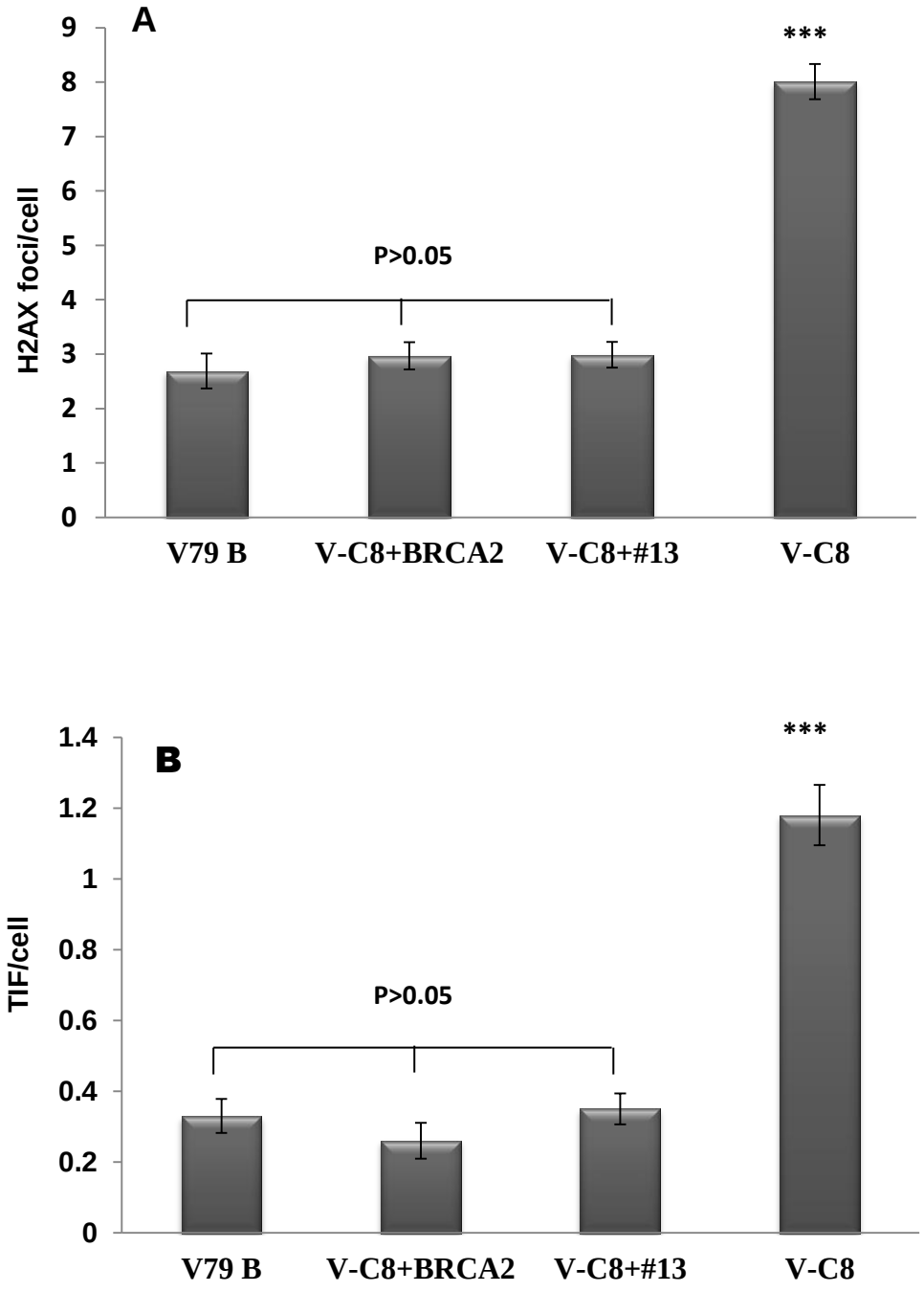

Figure 6.2 Frequency of γ-H2AX foci and TIF in hamster cell lines. A) γ-H2AX foci and B) TIF in untreated Chinese hamster cell lines. The error bars represent SEM, ***=P < 0.001.

6.3.2 Analysis DNA damage kinetics in hamster cell lines using γ-H2AX and TIF assay

Next, we analysed responses of the four Chinese hamster cell lines to ionizing radiation. All cells were irradiated with 1.0 Gy of gamma rays and DNA damage repair kinetics assessed at different time intervals after irradiation. Examples of H2AX and TIF foci in irradiated cells are shown in Figure 6.3. Green - γ-H2AX; Red – telomeric probe.

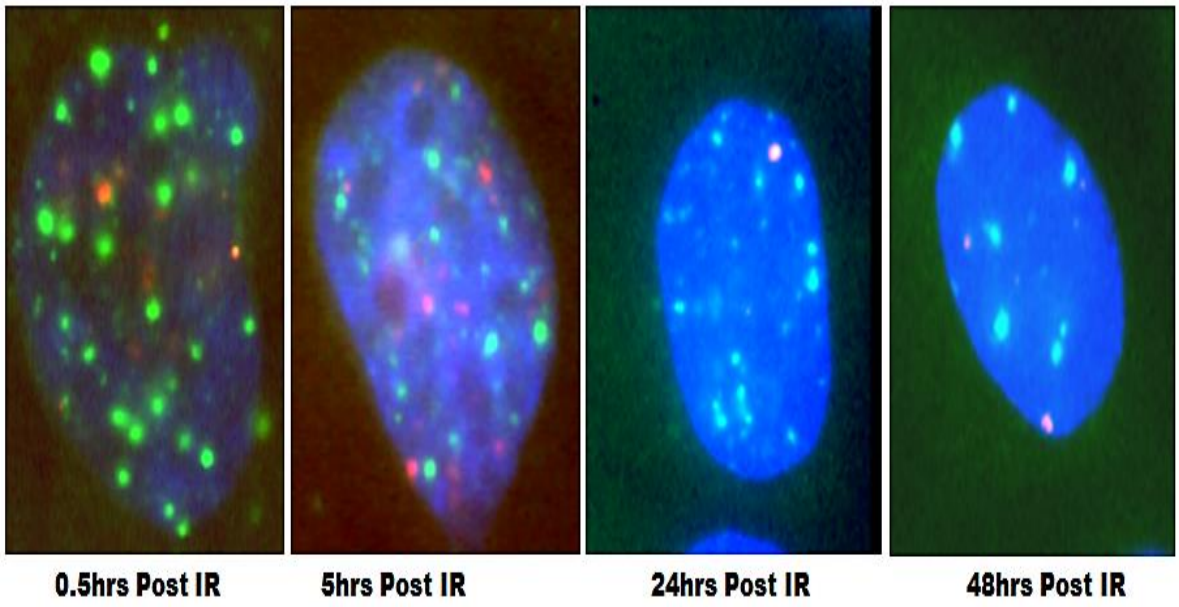

Figure 6.3 Chinese hamster cells at different time points following irradiation. An example of V-C8 interphase BRCA2 cells defective at four time points after 1Gy of irradiation. The reduction in frequency of γ-H2AX foci was clearly evident.

Results of our analysis are shown in Figure 6.4. It is clear from this analysis that BRCA2 proficient cell lines have been able to repair DNA damage effectively judging by the presence of approximately 3 foci/cell in control cells and cells observed 24 h and 48 h post-irradiation. However, BRCA2 defective cells have not been able to repair damage effectively judging by the presence of ~ 13 and ~ 9 foci/cell 24 h and 48 h after irradiation respectively, relative to 8 foci/cell in control non-irradiated cells (Figure 6.4). Therefore, these results are in line with expectation given that BRCA2 is involved in DNA damage response.

Cell lines	0.5 hrs	5hrs	24hrs	48hrs
V79B	***	***	P>0.05	P>0.05
V-C8+BRCA2	***	***	P>0.05	P>0.05
V-C8+#13	***	***	P>0.05	P>0.05
V-C8	***	***	***	*

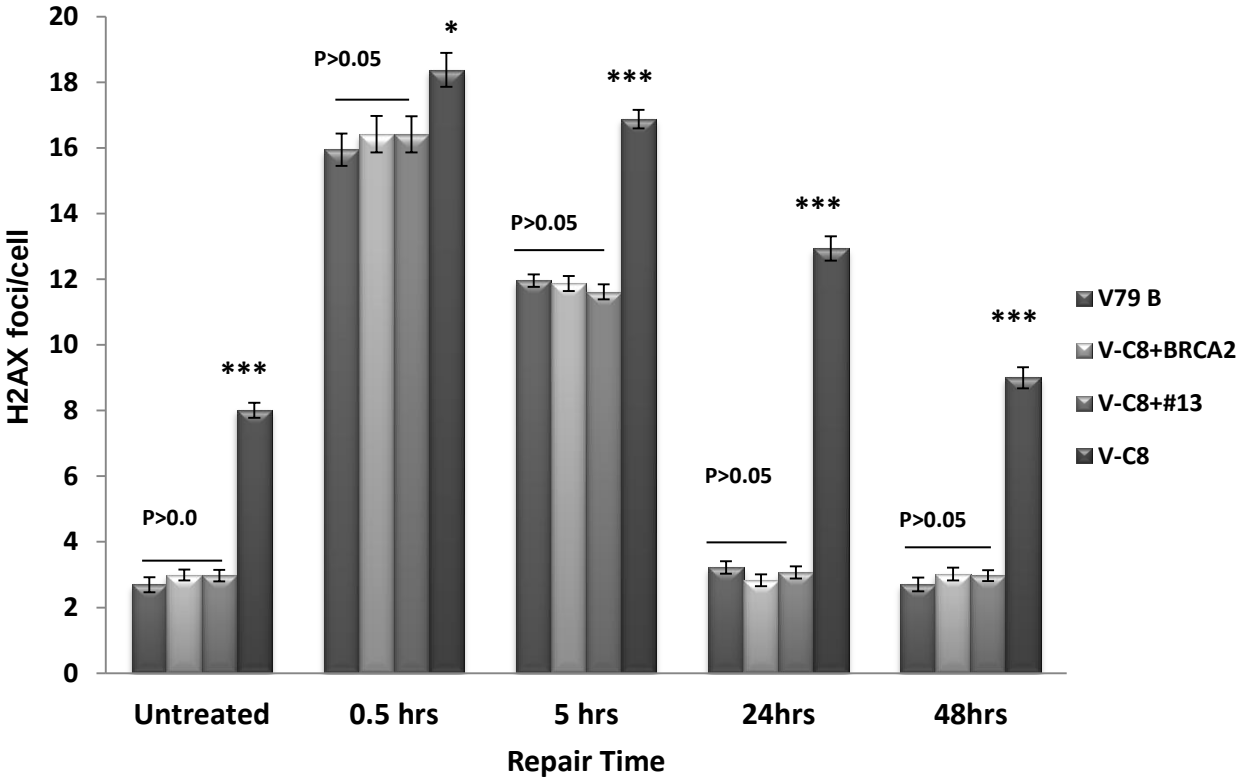

Figure 6.4 Frequencies of γH2AX foci after radiation in hamster cell lines. A normal and BRCA2 defective cell lines at different time intervals following 1.0 Gy gamma radiation. *=P<0.05, **=P<0.01, ***=P<0.001, Error bars represent SEM.

6.3.3 Telomere dysfunction Induced Foci (TIF) assay analysis in hamster cell lines

By using the TIF assay we have been able to assess repair kinetics within ITSs. All BRCA2 proficient cells have been able to repair DNA damage within telomeres effectively as frequencies of TIFs were similar in control cells and cells observed 24 h and 48 h after irradiation (Figure 6.5). However, BRCA2 defective cells showed different values of TIFs 24 h and 48 h after irradiation relative to control cells. In control cells TIF frequency was 1.18 TIF/cell, whereas cells observed 24 h and 48 h after irradiation showed values of 1.8 TIF/cell and 1.44 TIF/cell respectively (Figure 6.5). These results were statistically significant ($P<0.05$). Therefore, we can conclude that the BRCA2 defective cell line shows a defective DNA damage response when exposed to IR and that telomere dysfunction contributes significantly to this defective response (Figure 6.5).

Cell lines	0.5 hrs	5 hrs	24 hrs	48 hrs
V79B	***	*	P>0.05	P>0.05
V-C8+BRCA2	***	*	P>0.05	P>0.05
V-C8+#13	***	*	P>0.05	P>0.05
V-C8	***	***	***	*

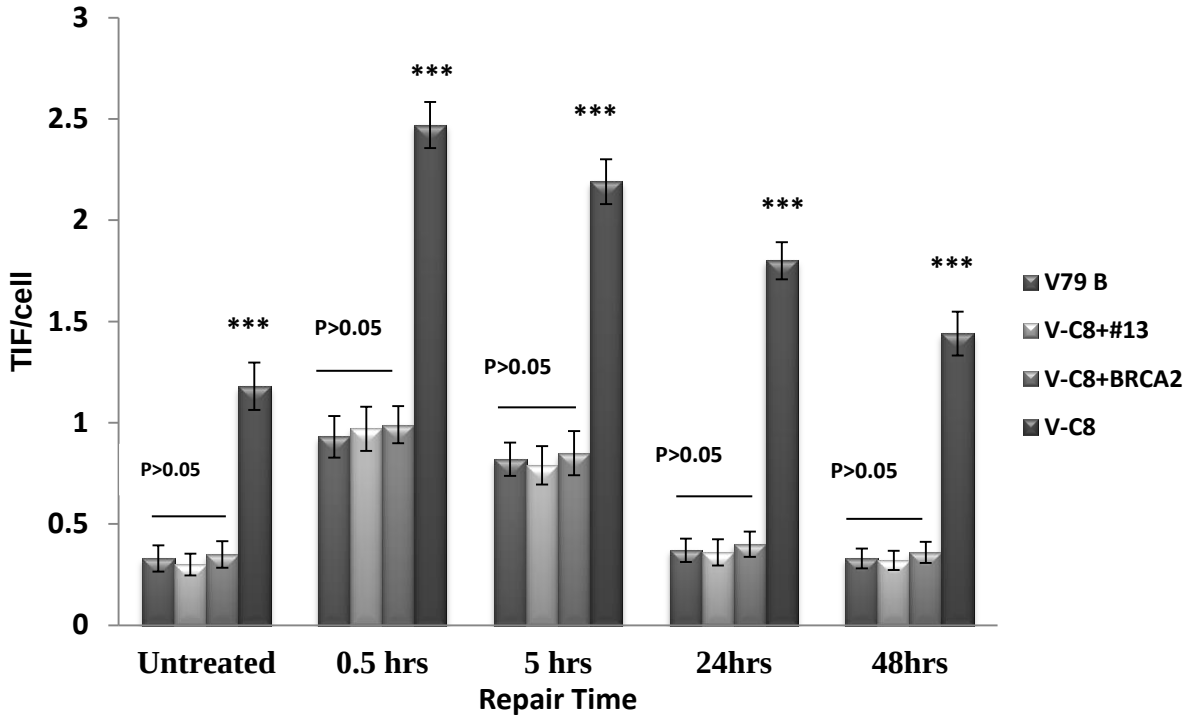

Figure 6.5 Frequency of TIF after radiation in Chinese hamster cell lines. Frequencies of TIF/cell in normal and BRCA2 defective cell lines at different time intervals following 1.0 Gy gamma radiation. *=P<0.05, **=P<0.01, ***=P<0.001, Error bars represent SEM.

6.3.4 Immunofluorescence detection of γ-H2AX in ITSs in metaphase cells

Given that our analysis of γ-H2AX foci and TIFs was carried out in interphase cells we ignored the fact that some of TIFs we observed may have not been localized within ITSs but rather within terminal telomeric sequences. As argued earlier (see Chapter 3) telomeres in Chinese hamster cell lines are short and the large majority of the fluorescence signal observed after FISH in interphase cells is likely to be due to ITSs. Nevertheless, it is important to determine the fraction of DNA damage occurring within terminal telomeric sequences.

This can be done only by analysing DNA damage in metaphase chromosomes. Classical metaphase chromosome preparation which uses strong fixatives (methanol and acetic acid) precludes the use of antibodies such as those against γ-H2AX. Therefore, a different protocol for chromosome preparation suitable for γ-H2AX and TIF detection needs to be developed.

Using a gentle fixation procedure (low concentration of formaldehyde) and the cytospin method for chromosome spreading we managed to obtain metaphase chromosome preparations suitable for γ-H2AX detection. Representative examples of spontaneous chromatid breaks detected by the γ-H2AX specific antibody are shown in Figure 6.6. However, our attempts to combine this protocol with the telomeric PNA probe in order to carry our TIF analysis have failed so far. However, we are confident that the TIF assay suitable for metaphase chromosome analysis will be developed within the next several months.

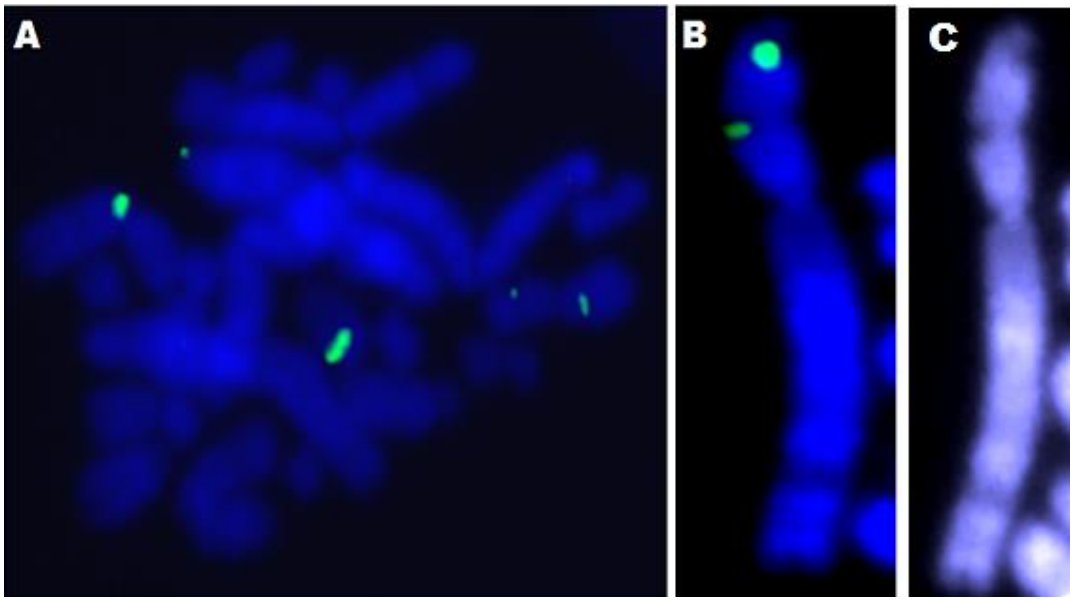

Figure 6.6 Detection of γ-H2AX foci in Chinese hamster metaphase cells. A) An example of a metaphase cell derived from BRCA2 defective hamster cell line V-C8. Green fluorescence represents DNA damage foci. Please note most of DNA damage are located within pericentromeric regions of chromosomes (sites of ITSs). B) A metaphase chromosomes showing localization of γ-H2AX within chromatid breaks. C) DAPI stain of picture B, showing localization of damage at chromosome.

In the absence of the means to detect telomeric sequences in metaphase chromosome preparations we resorted to karyotyping after hybridization with the telomeric PNA probe as shown in Figure 6.7 A-D. Using the generated karyotype information as a guide for detecting ITSs and telomeres we then classified spontaneous γ-H2AX foci into three categories:

(i) Those localizing within ITSs

(ii) Those localizing within terminal telomeric sequences

(iii) Those localizing outside ITSs and terminal telomeric sequences.

It is important to note that our method for γ-H2AX foci detection in metaphase chromosomes is not perfected yet to enable a simultaneous detection of γ-H2AX foci and telomeric sequences in the same slides. Results of our analysis are shown in Figure 6.7 E.

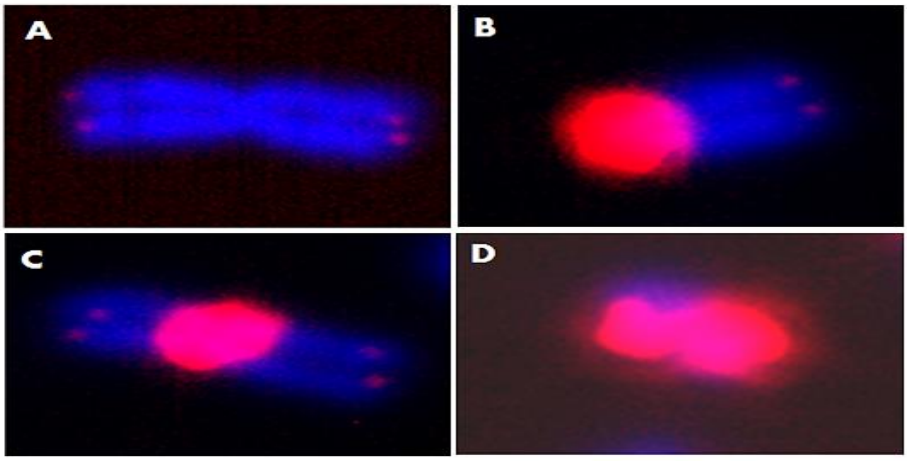

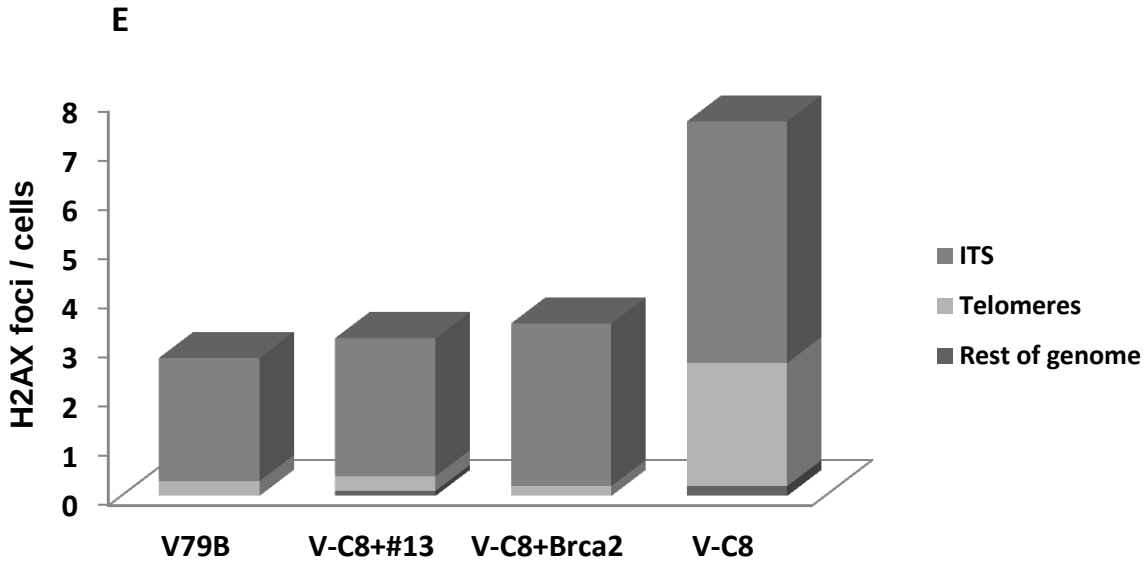

Figure 6.7 Frequencies of DNA damage foci in metaphase. A-D Individual Chinese hamster chromosomes showing typical hybridization patterns with the telomeric probe. E) Distribution of γ-H2AX foci within different regions of Chinese hamster chromosomes.

The average number of spontaneous γ-H2AX foci in three normal cell lines was similar and it ranged from 3-4 foci/cell (Figure 6.7 E). In contrast the BRCA2 defective V-C8 cell line had 8 foci/cell (Figure 6.7 E). It is clear from this analysis that, in the BRCA2 proficient cells, the large majority, >90%, of spontaneous γ-H2AX foci localize within ITSs with the

remaining foci being localised mostly within telomeres (Figure 6.7 E). The number of foci/cell localizing outside ITSs and telomeres was almost negligible. In contrast, BRCA2 defective V-C8 cells showed somewhat different pattern. The percentage of ITS localising γ-H2AX foci was in the region of 60-70%, whereas 30% γ-H2AX foci localized within telomeres with only a tiny fraction being localized outside ITSs and telomeres (Figure 6.7 E). However, when these results are compared with the results of γ-H2AX and TIF assays (Figure 6.4 and Figure 6.5) it is clear that the frequencies of DNA damage occurring within telomeric sequences as analysed in metaphase chromosomes is a gross over-estimate. This over-estimate is most likely caused by the lack of accuracy when classifying DNA damage foci using rough karyotyping as a guideline. Therefore, for the accurate estimate of DNA damage occurring within terminal telomeric sequences we need to complete development of the TIF protocol suitable for metaphase chromosomes.

6.3.5 Telomere dysfunctions in hamster BRCA2 defective cells

6.3.5.1 Anaphase bridge analysis in Chinese hamster cell lines

In the rest of this chapter we describe results of two more assays that detect DNA damage and can be used as confirmation of the results generated by the γ-H2AX assay. First we analysed frequencies of anaphase bridges. Anaphase bridges were first observed in maize by McClintock (McClintock, 1941, McClintock, 1942) and are today considered a hallmark of chromosome fusion resulting from telomere loss (Gisselsson et al., 2001, Rudolph et al., 2001). Examples of Telophase lags observed in Chinese hamster cells are shown in Figure 6.8.

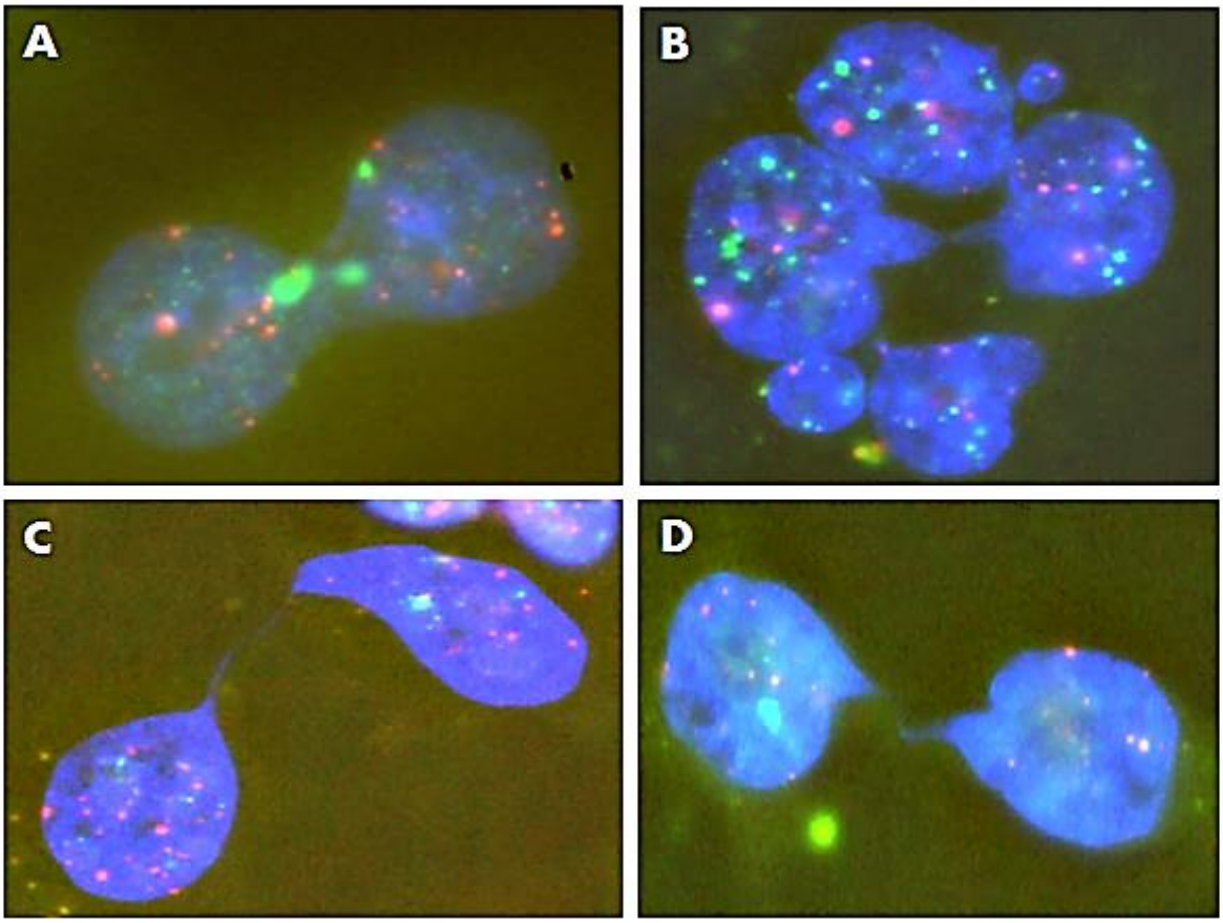

Figure 6.8 Telophase lags in the Chinese hamster cell line. A,B,C and D)The cells were captured in late anaphase-early telophase. A) Note the presence of red fluorescence within the Telophase lags. Red fluorescence represents telomeres. Green fluorescence is due to H2AX. Please note there are two Micronuclei in B.

We next quantified anaphase bridges observed in four Chinese hamster cell lines following irradiation. The pattern of repair was similar to that observed following the γ-H2AX assay (Figure 6.9).

Cell lines	0.5 hrs	5 hrs	24 hrs	48 hrs
V79B	P>0.05	P>0.05	P>0.05	P>0.05
V-C8+BRCA2	P>0.05	P>0.05	P>0.05	P>0.05
V-C8+#13	P>0.05	P>0.05	P>0.05	P>0.05
V-C8	***	***	***	P>0.05

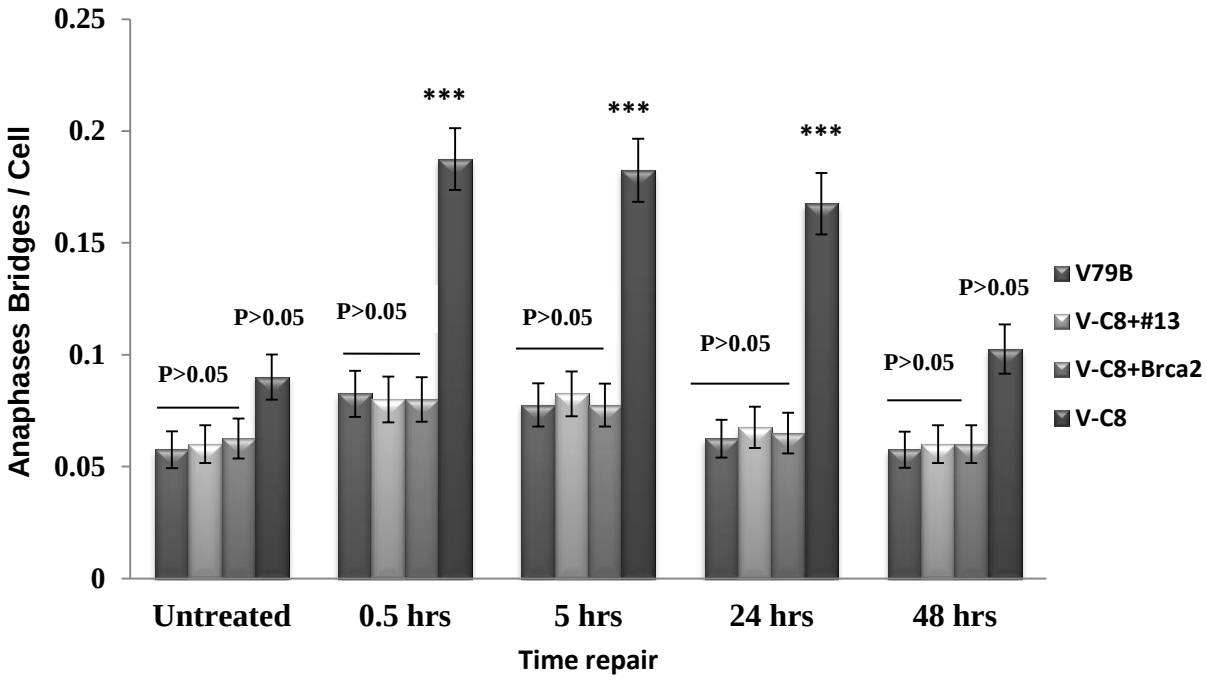

Figure 6.9 Anaphase bridge frequencies in Chinese hamster cell lines. Graph shows frequency of anaphase bridge at different time point following exposure to 1.0 Gy of gamma rays. *=P<0.05, **=P<0.01, *** = P < 0.001, Error bars represent SEM.

6.3.5.2 Micronuclei analysis in Chinese hamster cell lines

Next, we analysed micronuclei (MN) frequencies using the Cytochalasin B in four hamster cell lines. The cytokinesis-block MN assay in mammalian cells is one of the most commonly used technique for assessing DNA damage. MN resulting from whole chromosomes or chromosome fragments cannot attach to the mitotic spindle and lag behind the rest of chromosomes when the cell divides (Stewenius et al., 2005) (Figure 6.10).

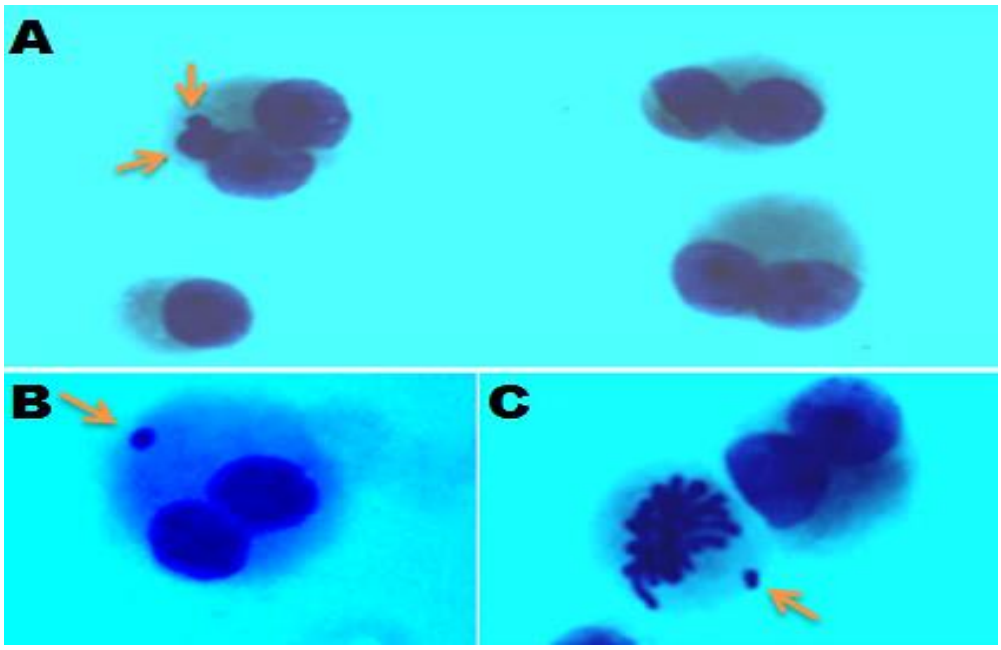

Figure 6.10 Examples of different MN forms in Chinese hamster cells. A) Three ideal binucleated cells one of which shows MN (arrows); B) Ideal binucleated cell with one clear MN; C) One binucleated cell and one metaphase cells containing a lagging chromosome fragment that will become a MN in anaphase.

Frequencies of radiation induced MN 24 hrs after ɣ-irradiation were assessed by scoring 500 binucleated cells in each cell line. Similarly to the patterns observed in this chapter, BRCA2 defective cells showed higher frequencies of MN relative to BRCA2 proficient cells (Figure 6.11).

Cell lines	2.0 Gy	4.0 Gy
V79B	*	*
V-C8+BRCA2	*	*
V-C8+#13	*	*
V-C8	***	***

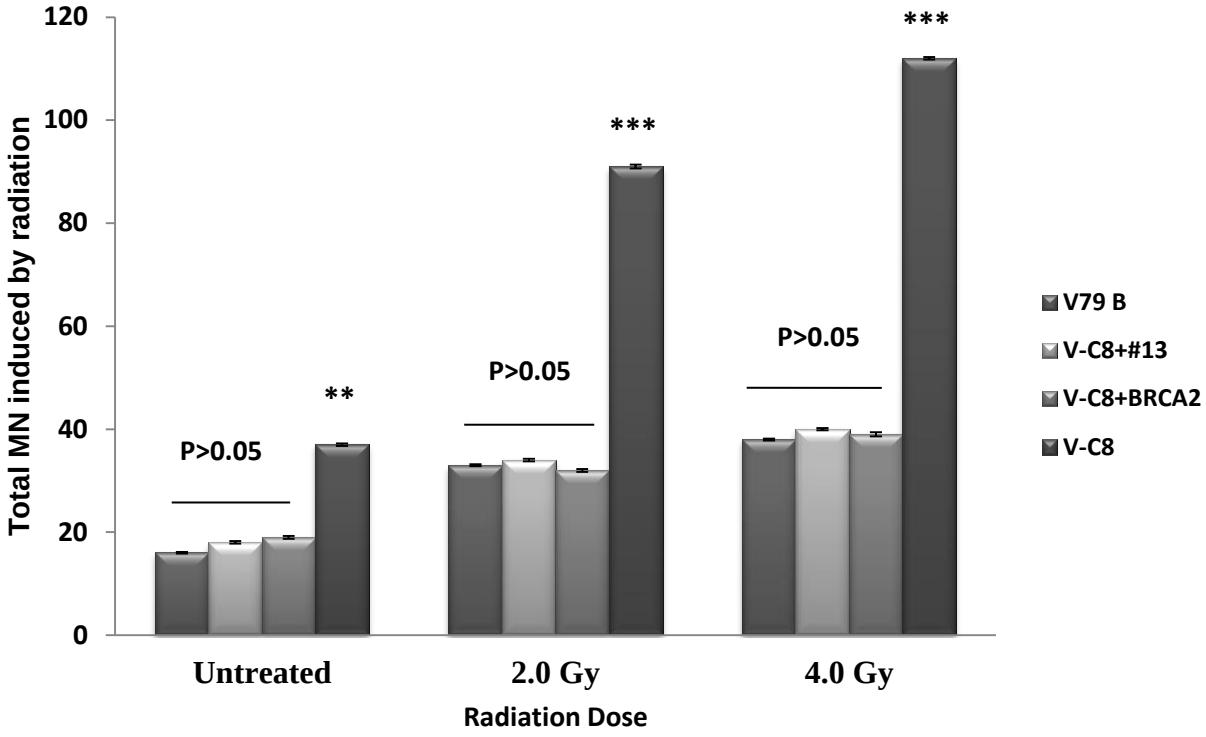

Figure 6.11 MN frequencies after irradiation in Chinese hamster cell lines. MN induced by IR 24 h after exposure to 2 and 4Gy in cultures of three BRCA2 normal (V79B , VC8+#13 and V-C8+BRCA2) and BRCA2 defective (V-C8)cell lines, treated with 6 µg/ml of Cyt-B. *=P<0.05, **=P<0.01, *** = P < 0.001. Mean ± S.E. from 500 scored cells.

.

6.4 Discussion

A number of studies have indicated that ITSs in the Chinese hamster genome are preferentially involved in spontaneous and radiation-induced chromosome breakage (Bertoni et al., 1994, Alvarez et al., 1993). Mechanisms behind this preferential involvement are not fully understood at present. It has been postulated that ITSs may (i) behave as fragile sites (Slijepcevic et al., 1996, Bolzan et al., 2001), (ii) act as unstable sites during DNA DSB repair (Bolzan, 2012) or (iii) be targeted by telomerase in the process of chromosome healing leading to chromosome breakage (Slijepcevic et al., 1996). In this Chapter we tested the hypothesis that DSB repair may be affected within ITSs. To this end we irradiated a set of 4 BRCA2 proficient and deficient cell lines using a dose of 1.0 Gy of gamma rays and monitored repair of DSBs using γ-H2AX and TIF assays.

Monitoring of DSBs by the γ-H2AX assay revealed somewhat higher frequencies of spontaneous DSBs in 3 BRCA2 proficient cell lines including the normal cell lines, V79B (Figure 6.4) relative to normal human cell lines used in our laboratory. However, the analysis of radiation induced chromosome breakage in the same cell lines using Giemsa staining revealed lack of spontaneous breakage (see Chapter 3; Figure 3-15). The expectation is that a higher frequency of DSBs will lead to a higher frequency of chromosome aberrations as it has been recognised that the molecular lesion responsible for chromosomal breakage is DSB (Natarajan and Obe 1985; Bryant 1985). Given the lack of correlation between the two it is possible that some γ-H2AX positive foci observed in untreated Chinese hamster cells may be not due to DSBs but rather due to chromatin modification changes as reported in embryonic stem cells (Turinetto et al., 2012). Embryonic stem cells show high frequencies of spontaneous γ-H2AX positive foci but their genome maintenance is normal judging by the absence of chromosomal aberrations. Alternatively, some other currently unknown

mechanisms may be implicated in this higher rate of spontaneous γ-H2AX positive foci in Chinese hamster cells.

Regarding the distribution of γ-H2AX positive foci within the telomeres as observed by the TIF assay it was clear that in normal cell lines approximately 10% of DSBs were located within ITSs (Figure 6.5). This seems to be an expected frequency as large blocks of ITSs in the Chinese hamster genome are unlikely to exceed 10% of the total Chinese hamster genome. However, in the case of the BRCA2 defective cell line this frequency was approximately 17% (Figure 6.5) suggesting that the BRCA2 defect may indeed affect repair of DSBs within ITSs. This is in line with the observed increase in recombination rates at telomeres in BRCA2 defective cells (see Chapter 3) (Sapir et al., 2011, Bodvarsdottir et al., 2012).

Exposure of cells to IR allowed us to test more directly the possibility that the BRCA2 deficiency may also affect repair kinetics within ITSs but also whether normal cells show different repair kinetics within ITSs.

As far as normal cells (BRCA2 proficient) are concerned repair kinetics within ITSs did not differ from the repair kinetics in the whole genome (Figure 6.4 and Figure 6.5). For example, the frequency of γ-H2AX positive foci in the normal V79B cell line 24 and 48 h after irradiation was the same as that before irradiation (Figure 6.4) indicating full repair. Similarly, frequencies of TIFs were the same in V79B cells before irradiation and 24/48 h after irradiation (Figure 6.5) again indicating full repair within these sequences. However, in the case of the V-C8 cell line (BRCA2 defective) repair kinetics was not as effective. For example, 24h and 48h after irradiation these cells had 13 foci/cell and 9 foci/cell respectively as opposed to 8 foci/cell in control non-irradiated cells (Figure 6.4). This suggests (i) slower

repair kinetics and (ii) inability to fully repair DNA damage long time after irradiation. Most normal cells will repair DSBs within 24h after irradiation (Gordon et al., 2002).

Therefore, BRCA2 deficiency confers general DSB repair deficiency. This general DSB repair deficiency also affects repair kinetics within ITSs. While normal cells are able to fully repair DSBs within ITSs in 24 h, BRCA2 defective cells cannot carry out full repair. For example, 24h and 48h after irradiation numbers of TIFs were 1.8/cell and 1.44/cell as opposed to 1.18/cell in control cells (Figure 6.7). Therefore, we can conclude that repair kinetics within ITSs in BRCA2 defective cells is slower/incomplete relative to BRCA2 normal cells.

Taken together, these results do not offer any major new insights into the mechanisms of ITS sensitivity to radiation-induced damage but allow us to add some refinements to the current understanding. Our results indeed replicate cytogenetic results which showed excess of chromosome breakpoints localizing within ITSs (Bertoni et al., 1994, Alvarez et al., 1993, Slijepcevic et al., 1996, Balajee et al., 1994). For example, spontaneous levels of γ-H2AX positive foci localizing within ITSs in normal cells were roughly 10% (see above). It has been estimated that the percentage of telomeric sequences in the genomes of immortalized Chinese hamster cells like those used in this study is roughly 3% (Bolzan et al. 2001). Therefore, the DNA damage excess of 300% relative to the expected level based on the random distribution of DSBs within the genome is largely in line with previous estimates one of which suggested a 4-6 times higher levels of chromosome breakage in ITSs relative to the rest of the genome. In the case of DSBs defective cells (V-C8) the excess of DNA damage localizing within ITSs, relative to the rest of the genome, is 600% suggesting that DSB repair defects enhance the overall effect.

However, surprisingly DSB repair kinetics within ITSs was proficient in normal Chinese hamster cells (Figures 6.5) suggesting that the hypothesis implying the role of ineffective DSB repair within ITSs may be discarded.

It is important to note that the present study had a minor limitation which, we believe, will be resolved in our future studies. This limitation is the reliance on interphase cells to carry out the TIF assay. As shown in (Figure 6.6) at present we are not able to carry out γ-H2AX detection in metaphase cells in combination with telomeric sequences. This is caused by our inabilities to merge two separate protocols (immuno-FISH and metaphase chromosome preparation by non-standard methods) into one effective protocol. However, we believe that we can achieve this within the next several months. The fully functioning protocol will enable us to calculate precisely percentages of DNA damage occurring within ITSs and terminal telomeric sequences relative to total DNA damage induced in the genome.

Chapter -7

General Discussion and Future work

7-1 General Discussion and future works

The key findings of this thesis can be summarized as follows. Defective BRCA2 causes telomere dysfunction, which manifests in telomere shortening, increased frequencies of ECFs and increased frequencies of T-SCEs (Sapir et al., 2011; Chapter 3). Increased T-SCE frequencies are consistent with the notion that BRCA2 may act as repressor of recombination at telomeres. However, in ALT positive cells the opposite is true, namely BRCA2 knock-down in these cells leads to a reduction in T-SCEs (Sapir et al., 2011; see also Chapter 4). We speculate that ALT positive and ALT negative cells may represent two different cellular environments in which DDR mechanisms are regulated in different fashions as suggested by a recent publication (Lovejoy et al., 2012). It is well established that most DDR response mechanisms, including DNA repair mechanisms, are characterized by functional plasticity. A good example is the NHEJ pathway, which has an alternative, or back-up form that was not appreciated in the past (Mladenov and Iliakis 2012). It is therefore possible that BRCA2 may play differential roles in cellular environments that show differences in DDR mechanisms and their regulation. Finally, our analysis of DSB repair kinetics within ITSs showed no major differences in repair capacities of ITSs relative to the rest of the genome (see Chapter 6). This disproves the hypothesis that ineffective repair of DSBs within ITSs may be responsible for their sensitivity to DNA damaging agents (Azzalin et al., 2001). The reason for this unusual sensitivity therefore must be searched for within the alternative hypothesis which points to the possibility that ITSs may behave as fragile sites (Bosco and de Lange, 2012).

The work on this project started in 2010 and at that time very little was known about the role of BRCA2 at telomeres. The first study that indicated a potential role of BRCA2 in this respect was that of Badie et al. (2009). Some of our results were published soon after that and the main contribution of this work to the current understanding of BRCA2 at telomeres is the

observation that BRCA2 may act as repressor of recombination at telomeres in ALT negative cells (Sapir et al. 2011; see also Chapter 3). Our finding was confirmed by a study of Bodvarsdottir et al., (2012).

Our ambition was to expand on this finding and explore its potential for cancer therapeutics. One scenario seemed particularly interesting. Given that BRCA2 dysfunction leads to reduction in T-SCE frequencies in ALT positive cells (Sapir et al. 2011; see Chapter 4) it seemed reasonable to argue that BRCA2 dysfunction may disable telomere maintenance by the ALT pathway. This pathway requires recombination and disabling the protein like BRCA2, which plays a key role in the process, may disrupt the whole recombination machinery. If this is indeed the case the expectation would be that creating BRCA2 deficiency together with inhibiting telomerase mechanisms could disable the process of telomere maintenance. Given that this process seems vital for proliferation of cancer cells the approach may constitute a valid avenue for cancer therapeutics.

The key test for the above scenario is to create a long term BRCA2 deficiency in the ALT positive environment and assess its effect on cell proliferation and other relevant phenotypic parameters. Unfortunately, our attempt to create a permanent BRCA2 knock-down in ALT positive U2OS cells did not work as described in Chapter 5.

One of the points for the future research is a more detailed examination of the failure of a permanent BRCA2 knock-down using the SMARTvector 2.0 system. While our preliminary results point to the epigenetic alterations of the promoter region in the vector system as a cause, other potential causes must be examined. It is worth noting that any attempt at knocking down expression of proteins involved in DDR will inevitably create a significant cell cycle block and cell proliferation problems. We observed a very strong proliferation block after transient BRCA2 knock-down (Sapir et al., 2011; see also Chapter 4). The same

situation was replicated when we attempted knock-down using the SMARTvector 2.0 system (see Chapter 5). The cell cycle block lasted for many days and it is possible that this situation created conditions that accelerated epigenetic changes including those affecting the promoter within the vector system. This occurred in the case of both ALT positive and ALT negative cells (see Chapter 5). One encouraging sign is that if the BRCA2 knock-down is long lasting then it may have a negative effect on cell proliferation which is a pre-requisite for a successful cancer therapy.

Another area that can be explored further is the examination of repair kinetics within ITSs and terminal telomeric sequences using the metaphase chromosome approach described in Chapter 6. We are very close to making this method work. Once we are able to simultaneously detect sites of DNA damage and telomeric sequences in metaphase chromosomes this will allow us to examine repair kinetics within telomeric sequences in the Chinese hamster genome with a greater accuracy.

Furthermore, interactions between BRCA2 and individual shelterin components are addressed only partially. Only when all protein interactions including those between shelterin components and BRCA2 and its interacting partners are mapped, only then a full biochemical picture of the BRCA2 involvement at telomeres may be obtained.

In conclusion, results presented in this thesis show that BRCA2 deficiency leads to telomere dysfunction. Future work is required to test whether this finding can be explored further from the perspective of cancer therapeutics.

References

AHNESORG, P., SMITH, P. & JACKSON, S. P. 2006. XLF interacts with the XRCC4-DNA ligase IV complex to promote DNA nonhomologous end-joining. *Cell,* 124**,** 301-313.

AISNER, D. L., WRIGHT, W. E. & SHAY, J. W. 2002. Telomerase regulation: not just flipping the switch. *Current Opinion in Genetics & Development,* 12**,** 80-85.

AL-WAHIBY, S. & SLIJEPCEVIC, P. 2005. Chromosomal aberrations involving telomeres in BRCA1 deficient human and mouse cell lines. *Cytogenet Genome Res,* 109**,** 491-496.

ALTER, B. P., ROSENBERG, P. S. & BRODY, L. C. 2007. Clinical and molecular features associated with biallelic mutations in FANCD1/BRCA2. *Journal of Medical Genetics,* 44**,** 1-9.

ALVAREZ, L., EVANS, J. W., WILKS, R., LUCAS, J. N., BROWN, J. M. & GIACCIA, A. J. 1993. Chromosomal Radiosensitivity at Intrachromosomal Telomeric Sites. *Genes Chromosomes & Cancer,* 8**,** 8-14.

AME 2004. The PARP superfamily (vol 26, pg 882, 2004). *Bioessays,* 26**,** 1148-1148.

ARTANDI, S. E. 2006a. Focus on research: Telomeres, telomerase, and human disease. *New England Journal of Medicine,* 355**,** 1195-1197.

ARTANDI, S. E. 2006b. Telomerase flies the coop: the telomerase RNA component as a viral-encoded oncogene. *Journal of Experimental Medicine,* 203**,** 1143-1145.

AZZALIN, C. M., NERGADZE, S. G. & GIULOTTO, E. 2001. Human intrachromosomal telomeric-like repeats: sequence organization and mechanisms of origin. *Chromosoma,* 110**,** 75-82.

AZZALIN, C. M., REICHENBACH, P., KHORIAULI, L., GIULOTTO, E. & LINGNER, J. 2007. Telomeric repeat-containing RNA and RNA surveillance factors at mammalian chromosome ends. Science, 318, 798-801.

BADIE, S., ESCANDELL, J. M., BOUWMAN, P., CARLOS, A. R., THANASOULA, M., GALLARDO, M. M., SURAM, A., JACO, I., BENITEZ, J., HERBIG, U., BLASCO, M. A., JONKERS, J. & TARSOUNAS, M. 2010. BRCA2 acts as a RAD51 loader to facilitate telomere replication and capping. *Nat Struct Mol Biol,* 17**,** 1461-U93.

BAILEY, S. M., BRENNEMAN, M. A. & GOODWIN, E. H. 2004. Frequent recombination in telomeric DNA may extend the proliferative life of telomerase-negative cells. *Nucleic Acids Res,* 32**,** 3743-3751.

BAIRD, D. M., ROWSON, J., WYNFORD-THOMAS, D. & KIPLING, D. 2003. Extensive allelic variation and ultrashort telomeres in senescent human cells. *Nat Genet,* 33**,** 203-207.

BALAJEE, A. S., OH, H. J. & NATARAJAN, A. T. 1994. Analysis of Restriction Enzyme-Induced Chromosome-Aberrations in the Interstitial Telomeric Repeat Sequences of Cho and Che Cells by Fish. *Mutat Res,* 307**,** 307-313.

BECHTER, O. E., ZOU, Y., WALKER, W., WRIGHT, W. E. & SHAY, J. W. 2004. Telomeric recombination in mismatch repair deficient human colon cancer cells after telomerase inhibition. *Cancer Research,* 64**,** 3444-3451.

BERNARDI, R. & PANDOLFI, P. P. 2007. Structure, dynamics and functions of promyelocytic leukaemia nuclear bodies. *Nature Reviews Molecular Cell Biology,* 8**,** 1006-1016.

BERTONI, L., ATTOLINI, C., TESSERA, L., MUCCIOLO, E. & GIULOTTO, E. 1994. Telomeric and Nontelomeric (Ttagcc)(N) Sequences in Gene Amplification and Chromosome Stability. *Genomics,* 24**,** 53-62.

BIGNELL, G., MICKLEM, G., STRATTON, M. R., ASHWORTH, A. & WOOSTER, R. 1997. The BRC repeats are conserved in mammalian BRCA2 proteins. *Human Molecular Genetics,* 6**,** 53-58.

BLACKBURN, E. H. 1991. Structure and Function of Telomeres. *Nature,* 350**,** 569-573.

BLACKBURN, E. H. 2000a. Telomere states and cell fates. *Nature,* 408**,** 53-56.

BLACKBURN, E. H. 2000b. Telomeres and their cellular growth effects. *Faseb Journal,* 14**,** A1310-A1310.

BLASCO, M. A. & HAHN, W. C. 2003. Evolving views of telomerase and cancer. *Trends in Cell Biology,* 13**,** 289-294.

BODVARSDOTTIR, S. K., STEINARSDOTTIR, M., BJARNASON, H. & EYFJORD, J. E. 2012. Dysfunctional telomeres in human BRCA2 mutated breast tumors and cell lines. *Mutat Res,* 729**,** 90-9.

BOLZAN, A. D. 2012. Chromosomal aberrations involving telomeres and interstitial telomeric sequences. *Mutagenesis,* 27**,** 1-15.

BOLZAN, A. D. & BIANCHI, M. S. 2006. Telomeres, interstitial telomeric repeat sequences, and chromosomal aberrations. *Mutation Research-Reviews in Mutation Research,* 612**,** 189-214.

BOLZAN, A. D., PAEZ, G. L. & BIANCHI, M. S. 2001. FISH analysis of telomeric repeat sequences and their involvement in chromosomal aberrations induced by radiomimetic compounds in hamster cells. *Mutation Research-Fundamental and Molecular Mechanisms of Mutagenesis,* 479**,** 187-196.

BROOKS, A. R., HARKINS, R. N., WANG, P. Y., QIAN, H. S., LIU, P. X. & RUBANYI, G. M. 2004. Transcriptional silencing is associated with extensive methylation of the CMV promoter following adenoviral gene delivery to muscle. *Journal of Gene Medicine,* 6**,** 395-404.

BRYAN, T. M. & REDDEL, R. R. 1997. Telomere dynamics and telomerase activity in in vitro immortalised human cells. *Eur J Cancer,* 33**,** 767-773.

BUCK, D., MALIVERT, L., DE CHASSEVAL, P., BARRAUD, A., FONDANECHE, M. C., SANAL, O., PLEBANI, A., STEPHAN, J. L., HUFNAGEL, M., LE DEIST, F., FISCHER, A., DURANDY, A., DE VILLARTAY, J. P. & REVY, P. 2006. Cernunnos, a novel nonhomologous end-joining factor, is mutated in human immunodeficiency with microcephaly. *Cell,* 124**,** 287-299.

BUSCEMI, G., CARLESSI, L., ZANNINI, L., LISANTI, S., FONTANELLA, E., CANEVARI, S. & DELIA, D. 2006. DNA damage-induced cell cycle regulation and function of novel Chk2 phosphoresidues. *Mol Cell Biol,* 26**,** 7832-7845.

CALLEN, E. & SURRALLES, J. 2004. Telomere dysfunction in genome instability syndromes. *Mutation Research-Reviews in Mutation Research,* 567**,** 85-104.

CAMPISI, J. 2001. Cellular senescence as a tumor-suppressor mechanism. *Trends in Cell Biology,* 11**,** S27-S31.

CERONE, M. A., AUTEXIER, C., LONDONO-VALLEJO, J. A. & BACCHETTI, S. 2005. A human cell line that maintains telomeres in the absence of telomerase and of key markers of ALT. *Oncogene,* 24**,** 7893-7901.

CESARE, A. J. & GRIFFITH, J. D. 2004. Telomeric DNA in ALT cells is characterized by free telomeric circles and heterogeneous t-loops. *Mol Cell Biol,* 24**,** 9948-57.

CESARE, A. J. & REDDEL, R. R. 2010. Alternative lengthening of telomeres: models, mechanisms and implications. *Nature Reviews Genetics,* 11**,** 319-330.

CHAKHPARONIAN, M. & WELLINGER, R. J. 2003. Telomere maintenance and DNA replication: how closely are these two connected? *Trends in Genetics,* 19**,** 439-446.

CHAN, S. R. W. L. & BLACKBURN, E. H. 2004. Telomeres and telomerase. *Philosophical Transactions of the Royal Society of London Series B-Biological Sciences,* 359**,** 109-121.

CHAN, S. W. L. & BLACKBURN, E. H. 2002. New ways not to make ends meet: telomerase, DNA damage proteins and heterochromatin. *Oncogene,* 21**,** 553-563.

CHANG, E. & HARLEY, C. B. 1995. Telomere Length and Replicative Aging in Human Vascular Tissues. *Proc Natl Acad Sci U S A,* 92**,** 11190-11194.

CHEN, C., QIU, H., GONG, J., LIU, Q., XIAO, H., CHEN, X. W., SUN, B. L. & YANG, R. G. 2012. (-)-Epigallocatechin-3-gallate inhibits the replication cycle of hepatitis C virus. *Archives of Virology,* 157**,** 1301-1312.

CHEN, H. J., LIANG, C. L., LU, K., LIN, J. W. & CHO, C. L. 2000. Implication of telomerase activity and alternations of telomere length in the histologic characteristics of intracranial meningiomas. *Cancer,* 89**,** 2092-2098.

CHEN, J. J., SILVER, D. P., WALPITA, D., CANTOR, S. B., GAZDAR, A. F., TOMLINSON, G., COUCH, F. J., WEBER, B. L., ASHLEY, T., LIVINGSTON, D. M. & SCULLY, R. 1998a. Stable interaction between the products of the BRCA1 and BRCA2 tumor suppressor genes in mitotic and meiotic cells. *Molecular Cell,* 2**,** 317-328.

CHEN, P. L., CHEN, C. F., CHEN, Y., XIAO, J., SHARP, Z. D. & LEE, W. H. 1998b. The BRC repeats in BRCA2 are critical for RAD51 binding and resistance to methyl methanesulfonate treatment. *Proc Natl Acad Sci U S A,* 95**,** 5287-92.

CHEUNG, A. L. M. & DENG, W. 2008. Telomere dysfunction, genome instability and cancer. *Frontiers in Bioscience-Landmark,* 13**,** 2075-2090.

CLETONJANSEN, A. M., COLLINS, N., LAKHANI, S. R., WEISSENBACH, J., DEVILEE, P., CORNELISSE, C. J. & STRATTON, M. R. 1995. Loss of Heterozygosity in Sporadic Breast-Tumors at the Brca2 Locus on Chromosome 13q12-Q13. *Br J Cancer,* 72**,** 1241-1244.

COLLINS, K. 2008. Physiological assembly and activity of human telomerase complexes. *Mechanisms of Ageing and Development,* 129**,** 91-98.

COLLINS, N., MCMANUS, R., WOOSTER, R., MANGION, J., SEAL, S., LAKHANI, S. R., ORMISTON, W., DALY, P. A., FORD, D., EASTON, D. F. & STRATTON, M. R. 1995. Consistent Loss of the Wild-Type Allele in Breast Cancers from a Family Linked to the Brca2 Gene on Chromosome 13q12-13. *Oncogene,* 10**,** 1673-1675.

CONNOR, F., BERTWISTLE, D., MEE, P. J., ROSS, G. M., SWIFT, S., GRIGORIEVA, E., TYBULEWICZ, V. L. J. & ASHWORTH, A. 1997. Tumorigenesis and a DNA repair defect in mice with a truncating Brca2 mutation. *Nat Genet,* 17**,** 423-430.

COX, M. M., GOODMAN, M. F., KREUZER, K. N., SHERRATT, D. J., SANDLER, S. J. & MARIANS, K. J. 2000. The importance of repairing stalled replication forks. *Nature,* 404**,** 37-41.

CULLEN, B. R. 2005. RNAi the natural way. *Nat Genet,* 37**,** 1163-1165.

DAS, P. M. & SINGAL, R. 2004. DNA methylation and cancer. *Journal of Clinical Oncology,* 22**,** 4632-4642.

DAY, J. P., LIMOLI, C. L. & MORGAN, W. F. 1998. Recombination involving interstitial telomere repeat-like sequences promotes chromosomal instability in Chinese hamster cells. *Carcinogenesis,* 19**,** 259-266.

DECKER, M. L., CHAVEZ, E., VULTO, I. & LANSDORP, P. M. 2009. Telomere length in Hutchinson-Gilford Progeria Syndrome. *Mechanisms of Ageing and Development,* 130**,** 377-383.

DE LANGE, T. 2005. Shelterin: the protein complex that shapes and safeguards human telomeres. Genes & Development, 19, 2100-2110.

DHAENE, K., VANCOILLIE, G., LAMBERT, J., NAEYAERT, J. M. & VAN MARCK, E. 2000. Absence of telomerase activity and telomerase catalytic subunit mRNA in melanocyte cultures. *Br J Cancer,* 82**,** 1051-1057.

DI FAGAGNA, F. D., HANDE, M. P., TONG, W. M., ROTH, D., LANSDORP, P. M., WANG, Z. Q. & JACKSON, S. P. 2001. Effects of DNA nonhomologous end-joining factors on telomere length and chromosomal stability in mammalian cells. *Current Biology,* 11**,** 1192-1196.

DUNHAM, M. A., NEUMANN, A. A., FASCHING, C. L. & REDDEL, R. R. 2000. Telomere maintenance by recombination in human cells. *Nat Genet,* 26**,** 447-50.

ESPEJEL, S. & BLASCO, M. A. 2002. Identification of telomere-dependent "senescence-like" arrest in mouse embryonic fibroblasts. *Experimental Cell Research,* 276**,** 242-248.

FAN, Q., ZHANG, F., BARRETT, B., REN, K. Q. & ANDREASSEN, P. R. 2009. A role for monoubiquitinated FANCD2 at telomeres in ALT cells. *Nucleic Acids Res,* 37**,** 1740-1754.

FARMER, H., MCCABE, N., LORD, C. J., TUTT, A. N., JOHNSON, D. A., RICHARDSON, T. B., SANTAROSA, M., DILLON, K. J., HICKSON, I., KNIGHTS, C., MARTIN, N. M., JACKSON, S. P., SMITH, G. C. & ASHWORTH, A. 2005. Targeting the DNA repair defect in BRCA mutant cells as a therapeutic strategy. *Nature,* 434**,** 917-21.

FENG, J. L., FUNK, W. D., WANG, S. S., WEINRICH, S. L., AVILION, A. A., CHIU, C. P., ADAMS, R. R., CHANG, E., ALLSOPP, R. C., YU, J. H., LE, S. Y., WEST, M. D., HARLEY, C. B., ANDREWS, W. H., GREIDER, C. W. & VILLEPONTEAU, B. 1995. The Rna Component of Human Telomerase. *Science,* 269**,** 1236-1241.

FOGH, J., FOGH, J. M. & ORFEO, T. 1977. 127 Cultured Human Tumor-Cell Lines Producing Tumors in Nude Mice. *Journal of the National Cancer Institute,* 59**,** 221-226.

FONG, P. C., BOSS, D. S., YAP, T. A., TUTT, A., WU, P. J., MERGUI-ROELVINK, M., MORTIMER, P., SWAISLAND, H., LAU, A., O'CONNOR, M. J., ASHWORTH, A., CARMICHAEL, J., KAYE, S. B., SCHELLENS, J. H. M. & DE BONO, J. S. 2009. Inhibition of Poly(ADP-Ribose) Polymerase in Tumors from BRCA Mutation Carriers. *New England Journal of Medicine,* 361**,** 123-134.

FORD, D., EASTON, D. F., STRATTON, M., NAROD, S., GOLDGAR, D., DEVILEE, P., BISHOP, D. T., WEBER, B., LENOIR, G., CHANG-CLAUDE, J., SOBOL, H., TEARE, M. D., STRUEWING, J., ARASON, A., SCHERNECK, S., PETO, J., REBBECK, T. R., TONIN, P., NEUHAUSEN, S., BARKARDOTTIR, R., EYFJORD, J., LYNCH, H., PONDER, B. A. J., GAYTHER, S. A., BIRCH, J. M., LINDBLOM, A., STOPPA-LYONNET, D., BIGNON, Y., BORG, A., HAMANN, U., HAITES, N., SCOTT, R. J., MAUGARD, C. M., VASEN, H. & CONSORTIUM, B. C. L. 1998. Genetic heterogeneity and penetrance analysis of the BRCA1 and BRCA2 genes in breast cancer families. *Am J Hum Genet,* 62**,** 676-689.

FUTAMURA, M., ARAKAWA, H., MATSUDA, K., KATAGIRI, T., SAJI, S., MIKI, Y. & NAKAMURA, Y. 2000. Potential role of BRCA2 in a mitotic checkpoint after phosphorylation by hBUBR1. *Cancer Research,* 60**,** 1531-1535.

GHOSHAL, K., DATTA, J., MAJUMDER, S., BAI, S. M., KUTAY, H., MOTIWALA, T. & JACOB, S. T. 2005. 5-Aza-deoxycytidine induces selective degradation of DNA methyltransferase 1 by a proteasomal pathway that requires the KEN box, bromo-adjacent homology domain, and nuclear localization signal. *Mol Cell Biol,* 25**,** 4727-4741.

GILLEY, D. & BLACKBURN, E. H. 1999. The telomerase RNA pseudoknot is critical for the stable assembly of a catalytically active ribonucleoprotein. *Proc Natl Acad Sci U S A,* 96**,** 6621-6625.

GISSELSSON, D., JONSON, T., PETERSEN, A., STROMBECK, B., DAL CIN, P., HOGLUND, M., MITELMAN, F., MERTENS, F. & MANDAHL, N. 2001. Telomere dysfunction triggers extensive DNA fragmentation and evolution of complex chromosome abnormalities in human malignant tumors. *Proc Natl Acad Sci U S A,* 98**,** 12683-12688.

GOGGINS, M., SCHUTTE, M., LU, J., MOSKALUK, C. A., WEINSTEIN, C. L., PETERSEN, G. M., YEO, C. J., JACKSON, C. E., LYNCH, H. T., HRUBAN, R. H. & KERN, S. E. 1996. Germline BRCA2 gene mutations in patients with apparently sporadic pancreatic carcinomas. *Cancer Research,* 56**,** 5360-5364.

GOLDBERG, A. D., BANASZYNSKI, L. A., NOH, K. M., LEWIS, P. W., ELSAESSER, S. J., STADLER, S., DEWELL, S., LAW, M., GUO, X. Y., LI, X., WEN, D. C., CHAPGIER, A., DEKELVER, R. C., MILLER, J. C., LEE, Y. L., BOYDSTON, E. A., HOLMES, M. C., GREGORY, P. D., GREALLY, J. M., RAFII, S., YANG, C. W., SCAMBLER, P. J., GARRICK, D., GIBBONS, R. J., HIGGS, D. R., CRISTEA, I. M., URNOV, F. D., ZHENG, D. Y. & ALLIS, C. D. 2010. Distinct Factors Control Histone Variant H3.3 Localization at Specific Genomic Regions. *Cell,* 140, 678-691.

GORDON, W. C., CASEY, D. M., LUKIW, W. J. & BAZAN, N. G. 2002. DNA damage and repair in light-induced photoreceptor degeneration. *Investigative Ophthalmology & Visual Science,* 43**,** 3511-3521.

GOYTISOLO, F. A., SAMPER, E., EDMONSON, S., TACCIOLI, G. E. & BLASCO, M. A. 2001. The absence of the DNA-dependent protein kinase catalytic subunit in mice results in anaphase bridges and in increased telomeric fusions with normal telomere length and G-strand overhang. *Mol Cell Biol,* 21**,** 3642-3651.

GOYTISOLO, F. A., SAMPER, E., MARTIN-CABALLERO, J., FINNON, P., HERRERA, E., FLORES, J. M., BOUFFLER, S. D. & BLASCO, M. A. 2000. Short telomeres result in organismal hypersensitivity to ionizing radiation in mammals. *Journal of Experimental Medicine,* 192**,** 1625-1636.

GREIDER, C. W. & BLACKBURN, E. H. 1985a. Identification of a Specific Telomere Terminal Transferase-Activity in Tetrahymena Extracts. *Cell,* 43**,** 405-413.

GREIDER, C. W. & BLACKBURN, E. H. 1985b. Identification of a specific telomere terminal transferase activity in Tetrahymena extracts. *Cell,* 43**,** 405-13.

GREIDER, C. W. & BLACKBURN, E. H. 1996. Telomeres, telomerase and cancer. *Scientific American,* 274**,** 92-97.

GRIFFIN, C. S. & THACKER, J. 2004. The role of homologous recombination repair in the formation of chromosome aberrations. *Cytogenet Genome Res,* 104**,** 21-27.

GRIFFITH, J. D., COMEAU, L., ROSENFIELD, S., STANSEL, R. M., BIANCHI, A., MOSS, H. & DE LANGE, T. 1999. Mammalian telomeres end in a large duplex loop. *Cell,* 97**,** 503-514.

GROBELNY, J. V., GODWIN, A. K. & BROCCOLI, D. 2000. ALT-associated PML bodies are present in viable cells and are enriched in cells in the G(2)/M phase of the cell cycle. *J Cell Sci,* 113**,** 4577-4585.

GROMPE, M. & D'ANDREA, A. 2001. Fanconi anemia and DNA repair. *Human Molecular Genetics,* 10**,** 2253-2259.

GUDMUNDSSON, J., JOHANNESDOTTIR, G., BERGTHORSSON, J. T., ARASON, A., INGVARSSON, S., EGILSSON, V. & BARKARDOTTIR, R. B. 1995. Different Tumor Types from Brca2 Carriers Show Wild-Type Chromosome Deletions on 13q12q13. *Cancer Research,* 55**,** 4830-4832.

HABER, J. E. 2000. Partners and pathways - repairing a double-strand break. *Trends in Genetics,* 16**,** 259-264.

HAKIN-SMITH, V., JELLINEK, D. A., LEVY, D., CARROLL, T., TEO, M., TIMPERLEY, W. R., MCKAY, M. J., REDDEL, R. R. & ROYDS, J. A. 2003. Alternative lengthening of telomeres and survival in patients with glioblastoma multiforme. *Lancet,* 361**,** 836-838.

HARLEY, C. B., FUTCHER, A. B. & GREIDER, C. W. 1990. Telomeres Shorten during Aging of Human Fibroblasts. *Nature,* 345**,** 458-460.

HARRINGTON, L., ZHOU, W., MCPHAIL, T., OULTON, R., YEUNG, D. S. K., MAR, V., BASS, M. B. & ROBINSON, M. O. 1997. Human telomerase contains evolutionarily conserved catalytic and structural subunits. *Genes & Development,* 11**,** 3109-3115.

HE, J., YANG, Q. & CHANG, L. J. 2005. Dynamic DNA methylation and histone modifications contribute to lentiviral transgene silencing in murine embryonic carcinoma cells. *J Virol,* 79**,** 13497-13508.

HEAPHY, C. M., DE WILDE, R. F., JIAO, Y. C., KLEIN, A. P., EDIL, B. H., SHI, C. J., BETTEGOWDA, C., RODRIGUEZ, F. J., EBERHART, C. G., HEBBAR, S., OFFERHAUS, G. J., MCLENDON, R., RASHEED, B. A., HE, Y. P., YAN, H., BIGNER, D. D., OBA-SHINJO, S. M., MARIE, S. K. N., RIGGINS, G. J., KINZLER, K. W., VOGELSTEIN, B., HRUBAN, R. H., MAITRA, A., PAPADOPOULOS, N. & MEEKER, A. K. 2011. Altered Telomeres in Tumors with ATRX and DAXX Mutations. *Science*, 333, 425-425.

HELLEDAY, T. 2003. Pathways for mitotic homologous recombination in mammalian cells. *Mutation Research-Fundamental and Molecular Mechanisms of Mutagenesis,* 532**,** 103-115.

HENSON, J. D., HANNAY, J. A., MCCARTHY, S. W., ROYDS, J. A., YEAGER, T. R., ROBINSON, R. A., WHARTON, S. B., JELLINEK, D. A., ARBUCKLE, S. M., YOO, J. Y., ROBINSON, B. G., LEAROYD, D. L., STALLEY, P. D., BONAR, S. F., YU, D. H., POLLOCK, R. E. & REDDEL, R. R. 2005. A robust assay for alternative lengthening of telomeres in tumors shows the significance of alternative lengthening of telomeres in sarcomas and astrocytomas. *Clinical Cancer Research,* 11**,** 217-225.

HENSON, J. D., NEUMANN, A. A., YEAGER, T. R. & REDDEL, R. R. 2002. Alternative lengthening of telomeres in mammalian cells. *Oncogene,* 21**,** 598-610.

HENSON, J. D. & REDDEL, R. R. 2010. Assaying and investigating Alternative Lengthening of Telomeres activity in human cells and cancers. *FEBS Lett,* 584**,** 3800-3811.

HERCEG, Z. & WANG, Z. Q. 2001. Functions of poly(ADP-ribose) polymerase (PARP) in DNA repair, genomic integrity and cell death. *Mutation Research-Fundamental and Molecular Mechanisms of Mutagenesis,* 477**,** 97-110.

HESELMEYER-HADDAD, K., JANZ, V., CASTLE, P. E., CHAUDHRI, N., WHITE, N., WILBER, K., MORRISON, L. E., AUER, G., BURROUGHS, F. H., SHERMAN, M. E. & RIED, T. 2003. Detection of genomic amplification of the human telomerase gene (TERC) in cytologic specimens as a genetic test for the diagnosis of cervical dysplasia. *American Journal of Pathology,* 163**,** 1405-1416.

HESELMEYER-HADDAD, K., SOMMERFELD, K., WHITE, N. M., CHAUDHRI, N., MORRISON, L. E., PALANISAMY, N., WANG, Z. Y., AUER, G., STEINBERG, W. & RIED, T. 2005. Genomic amplification of the human telomerase gene (TERC) in pap smears predicts the development of cervical cancer. *American Journal of Pathology,* 166**,** 1229-1238.

HILLS, M., LUCKE, K., CHAVEZ, E. A., EAVES, C. J. & LANSDORP, P. M. 2009. Probing the mitotic history and developmental stage of hematopoietic cells using single telomere length analysis (STELA). *Blood,* 113**,** 5765-5775.

HOUGHTALING, B. R., CUTTONARO, L., CHANG, W. & SMITH, S. 2004. A dynamic molecular link between the telomere length regulator TRF1 and the chromosome end protector TRF2. *Curr Biol,* 14**,** 1621-31.

HOWLETT, N. G., TANIGUCHI, T., OLSON, S., COX, B., WAISFISZ, Q., DE DIE-SMULDERS, C., PERSKY, N., GROMPE, M., JOENJE, H., PALS, G., IKEDA, H.,

FOX, E. A. & D'ANDREA, A. D. 2002. Biallelic inactivation of BRCA2 in Fanconi anemia. *Science,* 297**,** 606-9.

HUGHES-DAVIES, L., HUNTSMAN, D., RUAS, M., FUKS, F., BYE, J., CHIN, S. F., MILNER, J., BROWN, L. A., HSU, F., GILKS, B., NIELSEN, T., SCHULZER, M., CHIA, S., RAGAZ, J., CAHN, A., LINGER, L., OZDAG, H., CATTANEO, E., JORDANOVA, E. S., SCHUURING, E., YU, D. S., VENKITARAMAN, A., PONDER, B., DOHERTY, A., APARICIO, S., BENTLEY, D., THEILLET, C., PONTING, C. P., CALDAS, C. & KOUZARIDES, T. 2003. EMSY links the BRCA2 pathway to sporadic breast and ovarian cancer. *Cell,* 115**,** 523-35.

JEGGO, R. D., KELLETT, D. O., WANG, Y., RAMAGE, A. G. & JORDAN, D. 2005. The role of central 5-HT(3) receptors in vagal reflex inputs to neurones in the nucleus tractus solitarius of anaesthetized rats. *Journal of Physiology-London,* 566**,** 939-953.

JIN, Q., LIU, C., YAN, C., TAO, B., LI, Z. & CAI, Z. 2012a. 5-aza-CdR induces the demethylation of Syk promoter in nasopharyngeal carcinoma cell. *Gene,* 511**,** 224-6.

JIN, Q. Z., LIU, C. B., YAN, C., TAO, B. H., LI, Z. H. & CAI, Z. Y. 2012b. 5-aza-CdR induces the demethylation of Syk promoter in nasopharyngeal carcinoma cell. *Gene,* 511**,** 224-226.

KANAYA, T., KYO, S., TAKAKURA, M., ITO, H., NAMIKI, M. & INOUE, M. 1998. hTERT is a critical determinant of telomerase activity in renal-cell carcinoma. *International Journal of Cancer,* 78**,** 539-543.

KARRAN, P. 2000. DNA double strand break repair in mammalian cells. *Curr Opin Genet Dev,* 10**,** 144-50.

KATO, M., YANO, K., MATSUO, F., SAITO, H., KATAGIRI, T., KURUMIZAKA, H., YOSHIMOTO, M., KASUMI, F., AKIYAMA, F., SAKAMOTO, G., NAGAWA, H., NAKAMURA, Y. & MIKI, Y. 2000. Identification of Rad51 alteration in patients with bilateral breast cancer. *Journal of Human Genetics,* 45**,** 133-137.

KELLAND, L. 2007. The resurgence of platinum-based cancer chemotherapy. *Nature Reviews Cancer,* 7**,** 573-584.

KENNEDY, R. D. & D'ANDREA, A. D. 2005. The Fanconi Anemia/BRCA pathway: new faces in the crowd. *Genes & Development,* 19**,** 2925-2940.

KERR, P. & ASHWORTH, A. 2001. New complexities for BRCA1 and BRCA2. *Current Biology,* 11**,** R668-R676.

KILIAN, A., BOWTELL, D. D., ABUD, H. E., HIME, G. R., VENTER, D. J., KEESE, P. K., DUNCAN, E. L., REDDEL, R. R. & JEFFERSON, R. A. 1997. Isolation of a

candidate human telomerase catalytic subunit gene, which reveals complex splicing patterns in different cell types. *Hum Mol Genet,* 6**,** 2011-9.

KIM, N. W., PIATYSZEK, M. A., PROWSE, K. R., HARLEY, C. B., WEST, M. D., HO, P. L. C., COVIELLO, G. M., WRIGHT, W. E., WEINRICH, S. L. & SHAY, J. W. 1994. Specific Association of Human Telomerase Activity with Immortal Cells and Cancer. *Science,* 266**,** 2011-2015.

KIM, N. W. & WU, F. 1997. Advances in quantification and characterization of telomerase activity by the telomeric repeat amplification protocol (TRAP). *Nucleic Acids Res,* 25**,** 2595-2597.

KING, R. W., JACKSON, P. K. & KIRSCHNER, M. W. 1994. Mitosis in Transition. *Cell,* 79**,** 563-571.

KIYONO, T., FOSTER, S. A., KOOP, J. I., MCDOUGALL, J. K., GALLOWAY, D. A. & KLINGELHUTZ, A. J. 1998. Both Rb/p16INK4a inactivation and telomerase activity are required to immortalize human epithelial cells. *Nature,* 396**,** 84-8.

KRAAKMAN-VAN DER ZWET, M., OVERKAMP, W. J. I., VAN LANGE, R. E. E., ESSERS, J., VAN DUIJN-GOEDHART, A., WIGGERS, I., SWAMINATHAN, S., VAN BUUL, P. P. W., ERRAMI, A., TAN, R. T. L., JASPERS, N. G. J., SHARAN, S. K., KANAAR, R. & ZDZIENICKA, M. Z. 2002. Brca2 (XRCC11) deficiency results in radioresistant DNA synthesis and a higher frequency of spontaneous deletions. *Mol Cell Biol,* 22**,** 669-679.

KRISHNAN, B. & NAMPOORI, V. P. N. 2006. Line narrowing effects and enhanced back scattering from ZnO colloids. *Journal of Materials Science,* 41**,** 2387-2391.

LANCASTER, J. M., WOOSTER, R., MANGION, J., PHELAN, C. M., COCHRAN, C., GUMBS, C., SEAL, S., BARFOOT, R., COLLINS, N., BIGNELL, G., PATEL, S., HAMOUDI, R., LARSSON, C., WISEMAN, R. W., BERCHUCK, A., IGLEHART, J. D., MARKS, J. R., ASHWORTH, A., STRATTON, M. R. & FUTREAL, P. A. 1996. BRCA2 mutations in primary breast and ovarian cancers. *Nat Genet,* 13**,** 238-240.

LANSDORP, P. M. 2009. Telomeres and disease. *Embo Journal,* 28**,** 2532-2540.

LEE, J. & DUNPHY, W. G. 2013. The Mre11-Rad50-Nbs1 (MRN) complex has a specific role in the activation of Chk1 in response to stalled replication forks. *Mol Biol Cell,* 24**,** 1343-53.

LEONG, C. O., VIDNOVIC, N., DEYOUNG, M. P., SGROI, D. & ELLISEN, L. W. 2007. The p63/p73 network mediates chemosensitivity to cisplatin in a biologically defined subset of primary breast cancers. *Journal of Clinical Investigation,* 117**,** 1370-1380.

LEVY, M. Z., ALLSOPP, R. C., FUTCHER, A. B., GREIDER, C. W. & HARLEY, C. B. 1992. Telomere End-Replication Problem and Cell Aging. *J Mol Biol,* 225**,** 951-960.

LEWIS, P. W., ELSAESSER, S. J., NOH, K. M., STADLER, S. C. & ALLIS, C. D. 2010. Daxx is an H3.3-specific histone chaperone and cooperates with ATRX in replication-independent chromatin assembly at telomeres. *Proc Natl Acad Sci U S A,* 107, 14075-14080.

LIANG, F., HAN, M. G., ROMANIENKO, P. J. & JASIN, M. 1998. Homology-directed repair is a major double-strand break repair pathway in mammalian cells. *Proc Natl Acad Sci U S A,* 95**,** 5172-5177.

LIN, K. W. & YAN, J. 2008. Endings in the middle: Current knowledge of interstitial telomeric sequences. *Mutation Research-Reviews in Mutation Research,* 658**,** 95-110.

LIN, Y. L., SENGUPTA, S., GURDZIEL, K., BELL, G. W., JACKS, T. & FLORES, E. R. 2009. p63 and p73 Transcriptionally Regulate Genes Involved in DNA Repair. *Plos Genetics,* 5.

LINGNER, J. & CECH, T. R. 1998. Telomerase and chromosome end maintenance. *Current Opinion in Genetics & Development,* 8**,** 226-232.

LIU, D., O'CONNOR, M. S., QIN, J. & SONGYANG, Z. 2004. Telosome, a mammalian telomere-associated complex formed by multiple telomeric proteins. *Journal of Biological Chemistry,* 279**,** 51338-51342.

LIU, L., BAILEY, S. M., OKUKA, M., MUNOZ, P., LI, C., ZHOU, L. J., WU, C., CZERWIEC, E., SANDLER, L., SEYFANG, A., BLASCO, M. A. & KEEFE, D. L. 2007. Telomere lengthening early in development. *Nature Cell Biology,* 9**,** 1436-U185.

LOMONOSOV, M., ANAND, S., SANGRITHI, M., DAVIES, R. & VENKITARAMAN, A. R. 2003. Stabilization of stalled DNA replication forks by the BRCA2 breast cancer susceptibility protein. *Genes & Development,* 17**,** 3017-3022.

LONDONO-VALLEJO, J. A., DER-SARKISSIAN, H., CAZES, L., BACCHETTI, S. & REDDEL, R. R. 2004. Alternative lengthening of telomeres is characterized by high rates of telomeric exchange. *Cancer Research,* 64**,** 2324-2327.

LONGHESE, M. P. 2008. DNA damage response at functional and dysfunctional telomeres. *Genes Dev,* 22**,** 125-40.

LOVEJOY, C. A., LI, W., REISENWEBER, S., THONGTHIP, S., BRUNO, J., DE LANGE, T., DE, S., PETRINI, J. H., SUNG, P. A., JASIN, M., ROSENBLUH, J., ZWANG, Y., WEIR, B. A., HATTON, C., IVANOVA, E., MACCONAILL, L., HANNA, M., HAHN, W. C., LUE, N. F., REDDEL, R. R., JIAO, Y., KINZLER, K., VOGELSTEIN, B., PAPADOPOULOS, N. & MEEKER, A. K. 2012. Loss of ATRX, genome instability, and an altered DNA damage response are hallmarks of the alternative lengthening of telomeres pathway. *PLoS Genet,* 8**,** e1002772.

LOWER, K., LAW, M., DUNHAM, I., HUGHES, J., AYYUB, H., HIGGS, D. & GIBBONS, R. 2010. ATRX targets variable number tandem repeats and thereby influences allele-specific expression. *Journal of Medical Genetics*, 47, S35-S35.

LU, J., GETZ, G., MISKA, E. A., ALVAREZ-SAAVEDRA, E., LAMB, J., PECK, D., SWEET-CORDERO, A., EBET, B. L., MAK, R. H., FERRANDO, A. A., DOWNING, J. R., JACKS, T., HORVITZ, H. R. & GOLUB, T. R. 2005. MicroRNA expression profiles classify human cancers. *Nature,* 435**,** 834-838.

LUNDBERG, G., SEHIC, D., LANSBERG, J. K., ORA, I., FRIGYESI, A., CASTEL, V., NAVARRO, S., PIQUERAS, M., MARTINSSON, T., NOGUERA, R. & GISSELSSON, D. 2011. Alternative Lengthening of Telomeres-An Enhanced Chromosomal Instability in Aggressive Non-MYCN Amplified and Telomere Elongated Neuroblastomas. *Genes Chromosomes & Cancer,* 50**,** 250-262.

LUNDIN, C., ERIXON, K., ARNAUDEAU, C., SCHULTZ, N., JENSSEN, D., MEUTH, M. & HELLEDAY, T. 2002. Different roles for nonhomologous end joining and homologous recombination following replication arrest in mammalian cells. *Mol Cell Biol*, 22**,** 5869-5878.

LUSTIG, A. J. 2009. Separating the effects of telomere size from the mechanism of telomere elongation. *Embo Journal,* 28**,** 793-794.

MA, Y. M., PANNICKE, U., SCHWARZ, K. & LIEBER, M. R. 2002. Hairpin opening and overhang processing by an Artemis/DNA-dependent protein kinase complex in nonhomologous end joining and V(D)J recombination. *Cell,* 108**,** 781-794.

MAKAROV, V. L., HIROSE, Y. & LANGMORE, J. P. 1997. Long G tails at both ends of human chromosomes suggest a C strand degradation mechanism for telomere shortening. *Cell,* 88**,** 657-666.

MALDONADO, E., HAMPSEY, M. & REINBERG, D. 1999. Repression: Targeting the heart of the matter. *Cell,* 99**,** 455-458.

MARDER, B. A. & MORGAN, W. F. 1993. Delayed Chromosomal Instability Induced by DNA-Damage. *Mol Cell Biol,* 13**,** 6667-6677.

MARMORSTEIN, L. Y., KINEV, A. V., CHAN, G. K. T., BOCHAR, D. A., BENIYA, H., EPSTEIN, J. A., YEN, T. J. & SHIEKHATTAR, R. 2001. A human BRCA2 complex containing a structural DNA binding component influences cell cycle progression. *Cell,* 104**,** 247-257.

MASUTOMI, K., YU, E. Y., KHURTS, S., BEN-PORATH, I., CURRIER, J. L., METZ, G. B., BROOKS, M. W., KANEKO, S., MURAKAMI, S., DECAPRIO, J. A., WEINBERG, R. A., STEWART, S. A. & HAHN, W. C. 2003. Telomerase maintains telomere structure in normal human cells. *Cell,* 114**,** 241-253.

MAZUMDAR, T., SANDHU, R., QADAN, M., DEVECCHIO, J., MAGLOIRE, V., AGYEMAN, A., LI, B. B. & HOUGHTON, J. A. 2013. Hedgehog Signaling Regulates Telomerase Reverse Transcriptase in Human Cancer Cells. *PLoS One,* 8.

MCEACHERN, M. J., KRAUSKOPF, A. & BLACKBURN, E. H. 2000. Telomeres and their control. *Annual Review of Genetics,* 34**,** 331-358.

MCILWRAITH, M. J. & WEST, S. C. 2001. The efficiency of strand invasion by Escherichia coli RecA is dependent upon the length and polarity of ssDNA tails. *J Mol Biol,* 305**,** 23-31.

MEEKER, A. K. & COFFEY, D. S. 1997. Telomerase: a promising marker of biological immortality of germ, stem, and cancer cells. A review. *Biochemistry-Moscow,* 62**,** 1323-1331.

MERRITT, W. M., LIN, Y. G., HAN, L. Y., KAMAT, A. A., SPANNUTH, W. A., SCHMANDT, R., URBAUER, D., PENNACCHIO, L. A., CHENG, J., NICK, A. M., DEAVERS, M. T., MOURAD-ZEIDAN, A., WANG, H., MUELLER, P., LENBURG, M. E., GRAY, J. W., MOK, S., BIRRER, M. J., LOPEZ-BERESTEIN, G., COLEMAN, R. L., BAR-ELI, M. & SOOD, A. K. 2008. Dicer, Drosha, and Outcomes in Patients with Ovarian Cancer. *New England Journal of Medicine,* 359**,** 2641-2650.

MEYERSON, M., COUNTER, C. M., EATON, E. N., ELLISEN, L. W., STEINER, P., CADDLE, S. D., ZIAUGRA, L., BEIJERSBERGEN, R. L., DAVIDOFF, M. J., LIU, Q. Y., BACCHETTI, S., HABER, D. A. & WEINBERG, R. A. 1997. hEST2, the putative human telomerase catalytic subunit gene, is up-regulated in tumor cells and during immortalization. *Cell,* 90**,** 785-795.

MCCLINTOCK, B. 1941. The Stability of Broken Ends of Chromosomes in Zea Mays. Genetics, 26, 234-82.

MCCLINTOCK, B. 1942. The Fusion of Broken Ends of Chromosomes Following Nuclear Fusion. Proc Natl Acad Sci U S A, 28, 458-63.

MEYNE, J., BAKER, R. J., HOBART, H. H., HSU, T. C., RYDER, O. A., WARD, O. G., WILEY, J. E., WURSTERHILL, D. H., YATES, T. L. & MOYZIS, R. K. 1990. Distribution of Nontelomeric Sites of the (Ttaggg)N Telomeric Sequence in Vertebrate Chromosomes. *Chromosoma,* 99**,** 3-10.

MIKAELSDOTTIR, E. K., VALGEIRSDOTTIR, S., EYFJORD, J. E. & RAFNAR, T. 2004. The Icelandic founder mutation BRCA2 999del5: analysis of expression. *Breast Cancer Research,* 6**,** R284-R290.

MILLER, K. M. & COOPER, J. P. 2003. The telomere protein taz1 is required to prevent and repair genomic DNA breaks. *Molecular Cell,* 11**,** 303-313.

MOMPARLER, R. L., ELIOPOULOS, N. & AYOUB, J. 2000. Evaluation of an inhibitor of DNA methylation, 5-AZA-2 '-deoxycytidine, for the treatment of lung cancer and the future role of gene therapy. *Cancer Gene Therapy,* 465**,** 433-446.

MORIN, G. B. 1989. The Human Telomere Terminal Transferase Enzyme Is a Ribonucleoprotein That Synthesizes Ttaggg Repeats. *Cell,* 59**,** 521-529.

MOYNAHAN, M. E., PIERCE, A. J. & JASIN, M. 2001. BRCA2 is required for homology-directed repair of chromosomal breaks. *Molecular Cell,* 7**,** 263-272.

MOYZIS, R. K., BUCKINGHAM, J. M., CRAM, L. S., DANI, M., DEAVEN, L. L., JONES, M. D., MEYNE, J., RATLIFF, R. L. & WU, J. R. 1988. A Highly Conserved Repetitive DNA-Sequence, (Ttaggg)N, Present at the Telomeres of Human-Chromosomes. *Proc Natl Acad Sci U S A,* 85**,** 6622-6626.

MUNTONI, A., NEUMANN, A. A., HILLS, M. & REDDEL, R. R. 2009. Telomere elongation involves intra-molecular DNA replication in cells utilizing alternative lengthening of telomeres. *Human Molecular Genetics,* 18**,** 1017-1027.

MURNANE, J. P., SABATIER, L., MARDER, B. A. & MORGAN, W. F. 1994. Telomere Dynamics in an Immortal Human Cell-Line. *Embo Journal,* 13**,** 4953-4962.

NABETANI, A. & ISHIKAWA, F. 2009. Unusual Telomeric DNAs in Human Telomerase-Negative Immortalized Cells. *Mol Cell Biol,* 29**,** 703-713.

NAKAYAMA, J. I., TAHARA, H., TAHARA, E., SAITO, M., ITO, K., NAKAMURA, H., NAKANISHI, T., TAHARA, E., IDE, T. & ISHIKAWA, F. 1998. Telomerase

activation by hTRT in human normal fibroblasts and hepatocellular carcinomas. *Nat Genet,* 18**,** 65-68.

NATHANSON, K. L., WOOSTER, R. & WEBER, B. L. 2001. Breast cancer genetics: what we know and what we need (vol 7, pg 552, 2001). *Nature Medicine,* 7**,** 749-749.

NOWACKA-ZAWISZA, M., BRYS, M., ROMANOWICZ-MAKOWSKA, H., KULIG, A. & KRAJEWSKA, W. M. 2008. Loss of heterozygosity in the RAD51 and BRCA2 regions in breast cancer. *Cancer Detection and Prevention,* 32**,** 144-148.

O'DRISCOLL, M. & JEGGO, P. A. 2006. The role of double-strand break repair - insights from human genetics. *Nature Reviews Genetics,* 7**,** 45-54.

O'SULLIVAN, J. N., BRONNER, M. P., BRENTNALL, T. A., FINLEY, J. C., SHEN, W. T., EMERSON, S., EMOND, M. J., GOLLAHON, K. A., MOSKOVITZ, A. H., CRISPIN, D. A., POTTER, J. D. & RABINOVITCH, P. S. 2002. Chromosomal instability in ulcerative colitis is related to telomere shortening. *Nat Genet,* 32**,** 280-4.

ODDOUX, C., STRUEWING, J. P., CLAYTON, C. M., NEUHAUSEN, S., BRODY, L. C., KABACK, M., HAAS, B., NORTON, L., BORGEN, P., JHANWAR, S., GOLDGAR, D., OSTRER, H. & OFFIT, K. 1996. The carrier frequency of the BRCA2 6174delT mutation among Ashkenazi Jewish individuals is approximately 1%. *Nat Genet,* 14**,** 188-190.

OKANO, M., XIE, S. P. & LI, E. 1998. Cloning and characterization of a family of novel mammalian DNA (cytosine-5) methyltransferases. *Nat Genet,* 19**,** 219-220.

OLOVNIKOV, A. M. 1971. [Principle of marginotomy in template synthesis of polynucleotides]. *Dokl Akad Nauk SSSR,* 201**,** 1496-9.

OPRESKO, P. L., FAN, J. H., DANZY, S., WILSON, D. M. & BOHR, V. A. 2005. Oxidative damage in telomeric DNA disrupts recognition by TRF1 and TRF2. *Nucleic Acids Res,* 33**,** 1230-1239.

PATEL, K. J., YU, V. P. C. C., LEE, H. S., CORCORAN, A., THISTLETHWAITE, F. C., EVANS, M. J., COLLEDGE, W. H., FRIEDMAN, L. S., PONDER, B. A. J. & VENKITARAMAN, A. R. 1998. Involvement of Brca2 in DNA repair. *Molecular Cell,* 1**,** 347-357.

PAULL, T. T., CORTEZ, D., BOWERS, B., ELLEDGE, S. J. & GELLERT, M. 2001. Direct DNA binding by Brca1. *Proc Natl Acad Sci U S A,* 98**,** 6086-6091.

PATEL, K. J., YU, V. P. C. C., LEE, H. S., CORCORAN, A., THISTLETHWAITE, F. C., EVANS, M. J., COLLEDGE, W. H., FRIEDMAN, L. S., PONDER, B. A. J. &

VENKITARAMAN, A. R. 1998. Involvement of Brca2 in DNA repair. *Molecular Cell,* 1**,** 347-357.

PAULL, T. T., CORTEZ, D., BOWERS, B., ELLEDGE, S. J. & GELLERT, M. 2001. Direct DNA binding by Brca1. *Proc Natl Acad Sci U S A,* 98**,** 6086-6091.

POWELL, S. N. & KACHNIC, L. A. 2003. Roles of BRCA1 and BRCA2 in homologous recombination, DNA replication fidelity and the cellular response to ionizing radiation. *Oncogene,* 22**,** 5784-91.

PERREM, K., BRYAN, T. M., ENGLEZOU, A., HACKL, T., MOY, E. L. & REDDEL, R. R. 1999. Repression of an alternative mechanism for lengthening of telomeres in somatic cell hybrids. *Oncogene,* 18**,** 3383-3390.

PERREM, K., COLGIN, L. M., NEUMANN, A. A., YEAGER, T. R. & REDDEL, R. R. 2001. Coexistence of alternative lengthening of telomeres and telomerase in hTERT-transfected GM847 cells. *Mol Cell Biol,* 21**,** 3862-3875.

PISANO, M., COSSU, A., PERSICO, I., PALMIERI, G., ANGIUS, A., CASU, G., PALOMBA, G., SAROBBA, M. G., ROCCA, P. C. O., DEDOLA, M. F., OLMEO, N., PASCA, A., BUDRONI, M., MARRAS, V., PISANO, A., FARRIS, A., MASSARELLI, G., PIRASTU, M. & TANDA, F. 2000. Identification of a founder BRCA2 mutation in Sardinia. *Br J Cancer,* 82**,** 553-559.

POLO, S. E. & JACKSON, S. P. 2011. Dynamics of DNA damage response proteins at DNA breaks: a focus on protein modifications. *Genes Dev,* 25**,** 409-33.

PRADHAN, S., BACOLLA, A., WELLS, R. D. & ROBERTS, R. J. 1999. Recombinant human DNA (cytosine-5) methyltransferase I. Expression, purification, and comparison of de novo and maintenance methylation. *Journal of Biological Chemistry,* 274**,** 33002-33010.

PROSCH, S., STEIN, J., STAAK, K., LIEBENTHAL, C., VOLK, H. D. & KRUGER, D. H. 1996. Inactivation of the very strong HCMV immediate early promoter by DNA CpG methylation in vitro. *Biol Chem Hoppe Seyler,* 377**,** 195-201.

RAHMAN, N. & STRATTON, M. R. 1998. The genetics of breast cancer susceptibility. *Annual Review of Genetics,* 32**,** 95-121.

RAO, D. D., VORHIES, J. S., SENZER, N. & NEMUNAITIS, J. 2009. siRNA vs. shRNA: similarities and differences. *Adv Drug Deliv Rev,* 61**,** 746-59.

REDDEL, R. R., BRYAN, T. M., COLGIN, L. M., PERREM, K. T. & YEAGER, T. R. 2001. Alternative lengthening of telomeres in human cells. *Radiation Research,* 155**,** 194-200.

RIVERO, M. T., MOSQUERA, A., GOYANES, V., SLIJEPCEVIC, P. & FERNANDEZ, J. L. 2004. Differences in repair profiles of interstitial telomeric sites between normal and DNA double-strand break repair deficient Chinese hamster cells. *Experimental Cell Research,* 295**,** 161-172.

RODIER, F., KIM, S. H., NIJJAR, T., YASWEN, P. & CAMPISI, J. 2005. Cancer and aging: the importance of telomeres in genome maintenance. *International Journal of Biochemistry & Cell Biology,* 37**,** 977-990.

RODRIGUEZ, A. O., LLACUACHAQUI, M., PARDO, G. G., ROYER, R., LARSON, G., WEITZEL, J. N. & NAROD, S. A. 2012. BRCA1 and BRCA2 mutations among ovarian cancer patients from Colombia. *Gynecol Oncol,* 124**,** 236-243.

ROTH, C. W., KOBESKI, F., WALTER, M. F. & BIESSMANN, H. 1997. Chromosome end elongation by recombination in the mosquito Anopheles gambiae. *Mol Cell Biol,* 17**,** 5176-5183.

ROTHKAMM, K., KRUGER, I., THOMPSON, L. H. & LOBRICH, M. 2003. Pathways of DNA double-strand break repair during the mammalian cell cycle. *Mol Cell Biol,* 23**,** 5706-5715.

RUDOLPH, K. L., MILLARD, M., BOSENBERG, M. W. & DEPINHO, R. A. 2001. Telomere dysfunction and evolution of intestinal carcinoma in mice and humans. *Nat Genet,* 28**,** 155-159.

RUIZ-HERRERA, A., NERGADZE, S. G., SANTAGOSTINO, M. & GIULOTTO, E. 2008. Telomeric repeats far from the ends: mechanisms of origin and role in evolution. *Cytogenet Genome Res,* 122**,** 219-228.

SAMPER, E., GOYTISOLO, F. A., SLIJEPCEVIC, P., VAN BUUL, P. P. W. & BLASCO, M. A. 2000. Mammalian Ku86 protein prevents telomeric fusions independently of the length of TTAGGG repeats and the G-strand overhang. *Embo Reports,* 1**,** 244-252.

SAPIR, E., GOZALY-CHIANEA, Y., AL-WAHIBY, S., RAVINDRAN, S., YASAEI, H. & SLIJEPCEVIC, P. 2011. Effects of BRCA2 deficiency on telomere recombination in non-ALT and ALT cells. *Genome Integr,* 2**,** 9.

SCHMITTER, D., FILKOWSKI, J., SEWER, A., PILLAI, R. S., OAKELEY, E. J., ZAVOLAN, M., SVOBODA, P. & FILIPOWICZ, W. 2006. Effects of Dicer and Argonaute down-regulation on mRNA levels in human HEK293 cells. *Nucleic Acids Res,* 34**,** 4801-15.

SHARAN, S. K., MORIMATSU, M., ALBRECHT, U., LIM, D. S., REGEL, E., DINH, C., SANDS, A., EICHELE, G., HASTY, P. & BRADLEY, A. 1997. Embryonic lethality and radiation hypersensitivity mediated by Rad51 in mice lacking Brca2. *Nature,* 386**,** 804-810.

SHAY, J. W. & BACCHETTI, S. 1997. A survey of telomerase activity in human cancer. *Eur J Cancer,* 33**,** 787-791.

SHAY, J. W. & KEITH, W. N. 2008. Targeting telomerase for cancer therapeutics. *Br J Cancer,* 98**,** 677-683.

SHILOH, Y. & LEHMANN, A. R. 2004. Maintaining integrity. *Nature Cell Biology,* 6**,** 923-928.

SHORE, D. 1997. Telomerase and telomere-binding proteins: Controlling the endgame. *Trends in Biochemical Sciences,* 22**,** 233-235.

SINHA, R. P. & HADER, D. P. 2002. UV-induced DNA damage and repair: a review. *Photochemical & Photobiological Sciences,* 1**,** 225-236.

SLIJEPCEVIC, P. 2006. The role of DNA damage response proteins at telomeres--an "integrative" model. *DNA Repair (Amst),* 5**,** 1299-306.

SLIJEPCEVIC, P. & AL-WAHIBY, S. 2005. Telomere biology: integrating protection with DNA damage chromosomal end response. *Chromosoma,* 114**,** 275-285.

SLIJEPCEVIC, P., XIAO, Y., DOMINGUEZ, I. & NATARAJAN, A. T. 1996. Spontaneous and radiation-induced chromosomal breakage at interstitial telomeric sites. *Chromosoma,* 104**,** 596-604.

SMOGORZEWSKA, A., VAN STEENSEL, B., BIANCHI, A., OELMANN, S., SCHAEFER, M. R., SCHNAPP, G. & DE LANGE, T. 2000. Control of human telomere length by TRF1 and TRF2. *Mol Cell Biol,* 20**,** 1659-1668.

SPARDY, N., DUENSING, A., HOSKINS, E. E., WELLS, S. I. & DUENSING, S. 2008. HPV-16 E7 Reveals a Link between DNA Replication Stress, Fanconi Anemia D2 Protein, and Alternative Lengthening of Telomere-Associated Promyelocytic Leukemia Bodies. *Cancer Research,* 68**,** 9954-9963.

STEWENIUS, Y., GORUNOVA, L., JONSON, T., LARSSON, N., HOGLUND, M., MANDAHL, N., MERTENS, F., MITELMAN, F. & GISSELSSON, D. 2005. Structural and numerical chromosome changes in colon cancer develop through telomere-mediated anaphase bridges, not through mitotic multipolarity. *Proc Natl Acad Sci U S A,* 102**,** 5541-5546.

SUNG, P., KREJCI, L., VAN KOMEN, S. & SEHORN, M. G. 2003. Rad51 recombinase and recombination mediators. *Journal of Biological Chemistry,* 278**,** 42729-42732.

SY, S. M. H., HUEN, M. S. Y. & CHEN, J. J. 2009. PALB2 is an integral component of the BRCA complex required for homologous recombination repair. *Proc Natl Acad Sci U S A,* 106**,** 7155-7160.

TAKANO, H., MURASAWA, S. & ASAHARA, T. 2008. Functional and gene expression analysis of hTERT overexpressed endothelial cells. *Biologics,* 2**,** 547-54.

THOMPSON, L. H. 2005. Unraveling the Fanconi anemia-DNA repair connection. *Nat Genet,* 37**,** 921-922.

THORLACIUS, S., SIGURDSSON, S., BJARNADOTTIR, H., OLAFSDOTTIR, G., JONASSON, J. G., TRYGGVADOTTIR, L., TULINIUS, H. & EYFJORD, J. E. 1997. Study of a single BRCA2 mutation with high carrier frequency in a small population. *Am J Hum Genet,* 60**,** 1079-1084.

THORSLUND, T., ESASHI, F. & WEST, S. C. 2007. Interactions between human BRCA2 protein and the meiosis-specific recombinase DMC1. *Embo Journal,* 26**,** 2915-2922.

TONIN, P. N., MES-MASSON, A. M., NAROD, S. A., GHADIRIAN, P. & PROVENCHER, D. 1999. Founder BRCA1 and BRCA2 mutations in French Canadian ovarian cancer cases unselected for family history. *Clinical Genetics,* 55**,** 318-324.

TRENZ, K., ROTHFUSS, A., SCHUTZ, P. & SPEIT, G. 2002. Mutagen sensitivity of peripheral blood from women carrying a BRCA1 or BRCA2 mutation. *Mutation Research-Fundamental and Molecular Mechanisms of Mutagenesis,* 500**,** 89-96.

TURINETTO, V., ORLANDO, L., SANCHEZ-RIPOLL, Y., KUMPFMUELLER, B., STORM, M. P., PORCEDDA, P., MINIERI, V., SAVIOZZI, S., ACCOMASSO, L., CIBRARIO ROCCHIETTI, E., MOORWOOD, K., CIRCOSTA, P., CIGNETTI, A., WELHAM, M. J. & GIACHINO, C. 2012. High basal gammaH2AX levels sustain self-renewal of mouse embryonic and induced pluripotent stem cells. *Stem Cells,* 30**,** 1414-23.

TUTT, A., BERTWISTLE, D., VALENTINE, J., GABRIEL, A., SWIFT, S., ROSS, G., GRIFFIN, C., THACKER, J. & ASHWORTH, A. 2001. Mutation in Brca2 stimulates error-prone homology-directed repair of DNA double-strand breaks occurring between repeated sequences. *Embo Journal,* 20**,** 4704-4716.

TUTT, A., GABRIEL, A., BERTWISTLE, D., CONNOR, F., PATERSON, H., PEACOCK, J., ROSS, G. & ASHWORTH, A. 1999. Absence of Brca2 causes genome instability

by chromosome breakage and loss associated with centrosome amplification. *Current Biology,* 9**,** 1107-1110.

ULANER, G. A. & GIUDICE, L. C. 1997. Developmental regulation of telomerase activity in human fetal tissues during gestation. *Molecular Human Reproduction,* 3**,** 769-773.

ULANER, G. A., HU, J. F., VU, T. H., GIUDICE, L. C. & HOFFMAN, A. R. 1998. Telomerase activity in human development is regulated by human telomerase reverse transcriptase (hTERT) transcription and by alternate splicing of hTERT transcripts. *Cancer Research,* 58**,** 4168-4172.

VAN STEENSEL, B., SMOGORZEWSKA, A. & DE LANGE, T. 1998. TRF2 protects human telomeres from end-to-end fusions. Cell, 92, 401-13.

VAN STEENSEL, B., SMOGORZEWSKA, A. & DE LANGE, T. 1998. TRF2 protects human telomeres from end-to-end fusions. *Cell,* 92**,** 401-413.

VENKITARAMAN, A. R. 2001a. Functions of BRCA1 and BRCA2 in the biological response to DNA damage. *J Cell Sci,* 114**,** 3591-8.

VENKITARAMAN, A. R. 2001b. Functions of BRCA1 and BRCA2 in the biological response to DNA damage. *J Cell Sci,* 114**,** 3591-3598.

VENKITARAMAN, A. R. 2002a. Cancer susceptibility and the functions of BRCA1 and BRCA2. *Cell,* 108**,** 171-182.

VENKITARAMAN, A. R. 2002b. Connecting Fanconi's anaemia to breast cancer predisposition. *Lancet,* 360**,** 1344-1345.

VENTURELLI, S., ARMEANU, S., PATHIL, A., HSIEH, C. J., WEISS, T. S., VONTHEIN, R., WEHRMANN, M., GREGOR, M., LAUER, U. M. & BITZER, M. 2007. Epigenetic combination therapy as a tumor-selective treatment approach for hepatocellular carcinoma. *Cancer,* 109**,** 2132-41.

VERDUN, R. E. & KARLSEDER, J. 2007. Replication and protection of telomeres. *Nature,* 447**,** 924-931.

VERHOOG, L. C., VAN DEN OUWELAND, A. M. W., BERNS, E., VAN VEGHEL-PLANDSOEN, M. M., VAN STAVEREN, I. L., WAGNER, A., BARTELS, C. C. M., TILANUS-LINTHORST, M. M. A., DEVILEE, P., SEYNAEVE, C., HALLEY, D. J. J., NIERMEIJER, M. F., KLIJN, J. G. M. & MEIJERS-HEIJBOER, H. 2001. Large regional differences in the frequency of distinct BRCA1/BRCA2 mutations in 517 Dutch breast and/or ovarian cancer families. *Eur J Cancer,* 37**,** 2082-2090.

VOGEL, C. & MARCOTTE, E. M. 2012. Insights into the regulation of protein abundance from proteomic and transcriptomic analyses. *Nat Rev Genet,* 13**,** 227-32.

VON FIGURA, G., HARTMANN, D., SONG, Z. F. & RUDOLPH, K. L. 2009. Role of telomere dysfunction in aging and its detection by biomarkers. *Journal of Molecular Medicine-Jmm,* 87**,** 1165-1171.

WANG, W. D. 2007. Emergence of a DNA-damage response network consisting of Fanconi anaemia and BRCA proteins. *Nature Reviews Genetics,* 8**,** 735-748.

WANG, X. Z., ANDREASSEN, P. R. & D'ANDREA, A. D. 2004. Functional interaction of monoubiquitinated FANCD2 and BRCA2/FANCD1 in chromatin. *Mol Cell Biol,* 24**,** 5850-5862.

WANG, Y., CORTEZ, D., YAZDI, P., NEFF, N., ELLEDGE, S. J. & QIN, J. 2000. BASC, a super complex of BRCA1-associated proteins involved in the recognition and repair of aberrant DNA structures. *Genes & Development,* 14**,** 927-939.

WARD, J. F. 2000. Complexity of damage produced by ionizing radiation. *Cold Spring Harbor Symposia on Quantitative Biology,* 65**,** 377-382.

WARREN, M., SMITH, A., PARTRIDGE, N., MASABANDA, J., GRIFFIN, D. & ASHWORTH, A. 2002. Structural analysis of the chicken BRCA2 gene facilitates identification of functional domains and disease causing mutations. *Human Molecular Genetics,* 11**,** 841-851.

WATSON, J. D. 1972. Origin of Concatemeric T7 DNA. *Nature-New Biology,* 239**,** 197-&.

WEINRICH, S. L., PRUZAN, R., MA, L., OUELLETTE, M., TESMER, V. M., HOLT, S. E., BODNAR, A. G., LICHTSTEINER, S., KIM, N. W., TRAGER, J. B., TAYLOR, R. D., CARLOS, R., ANDREWS, W. H., WRIGHT, W. E., SHAY, J. W., HARLEY, C. B. & MORIN, G. B. 1997. Reconstitution of human telomerase with the template RNA component hTR and the catalytic protein subunit hTRT. *Nat Genet,* 17**,** 498-502.

WELLINGER, R. J. & SEN, D. 1997. The DNA structures at the ends of eukaryotic chromosomes. *Eur J Cancer,* 33**,** 735-749.

WEST, S. C. 2003. Cross-links between Fanconi anaemia and BRCA2. *DNA Repair (Amst),* 2**,** 231-234.

WILSON, D. M. & THOMPSON, L. H. 2007. Molecular mechanisms of sister-chromatid exchange. *Mutation Research-Fundamental and Molecular Mechanisms of Mutagenesis,* 616**,** 11-23.

WOJTYLA, A., GLADYCH, M. & RUBIS, B. 2011. Human telomerase activity regulation. *Molecular Biology Reports,* 38**,** 3339-3349.

WOOSTER, R., BIGNELL, G., LANCASTER, J., SWIFT, S., SEAL, S., MANGION, J., COLLINS, N., GREGORY, S., GUMBS, C., MICKLEM, G., BARFOOT, R., HAMOUDI, R., PATEL, S., RICE, C., BIGGS, P., HASHIM, Y., SMITH, A., CONNOR, F., ARASON, A., GUDMUNDSSON, J., FICENEC, D., KELSELL, D., FORD, D., TONIN, P., BISHOP, D. T., SPURR, N. K., PONDER, B. A. J., EELES, R., PETO, J., DEVILEE, P., CORNELISSE, C., LYNCH, H., NAROD, S., LENOIR, G., EGILSSON, V., BARKADOTTIR, R. B., EASTON, D. F., BENTLEY, D. R., FUTREAL, P. A., ASHWORTH, A. & STRATTON, M. R. 1995. Identification of the Breast-Cancer Susceptibility Gene Brca2. *Nature,* 378**,** 789-792.

WU, G. K., LEE, W. H. & CHEN, P. L. 2000. NBS1 and TRF1 colocalize at promyelocytic leukemia bodies during late S/G(2) phases in immortalized telomerase-negative cells - Implication of NBS1 in alternative lengthening of telomeres. *Journal of Biological Chemistry,* 275**,** 30618-30622.

XIA, B., SHENG, Q., NAKANISHI, K., OHASHI, A., WU, J. M., CHRIST, N., LIU, X. G., JASIN, M., COUCH, F. J. & LIVINGSTON, D. M. 2006. Control of BRCA2 cellular and clinical functions by a nuclear partner, PALB2. *Molecular Cell,* 22**,** 719-729.

YANG, H. J., JEFFREY, P. D., MILLER, J., KINNUCAN, E., SUN, Y. T., THOMA, N. H., ZHENG, N., CHEN, P. L., LEE, W. H. & PAVLETICH, N. P. 2002. BRCA2 function in DNA binding and recombination from a BRCA2-DSS1-ssDNA structure. *Science,* 297**,** 1837-1848.

YASAEI, H., GOZALY-CHIANEA, Y. & SLIJEPCEVIC, P. 2013. Analysis of telomere length and function in radiosensitive mouse and human cells in response to DNA-PKcs inhibition. Genome Integr, 4, 2.

YEAGER, T. R., NEUMANN, A. A., ENGLEZOU, A., HUSCHTSCHA, L. I., NOBLE, J. R. & REDDEL, R. R. 1999. Telomerase-negative immortalized human cells contain a novel type of promyelocytic leukemia (PML) body. *Cancer Research,* 59**,** 4175-4179.

YI, X. M., SHAY, J. W. & WRIGHT, W. E. 2001. Quantitation of telomerase components and hTERT mRNA splicing patterns in immortal human cells. *Nucleic Acids Res,* 29**,** 4818-4825.

YU, V. P. C. C., KOEHLER, M., STEINLEIN, C., SCHMID, M., HANAKAHI, L. A., VAN GOOL, A. J., WEST, S. C. & VENKITARAMAN, A. R. 2000. Gross chromosomal

rearrangements and genetic exchange between nonhomologous chromosomes following BRCA2 inactivation. *Genes & Development,* 14**,** 1400-1406.

ZAKIAN, V. A. 1995. Telomeres - Beginning to Understand the End. *Science,* 270**,** 1601-1607.

ZHONG, Q., CHEN, C. F., LI, S., CHEN, Y. M., WANG, C. C., XIAO, J., CHEN, P. L., SHARP, Z. D. & LEE, W. H. 1999. Association of BRCA1 with the hRad50-hMre11-p95 complex and the DNA damage response. *Science,* 285**,** 747-750.

ZHONG, Z. H., JIANG, W. Q., CESARE, A. J., NEUMANN, A. A., WADHWA, R. & REDDEL, R. R. 2007. Disruption of telomere maintenance by depletion of the MRE11/RAD50/NBS1 complex in cells that use alternative lengthening of telomeres. *Journal of Biological Chemistry,* 282**,** 29314-29322.

ZHOU, Y. L., SHI, H. Y., LI, X. N., LV, P., LI, G. S., LIU, Q. Y. & XU, H. 2013. Role of Endoplasmic Reticulum Stress in Aberrant Activation of Fluoride-Treated Osteoblasts. *Biological Trace Element Research,* 154**,** 448-456.

Appendix

Appendix I

Three different target sequences of Lentiviral shRNA particles that purchased from the thermo scientific SMART choice Lentiviral shRNA Particles for BRCA2 stable knockdown. The SMARTvector 2.0 contained three unique BRCA2 hairpin sequences as shown in (Packing list & COSHH form) below. The three sequences were then mixed at equal Titer to generate a pool SMARTvector 2.0. A pool of shRNAs helps to increase the target knock-down efficiency.

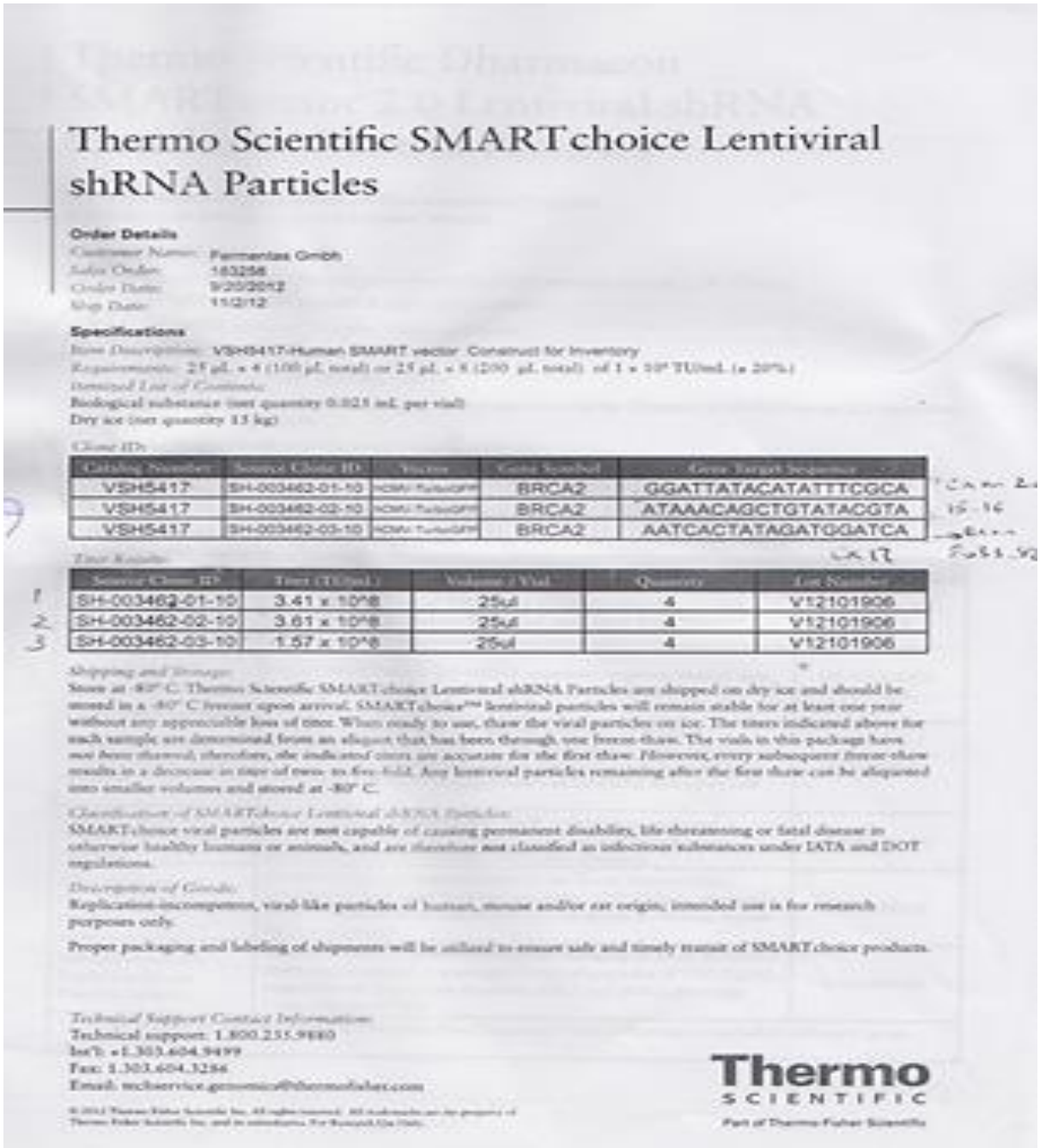

Thermo Scientific SMARTchoice Lentiviral shRNA Particles

Order Details

Customer Name: Fermentas GmbH
Sales Order: 183256
Order Date: 9/20/2012
Ship Date: 11/2/12

Specifications

Item Description: VSH5417-Human SMART vector Construct for Inventory
Requirements: 25 µL x 4 (100 µL total) or 25 µL x 8 (200 µL total) of 1 x 10⁵ TU/mL (± 20%)
Itemized List of Contents:
Biological substance (net quantity 0.025 mL per vial)
Dry ice (net quantity 15 kg)

Clone ID:

Catalog Number	Source Clone ID	Vector	Gene Symbol	Gene Target Sequence
VSH5417	SH-003462-01-10	pGIPZ	BRCA2	GGATTATACATATTTCGCA
VSH5417	SH-003462-02-10	pGIPZ	BRCA2	ATAAACAGCTGTATACGTA
VSH5417	SH-003462-03-10	pGIPZ	BRCA2	AATCACTATAGATGGATCA

Titer Results:

Source Clone ID	Titer (TU/mL)	Volume / Vial	Quantity	Lot Number
SH-003462-01-10	3.41 x 10^8	25µl	4	V12101906
SH-003462-02-10	3.61 x 10^8	25µl	4	V12101906
SH-003462-03-10	1.57 x 10^8	25µl	4	V12101906

Shipping and Storage:
Store at -80° C. Thermo Scientific SMARTchoice Lentiviral shRNA Particles are shipped on dry ice and should be stored at -80° C freezer upon arrival. SMARTchoice™ lentiviral particles will remain stable for at least one year without any appreciable loss of titer. When ready to use, thaw the viral particles on ice. The titers indicated above for each sample are determined from an aliquot that has been through one freeze-thaw. The vials in this package have not been thawed; therefore, the indicated titers are accurate for the first thaw. However, every subsequent freeze-thaw results in a decrease in titer of two- to five-fold. Any lentiviral particles remaining after the first thaw can be aliquoted into smaller volumes and stored at -80° C.

Classification of SMARTchoice Lentiviral shRNA Particles:
SMARTchoice viral particles are **not** capable of causing permanent disability, life-threatening or fatal disease in otherwise healthy humans or animals, and are therefore **not** classified as infectious substances under IATA and DOT regulations.

Description of Goods:
Replication-incompetent, viral-like particles of human, mouse and/or rat origin; intended use is for research purposes only.

Proper packaging and labeling of shipments will be utilized to ensure safe and timely transit of SMARTchoice products.

Technical Support Contact Information:
Technical support: 1.800.255.9880
Int'l: +1.303.604.9499
Fax: 1.303.604.3284
Email: mchservice.genomics@thermofisher.com

Thermo SCIENTIFIC
Part of Thermo Fisher Scientific

HAZARD IDENTIFICATION & COSHH | **BIOSCIENCES**

PROCEDURE: SMARTvector Lentivirus shRNA Particles | **DATE:** 06/09/2012

COMPANY NAME & NUMBER: ThermoFisher Scientific Chemtrec (EU): (202) 483-7616

Substance to be assessed and amount used	HAZARD CLASSIFICATION										ROUTE OF CONTACT						CONTROL							DISPOSAL METHOD					RISK ASSESSMENT				
	Very Toxic	Toxic	Corrosive	Harmful	Irritant	Sensitiser	Dust	Teratogenic	Carcinogenic	Long term effects	Inhalation	Ingestion	Absorption via skin	Injection	Skin/eye damage		Goggles	Face Shield	Gloves	Respiratory Apparatus	Labcoat	Fume Cupboard	Sink	Solvent Wast	Solid Waste	Clinical Waste	Other	None	Low	Medium	High	Very High
Lentivirus particles					X						X	X	X		X				X		X	X				X			X			

Spillage:

Treat spillage the same way as doing any cell culturing.

Comments:
SMARTvector 2.0 lentiviral shRNA particles can be employed in standard Biosafety Level 2 tissue culture facilities and should be treated with the same level of caution as any other potentially infectious agent

Appendix II

Detail of Chromosomal abnormalities experiments.

Two sets of experiments were carried out using Giemsa stained techniques. In each experiment at least 30- 50 metaphases were analysed.

Date: 08/03/12

Experiment: V79-B Radiation 2Gy -G1 Chrom- Radiation 2Gy G1

No. of Cells	No. of Chromosome	Di	Frag	Ring	Other	No. of Cells	No. of Chromosome	Di	Frag	Ring	Other
1					1	51					1
2						52					
3						53					
4						54					
5						55		2			a1
6		1				56		2			1
7			1			57		1			
8						58					
9						59					
10						60					
11			1			61		2			1
12						62					
13				1		63		1			
14						64					
15			1			65					
16						66					
17						67					
18						68					
19						69					
20						70					
21						71					
22						72					
23						73					
24						74					
25						75					
26						76					
27						77					
28						78					
29						79					
30						80					
31						81					
32						82					
33						83					
34						84					
35						85					
36			1			86					
37						87		1			
38						88					
39						89					
40						90				1	
41			1			91					
42						92					
43						93					
44						94					
45						95					
46						96					
47		1		1		97					
48						98					
49						99					
50						100					

V79-B

Date:

Experiment: G1 -

No. of Cells	No. of Chromosome	DI	Frag	Ring	Other
1					
2					
3					
4					
5					
6					
7					
8					
9					
10					
11					
12					
13					
14					1
15					
16					
17					
18					
19					
20					
21					
22					
23					
24					
25					
26					
27					
28		1			
29					
30					
31					
32					
33					
34					
35					
36					
37					
38					
39					
40					
41					
42					
43				3	
44					
45				1	
46					
47					
48					
49					
50					

VC8 - chrom

G1 control

No. of Cells	No. of Chromosome	Di	Frag	Ring	Other
51		1			
52					
53					
54					
55					
56					
57					
58		1			
59					
60					
61					
62					
63					
64					1
65		1			
66					
67					
68					
69					
70		1			
71					
72					
73					
74					
75					
76					
77					
78			1		
79					
80					
81					
82					
83					
84					
85					
86					
87		1			
88					
89					
90					
91		1			
92					
93					1
94					
95					
96					
97					
98					
99					
100					

Appendix III

Determination of telomerase activity by conventional Telomeric Repeat Amplification Protocol (TRAP) assay

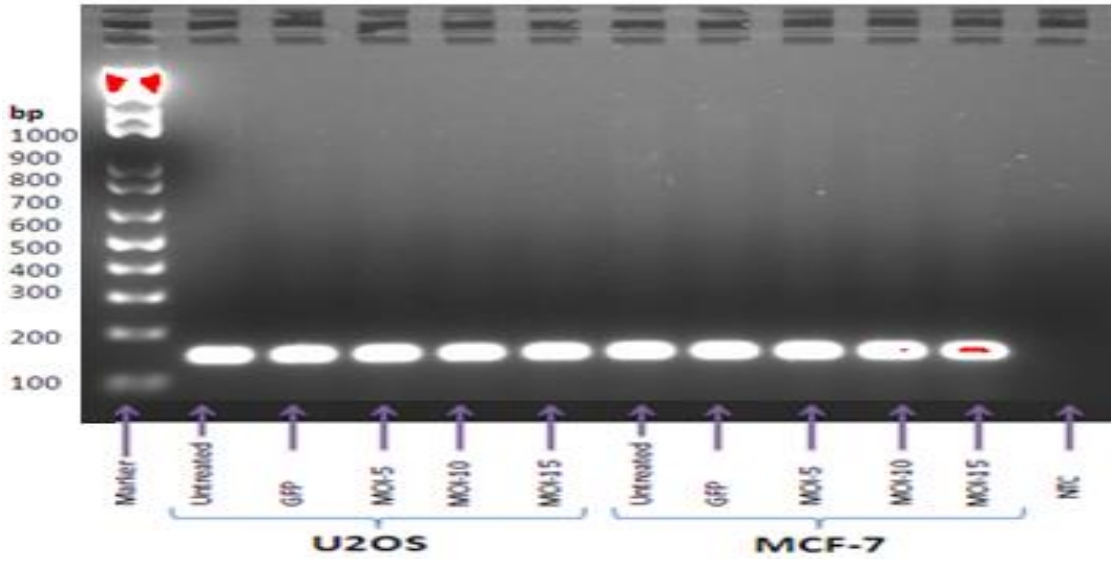

Figure 1 - Optimisation of shBRCA2 CDNs
The image shows the running of cDNA obtained from two cell lines, U2OS and MCF-7 after transfected with Lentiviral shBRCA2 in order to determine the annealing efficiency and cycle at 57°C. The cycles in A and B was 25 and 35.

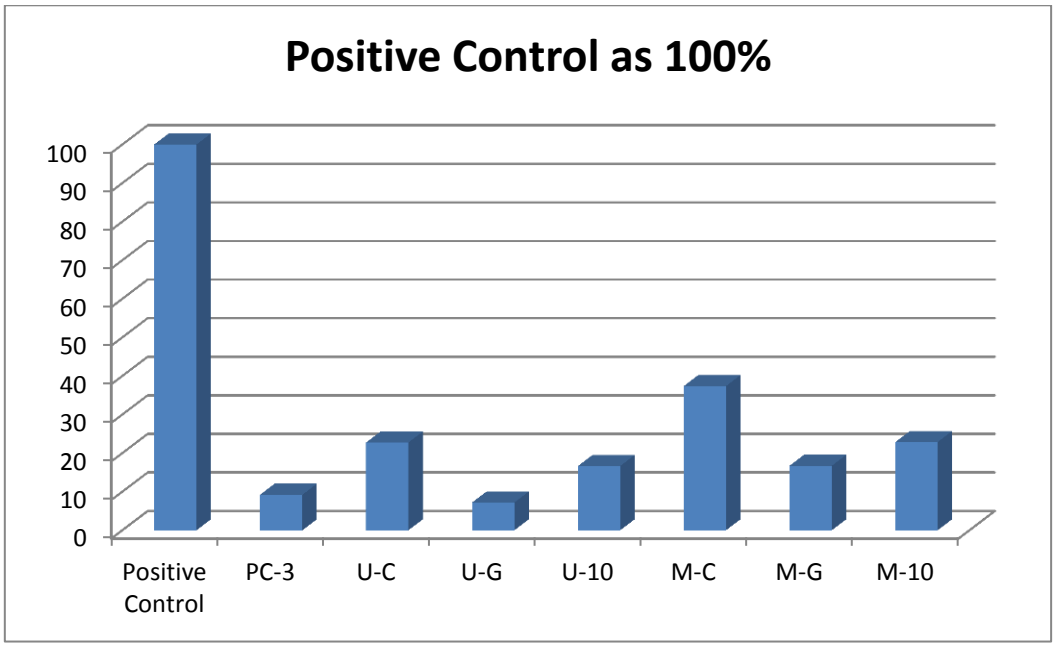

Figure 2- Telomerase activity was assessed by the q-PCR-based telomerase activity detection method, Telomeric Repeat Amplification Protocol (TRAP). As controls we used two cell lines, PC3 and PC3/hTERT, known to have robust telomerase activity. PC-3/hTERT cells showed robust telomerase activity as expected.

Appendix IV

These are the list of applies for permission to reproduce the images that haven been used in this thesis.

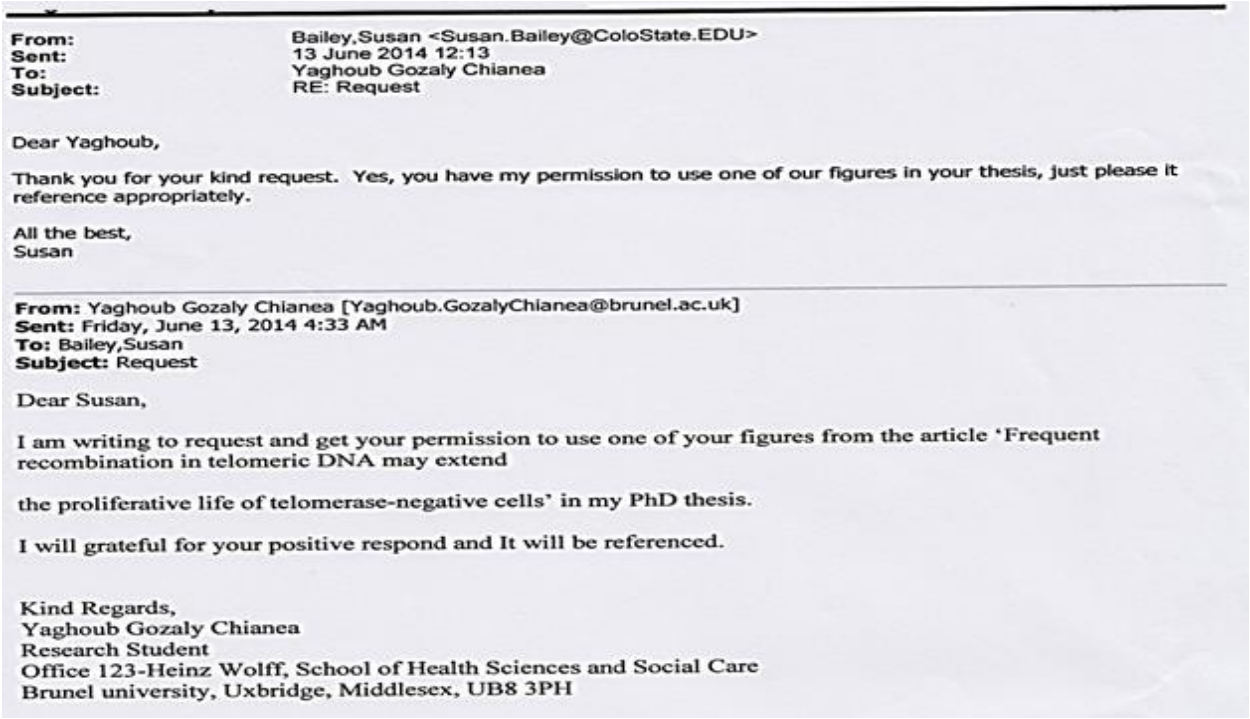

From: Bailey,Susan <Susan.Bailey@ColoState.EDU>
Sent: 13 June 2014 12:13
To: Yaghoub Gozaly Chianea
Subject: RE: Request

Dear Yaghoub,

Thank you for your kind request. Yes, you have my permission to use one of our figures in your thesis, just please it reference appropriately.

All the best,
Susan

From: Yaghoub Gozaly Chianea [Yaghoub.GozalyChianea@brunel.ac.uk]
Sent: Friday, June 13, 2014 4:33 AM
To: Bailey,Susan
Subject: Request

Dear Susan,

I am writing to request and get your permission to use one of your figures from the article 'Frequent recombination in telomeric DNA may extend

the proliferative life of telomerase-negative cells' in my PhD thesis.

I will grateful for your positive respond and It will be referenced.

Kind Regards,
Yaghoub Gozaly Chianea
Research Student
Office 123-Heinz Wolff, School of Health Sciences and Social Care
Brunel university, Uxbridge, Middlesex, UB8 3PH

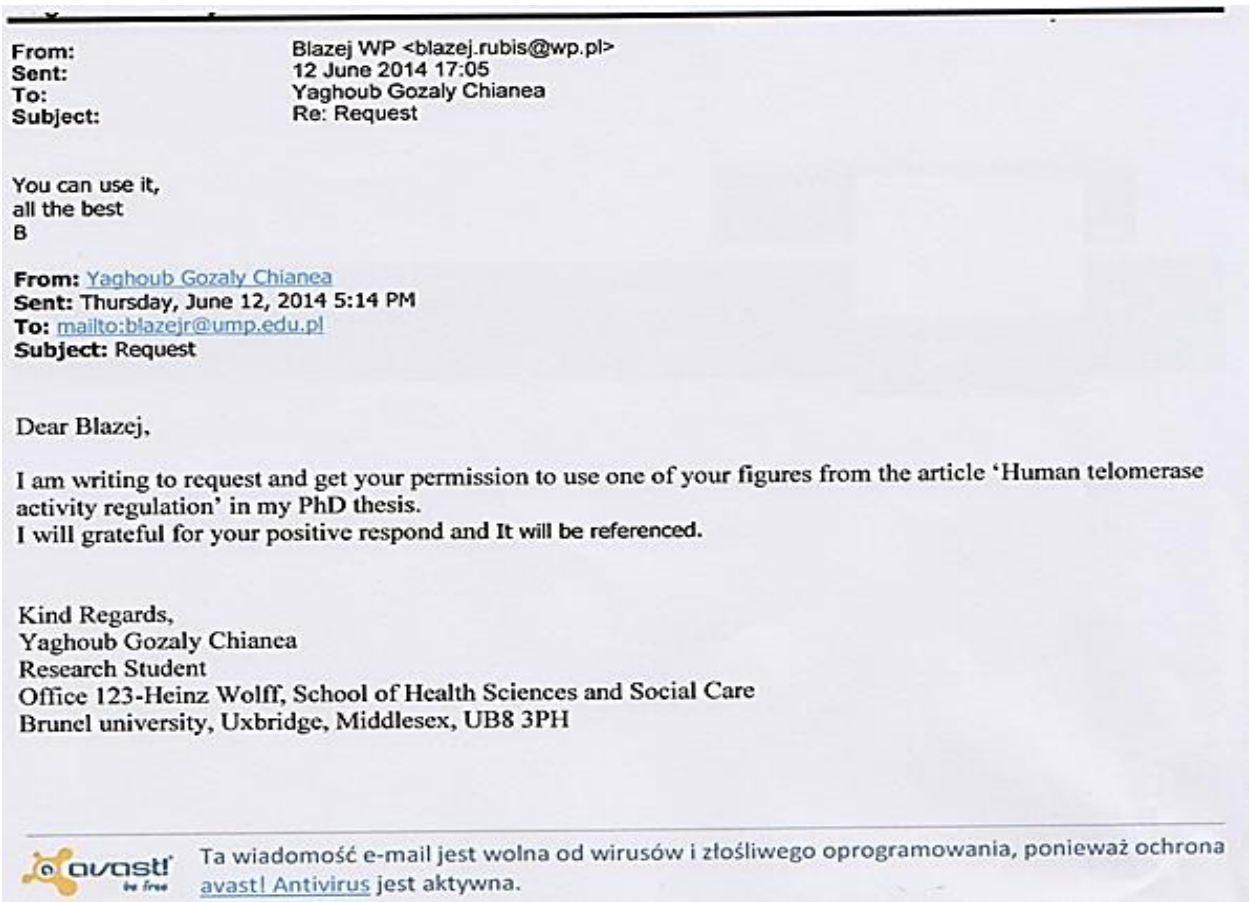

From: Blazej WP <blazej.rubis@wp.pl>
Sent: 12 June 2014 17:05
To: Yaghoub Gozaly Chianea
Subject: Re: Request

You can use it,
all the best
B

From: Yaghoub Gozaly Chianea
Sent: Thursday, June 12, 2014 5:14 PM
To: mailto:blazejr@ump.edu.pl
Subject: Request

Dear Blazej,

I am writing to request and get your permission to use one of your figures from the article 'Human telomerase activity regulation' in my PhD thesis.
I will grateful for your positive respond and It will be referenced.

Kind Regards,
Yaghoub Gozaly Chianea
Research Student
Office 123-Heinz Wolff, School of Health Sciences and Social Care
Brunel university, Uxbridge, Middlesex, UB8 3PH

From: Jordi Surrallés Calonge <Jordi.Surralles@uab.cat>
Sent: 12 June 2014 21:05
To: Yaghoub Gozaly Chianea
Subject: RE: Request

Yes, of course Yaghoub, feel free to use this figure. Are your woking in Predrag's lab? if so, please send him my warm regards
Best
Jordi

De: Yaghoub Gozaly Chianea <Yaghoub.GozalyChianea@brunel.ac.uk>
Enviat el: dijous, 12 de juny de 2014 21:35
Per a: Jordi Surrallés Calonge
Tema: Request

Dear Surralles,

I am writing to request and get your permission to use one of your figures from the article 'Telomere dysfunction in genome instability syndromes' in my PhD thesis.
I will grateful for your positive respond and it will be referenced.

Kind Regards,
Yaghoub Gozaly Chianea
Research Student
Office 123-Heinz Wolff, School of Health Sciences and Social Care
Brunel university, Uxbridge, Middlesex, UB8 3PH

From: Roger Reddel <RReddel@cmri.org.au>
Sent: 12 June 2014 13:58
To: Yaghoub Gozaly Chianea
Subject: RE: Request

Dear Yaghoub,

That's fine with me, provided it is attributed in the usual way.

Best wishes,

Roger Reddel

From: Yaghoub Gozaly Chianea [mailto:Yaghoub.GozalyChianea@brunel.ac.uk]
Sent: Thursday, 12 June 2014 10:56 PM
To: Roger Reddel
Subject: Request

Dear Reddel,

I am writing to request and get your permission to use one of your figures from the review 'alternative lengthening of telomeres:models, mechanisms and implications' in my PhD thesis.
I will grateful for your positive respond.

Kind Regards,
Yaghoub Gozaly Chianea
Research Student
Office 123-Heinz Wolff, School of Health Sciences and Social Care
Brunel university, Uxbridge, Middlesex, UB8 3PH